ISSN 0003-2670

ANALYTICA CHIMICA ACTA

International monthly devoted to all branches of analytical chemistry
Revue mensuelle internationale consacrée à tous les domaines de la chimie analytique
Internationale Monatsschrift für alle Gebiete der analytischen Chemie

ELSEVIER SCIENTIFIC PUBLISHING COMPANY

AMSTERDAM

Anal. Chim. Acta, Vol. 85, No. 1, 1–218, August 1976

Published monthly

ANALYTICA CHIMICA ACTA

Publication Schedule for 1976

Vol. 81, No. 1	January 1976	
Vol. 81, No. 2	February 1976	**(completing Vol. 81)**
Vol. 82, No. 1	March 1976	
Vol. 82, No. 2	April 1976	**(completing Vol. 82)**
Vol. 83	May 1976	**(complete in one issue)**
Vol. 84, No. 1	June 1976	
Vol. 84, No. 2	July 1976	**(completing Vol. 84)**
Vol. 85, No. 1	August 1976	
Vol. 85, No. 2	September 1976	**(completing Vol. 85)**
Vol. 86	October 1976	**(complete in one issue)**
Vol. 87, No. 1	November 1976	
Vol. 87, No. 2	December 1976	**(completing Vol. 87)**

Subscription price for 1976 (covering November '75/December '76, Vols. 80–87): Dfl. 840.00 plus Dfl. 96.00 postage. Subscribers in the U.S.A. and Canada receive their copies by airmail. Additional charges for airmail to other countries are available on request. For advertising rates apply to the publishers.

Subscriptions should be sent to:
Elsevier Scientific Publishing Company, P.O. Box 211, Amsterdam, The Netherlands.

GENERAL INFORMATION

Languages

Papers will be published in English, French or German.

Detailed information

Authors should consult Vol. 73, p. 435 for detailed instructions. Reprints of this information are obtainable from Dr. Macdonald or from: Elsevier Editorial Services Ltd., Mayfield House, 256 Banbury Road, Oxford (Great Britain)

Submission of papers

Papers should be sent to:

Prof. Philip W. West,
Coates Chemical Laboratories,
College of Chemistry and Physics,
Louisiana State University,
Baton Rouge 3,
La. 70803 (U.S.A.)

or to:

Dr. A.M.G. Macdonald,
Department of Chemistry,
The University,
P.O. Box 363,
Birmingham, B15 2TT (Great Britain)

Reprints

Fifty reprints will be supplied free of charge. Additional reprints (minimum 100) can be ordered at quoted prices. They must be ordered on order forms which are sent together with the proofs.

ANALYTICA CHIMICA ACTA
Vol. 85 (1976)

ANALYTICA CHIMICA ACTA

International monthly devoted to all branches of analytical chemistry
Revue mensuelle internationale consacrée à tous les domaines de la chimie analytique
Internationale Monatsschrift für alle Gebiete der analytischen Chemie

ELSEVIER SCIENTIFIC PUBLISHING COMPANY

AMSTERDAM

Anal. Chim. Acta, Vol. 85, (1976)

PRINTED IN THE NETHERLANDS

Analytica Chimica Acta, 85 (1976) 1—16

NEW NITRATE ION-SELECTIVE ELECTRODES BASED ON QUATERNARY AMMONIUM COMPOUNDS IN NONPOROUS POLYMER MEMBRANES

HANS JØRGEN NIELSEN* and ELO HARALD HANSEN

Chemistry Department A, The Technical University of Denmark, Building 207, DK-2800 Lyngby (Denmark)

(Received 26th February 1976)

SUMMARY

A new theory based on the concept of solubility parameters has been developed which has made it possible to establish additional rules for selecting the membrane constituents of liquid-exchanger ion-selective electrodes in order to obtain optimum electrode parameters. This theory has been used in developing nitrate-selective electrodes with various quaternary ammonium compounds in non-porous PVC-based membranes. These new nitrate electrodes are superior in stability and sensitivity to earlier electrodes. An explanation is offered as to which parameters are most significant in obtaining improved electrode characteristics.

Selective, precise and rapid measurements of nitrate are frequently required in many analytical problems. While determination of high contents of nitrate, e.g., in fertilizers, can be readily accomplished by colorimetry or even by gravimetry, the determination of trace amounts is difficult; yet, it is of vital importance in fertility and nitrate residue pollution studies.

With the advent, within the last decade, of nitrate ion-selective electrodes [1—7], one of the most promising tools for this purpose seemed to have emerged, since the use of electrodes is simple and fast as well as potentially suitable for continuous measurements. Unfortunately, the commercially available nitrate electrodes, e.g. from Orion [1] and Corning [2], have not come up to expectations. These electrodes may suffer from pronounced and erratic potential drifts (see, e.g. ref. 8), and are characterized by fairly poor sensitivity and gradual changes of sensitivy and selectivity. These drawbacks are partly due to the fact that the electrodes utilize porous membranes holding a water-immiscible mixture of ion-exchanger and solvent. This construction is disadvantageous from a mechanical viewpoint, because the organic liquid during operation must leak constantly into the aqueous sample solution, and because pressure and temperature fluctuations adversely influence the barrier formed by the organic liquid in the membrane pores.

*Present address: F. L. Smidth & Co. A/S, Vigerslev Allé 77, 2500 Valby, Denmark

One of the most significant contributions in the construction of liquid-exchanger ion-selective electrodes was the introduction of the non-porous PVC-membranes suggested by Moody et al. [9]. Cast to contain both liquid ion-exchanger and solvent, these polymer membranes not only improve and simplify the construction of electrodes, but as the ion-exchanger is stabilized within the polymer framework, better mechanical properties of the membranes and thus better electrode potential stabilities are obtained. PVC-membranes have also successfully been used by Růžička et al. [10], and Fiedler and Růžička [11] have outlined rules for preparing this type of membrane. It might therefore appear that stable nitrate electrodes could be made by embodying a commercial ion-exchanger into a suitable polymer matrix. However, Davies et al. [12] found that when the ion-exchanger materials used in the Orion and Corning nitrate electrodes were incorporated into PVC, no significant improvements of the operational parameters were obtained although the electrode lifetimes were prolonged. This is partly because both electroactive materials tested are too soluble in water, and partly because the solvents or plasticizers used are not compatible with the electroactive materials.

The stability of liquid-exchanger electrodes depends on how readily the electroactive material is dissolved in the aqueous sample phase [9—11, 13]. This solubility is closely related to the distribution ratio q of the electroactive material between the membrane and the aqueous phases as the electrode stability will improve with an increase in q. Additionally, as the limit of detection is a function of this distribution ratio, a combination of electroactive material and membrane material yielding as high a q-value as possible, should lead not only to improved electrode stability, but also to a decrease in the limit of detection, i.e. an extension of the dynamic measuring range.

In order to optimize the q-value, a detailed study of electroactive materials and plasticizers as well as membrane materials has been made. With quaternary ammonium compounds as the electroactive materials, and with the aid of computations based on solubility parameters, the applicability of the general approach is demonstrated for the development of new nitrate ion-selective electrodes, electrodes with much higher sensitivity and stability than those described previously.

THEORY

According to Small [14], the enthalpy of dissolution (ΔH) associated with the process of dissolving compound i in solvent j can be described by

$$\Delta H_{i,j} = V_i V_j (d_i - d_j)^2 \quad (1)$$

where V denotes the volume fraction in the resulting system and d is the solubility parameter. The solubility parameter can either be ascertained by solubility experiments in various organic solvents of different solubility parameters, or as suggested by Small [14], calculated from the expression

$d = (\rho \Sigma G)/M$, where ρ is the density of the material, $\Sigma\ G$ is the sum of the molar attraction constants of the structural units in the material, and M is its molecular weight.

Applied to the process of dissolving an electroactive material (e) in a membrane matrix (m), eqn. (1) can be written as

$$\Delta H_{e,m} = V_e V_m\ (d_e - d_m)^2 \tag{2}$$

while the corresponding process of dissolving the electroactive material in an aqueous phase (aq) is

$$\Delta H_{e,aq} = V_e V_{aq}\ (d_e - d_{aq})^2 \tag{3}$$

If the pure (solid) electroactive material is denoted by e(s), the reaction sequence

$$e(s) \rightarrow e_{aq} \rightarrow e_m \rightarrow e(s) \tag{4}$$

shows that ΔH for the process of transferring from the aqueous phase to the membrane phase a quantity of electroactive material equalling in the aqueous phase that of V_e in the membrane phase is given by

$$\Delta H_{aq,m} = \Delta H_{e,m} - \Delta H_{e,aq} \tag{5}$$

As the change in free energy, ΔG, is generally given by the expression $\Delta G = \Delta H - T\Delta S$ (where ΔS is the coupled change in entropy), ΔG for the process mentioned is therefore given by

$$\Delta G_{aq,m} = \Delta H_{e,m} - \Delta H_{e,aq} + T\,(\Delta S_{e,aq} - \Delta S_{e,m}) \tag{6}$$

If it is assumed that the statistical distribution or order is approximately identical in both liquid phases, i.e. $\Delta S_{e,m} \simeq \Delta S_{e,aq}$, and that the electroactive material (e) is present as a monomer in the membrane phase as well as in the aqueous phase, the distribution ratio of electroactive material between these two phases, $q = [e_m]/[e_{aq}]$, may therefore, by combining eqn. (6) with eqns. (2) and (3), be expressed as

$$\Delta G_{aq,m} = -RT \ln q = V_e V_m\ [(d_e - d_m)^2 - (d_e - d_{aq})^2] \tag{7}$$

i.e.,

$$q = \exp.\ (V_e V_m / RT[(d_e - d_{aq})^2 - (d_e - d_m)^2]) \tag{8}$$

The case where the electroactive material might also be present in other than the monomeric form, i.e. where the distribution ratio q is different from the partition coefficient K, has been discussed in detail by Růčička et al. [10].

Since the electrode parameters, i.e. limit of detection, selectivity and long-term stability, all are functions of q, and will improve with increasing value of q, eqn. (8) offers a guide as to how the individual membrane constituent should be selected in order to obtain electrodes with optimal characteristics.

EXPERIMENTAL

Reagents

Electroactive materials. Tetraheptylammonium iodide (THAI) and trioctylmethylammonium nitrate (TOMAN) were donated by Radiometer A/S, Copenhagen. Tetraoctylammonium bromide (TOAB) was synthesized as described by Hughes and Prices [15]. Tetradodecylammonium bromide (TDDAB) and tetratetradecylammonium bromide (TTDAB) were synthesized as outlined by Eriksen et al. [16]. The latter two compounds were purified by successive recrystallizations from saturated solutions of potassium hydroxide in ethanol. After each recrystallization the compound obtained was incorporated into a membrane matrix of dibutylphthalate—PVC, and the membrane was mounted on an electrode tube. After conditioning, potential—pH curves for the electrodes were recorded, and when the potentials at different pNO_3-values were nearly independent of pH, the recrystallizations were terminated. Additionally, the purities of the TOAB and TDDAB materials were verified by mass spectrometry.

Plasticizers (solvents). All plasticizers, which were a gift from Scandinol, Copenhagen, were of technical grade.

Polymers. Polyvinylchloride (PVC; Breon 113; B.P. Chemicals Ltd), and polyurethane (Estane; B.F. Goodrich Chemical Company) were used.

Calibration solutions

Calibration solutions for nitrate cannot be prepared by means of ion buffer solutions; dilutions of standard potassium nitrate solutions were therefore used. The solutions were not adjusted to identical ionic strength (I), and all concentrations were converted to activities by means of the expression: $\log f = -0.511\ [\sqrt{I}/(1 + \sqrt{I})]$, where f is the activity coefficient ($z_{NO_3} = -1$).

Membrane and electrode preparation

The membranes were prepared by dissolving 75 mg of PVC, 180 mg of plasticizer and an appropriate amount of electroactive material (see Results) in 5 ml of tetrahydrofuran (A.R.-grade) [11]. This solution was poured into a 26-mm i.d. glass ring resting on a glass plate, followed by slow evaporation of the solvent. From this membrane (0.3-mm thick) a 6-mm diameter disc was cut with a cork borer. The disc was glued with a solution of 4 % (w/w) PVC in tetrahydrofuran to a PVC tube of the type used for the Radiometer calcium Selectrode. The inner reference electrode was identical to that used in the Radiometer Selectrode (Ag/AgCl, Type F 2002) while the inner reference solution consisted of 0.01 M NaCl and 0.01 M $NaNO_3$.

For pH checks and recordings a glass electrode (Radiometer G 202 B) and a reference calomel electrode (Radiometer K 401) were used.

Apparatus

All potential measurements were done with a digital pH meter (Radiometer PHM 52) accurate to within ± 0.1 mV. For automatic potential — pH measurements, an automatic scanning potentiometer, an autoburette ABU 13, two pH meters (Radiometer PHM 51) and an X-Y recorder (Watanabe) were used.

Measurement techniques

pNO_3 response. After mounting, each electrode was conditioned for 24 h in a 0.1 M KNO_3 solution, whereupon the electrode was ready for use. This conditioning was necessary in order to replace the iodide or bromide in the membrane with nitrate. Accordingly, all the electroactive materials are denoted with a suffix N in the subsequent discussion. After conditioning, the potentials (against a saturated calomel electrode, SCE) were measured in separate standard calibration solutions during constant stirring.

Selectivity coefficients. These were measured by the fixed interference method [17] where the concentration of the interfering ion in all instances was fixed at 0.01 M.

Potential—pH curves. These were recorded automatically at a speed of one pH unit per 2 min. The scanning always started at pH 3 and was done by automated addition of sodium hydroxide. Potential values below pH 3 and above pH 10 were obtained manually, point-wise.

Computations

All slopes were calculated by means of regression analysis on the linear part of the calibration curves. The E^0 values were obtained by extrapolation to $pNO_3 = 2.06$, and the intercept between a calibration curve and the lower limit of detection determined the selectivity coefficient in the solution used. Selectivity coefficients $k_{NO_3,X}$, are expressed as $pk_{NO_3,X} = -\log k_{NO_3,X}$.

RESULTS

The properties of electrodes containing tetraoctylammonium nitrate and tetradodecylammonium nitrate as electroactive materials in non-porous polymer membranes are described in detail; electrodes applying other quaternary ammonium compounds are briefly mentioned. Each membrane was tested in the following cell

$$Ag|AgCl|Cl^- \ (0.01M),\ NO_3^- \ (0.01M)|Membrane|Sample\ ..||KCl\ (sat.)\ |Hg_2Cl_2|Hg$$

The behaviour of the electrodes was judged, in the usual manner, by the extent to which the cell e.m.f. agreed with the value predicted by the extended Nernst equation

$$E = E^0 - \frac{2.303\,RT}{F} \log (a_{NO_3^-} + k_{NO_3,X} \cdot a_X^{1/z_X}) \quad (9)$$

where the symbols have their usual meaning. As pNO_3 in the internal reference solution was 2.06, the theoretical value of E^0 of the cell at 20 °C is thus

$$E^0 = E^0_{Ag/AgCl} + \frac{59.15 \cdot 293}{298}(2.06) - E_{SCE} = 96 \text{ mV}$$

In practice, the E^0-value of each cell was determined by extrapolating to $pNO_3 = 2.06$ on the calibration curves.

Electrodes containing tetraoctylammonium nitrate

The solubility parameter of the tetraoctylammonium nitrate (TOAN) determined by solubility experiments and by calculations as outlined under Experimental, was 9.7 ± 0.5 $(cal/cm^3)^{\frac{1}{2}}$. In order to evaluate the optimal membrane constitution, i.e. the kind of plasticizer and quantity of TOAN, a series of membranes containing 7 % (w/w) of TOAN, which corresponded to the maximum solubility of TOAN in the membrane matrix, dissolved in plasticized PVC (and in one instance polyurethane), was prepared, with solvents of different solubility parameters. The solubility parameters of the resulting membranes were calculated from

$$d_m = w_{PVC} \cdot d_{PVC} + w_{solv.} \cdot d_{solv.} \quad (10)$$

where w refers to weight per cent and d is the solubility parameter.

After mounting and conditioning, each electrode was calibrated in a series of nitrate standard solutions covering the range $10^{-1} - 10^{-6}$ M. The composition and parameters for each electrode are shown in Table 1. On the basis of these experiments, the electrode based on a dibutylphthalate—PVC membrane was selected for further investigation. This electrode showed an E^0-value of 94 mV, and thus an asymmetry potential of ca. 2 mV, and an almost Nernstian slope of 56.5 mV/decade.

The TOAN was then incorporated in different weight ratios in dibutylphthalate—PVC membranes, and the resulting electrodes were calibrated. The results (Table 1) proved that the optimal membrane composition with TOAN as electroactive material was (w/w): 29 % PVC, 65 % dibutylphthalate (DBP), and 6—7 % TOAN. A typical calibration curve for an electrode based on this membrane composition is shown in Fig. 1; the response time was a few seconds or less, irrespective of the magnitude of the concentration changes.

The long-term stability of this electrode was tested over a period of 8 weeks; at weekly intervals, the electrode was calibrated in $10^{-1} - 10^{-6}$ M nitrate standard solutions, being stored between measurements in 10^{-1} M sodium nitrate solution. Over the 8-week period the electrode showed an average E^0-value of 94.34 mV with a standard deviation of 0.22 mV, and a slope of 56.90 ± 0.12 mV/decade; the limit of detection remained constant at pNO_3 5.25, the linear detection limit being pNO_3 4.8.

TABLE 1

Nitrate-selective electrodes incorporating tetraoctylammonium nitrate as electroactive material

Polymer and content[a] %	Solvent[b]	d_m $(cal/cm^3)^{\frac{1}{2}}$	% TOAN	E^o (mV)	Slope (mV/pNO_3)	Limit of detection (pNO_3)
29 PVC	DIDP	7.8	7	72	56.1	5.25
29 PVC	DOP	8.2	7	77	56.1	5.25
29 PVC	DBP	9.3	7	94	56.5	5.27
29 PVC	DEP	9.9	7	99	56.5	5.28
80 PU	DEP	10.0	7	99	56.5	5.28
29 PVC	DBP	9.3	1	120	52	3.55
29 PVC	DBP	9.3	2	103	54	3.85
29 PVC	DBP	9.3	3	99	54	4.15
29 PVC	DBP	9.3	6	95	56.1	5.25

[a]PVC = polyvinylchloride. PU = polyurethane.
[b]DIDP = diisodecylphthalate. DOP = dioctylphthalate. DBP = dibutylphthalate. DEP = diethylphthalate.

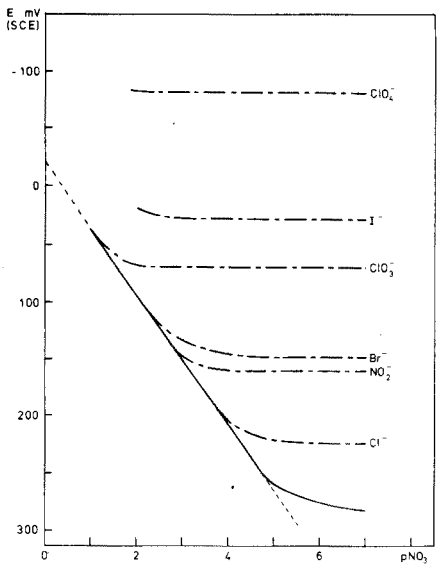

Fig. 1. Calibration curve and selectivity parameters for the tetraoctylammonium nitrate—dibutylphthalate—PVC membrane electrode. The concentration of all interfering anions is 10^{-2} M.

The selectivity coefficients, $k_{NO_3,X}$, for a series of anions are shown in Fig. 1 and in Table 2. To ascertain whether cations interfered, aqueous 10^{-3} M solutions of the nitrate salts of the following cations were prepared: NH_4^+, Na^+, K^+, Ag^+, Mg^{2+}, Ca^{2+} and Cu^{2+}. None of these ions interfered; in all cases the electrode potential deviated less than 1 mV from the theoretical value. Mercury(II) chloride, however, exerted some interference; in trace amounts, it affected the electrode potential even in 10^{-1} M sodium nitrate solutions.

In order to check the pH-dependence of the potential of the TOAN-containing electrode, potential—pH curves at various nitrate concentrations were recorded. The plots (Fig. 2) show that between pH 4 and 9 the potential is independent of pH. During the 8 weeks of testing, no discernible change in the potential/pH behaviour was observed.

Electrodes containing tetradodecylammonium nitrate

The solubility parameter of tetradodecylammonium nitrate (TDDAN) was found to be 9.5 ± 0.5 $(cal/cm^3)^{\frac{1}{2}}$.

In order to determine the optimal combination of electroactive material and PVC-solvent, experiments similar to those described for the TOAN material were executed. Table 3 shows the operational parameters of three 4 % (w/w) TDDAN-containing membranes of different solubility parameters. Again dibutylphthalate (DBP) was found to be the best solvent. In further experiments, TDDAN was dissolved in different weight ratios in dibutyl-phthalate—PVC membranes, with the results shown in Table 3. These experiments proved that the optimal membrane constitution was (w/w): 29 % PVC, 67 % DBP and 4 % TDDAN. The calibration curve for an electrode based on this membrane is shown in Fig. 3.

Except for exhibiting a lower limit of detection ($pNO_3 = 6.1$), the electrode based on the TDDAN—DBP—PVC membrane expectedly showed characteristics

TABLE 2

Selectivity coefficients of tetraoctyl- (TOAN) and tetradodecyl-ammonium nitrate (TDDAN)-based electrodes, measured by the fixed interference method (All selectivity coefficients expressed as $-\log k_{NO_3,X} = pk_{NO_3,X}$)

Interfering anion (10^{-2} M)	TOAN	TDDAN
ClO_4^-	−3.10	—
I^-	−1.15	--
ClO_3^-	−0.48	—
Br^-	0.89	—
NO_2^-	1.15	1.15
Cl^-	2.30	2.30
F^-		3.00
Ac^-, SO_4^{2-}		
$H_2PO_4^-$, HPO_4^{2-}, HCO_3^-	> 3.00	> 3.30

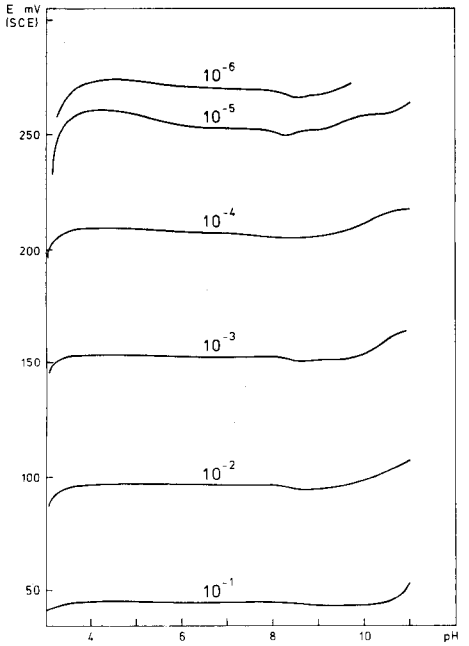

Fig. 2. Potential– pH diagram for the tetraoctylammonium nitrate—dibutylphthalate–PVC membrane electrode in 10^{-1} — 10^{-6} M potassium nitrate solutions.

TABLE 3

Nitrate-selective electrodes incorporating various quaternary ammonium compounds as electroactive materials in membranes containing 29 % PVC

Solvent[a]	Active material[b]	d_m $(cal/cm^3)^{\frac{1}{2}}$	Concn. of active material (%)	E^0 (mV)	Slope (mV/pNO_3)	Limit of detection (pNO_3)
DIDP	TDDAN	7.8	4	89	54.0	5.60
DOP	TDDAN	8.2	4	88	56.0	5.60
DBP	TDDAN	9.3	4	98	56.2	6.08
DBP	TDDAN	9.3	2	70	56.0	5.20
DBP	TDDAN	9.3	3	85	56.0	5.70
DBP	TDDAN	9.3	7	102	56.2	6.10
DBP	TOMAN	9.3	7	88	54.2	4.60
DBP	THAN	9.3	7	85	55.6	4.70
DBP	TTDAN	9.3	4	99	58.8	5.70

[a] For abbreviations, see Table 1.
[b] TDDAN = tetradodecylammonium nitrate. TOMAN = trioctylmethylammonium nitrate. THAN = tetraheptylammonium nitrate. TTDAN = tetratetradecylammonium nitrate.

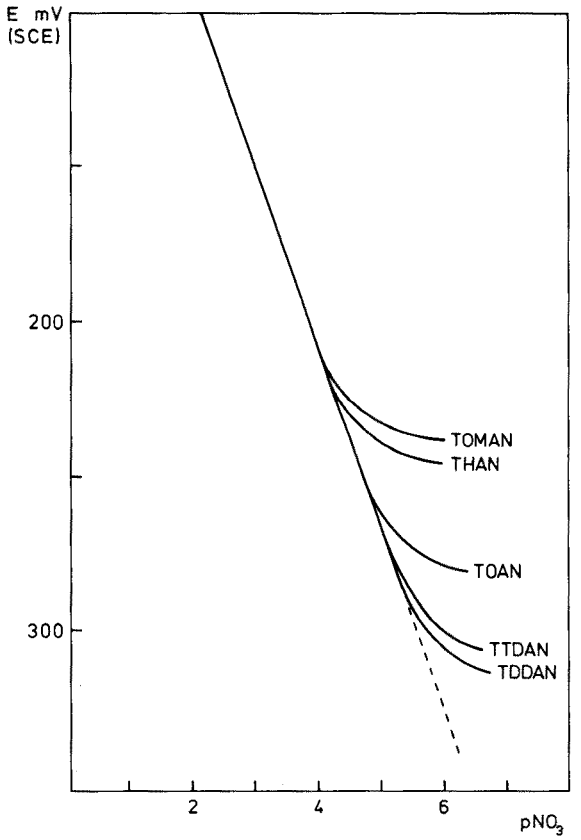

Fig. 3. Calibration curves for electrodes incorporating trioctylmethyl- (TOMAN), tetraheptyl- (THAN), tetraoctyl- (TOAN), tetratetradecyl- (TTDAN) and tetradodecylammonium nitrate (TDDAN), respectively, as electroactive material, all in dibutylphthalate—PVC-based membranes. For the sake of comparison, all electrodes are adjusted to the same E°-value.

very similar to those reported above for the TOAN—DBP—PVC membrane electrode, i.e., rapid response, long-term potential stability (as tested over 4 weeks), almost identical selectivity parameters (Table 2), and no potential/pH dependency within the pH-range 4—9 (cf. Fig. 5).

Electrodes containing other quaternary ammonium nitrate compounds

Three other quaternary ammonium nitrate compounds, tetratetradecylammonium nitrate (TTDAN), trioctylmethylammonium nitrate (TOMAN) and tetraheptylammonium nitrate (THAN), were incorporated into dibutylphthalate—PVC membranes. The constitution of the membranes in all cases was (w/w): 29 % PVC, 64 % DBP, and 7 % electroactive material, except for the TTDAN where only 4 % of quaternary ammonium nitrate was used. The

electrode parameters are shown in Table 3, and the corresponding calibration curves are reproduced in Fig. 3. Despite repeated recrystallization efforts it was, unfortunately, as judged by a potential—pH diagram, impossible to obtain the TTDAN entirely pure. Thus, it can be seen that the limit of detection of the TTDAN electrode, contrary to expectations, is slightly poorer than that obtained with the TDDAN electrode.

Preliminary applications

To check the practical potentials of these new sensors, the TOAN—DBP—PVC membrane electrode was used to determine the nitrate content in a series of waste-water samples and four soil extracts. The waste-water samples, collected by the Department of Sanitary Engineering of this University and analyzed there by the AutoAnalyzer brucine-method, were measured without any pretreatment and the equilibrium potentials obtained were evaluated by means of the calibration curve. The results are shown in Table 4.

The soil extracts, prepared by the State Laboratory for Soil and Crop Research, Lyngby (SLSCR) by extraction of soil samples with 0.022M acetic acid, were analyzed in the same manner, with a calibration curve of nitrate standard solutions in dilute acetic acid, and by the standard addition method. The results are shown in Table 5 where the results obtained by the SLSCR with an Orion nitrate electrode are also given.

Further applications of these new nitrate electrodes, including incorporation in the recently developed Flow Injection Analyzer system [18], are currently being investigated.

DISCUSSION

The results with the quaternary ammonium nitrate-based electrodes described here, together with experiments on valinomycin-based potassium [11] and organophosphate-based calcium electrodes [10], confirm the

TABLE 4

Determination of nitrate in waste-water samples with the tetraoctylammonium nitrate—dibutylphthalate—PVC membrane electrode

Sample No.	p.p.m. $N—NO_3^-$ found		Sample No.	p.p.m. $N—NO_3^-$ found	
	AutoAnal.[a]	Electrode		AutoAnal.[a]	Electrode
1	9.5	9.8	6	29.5	30.6
2	4.0	4.1	7	21.0	21.7
3	8.0	7.8	8	11.3	11.0
4	1.5[b]	2.4	9	3.0	1.9
5	6.5	7.0			

[a]By the brucine method (± 1 p.p.m.)
[b]Containing 0.29 p.p.m. $N—NO_2^-$.

TABLE 5

Determination of nitrate in soil extracts with the tetratoctylammonium nitrate—dibutylphthalate—PVC membrane electrode

Soil sample	Nitrate content (p.p.m.-NO_3^-)		
	Eq. detn.	Stand. addn.	SLSCR[a]
1	6	6	6
2	26	28	25
3	121	117	118
4	84	82	78

[a]Orion nitrate electrode, calibrated every 15 min.

superiority of polymer non-porous membranes. As the operational parameters of a membrane electrode are a function of the distribution ratio q of electroactive material between the membrane and aqueous phases [9, 13], the optimization of q according to eqn. (8) requires that:

1. the solubility parameter of the electroactive material should be as low as possible;

2. the difference between the solubility parameters of the electroactive material and the membrane material should be as small as possible, ideally zero;

3. as much electroactive material as possible — and ideally so much that the volume fractions V_e and V_m are identical — should be incorporated into the membrane.

In order to attain the lowest possible limit of detection, the first rule simply requires that since the solubility parameter of water is constant (d_{aq} = 23.4 $(cal/cm^3)^{\frac{1}{2}}$), the electroactive material must be as organic as possible. In Fig. 3, which shows the calibration curves for nitrate electrodes incorporating trioctylmethyl- (TOMAN), tetraheptyl- (THAN), tetraoctyl- (TOAN), tetradodecyl- (TDDAN) and tetratetradecyl-ammonium nitrate (TTDAN) as electroactive materials, it can indeed by seen that the sensitivity of the electrodes improves with increasing organic properties of the quaternary ammonium nitrate compounds. The reversal of the sequence for TDDAN and TTDAN is due to impurities in the latter compound. Although the solubility parameter of quaternary ammonium compounds, R_4N^+, decreases with increasing chain length of R, the gradual changes at longer chain lengths are so small that the solubility parameter remains almost constant at ca. 9.5 $(cal/cm^3)^{\frac{1}{2}}$ provided that each chain contains at least 7 carbon atoms. The apparent paradox that the limit of detection is lowered by increasing the carbon-chain length above 7, whether V_e is kept constant or even decreased, is simply due to the increase in the molecular weight of the quaternary ammonium compound, as ln q (eqn. 7) will increase with increasing molecular weight.

Thus (symmetrical) quaternary ammonium compounds with sufficiently

long carbon-chains, should theoretically provide nitrate electrodes of higher sensitivity. At longer chain lengths, however, the selectivity parameters remain almost constant (cf. Table 2), so that in practice very little is gained by using substituents with chain lengths exceeding 12—14 carbon atoms. Besides, the synthesis and purification of the higher quaternary ammonium compounds becomes disproportionately more difficult with increasing chain lengths (the TTDAN-compound).

The second rule requires that the plasticized membrane material should possess a solubility parameter equal to that of the electroactive material, i.e. ca. 9.5 $(cal/cm^3)^{\frac{1}{2}}$. Equation (7) shows, however, that even a difference of 1.5 $(cal/cm^3)^{\frac{1}{2}}$ between d_e and d_m will result in change in ln q of only a few per cent. Therefore, approximately similar limits of detection would be expected for electrodes based on identical electroactive materials dissolved in different solvents. That this is true can be seen from Tables 1 and 3.

The asymmetry potential, however, increases significantly with increasing numerical difference between the solubility parameters of the electroactive material and the membrane matrix, as can be seen from Fig. 4, which shows the measured E^0-values of 7 %-TOAN-based electrodes as a function of their d_m-values. The difference $E^0_{theor.} - E^0_{meas.}$ is positive for $d_e < d_m$, negative for $d_e > d_m$, and zero for $d_e = d_m$. The asymmetry potential seems therefore to constitute a measure of the compatibility of the electroactive material and the membrane material, i.e. of their solubility parameters. Conversely, if an electrode exhibits an asymmetry potential, its sign and magnitude will indicate in which direction the solubility parameters and thus the constitution of the membrane material should be altered in order to obtain a zero asymmetry potential.

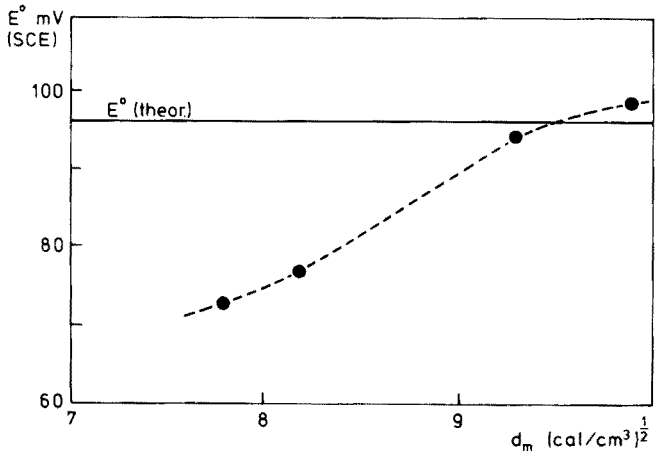

Fig. 4. The E^0-value of electrodes based on tetraoctylammonium nitrate (7 %), dissolved in PVC-membranes incorporating various solvents, as a function of the solubility parameter of the membrane, d_m.

From the theory of glass electrodes, it is known that these electrodes yield optimal operational parameters when the ion-exchanging gel-sites and the polymeric silica back-bone material dissolve into the aqueous phase at identical rates. Similarly, it may be assumed that the best electrode characteristics of liquid-exchanger electrodes are obtained when the membrane material and the electroactive material have identical solubility in water, i.e., when the solubility parameter of the membrane material is adjusted to that of the electroactive material.

It has long been recognized that a drift in the E^0-value is closely associated with the dissolution of electroactive material from the membrane phase. Hence, if it is assumed that the asymmetry potential is a function of the homogeneity across the ion-exchanging membrane, it can readily be understood why a zero asymmetry potential is beneficial in obtaining high electrode stability. While an equilibrium is established eventually at the interface between the membrane and the inner reference solution of the electrode, materials will normally be dissolved continuously from the membrane at the membrane-sample solution boundary, because the collective volumes of sample solutions within the electrode lifetime are larger by many orders of magnitude than that of the inner reference solution.

If $d_e < d_m$, the membrane material will dissolve more readily than the electroactive material, with which the outer surface of the membrane thus becomes enriched. This inhomogeneity will cause a change in the asymmetry potential, which will be registered as a drift in the E^0-value of the electrode. If $d_e > d_m$, the membrane material will dissolve to a lesser extent than the electroactive material, and there will be a similar drift in the E^0-value, but in the opposite direction, In both cases, however, the drift in E^0 will increase the numerical value of the asymmetry potential. If $d_e = d_m$, the constitution of the membrane will remain constant despite the dissolution process, and the homogeneity of the membrane and thus a stable value of E^0 are ensured.

It was found previously that both the potassium electrode and the calcium electrode described by Růžička et al. [10, 11] exhibited maximum stability when the asymmetry potential was zero, thus sustaining the results discussed above.

The third rule requires that the plasticized membrane should dissolve as much of the electroactive material as possible, and ideally so much that V_e becomes equal to V_m. At low concentrations of electroactive material, V_m in eqn. (8) may be approximated to unity, and it is seen that the limit of detection decreases when V_e is increased. At higher concentrations, however, the membrane becomes saturated with electroactive material, and no further decrease in the limit of detection with increasing V_e can be expected. Theoretically, it can be shown that the solubility of quaternary ammonium compounds decreases with increasing carbon-chain lengths of the substituents. Experimentally, it was found that the saturation concentration of tetraoctylammonium nitrate in dibutylphthalate—PVC membranes was ca. 6 % while that of the tetradodecylammonium nitrate in a similar membrane matrix was ca. 4 %.

Finally, an apparent discrepancy between the results reported here and those obtained by Davies et al. [12] with the Corning nitrate electrode should be mentioned. In the Corning electrode, tridodecylhexadecylammonium nitrate is the electroactive material. It would be expected that this electrode and the tetradodecylammonium nitrate-containing electrode described here should behave rather similarly. However, the limit of detection of the Corning electrode is almost one decade poorer than that of the TDDAN–DBP–PVC-based electrode, and this difference cannot be due to the membrane material. An explanation may be found by comparing the potential–pH diagram of the Corning electrode [12] with those of the TDDAN-based electrode recorded during purification of the TDDAN (Fig. 5). Comparison indicates that the Corning material has not been successfully purified, for the potential–pH diagram [12] is very similar to that recorded for the partly purified TDDAN material (Fig. 5a). In addition to the tridodecylhexadecylammonium nitrate, the Corning material probably contains some tridodecylhydrogenammonium nitrate which will make the electrode strongly pH-dependent. Combined with an improper choice of membrane material so that $d_e \neq d_m$, this will lead to a further drift in the E^0-value of the electrode.

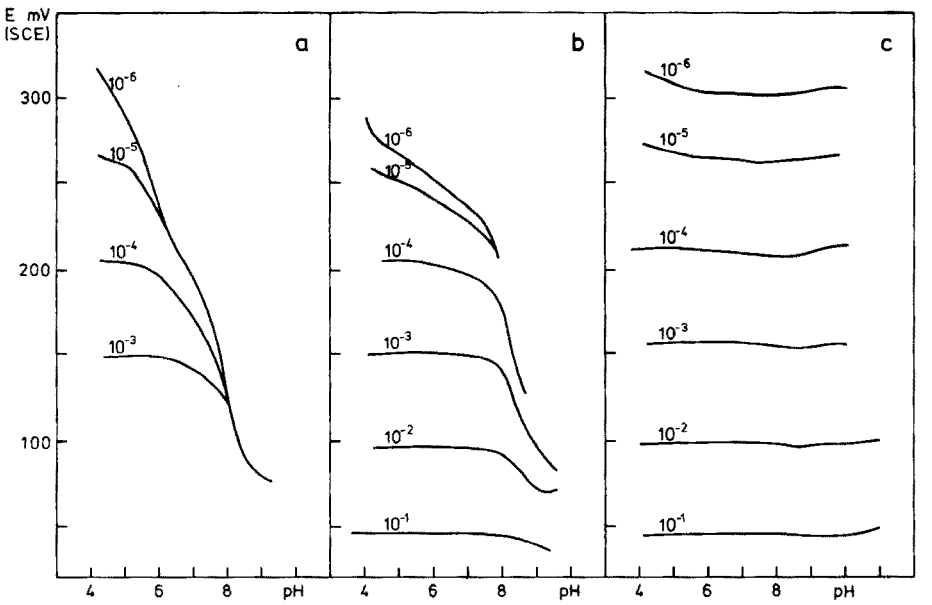

Fig. 5. Potential–pH diagrams of electrodes incorporating tetradodecylammonium nitrate (TDDAN) as electroactive material in dibutylphthalate–PVC-based membranes. (a) Unpurified TDDAN; (b) after 1 recrystallization procedure; (c) after 2 recrystallizations.

CONCLUSION

Based on the concept of solubility parameters, a new theory has been developed which has made it possible to establish additional rules for selecting the membrane constituents of liquid-exchanger ion-selective electrodes with optimum electrode parameters. To test the theory and in order to develop new nitrate-selective electrodes, a series of symmetrical quaternary ammonium compounds have been synthesized and purified, and have been used as electroactive materials in various non-porous PVC-membrane electrodes.

On the basis of these investigations, a simple explanation is offered as to which parameters are the most significant, and new nitrate electrodes have been developed [19] which are superior with respect to stability and sensitivity to any nitrate electrodes described previously. This in itself demonstrates the usefulness of the concept of solubility parameters in developing new ion-selective electrodes.

The authors express their sincere thanks to Dr. J. Růžička for critical comments and valuable discussions. This work was carried out in part under Research Agreement No. 1590/CF with the International Atomic Energy Agency, Vienna, Austria, in the coordinated programme on agricultural nitrogen residues with particular reference to their conservation as fertilizers and behaviour as potential pollutants.

REFERENCES

1 British Patent No. 1.197.264 (1968).
2 U.S. Patent No. 3.671.413 (1972).
3 G.J. Moody and J. D. R. Thomas, Selective Ion Sensitive Electrodes, Merrow, Watford, 1971, p. 22.
4 A. V. Gordievskii, V. S. Shterman, A. Ya. Syrchenkov, N. I. Savvin and A. F. Zhurkov, Zh. Anal. Khim., 27 (1972) 772.
5 A. V. Gordievskii, A. Ya. Syrchenkov, V. V. Sergievskii and N. I. Savvin, Elektrokhimiya, 8 (1972) 520.
6 A. L. Grekovich, E. A. Materova and V. E. Yurinskaya, Zh. Anal. Khim., 27 (1972) 1218.
7 A. L. Grekovich, E. A. Materova and G. I. Shchekina, Elektrokhimiya, 10 (1974) 342.
8 M. K. Mahendrappa, Soil. Sci., 108 (1969) 132.
9 G. J. Moody, R. B. Oke and J. D. R. Thomas, Analyst (London), 95 (1970) 910.
10 J. Růžička, E. H. Hansen and J. Chr. Tjell, Anal. Chim. Acta, 67 (1973) 155.
11 U. Fiedler and J. Růžička, Anal. Chim. Acta, 67 (1973) 179.
12 J. E. W. Davies, G. J. Moody and J. D. R. Thomas, Analyst (London), 97 (1972) 87.
13 G. H. Griffith, G. J. Moody and J. D. R. Thomas, Analyst (London), 97 (1972) 420.
14 P. A. Small, J. Appl. Chem., 3 (1953) 71.
15 S. R. C. Hughes and D. H. Prices, J. Chem. Soc., A (1967) 1093.
16 S. P. Eriksen, L. D. Tuck and J. F. Oneto, J. Org. Chem., 25 (1960) 849.
17 IUPAC. Inform. Bull., Appendices on Provisional Nomenclature, Symbols, Units and Standards, No. 43., Jan. 1975.
18 J. Růžička and E. H. Hansen, Anal. Chim. Acta, 78 (1975) 145.
19 H. J. Nielsen and E. H. Hansen, Dan. Pat. Appl. No. 5217/75, Nov. 1975.

Analytica Chimica Acta, 85 (1976) 17—30

STUDIES OF SOLID-STATE ION-SELECTIVE ELECTRODES PREPARED FROM SEMICONDUCTING ORGANIC RADICAL-ION SALTS

MICHAEL SHARP

Department of Analytical Chemistry, University of Umeå, S-901 87 Umeå (Sweden)

(Received 23rd February 1976)

SUMMARY

The primary redox reactions for solid-state ion-selective electrodes prepared from electronically semiconducting salts of 7,7,8,8-tetracyanoquinodimethane (tcnq) can be identified by considering the redox properties of their constituent ions or molecules. Three different processes involving the couples, M^{n+}/M^0, 2 $tcnq^0/(tcnq^{\cdot-})_2$ and $(tcnq^{\cdot-})_2/2\ tcnq^{2-}$ are possible depending on salt composition. Ionic product values determined by potentiometric and atomic absorption methods are in excellent agreement for several such salts; $K_s(K_2tcnq_2) = 5.8 \pm 1.2 \cdot 10^{-11}$ (pot.), $1.7 \pm 1 \cdot 10^{-11}$ (a.a.s.); $K_s(Cdtcnq_2) = 3.0 \pm 0.5 \cdot 10^{-9}$ (pot.), $2.9 \pm 0.3 \cdot 10^{-9}$ (a.a.s.); $K_s(Pbtcnq_2) = 1.3 \pm 0.3 \cdot 10^{-10}$ (pot.), $0.96 \pm 0.2 \cdot 10^{-10}$ (a.a.s.); and indicate that the lower activity limit for electrode response is controlled by the solubility of the sensor material itself. Comparisons of predicted and observed standard electrode potentials provide quantitative support for an ion-exchange mechanism of interference. The behaviour of electrodes prepared from Cu_2tcnq_2 (copper(I)) and $Cutcnq_2$ (copper(II)) is explained on the basis of an interference mechanism and considerations of solid-state equilibria.

Sparingly soluble salts prepared from certain organic radical-ion species can be employed as the electroactive components of solid-state ion-selective electrodes. In contrast to most of the inorganic compounds which are similarly used, these materials are electronic rather than ionic semiconductors. Anion-selective as well as cation-selective sensors have been constructed and their general properties have been reported [1—4]. A detailed discussion of electrode behaviour has not previously been given, however, although it was suggested at an early stage that radical-ion salt electrodes showed characteristics which largely conformed with those of electrodes of the second kind [1, 5]. This implies that electrode function is governed by a primary potential-determining redox process which is coupled to a solubility equilibrium. Definite evidence for such a mechanism was not put forward. A closer examination of electrode behaviour has recently been carried out in an attempt to define the functional mechanism more precisely. For this purpose the salts of the 7,7,8,8-tetracyanoquinodimethane radical-anion ($tcnq^{\cdot-}$) were chosen as a representative series of cation-selective materials. Details of synthetic methods, of solid-state properties, and of some aspects of solution

chemistry have been reported for tcnq and its salts [6]. From a consideration of the standard redox potentials relevant to a given salt composition, it was possible to derive a model for electrode function. Its validity was then assessed by comparing predicted and observed electrode characteristics, particularly standard electrode potentials. The results obtained are considered to be significant for establishing the mechanisms not only of other electrodes of similar type but of solid-state electrodes in general.

EXPERIMENTAL

Materials

Commercially available tcnq (Eastman Organic Chemicals) was recrystallized from dry tetrahydrofuran. The dry, yellow crystals melted sharply at 295 °C (lit. m.p. 293.6—296 °C).

The lithium salt of $tcnq^-$ was prepared by reacting lithium iodide with tcnq in hot, anhydrous acetonitrile. The Li_2tcnq_2 so obtained was then used to prepare the salts, Ag_2tcnq_2, $Cutcnq_2$, $Pbtcnq_2$, $Cdtcnq_2$, K_2tcnq_2, Na_2tcnq_2 and $(Et_4N)_2tcnq_2$ by metathesis in aqueous solution. The various products were isolated as sparingly soluble precipitates which were subsequently filtered off, washed and dried.

Copper(I) tcnq, Cu_2tcnq_2, was prepared by reacting copper(I) iodide with tcnq in hot, dry acetonitrile. The product precipitated as blue-black crystals. After filtration, the solid was washed with acetonitrile and dried.

The complex salt, $(Et_4N)_2tcnq_4$, was obtained from the reaction between Et_4NI and tcnq in hot acetonitrile. The black, crystalline precipitate was filtered off, washed with acetonitrile and dried.

Potentiometric measurements

Cell potentials for the system i.s.e. | sample solution (aq.) | reference electrode were measured at 25 °C with an Orion Model 701 digital pH-meter. The reference was either an SCE (Radiometer K 401) or an Ag—AgCl electrode. The ion-selective electrodes (i.s.e.) were prepared by the 'Selectrode' technique [7] which consists of the manual application of small amounts of a given electroactive substance to a graphite—teflon conducting surface. 'Selectrode' bodies were obtained commercially (Radiometer F 3012).

Response curves for the different electrodes were established from measurements with aqueous solutions of a single salt. In the case of Li_2tcnq_2, the solutions were deaerated and held under a nitrogen atmosphere. Corresponding standard potential values were obtained with a precision of approximately ±1 mV by extrapolating these E_i (cell) vs. log a_i plots to unit activity of the ion, i, concerned. Ionic concentrations were converted to activities with the aid of alignment charts based on the Davies equation [8].

Voltammetric measurements

Cyclic voltammetric measurements were carried out at 25 °C with an Amel Model 551/SU potentiostat connected to a Moseley 7030 AM X-Y recorder

at a scan-rate of 2 V min^{-1}. A three-electrode system comprising working (WIGE or Pt), reference (SCE) and counter (Pt) electrodes was employed. Wax-impregnated graphite working electrodes (WIGE) were prepared by immersing spectroscopic-grade graphite rods in molten ceresin wax under vacuum. The electrode body was insulated with a tight fitting teflon sleeve. Platinum working electrodes were pretreated with dichromate—sulphuric acid cleaning mixture for several min, dipped into hot 12 M HCl for 1—2 min and finally rinsed with distilled water. Measurements were made in deaerated, aqueous solutions of Li_2tcnq_2 under a nitrogen atmosphere. The supporting electrolyte was 0.1 M $LiClO_4$ and the stoichiometric concentration of $tcnq^{\cdot-}$ approximately $2 \cdot 10^{-3}$ M.

Atomic absorption measurements

Determinations of the lead, cadmium, and potassium concentrations in saturated aqueous solutions of their respective $tcnq^{\cdot-}$ salts were made with a Varian Techtron AA6 atomic absorption spectrophotometer.

RESULTS AND DISCUSSION

Table 1 shows a comparison between the standard electrode potentials for the cation response of electrodes prepared from several different metal—tcnq salts and the standard reduction potentials of the corresponding cation. (Since magnetic susceptibility and crystallographic data indicate dimerization of the $tcnq^{\cdot-}$ radical-anion species in the solid-state the formulae of these salts are written in terms of $(tcnq^{\cdot-})_2$ as the basic anionic unit [9]). Only in the case of Ag_2tcnq_2 does the agreement between these values clearly indicate that the redox process underlying electrode function involves the cationic component of the salt. In the remaining cases, the wide discrepancies point to more complicated behaviour. As the first stage in elucidating the mechanisms of these electrodes, it was considered necessary to examine the redox

TABLE 1

Comparison between standard electrode potentials for metal ion/metal tcnq salts and corresponding metal ion/metal systems

Electroactive substance	$E^0_{M^{n+}/M_{2/n}(tcnq)_2}$ (mV vs NHE)	$E^0_{M^{n+}/M^0}$ (mV vs NHE)
Ag_2tcnq_2	799	799
Cu_2tcnq_2	665 (Cu^{2+})	337
$Cutcnq_2$	667 (Cu^{2+})	337
$Pbtcnq_2$	404	−126
$Cdtcnq_2$	363	−403
K_2tcnq_2	414	−2952
Na_2tcnq_2	474	−2714

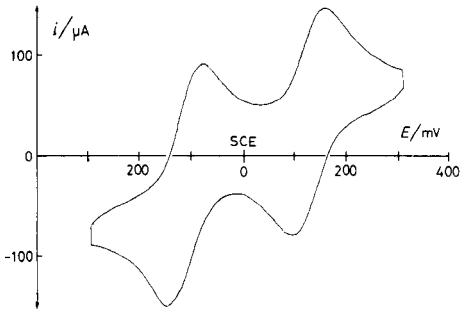

Fig. 1. Cyclic voltammetric curves for the $tcnq^0/(tcnq^{\cdot-})_2/tcnq^{2-}$ system obtained in aqueous solution with a Pt electrode at 25 °C and a scan-rate of 0.067 V s^{-1}.

properties of the anionic component of the salt, i.e., $(tcnq^{\cdot-})_2$, in aqueous media. Figure 1 shows a cyclic voltammogram obtained with a bright platinum electrode in an aqueous solution of Li_2tcnq_2 with a supporting electrolyte of 0.1 M $LiClO_4$. Peaks corresponding to two essentially reversible one-electron processes were observed. These were assigned to reduction of neutral tcnq to its radical-anion, followed, at more cathodic potentials, by reduction of the radical-anion to the corresponding dianionic form. These equilibria are simply represented by

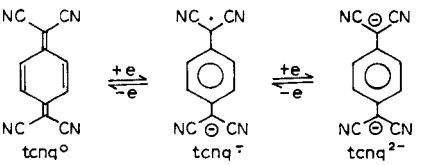

However, the interpretation of the voltammetric data must take into account the effects of extensive dimerization of $tcnq^{\cdot-}$ in aqueous solution according to

$$2\ tcnq^{\cdot-} \Leftrightarrow (tcnq^{\cdot-})_2 \qquad K_d = [(tcnq^{\cdot-})_2]/[tcnq^{\cdot-}]^2$$

where the dimerization constant is given by K_d. A value of $K_d = 2500\ l\ mol^{-1}$ has been given by Boyd and Phillips [10] on the basis of spectrophotometric data and this value was subsequently confirmed by the e.s.r. and spectrophotometric experiments of Blandamer et al. [11]. The mathematical treatment of Clark [12] appropriate to redox couples in which dimerization of the oxidant or reductant molecules occurs may be adapted readily to the present system by assuming that only the radical-anion species is capable of forming a dimer. Dimerization causes an anodic shift in the observed half-wave potentials with respect to that in the absence of complexation which is dependent on the stoichiometric concentration of the dimer-forming species and the dimerization constant K_d. At the concentration of radical-ions employed for the voltammetric measurements, $[tcnq^{\cdot-}] \simeq 2 \cdot 10^{-3}$ M, the

analysis predicts that the half-wave potentials observed should correspond within a few mV with values for the standard potentials for reductions involving the dimer species which are formally represented by:

$2\ tcnq^0 + 2\ e \Leftrightarrow (tcnq^-)_2$

and

$(tcnq^-)_2 + 2\ e \Leftrightarrow 2\ tcnq^{2-}$

The approximate standard potentials for these reactions were thus observed, see Fig. 1, to be, respectively,

$E^0_{2\ tcnq^0/(tcnq^-)_2} = 115 \pm 5$ mV (SCE) $= 359 \pm 5$ mV (NHE)

$E^0_{(tcnq^-)_2/2\ tcnq^{2-}} = -128 \pm 5$ mV (SCE) $= 116 \pm 5$ mV (NHE)

A more precise value for the latter, i.e., that which is most significant for an explanation of electrode mechanism, was obtained from potentiometric measurements with an electrode prepared from $Pbtcnq_2$. The response of this electrode towards $(tcnq^-)_2$ permits a value for $E^0_{(tcnq^-)_2/2\ tcnq^{2-}}$ to be obtained by extrapolation. Again the treatment of Clark was applied to account for the monomer–dimer equilibrium. Table 2 contains experimental data for six different solutions of Li_2tcnq_2 together with values for the standard potential of the reaction $tcnq^- + e \Leftrightarrow tcnq^{2-}$ thus derived. The standard potential for the formal reaction $(tcnq^-)_2 + 2\ e \Leftrightarrow 2\ tcnq^{2-}$ was calculated by means of the equation

$$E^0_{(tcnq^-)_2/2\ tcnq^{2-}} = E^0_{tcnq^-/tcnq^{2-}} + 29.6 \log K_d$$

from which

$E^0_{(tcnq^-)_2/2\ tcnq^{2-}} = -133 \pm 1$ mV (SCE) $= 111 \pm 1$ mV (NHE)

This is in good agreement with the value obtained voltammetrically and the value $E^0_{(tcnq^-)_2/2\ tcnq^{2-}} = 111 \pm 1$ mV (NHE) was employed in the following quantitative discussion.

TABLE 2

Determination of the standard redox potential, E^0_2, for the reaction $tcnq^- + e \Leftrightarrow tcnq^{2-}$ from measurements in the cell graphite|$Pbtcnq_2$|Litcnq, aq|SCE

[Litcnq](M) (stoichiometric)	$[tcnq^-]$(M)	E_{cell}(mV)	E^0_2(mV)
$9.27 \cdot 10^{-4}$	$3.44 \cdot 10^{-4}$	−27	−232
$6.01 \cdot 10^{-4}$	$2.60 \cdot 10^{-4}$	−23	−235
$2.17 \cdot 10^{-3}$	$5.66 \cdot 10^{-4}$	−42	−234
$2.09 \cdot 10^{-4}$	$1.28 \cdot 10^{-4}$	−4	−235
$2.85 \cdot 10^{-3}$	$6.62 \cdot 10^{-4}$	−46	−234
$4.89 \cdot 10^{-3}$	$8.94 \cdot 10^{-4}$	−53	−234
			Mean −234 ± 1

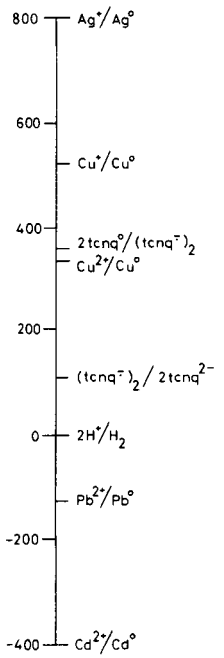

Fig. 2. Standard redox potentials in aqueous media at 25 °C (mV vs NHE).

On the basis of these results it was possible to determine the relative positions of the standard reduction potentials for the ionic components of a given salt from the electrochemical series shown in Fig. 2. Such knowledge then permitted the localization of the lowest available electron energy level in a given salt to be established and consequently the primary redox process could be identified. For Ag_2tcnq_2, for example, examination of Fig. 2 indicates that the Ag^+ ion presents the lowest electron energy level available to an added electron and the primary potential-determining redox process is expected to involve the Ag^+/Ag^0 couple. In contrast an electrode made from K_2tcnq_2 will be expected to function through a primary redox process involving the $(tcnq^-)_2$ dimer since the $(tcnq^-)_2$ component of the salt is more easily reduced than the cation K^+. Following such arguments it is possible to propose mechanisms for electrodes prepared from the different materials and to compare predicted behaviour with that observed. Particular emphasis was placed upon the degree of agreement between standard electrode potential values. For convenience, electrodes are discussed either separately or in groups where a common mechanism is applicable. A mechanism for the copper salts of $(tcnq^-)_2$, which is somewhat exceptional, is deferred until the mechanism of interference has been discussed.

Electrodes prepared from Ag_2tcnq_2

As discussed above, the primary redox process for the Ag_2tcnq_2 electrode is predicted by Fig. 2 to be $Ag^+ + e \Leftrightarrow Ag^0$, and the response of the electrode to Ag^+ thus follows the relation

$$E_{Ag^+} = E^0_{Ag^+/Ag^0} + 59.2 \log a_{Ag^+}$$

The standard electrode potential for Ag^+ response is that characteristic of the Ag^+/Ag^0 couple and this is found experimentally (see Table 1). Response towards $(tcnq^-)_2$ is found by substituting for a_{Ag^+} in the above equation from the ionic product relation

$$K_s(Ag_2tcnq_2) = (a_{Ag^+})^2 \cdot a_{(tcnq^-)_2}$$

Thus

$$E_{(tcnq^-)_2} = E^0_{Ag^+/Ag^0} + 29.6 \log K_s(Ag_2tcnq_2) - 29.6 \log a_{(tcnq^-)_2}$$

From measurements in aqueous solutions of Li_2tcnq_2 and with due consideration of the prevailing monomer—dimer equilibrium the standard electrode potential for response towards the radical-ion dimer, $E^s_{(tcnq^-)_2}$ was found to be

$$E^s_{(tcnq^-)_2} = E^0_{Ag^+/Ag^0} + 29.6 \log K_s(Ag_2tcnq_2) = 17 \pm 1 \text{ mV (NHE)}$$

from which the ionic product for Ag_2tcnq_2 was calculated to be

$$K_s(Ag_2tcnq_2) = 3.8 \pm 0.5 \cdot 10^{-27}$$

The detection limit for Ag^+ response for this electrode is therefore expected to be approximately $2 \cdot 10^{-9}$ M assuming a solubility limitation.

Electrodes prepared from simple salts of stoichiometric formula, $M^{n+}(tcnq^-)_n$, where $E^0_{M^{n+}/M^0}$ lies below $E^0_{(tcnq^-)_2/2tcnq^{2-}}$ in the electrochemical series

In such cases the $(tcnq^-)_2$ dimer is more easily reduced than the cationic component of the salt and the primary redox process is predicted to be

$$(tcnq^-)_2 + 2\,e \Leftrightarrow 2\,tcnq^{2-}$$

Taking the case of the electrode made from $Pbtcnq_2$ as example, the overall electrode reaction may be written

$$2\,Pbtcnq_2\,(s) + 2\,e \Leftrightarrow 2\,Pbtcnq\,(s) + (tcnq^-)_2$$

which involves reduction of the radical-anion dimer in the solid-state accompanied by release of $(tcnq^-)_2$ into the solution. By assuming that $a_{Pbtcnq_2\,(s)} = a_{Pbtcnq\,(s)} = 1$, the response of this electrode towards $(tcnq^-)_2$ should follow the relationship

$$E_{(tcnq^-)_2} = E^0_{(tcnq^-)_2/2tcnq^{2-}} - 29.6 \log a_{(tcnq^-)_2}$$

Such a dependence is found experimentally. From the ionic product of $Pbtcnq_2$,

TABLE 3

Comparison of solubility products determined potentiometrically with those obtained from measurements of cation concentration in saturated solutions by atomic absorption

Substance	K_s(pot.)	K_s(a.a.s.)
$Pbtcnq_2$	$1.3 \pm 0.3 \cdot 10^{-10}$	$0.96 \pm 0.2 \cdot 10^{-10}$
$Cdtcnq_2$	$3.0 \pm 0.5 \cdot 10^{-9}$	$2.9 \pm 0.3 \cdot 10^{-9}$
K_2tcnq_2	$5.8 \pm 1.2 \cdot 10^{-11}$	$1.7 \pm 1 \cdot 10^{-11}$

$K_s(Pbtcnq_2) = a_{Pb^{2+}} \cdot a_{(tcnq^{-})_2}$

the response to Pb^{2+} is found by substituting for $a_{(tcnq^{-})_2}$ in the above equation, i.e.,

$E_{Pb^{2+}} = E^0_{(tcnq^{-})_2/2tcnq^{2-}} - 29.6 \log K_s(Pbtcnq)_2 + 29.6 \log a_{Pb^{2+}}$

Again, such a relationship is found experimentally. Figure 3 shows the observed response curves for both Pb^{2+} and $(tcnq^{-})_2$. Analogous mechanisms apply to electrodes prepared from the salts, $Cdtcnq_2$, K_2tcnq_2, Na_2tcnq_2 and $(Et_4N)_2tcnq_2$ where the primary redox system also involves the $(tcnq^{-})_2/2tcnq^{2-}$ couple. Since the standard electrode potentials for cation response are readily determined and since $E^0_{(tcnq^{-})_2/2tcnq^{2-}}$ is known with fair precision, values for the ionic products of these salts may be determined. Table 3 contains results for the three compounds $Pbtcnq_2$, $Cdtcnq_2$ and K_2tcnq_2 and compares the potentiometrically determined ionic products with those evaluated from atomic absorption measurements of metal ion concentrations in saturated aqueous solutions of the respective salts. The assumption that the concentrations of metals so determined reflect free ion concentrations is reasonable. The agreement between the potentiometric and atomic absorption values is seen to be excellent. Such agreement may be taken as evidence in support of the model assumed for the electrode mechanism.

Electrodes prepared from a complex salt containing neutral tcnq

Complex radical-ion salts which contain both the $tcnq^{-}$ species and neutral $tcnq^0$ molecules, usually in a 1:1 molecular ratio, are obtained by reacting tcnq with the iodide salt of an organic or organometallic cation in a non-aqueous solvent such as acetonitrile. The general formula of such substances may be written in the form $M^{n+}(tcnq^{-})_n(tcnq^0)_n$. Electrodes prepared from complex salts are expected, by reference to Fig. 2, to show behaviour different from simple salt electrodes since the presence of neutral tcnq in the solid permits a change in the primary redox process from the $(tcnq^{-})_2/2tcnq^{2-}$ couple to the $2tcnq^0/(tcnq^{-})_2$ couple. This proposition can be quickly tested by comparing the response characteristics of electrodes made from $(Et_4N)_2tcnq_2$ (simple salt) and $(Et_4N)_2tcnq_4$ (complex salt), substances which

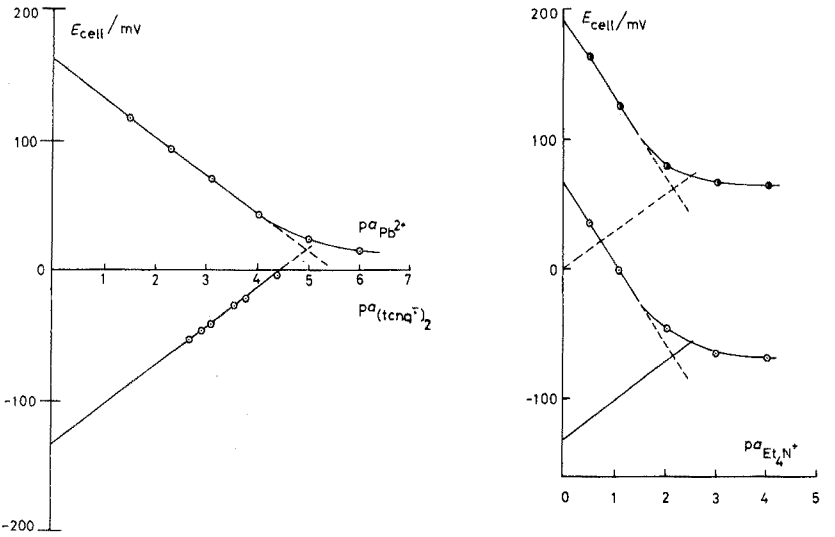

Fig. 3. Response of electrode made from $Pbtcnq_2$ towards Pb^{2+} and $(tcnq^-)_2$ ions in aqueous solution at 25 °C (E vs. SCE).

Fig. 4. Observed response curves for electrodes made from $(Et_4N)_2tcnq_4$ (complex salt, •) and $(Et_4N)_2tcnq_2$ (simple salt, ○) towards Et_4N^+ ions in aqueous solution at 25 °C (E vs. SCE).

are readily prepared by different synthetic procedures. The relevant equations describing the responses of these electrodes to Et_4N^+ cations are given by;

Simple salt

$$E_{Et_4N^+} = E^0_{(tcnq^-)_2/2tcnq^{2-}} - 29.6 \log K_s((Et_4N)_2tcnq_2) + 59.2 \log a_{Et_4N^+}$$

Complex salt

$$E_{Et_4N^+} = E^0_{2tcnq^0/(tcnq^-)_2} - 29.6 \log K_s((Et_4N)_2tcnq_2) + 59.2 \log a_{Et_4N^+}$$

where the ionic product

$$K_s((Et_4N)_2tcnq_2) = a^2_{Et_4N^+} \cdot a_{(tcnq^-)_2}$$

is common to both. Examination of these equations indicates that parallel response curves should be observed with that for the complex salt displaced to more positive potentials since $E^0_{2tcnq^0/(tcnq^-)_2}$ is more positive than $E^0_{(tcnq^-)_2/2tcnq^{2-}}$. Figure 4 shows the experimental results obtained and confirms the essential correctness of the above arguments. The difference between the standard potentials for Et_4N^+ response observed is, however, less than the expected difference of 245 mV (see Fig. 2). A re-examination of the voltammetric behaviour of the tcnq system was therefore carried out with a graphite electrode. The resulting voltammogram, shown in Fig. 5, is similar to that

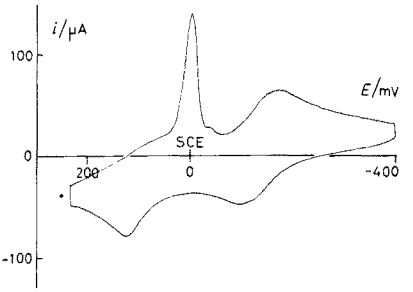

Fig. 5. Cyclic voltammetric curves for the $tcnq^0/(tcnq^-)_2/tcnq^{2-}$ system obtained in aqueous solution with a graphite electrode at 25 °C and a scan rate of 0.067 V s^{-1}.

obtained at platinum except that the reduction of $tcnq^0$ to the radical-anion occurs at a potential in the vicinity of that of the calomel electrode, i.e., at 244 mV (NHE) and corresponds to the cathodic dissolution of a film of $tcnq^0$ which is deposited on the graphite surface during the prior anodic scan. Deliberate manual application of $tcnq^0$ to a clean electrode produces closely similar voltammetric curves. Such behaviour predicts a difference between $E^0_{2tcnq^0/(tcnq^-)_2}$ and $E^0_{(tcnq^-)_2/2tcnq^{2-}}$ of the order of 130 mV which is in rough agreement with the difference observed between the standard potentials for the tetraethylammonium salt electrodes.

Mechanism of interference

For solid-state ion-selective electrodes the normally assumed mechanism of interference comprises an ion-exchange process at the surface of the electroactive material. By way of example, this equilibrium may be represented for the Ag_2tcnq_2 electrode in the presence of Cu^{2+} ions by

$$Ag_2tcnq_2\,(s) + Cu^{2+}\,(aq) \Leftrightarrow Cutcnq_2\,(s) + 2\,Ag^+\,(aq)$$

Assuming unit activities for the solid phases

$$\frac{a^2_{Ag^+}}{a_{Cu^{2+}}} = \frac{K_s(Ag_2\,tcnq_2)}{K_s(Cutcnq_2)}$$

where the K_s terms represent ionic products. For the Ag_2tcnq_2 electrode, which responds to Ag^+ ions according to

$$E_{Ag^+} = E^0_{Ag^+/Ag^0} + 59.2 \log a_{Ag^+}$$

substituting for a_{Ag^+} thus yields an expression for its response to Cu^{2+} ions of the form

$$E_{Cu^{2+}} = E^0_{Ag^+/Ag^0} + 29.6 \log \frac{K_s(Ag_2tcnq_2)}{K_s(Cutcnq_2)} + 29.6 \log a_{Cu^{2+}}$$

The standard potential for Cu^{2+} response is thus given by

$$E^{s}_{Cu^{2+}} = E^{0}_{Ag^{+}/Ag^{0}} + 29.6 \log \frac{K_s(Ag_2tcnq_2)}{K_s(Cutcnq_2)}$$

This expression can be tested experimentally by substituting values for the ionic products $K_s(Ag_2tcnq_2)$ and $K_s(Cutcnq_2)$ and comparing $E^{s}_{Cu^{2+}}$ (predicted) with $E^{s}_{Cu^{2+}}$ (observed). With $K_s(Ag_2tcnq_2) = 3.8 \pm 0.5 \cdot 10^{-27}$ and $K_s(Cutcnq_2) = 3.9 \pm 0.6 \cdot 10^{-19}$ (see below), $E^{s}_{Cu^{2+}}$ (predicted) was found to be 562 ± 3 mV (NHE) in excellent agreement with $E^{s}_{Cu^{2+}}$ (observed) = 560 ± 1 mV (NHE). The agreement implies that the adopted model for interference is satisfactory.

Additional confirmation is obtained by examining the predicted and observed behaviour of electrodes in which the $(tcnq^{\cdot-})_2/2tcnq^{2-}$ couple represents the primary redox process. Considering the interference of K^+ ions at an electrode prepared from $Pbtcnq_2$, the surface ion-exchange process is given by

$$Pb\ tcnq_2\ (s) + 2\ K^+\ (aq) \Leftrightarrow K_2\ tcnq_2\ (s) + Pb^{2+}\ (aq)$$

where

$$\frac{a_{Pb^{2+}}}{a^2_{K^+}} = \frac{K_s(Pbtcnq_2)}{K_s(K_2tcnq_2)}$$

The response of the $Pbtcnq_2$ electrode to Pb^{2+} ions follows the relation

$$E_{Pb^{2+}} = E^{0}_{(tcnq^{\cdot-})_2/2tcnq^{2-}} - 29.6 \log K_s(Pbtcnq_2) + 29.6 \log a_{Pb^{2+}}$$

and by substituting for $a_{Pb^{2+}}$ its response to the interferent ion K^+ is predicted to follow the equation:

$$E_{K^+} = E^{0}_{(tcnq^{\cdot-})_2/2tcnq^{2-}} - 29.6 \log K_s(K_2tcnq_2) + 59.2 \log a_{K^+}$$

This latter relationship is identical with the equation which describes the response of an electrode prepared from K_2tcnq_2 towards its primary ion K^+. Generalization of these arguments implies that, provided no change in primary redox process takes place, electrodes prepared from different tcnq-salts should yield one and the same response curve for a given cation. Support for this is shown by the data contained in Table 4 where the standard electrode potentials for cation response are collected for three different electrode materials. The agreement between the values contained in a given column

TABLE 4

Standard potentials observed for response of electrodes made from $Pbtcnq_2$, K_2tcnq_2 and $Cdtcnq_2$ towards different interfering cations (Potential values in mV vs. NHE.)

Electroactive salt	Interfering cation				
	Pb^{2+}	K^+	Cd^{2+}	Cu^{2+}	Ag^+
$Pbtcnq_2$	404	412	360	656	893
K_2tcnq_2	404	414	363	657	894
$Cdtcnq_2$	403	413	363	656	894

substantiates the above reasoning and further supports the assumed interference mechanism. It may be noted that the standard potentials observed for interference by Cu^{2+} and Ag^{+} ions allow values for the respective ionic products $K_s(Cutcnq_2)$ and $K_s(Ag_2tcnq_2)$ to be calculated. These were found to be $K_s(Cutcnq_2) = 3.9 \pm 0.6 \cdot 10^{-19}$ and $K_s(Ag_2tcnq_2) = 3.5 \pm 0.5 \cdot 10^{-27}$, the latter being in good agreement with that derived from the potentiometric response data for the Ag_2tcnq_2 electrode.

Electrodes prepared from Cu_2tcnq_2 and $Cutcnq_2$

Table 1 shows that identical standard electrode potentials for response to Cu^{2+} ions are obtained for electrodes prepared from copper(I) tcnq (Cu_2tcnq_2) and "copper(II)" tcnq ($Cutcnq_2$). A correlation between these values and the standard potentials of the Cu^{+}/Cu^{0} and the Cu^{2+}/Cu^{0} redox couples is not immediately apparent. An examination of the Cu_2tcnq_2 electrode, however, led to an adequate interpretation of its behaviour which was based on the interference mechanism discussed in the preceding section.

Figure 2 indicates that for the Cu_2tcnq_2 electrode, the primary redox process should involve the Cu^{+}/Cu^{0} couple and that the response of this sensor to Cu^{+} ions will be given by the equation

$$E_{Cu^+} = E^0_{Cu^+/Cu^0} + 59.2 \log a_{Cu^+}$$

Response to the anionic component of the salt, $(tcnq^-)_2$, is obtained by substituting from the ionic product:

$$K_s(Cu_2tcnq_2) = a^2_{Cu^+} \cdot a_{(tcnq^-)_2}$$

Thus

$$E_{(tcnq^-)_2} = E^0_{Cu^+/Cu^0} + 29.6 \log K_s(Cu_2tcnq_2) - 29.6 \log a_{(tcnq^-)_2}$$

By measuring the response of the electrode in solutions of Li_2tcnq_2, a value for the standard electrode potential $E^s_{(tcnq^-)_2}$ was obtained from which the ionic product $K_s(Cu_2tcnq)_2$ could be calculated. Since $E^s_{(tcnq^-)_2} = 120 \pm 1$ mV (NHE) and $E^0_{Cu^+/Cu^0} = 522$ mV (NHE), $K_s(Cu_2tcnq_2) = 2.6 \pm 0.5 \cdot 10^{-14}$. If it is assumed that response to Cu^{2+} occurs by means of an interference process involving ion-exchange, the appropriate response equation is found to be of the form:

$$E_{Cu^{2+}} = E^0_{Cu^+/Cu^0} + 29.6 \log \frac{K_s(Cu_2tcnq_2)}{K_s(Cutcnq_2)} + 29.6 \log a_{Cu^{2+}}$$

Since both $K_s(Cu_2tcnq_2)$ and $K_s(Cutcnq_2)$ are known, it is possible to evaluate the theoretical value for the standard electrode potential for Cu^{2+} response and to compare it with experiment. The agreement between $E^s_{Cu^{2+}}$ (predicted) $= 665 \pm 3$ mV (NHE) and $E^s_{Cu^{2+}}$ (observed) $= 665 \pm 1$ mV (NHE) supports the above arguments.

In the case of the "copper(II)" tcnq salts, with stoichiometric formula

$Cutcnq_2$, there exists evidence from magnetic susceptibility studies [6] of the solid which suggests that equilibria prevail which may be represented by the following structures:

$$2\ Cu^{2+}(tcnq^{\cdot-})_2 \Leftrightarrow (Cu^{+})_2(tcnq^{\cdot-})_2(tcnq^{0})_2 \Leftrightarrow (Cu^{+})_2(tcnq^{2-})\,(tcnq^{0})_3$$

The lack of significant contributions to the magnetic properties by Cu^{2+} and the free radical-anion, together with the fact that reaction between $tcnq^{2-}$ and $tcnq^0$ to form $(tcnq^{\cdot-})_2$ is strongly favoured, suggests that the solid phase may be more correctly described by the formula $(Cu^{+})_2(tcnq^{\cdot-})_2(tcnq^{0})$. Such a structure certainly conforms with the potentiometric behaviour observed, since it is to be expected that the primary redox process would be that involving the Cu^{+}/Cu^{0} couple and that response to Cu^{2+} would be accounted for by an interference mechanism as for the pure copper(I) compound. Identical response behaviour would be expected from both copper(I) and copper(II) salts and this is what is observed.

CONCLUSIONS

The behaviour of solid-state ion-selective electrodes made from the semi-conducting radical-ion salts of tcnq is satisfactorily explained by a mechanistic model analogous to that appropriate to electrodes of the second-kind. Considerations of the relative standard reduction potentials for the components of a particular sensing material allow the primary redox process to be identified. Three different primary redox processes, involving the M^{n+}/M^0, $(tcnq^{\cdot-})_2/2tcnq^{2-}$ or $2\ tcnq^0/(tcnq^{\cdot-})_2$ couples are possible depending on salt composition. Response ranges are accounted for by solubility equilibria relevant to the sensor material and interference effects are adequately interpreted on the basis of ion-exchange processes at the surface of the electroactive substance.

Despite the limitation of this study to salts of a single radical-forming molecule, similar arguments are considered to be valid in interpreting the behaviour of electrodes prepared from different materials of the same class. The results are also significant for the explanation of solid-state ion-selective electrode behaviour in general.

The author wishes to thank Prof. Gillis Johansson for his interest and helpful suggestions and Dr. Wolfgang Frech for carrying out the a.a.s. measurements. Financial support by the Swedish Natural Science Research Council is gratefully acknowledged.

REFERENCES

1 M. Sharp and G. Johansson, Anal. Chim. Acta, 54 (1971) 13.
2 M. Sharp, Anal. Chim. Acta, 59 (1972) 137.
3 M. Sharp, Anal. Chim. Acta, 61 (1972) 99.

4 M. Sharp, Anal. Chim. Acta, 62 (1972) 385.
5 P. Weidenthaler and E. Pelinka, Collect. Czech. Chem. Commun., 34 (1969) 1482.
6 L. R. Melby, R. J. Harder, W. R. Hertler, W. Mahler, R. E. Benson and W. E. Mochel, J. Am. Chem. Soc., 84 (1962) 3374.
7 J. Růžička and C. G. Lamm, Anal. Chim. Acta, 54 (1971) 1.
8 J. N. Butler, Ionic Equilibria, Addison-Wesley, Reading, Mass., 1964, p. 473.
9 E. P. Goodings, Endeavour, 34 (1975) 123 and references cited.
10 R. H. Boyd and W. D. Phillips, J. Chem. Phys., 43 (1965) 2927.
11 M. J. Blandamer, J. A. Brivati, M. F. Fox, M. C. R. Symons and G. S. P. Verma, Trans. Faraday Soc., 63 (1967) 1850.
12 W. M. Clark, Oxidation—Reduction Potentials of Organic Systems, Williams and Wilkins, Baltimore, 1960, Ch. 6.

Analytica Chimica Acta, 85 (1976) 31—40

RECHERCHE DES CONDITIONS OPTIMALES DE FONCTIONNEMENT D'UNE ÉLECTRODE À ENZYME SPÉCIFIQUE DU LACTATE APPLICATION AU DOSAGE DANS LE SANG

H. DURLIAT, M. COMTAT et J. MAHENC

Laboratoire de Chimie-Physique et d'Electrochimie, Université Paul Sabatier (laboratoire associé 192 au CNRS), 31077 Toulouse Cédex (France)

A. BAUDRAS

Centre de Recherche de Biochimie et de Génétique Cellulaires du C.N.R.S., 118, Route de Narbonne, 31077 Toulouse, Cédex (France)

(Reçu le 9 février 1976)

RÉSUMÉ

L'emploi d'une enzyme de levure aérobie permet de proposer une électrode spécifique basée sur l'association de la réaction catalytique d'oxydation du lactate par l'hexacyanoferrate(III) et de l'oxydation électrochimique de l'hexacyanoferrate(II) formé, sur électrode inattaquable. L'adoption de valeurs convenables pour les divers paramètres — épaisseur de la membrane et de la chambre réactionnelle, concentration de l'enzyme — rend possible le dosage d'échantillons de sang brut en des temps inférieurs à la minute avec une précision comparable à celle des dosages spectrophotométriques.

SUMMARY

L(+)-Lactate dehydrogenase, extracted from aerobic yeast, is used in a specific lactate electrode system in which the catalytic oxidation of lactate by hexacyanoferrate(III) is coupled with the electrochemical oxidation of the formed hexacyanoferrate(II) on an inert electrode. Selection of the optimal parameters particularly the thickness of the membrane and the thickness of the reaction chamber, allows the determination of lactate in blood without preliminary preparation, within a minute. This method is as accurate as the spectrophotometric method.

Depuis une dizaine d'années, des détecteurs électrochimiques ont été mis au point qui présentent une réponse rendue spécifique grâce à l'utilisation d'enzyme (électrodes à enzyme) et permettent le dosage de divers composés d'intérêt biologique. On peut distinguer les électrodes dont le principe est basé sur la mesure d'un potentiel proportionnel au logarithme de la concentration du substrat et celles qui conduisent à la mesure d'une intensité de courant directement proportionnelle à la concentration de l'espèce à doser. Pour la première catégorie, les plus répandues sont les électrodes spécifiques de l'urée [1, 2], du glucose [3]. Pour la deuxième catégorie on note essentiellement les électrodes mises au point pour doser le glucose [4—6], les alcools [7], les acides aminés [5, 8], et le lactate [6, 9—11].

En ce qui concerne ce dernier métabolite, on comprend aisément l'importance de son dosage dans les milieux biologiques végétaux et animaux en rappelant que ce composé est toujours associé au pyruvate, produit final des processus aérobie ou anaérobie de dégradation du glucose et également produit intermédiaire dans le catabolisme des protéines et des lipides.

Chez un être humain au repos, la concentration du lactate dans le sang est voisine de 1 mM. Toutefois, diverses circonstances pathologiques sont accompagnées d'une élévation de la concentration du lactate qui peut être importante (7 à 10 mM). L'acidose lactique se manifeste par des troubles circulatoires ou respiratoires et des troubles de la conscience pouvant aller jusqu'au coma. Ces signes cliniques n'étant pas spécifiques, le diagnostic ne peut être établi qu'à la suite d'un dosage du lactate. Il est en outre important de pouvoir connaître simplement et rapidement le taux de lactate lorsque le médecin est confronté à des cas d'urgences (services de réanimation). Actuellement, le lactate est dosé par une méthode spectrophotométrique qui présente deux inconvénients sérieux: un traitement préalable de l'échantillon de sang est nécessaire et, de plus, le résultat de l'analyse ne peut être connu en moins d'une heure. Pour ces raisons, le dosage du lactate est un cas typique pour lequel l'utilisation d'un détecteur électrochimique doit permettre de grandes améliorations.

Après avoir rappelé le principe du dosage du lactate en solution aqueuse effectué à l'aide d'une électrode ampérométrique, nous présentons une étude de l'influence de divers paramètres en vue d'optimiser les performances de l'électrode. Un traitement théorique réalisé à l'état stationnaire rend compte des résultats expérimentaux. Nous montrons enfin que cette électrode permet le dosage du lactate dans le sang non traité et fournit des valeurs de concentration qui sont en excellent accord avec les valeurs obtenues par la méthode spectrophotométrique classique.

DISPOSITIF EXPERIMENTAL ET RAPPEL DU PRINCIPE DE DOSAGE

Cellule

La cellule (Fig. 1) est tournée dans un rondin d'Altuglas. Une chemise externe permet le maintien d'une température constante grâce à une circulation d'eau fournie par un thermostat. Il faut toutefois signaler que l'isothermicité stricte ne s'impose pas: en effet, l'expérience a montré qu'une légère variation de température (1 à 2 degrés) n'entraîne pas de modifications notables dans la réponse de l'électrode. La cellule peut être commodément rincée entre les dosages grâce à deux orifices d'alimentation et d'évacuation de la solution.

Electrodes et circuit électrique

L'électrode indicatrice peut être en platine, en or ou en carbone vitreux; c'est un disque de 7.10^{-2} cm^2 de surface délimité par la section d'un cylindre de métal ou de carbone enchâssé dans un tube cylindrique en matière

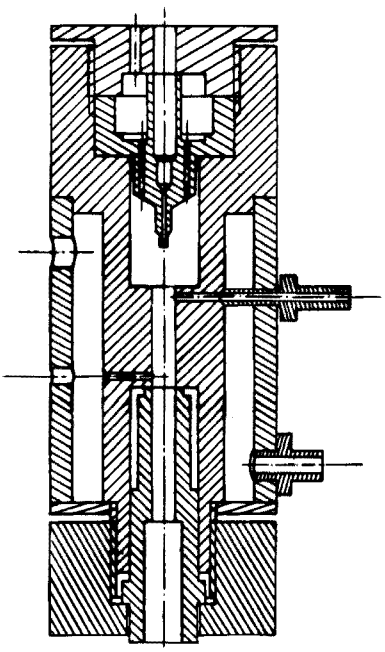

Fig. 1. Schéma de la cellule de mesure. Hauteur 80 mm, diam. 30 mm.

plastique vissé sur la cellule, ce qui assure une bonne étanchéité. Cette électrode est recouverte d'une membrane semi-perméable en cellophane que maintient une bague en "altuglas". Le faible volume (inférieur à 10^{-6} l) délimité par l'électrode et la membrane est appelé chambre réactionnelle. L'électrode auxiliaire est une électrode de deuxième espèce de type Ag/AgCl/Cl^-, de grande surface. L'électrode de référence au calomel saturé par rapport à laquelle sont exprimés les potentiels, se trouve dans un capillaire de Luggin dont l'extrémité est placée au voisinage immédiat de la membrane, ce qui assure la jonction et minimise la chute ohmique entre les électrodes indicatrice et de référence.

Un potentiostat assure la régulation du potentiel de l'électrode indicatrice par rapport à l'électrode de référence. L'intensité du courant d'électrolyse est mesurée à l'aide d'un galvanomètre enregistreur placé en série dans le circuit de l'électrode auxilliaire. Un voltmètre électronique à haute impédance d'entrée permet la mesure du potentiel d'équilibre de l'électrode indicatrice et le contrôle de son potentiel au cours de l'électrolyse.

Solution électrolytique. Le milieu utilisé est une solution tamponnée, mélange de phosphates monopotassique et disodique de concentration en phosphate égale à 0,2 M, dont le pH et la force ionique sont respectivement égaux à 7,20 et 0,5 M.

Traitement préalable de l'électrode indicatrice. Pour obtenir une bonne reproductibilité des mesures il est nécessaire de faire subir à l'électrode indicatrice un traitement préalable qui consiste à soumettre l'électrode immergée dans la solution tamponnée à des balayages alternés de potentiel linéairement variable entre les bornes −0,2 V et 1 V jusqu'à ce que les tracés des cycles se superposent. L'électrode est ensuite maintenue pendant 3 min à −0,03 V.

Dosage du lactate en solution aqueuse

L'enzyme utilisée est la L(+)-lacticodéshydrogénase de levure aérobie (1.1.2.3) qui catalyse la réaction d'oxydation du lactate par l'hexacyanoferrate(III).

$$CH_3CHOHCOO^- + 2Fe(CN)_6^{3-} \xrightarrow[LDH]{} CH_3COCOO^- + 2Fe(CN)_6^{4-} + 2H^+ \quad (1)$$

Cette réaction a lieu dans la chambre réactionnelle et l'hexacyanoferrate(II) formé est oxydé électrochimiquement. Pour effectuer un dosage on opère de la façon suivante: après l'introduction de la solution enzymatique dans la chambre réactionnelle, l'électrode est plongée d'abord dans la solution tamponnée afin que la membrane de cellophane s'hydrate, puis dans une solution tamponnée contenant de l'hexacyanoferrate (III) pendant 10 min, temps au bout duquel les concentrations sont égales de part et d'autre de la membrane après diffusion au-travers de cette dernière. La concentration de la solution d'hexacyanoferrate(III) utilisée doit rester inférieure à 3 mM pour éviter une dénaturation de l'enzyme. L'électrode indicatrice est ensuite vissée sur l'orifice fileté de la cellule. Dès que la solution de lactate est introduite dans la cellule, l'électrode indicatrice est portée au potentiel de + 250 mV par rapport à l'électrode de référence [11], potentiel pour lequel la concentration de l'hexacyanoferrate(II) est nulle à la surface de l'électrode et l'intensité du courant résiduel la plus faible possible. L'enregistrement de la courbe donnant l'intensité du courant en fonction du temps présente un palier lorsque la solution est agitée ou un maximum A en absence d'agitation (Fig. 2). Les deux caractéristiques essentielles de ces courbes sont la valeur de l'intensité maximale et le temps nécessaire pour l'atteindre (temps de réponse θ).

L'expérience montre que l'intensité du courant à l'état stationnaire est proportionnelle à la concentration du lactate dans la solution externe pour une gamme étendue de concentration comprise entre 0,1 mM et 8 mM (Fig. 3).

INFLUENCE DE QUELQUES PARAMETRES

Epaisseur de la membrane. Diverses membranes en cellophane d'épaisseur l' ont été utilisées pour doser une même solution de lactate non agitée. Les résultats sont consignés dans le Tableau 1(a). Il ressort de ces valeurs que l'intensité maximale du courant varie en sens inverse de l'épaisseur de la

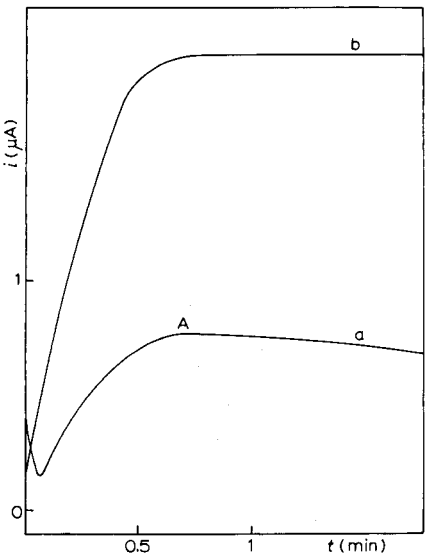

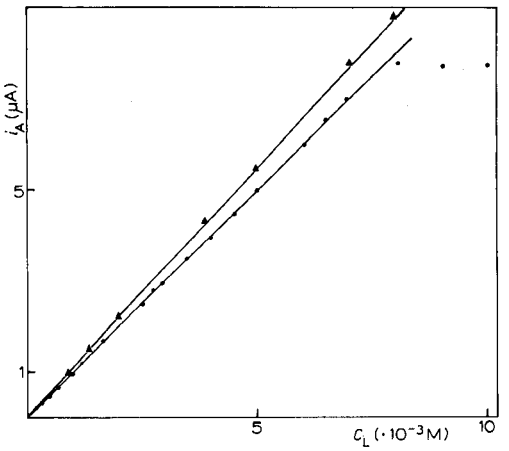

Fig. 2. Courbes de réponse de l'électrode (a) en l'absence d'agitation de la solution (b) avec agitation. $C_L = 10^{-3}$ M.

Fig. 3. Etalonnage de l'électrode en solution aqueuse. ▲Au · C ● Pt. $[Fe(CN)_6^{3-}] = 1.5$ mM.

TABLEAU 1

Influence (a) de l'épaisseur de la membrane (b) de la profondeur de la chambre réactionnelle sur les caractéristiques de l'électrode
[Solution non agitée électrode de platine. $C_L^{ext} = 1$ mM. $k_3 = 900$ s^{-1} (activité moléculaire de l'enzyme à 25 °C.)]

(a) $l = 80$ μm; $C_E = 40$ μM			(b) $l = 50$ μm; $C_E = 40$ μM		
l' (μm)	i_A (μA)	θ (s)	l (μm)	i_A (μA)	θ (s)
38 ± 2	1,15 ± 0,02	30	40 ± 10	1,50 ± 0,03	20
48 ± 2	1,09 ± 0,02	40	80 ± 10	1,38 ± 0,02	50
80 ± 2	0,68 ± 0,01	60	120 ± 10	1,00 ± 0,02	75
			180 ± 10	0,85 ± 0,02	480

membrane. D'autre part le temps de réponse est d'autant plus court que l' est petit.

Profondeur de la chambre réactionnelle. Des mesures de l'intensité de courant à l'état stationnaire ont été effectuées avec une solution de lactate non agitée, pour différentes valeurs de l'épaisseur l de la chambre réactionnelle: les valeurs de i_A sont reportées dans le Tableau 1(b). Quand la profondeur l croît, l'intensité i_A diminue et le temps de réponse augmente.

Concentration de la solution enzymatique. Pour une concentration donnée en lactate (1 mM) l'intensité i_A est indépendante (1,50 ± 0,03 μA; θ = 24 ± 15) de la concentration de l'enzyme dans la chambre réactionnelle (l = 40 μm; l' = 50 μm) dans un domaine étendu de concentration (0,4 μM—130,0 μM pour ces essais) sous réserve que cette concentration soit supérieure à 0,4 μM. Ce fait expérimental est intéressant sur le plan pratique. En effet une dénaturation lente de l'enzyme a été observée, qui correspond à une diminution progressive dans le temps de la concentration vraie d'enzyme active. Néanmoins ce phénomène n'a pas d'effet néfaste sur le comportement de l'électrode pour autant que la concentration de la solution d'enzyme introduite dans la chambre réactionnelle soit élevée.

Concentration de l'hexacyanoferrate(III) dans la solution de lactate étudiée. Pour les teneurs en hexacyanoferrate(III) supérieures à 1 mM (1,0—10,0 mM) l'intensité du courant à l'état stationnaire est indépendante de la concentration (i_A = 1,50 ± 0,04 μA; C_E = 40 μM). En dessous de 1 mM l'intensité du courant présente une variation monotone croissante en fonction de la concentration: i_A = 1,34 μA pour 0,8 mM $Fe(CN)_6^{3-}$ et 0,86 μA pour 0,08 mM.

Pour les fortes concentrations (10 mM) apparaissent deux maximums sur la courbe i (t). Ce phénomène a également été observé lorsque l'enzyme a perdu une grande partie de son activité. Comme nous l'avons signalé précédemment, nous nous trouvons dans des conditions de dénaturation de l'enzyme par l'hexacyanoferrate(III).

CALCUL THEORIQUE

Racine et coll. [9] ont, les premiers, proposé une ébauche de calcul qui conduit à la relation suivante entre l'intensité du courant à l'état stationnaire et la concentration du lactate dans la solution externe à doser.

$$i = nF \frac{D^m}{l'} C_L^{ext}$$

D^m étant le coefficient de diffusion du lactate dans la membrane, F la constante de Faraday, et n le nombre d'électrons échangés lors de la réaction électrochimique.

Cette relation ne prend pas en considération le paramètre "profondeur de la chambre réactionnelle" qui, comme nous l'avons montré, influe notablement sur les caractéristiques de la réponse. Par ailleurs, l'hypothèse selon laquelle la concentration du lactate dans la chambre réactionnelle serait constante nous semble contestable.

Nous proposons une relation théorique plus générale qui rend compte des résultats expérimentaux présentés précédemment. Les hypothèses et conditions de travail sont les suivantes.

(a) La concentration du lactate dans la chambre réactionnelle C_L^{int} est inférieure à la constante de Michaelis K_m (dans ces conditions la vitesse de la réaction enzymatique est d'ordre partiel 1 par rapport au lactate).

(b) La concentration de l'hexacyanoferrate(III) est suffisante pour que tout le lactate arrivant dans la chambre réactionnelle puisse être transformé. Elle est d'autre part comprise entre 0,1 et 3 mM, domaine pour lequel la vitesse de la réaction enzymatique est d'ordre partiel zéro parte rapport à l'hexacyanoferrate(III).

(c) La solution à l'extéreur de la chambre réactionnelle est agitée.

(d) Les gradients de concentration des différentes espèces dans la membrane sont constants.

(e) Le rapport des concentrations de chaque espèce de part et d'autre du plan de séparation entre chambre réactionnelle et membrane est pris égal à l'unité.

En outre, pour simplifier le calcul, et dans l'attente d'une détermination des valeurs exactes des coefficients de diffusion dans nos conditions expérimentales, nous avons pris une valeur unique pour ces coefficients de diffusion, soit D^s en solution et D^m dans la membrane.

Avec ces hypothèses il est possible d'établir une analogie entre le système étudié et un détecteur à enzyme immobilisée pour lequel une description théorique a été proposée par Blaedel et coll. [12]. La chambre réactionnelle et la membrane semi-perméable qui la limite, dans l'électrode, sont assimilables respectivement à la membrane porteuse d'enzyme fixée et à la couche de diffusion en solution du système décrit par Blaedel.

Dans la chambre réactionnelle se fait la réaction (1) dont la vitesse a pour expression

$$v = \frac{k_3 C_E}{K_m} C_L^{int}$$

k_3 étant activité moléculaire de l'enzyme, et C_E la concentration de l'enzyme.

Les différents produits et réactifs diffusent dans la solution présente dans la chambre réactionnelle. A l'état stationnaire le bilan effectué sur le lactate, le pyruvate et l'hexacyanoferrate(II) permet d'écrire

$$D^s \frac{d^2 C_L^{int}}{dx^2} = v \quad ; \quad D^s \frac{d^2 C_P^{int}}{dx^2} = -v \quad ; \quad D^s \frac{d^2 C_H^{int}}{dx^2} = -2v$$

L'intégration de ces équations différentielles conduit aux expressions des concentrations des différentes espèces dans la chambre réactionnelle en fonction de la distance x à la membrane et au calcul des flux des espèces aux interfaces membrane—solution externe, membrane—solution interne et électrode—solution interne. Il s'ensuit l'expression suivante de l'intensité du courant

$$i = n F A (J_H)_{x = l}$$

$$i = 2 F A \frac{D^s \cdot D^m}{l D^m + l' D^s} C_L^{ext}$$

qui fait apparaître l'influence de l et l' sur l'intensité i et l'indépendance de l'intensité du courant vis-à-vis de la concentration de l'enzyme [$(J_H)_{x = l}$ est le flux de l'hexacyanoferrate(III) dans la chambre réactionnelle.

La validité de cette relation est éprouvée en confrontant les valeurs calculées et expérimentales des paramètres (Tableau 2): on calcule d'abord l, l' étant fixé et D^m déterminé par approximations successives. On réalise ensuite le même calcul pour l' en prenant cette fois l constant. Comme le montre le Tableau 2 une bonne concordance existe entre les valeurs calculées et expérimentales pour l et l' respectivement; il conviendrait toutefois d'affiner ces calculs par l'introduction des valeurs réelles des coefficients de diffusion des espèces en présence.

APPLICATION AU DOSAGE DU LACTATE DANS LE SANG

L'électrode à enzyme est utilisée pour doser le lactate dans des échantillons de sang. Nous avons constaté qu'un tel dosage est possible sans aucun traitement préalable du sang, ce qui n'est pas le cas pour la méthode spectrophotométrique. Immédiatement après son prélèvement le sang est introduit dans la cellule d'électrolyse et l'intensité du courant est enregistrée au cours du temps. La courbe obtenue a la même allure générale que celle qui est observée lors du dosage d'une solution aqueuse de lactate. Pour un choix optima des valeurs des paramètres l et l', la concentration de lactate est connue moins d'une minute après l'introduction dans la cellule de la solution étudiée.

Les résultats obtenus par le dosage ampérométrique ont été contrôlés à l'aide de la méthode spectrophotométrique classiquement utilisée dans les services cliniques pour doser le lactate [13—15]. Le protocole de ce dernier dosage est le suivant: immédiatement après son prélèvement, le sang est déprotéinisé par l'acide perchlorique (la concentration finale est égale à 0,4 N), puis centrifugé. Au surnageant qui contient le lactate, on ajoute le coenzyme NAD^+ et la lacticodéshydrogénase du muscle. Il se produit la réaction suivante

$$CH_3—CHOH—COO^- + NAD^+ \xrightarrow[LDH]{} CH_3—CO—COO^- + NADH + H^+ \qquad (2)$$

Cette réaction équilibrée est en pratique déplacée dans le sens de l'oxydation du lactate grâce à l'addition d'hydrazine et à l'utilisation d'un milieu

TABLEAU 2

Comparaison des valeurs de l et l' expérimentales et calculées ($C_L^{ext} = 1$ mM; $C_E = 40$ μM; $k_3 = 700$ s^{-1}; $K_m = 1$ mM; $D^s = 5.10^{-6}$ cm^2 s^{-1})

$l = 40$ μm; $D^m = 1{,}1_5.10^{-6}$ cm^2 s^{-1}			$l' = 50$ μm; $D^m = 1{,}6_5.10^{-6}$ cm^2 s^{-1}		
i (μA)	l' (μm) calculé	l' (μm) mesuré	i (μA)	l (μm) calculé	l (μm) mesuré
3,0	36	38 ± 2	3,91	34	40 ± 10
2,35	51	50 ± 2	3,04	85	80 ± 10
1,76	75	77 ± 2	2,61	124	120 ± 10
			2,22	173	180 ± 10

réactionnel tamponné de pH 9. Dans ces conditions l'oxydation du lactate est terminée au bout d'une heure d'incubation à 30 °C et une mesure d'absorbance à 340 nm permet de calculer la concentration du lactate dans l'échantillon de sang analysé.

Dans le Tableau 3 sont comparées les valeurs des concentrations de lactate trouvées pour les mêmes prélèvements sanguins, soit par la méthode ampérométrique, soit par la dernière méthode spectrophotométrique classique: elles présentent un excellent accord, pour autant que le dosage ampérométrique soit effectué sans délai après le prélèvement de l'échantillon de sang.

L'électrode spécifique du lactate a été également employée avec succès pour le dosage d'autres liquides d'origine biologique, les vins par exemple (cette méthode permet de suivre commodément le déroulement de la fermentation malolactique des vins).

CONCLUSION

L'utilisation de la L(+)-lacticodéshydrogénase de levure aérobie permet de proposer une électrode spécifique du lactate qui rend possible le dosage de ce substrat dans les échantillons de sang non traités au préalable. La comparaison des résultats de la mesure électrochimique avec ceux obtenus par la méthode spectrophotométrique classique montre que la précision est identique dans les deux cas (erreur inférieure à 2 %).

Le dosage ampérométrique présente l'avantage d'être rapide: la mesure peut être faite en vingt secondes environ si l'on choisit au mieux les valeurs des paramètres qui ont une influence sur l'intensité du courant à l'état stationnaire.

Les résultats expérimentaux relatifs à la variation de cette intensité avec l'épaisseur de la membrane et la profondeur de la chambre réactionnelle, sont en accord avec l'expression théorique proposée.

D'autre part, sous réserve que la concentration de l'enzyme utilisée soit suffisamment élevée, l'électrode peut être employée pour un grand nombre de dosages, ce qui diminue son prix de revient.

TABLEAU 3

Comparison des valeurs des concentrations (en mM) de lactate dans le sang trouvées par deux méthodes

Spectrophotométrie	Electrode ampérométrique
0,62 ± 0,01	0,63 ± 0,01
1,06 ± 0,02	1,10 ± 0,02
1,30 ± 0,02	1,33 ± 0,02

BIBLIOGRAPHIE

1 G. G. Guilbault et J. G. Montalvo, J. Am. Chem. Soc., 91 (1969) 2164; G. G. Guilbault et W. Stokbro, Anal. Chim. Acta, 76 (1975) 237, et réfs en cela.
2 J. G. Montalvo, Anal. Chem., 41 (1969) 2093.
3 M. K. Weibel, Anal. Biochem., 52 (1973) 402.
4 G. G. Guilbault et G. J. Lubrano, Anal. Chim. Acta, 60 (1972) 254; Anal. Chim. Acta, 64 (1973) 439.
5 M. Nanjo et G. G. Guilbault, Anal. Chim. Acta, 73 (1974) 367.
6 D. L. Williams, A. R. Doig et A. Korosi, Anal. Chem., 42 (1970) 118.
7 G. G. Guilbault et G. J. Lubrano, Anal. Chim. Acta, 69 (1974) 189.
8 G. G. Guilbault et G. J. Lubrano, Anal. Chim. Acta, 69 (1974) 183.
9 P. Racine et W. Mindt, Experientia Suppl., 18 (1971) 525.
10 P. Racine, R. Engelhardt, J. G. Higelin et W. Mindt, Medical Instrumentation, 9 (1975) 11.
11 H. Durliat, M. Comtat, J. Mahenc et A. Baudras, J. Electroanal. Chem., 66 (1975) 73; H. Durliat, Doctorat de Spécialité, Toulouse, 1975.
12 W. J. Blaedel, T. R. Kissel et R. C. Boguslaski, Anal. Chem., 44 (1972) 2030.
13 B. Hess, Biochem. Z., 328 (1956) 110.
14 H. J. Hohorst, Biochem. Z., 328 (1957) 509.
15 P. Vaupel et H. Gunther., Pfluegers Arch., 323 (1971) 351.

Analytica Chimica Acta, 85 (1976) 41—46

THE BEHAVIOUR OF SILVER PHOSPHATE AS THE ELECTROACTIVE SENSOR IN A PHOSPHATE-SENSITIVE ELECTRODE

I. NOVOZAMSKY and W. H. van RIEMSDIJK

Laboratory of Soils and Fertilizers, Agricultural University, Wageningen (The Netherlands)

(Received 15th January 1976)

SUMMARY

A phosphate ion-selective electrode based on silver phosphate as the electroactive material is described. The behaviour of the electrode is Nernstian, the response time is 2 min, the detection limit is 10^{-5} M total phosphate, and the short-term stability is within 0.5 mV. The most serious interfering ion is chloride; no interferences were found from polyphosphates, nitrates or sulfates.

Several attempts have been made to construct an electrode which is selective for phosphate ions [1—5] but none of the materials tested has shown sufficient selectivity or a Nernstian response over a reasonable range of phosphate activities. All of these electrodes are based on the same concept, i.e. the exchange of phosphate from the membrane material with phosphate in the solution, which results in a measurable potential difference. The electrode described recently by Guilbault and Nanjo [6] is a dual-enzyme electrode, and is probably the most useful phosphate electrode developed so far. The purpose of the research described here was to test the usefulness of silver phosphate as a phosphate-sensitive membrane material.

EXPERIMENTAL

Construction of the electrode

The electroactive compound [7] for the electrode, silver phosphate, was made by slow stepwise titration of 0.01 or 0.1 M Na_2HPO_4 with 0.25 M silver nitrate at pH 9. The silver nitrate solution was added from a Radiometer ABU 12 buret, and the pH of the system was kept constant by the addition of 0.2 M sodium hydroxide by means of a Radiometer pH-stat. The suspension was stirred continuously, and the titration was stopped at intervals of about 1 ml of silver nitrate solution to allow attainment of equilibrium, which was indicated by the hydroxide addition. The reaction, after the addition of about 0.2 ml of silver(I) solution, followed the equation: $3\ Ag^+ + HPO_4^{2-} \rightleftharpoons Ag_3PO_4 + H^+$; this was clear from the amounts of silver(I) and hydroxide solution added at each step.

At the end of the titration, the silver activity was followed potentiometrically by means of a silver wire and a double-junction SCE with a 1 M sodium nitrate salt bridge to prevent chloride contamination. The titration was stopped at pAg 3.2—3.7, to prevent contamination by silver hydroxide or silver oxide. The precipitate was centrifuged off and washed several times with distilled water or with $10^{-3.7}$ M silver nitrate solution. The purified compound was then dried at 200 °C for 24 h.

Several systems are available for the construction of electrodes with solid membranes [8]. In the present case, the system proposed by Růžička et al. [9, 10] was selected. The electrode consists of a Teflon-impregnated graphite column, the electroactive material being rubbed into the end of the rod.

The conditioning of the electrode consisted of storage in 0.1 M total phosphate solution with a pH value of about 7 for periods ranging from 30 min to 48 h before use. All potential measurements were done in a constant-temperature room at 20 (±0.2) °C.

The reference electrode was a double-junction SCE with a 1 M $NaNO_3$ salt bridge to prevent chloride contamination. The ionic strength in all measurements was $\mu = 0.10 \pm 0.02$.

A Knick type 641 mV-pH meter (±0.1 mV) was used for mV measurements, and a Radiometer PHM 64 mV-pH meter for pH measurements.

THEORETICAL CONSIDERATIONS

The electroactive species is silver orthophosphate (Ag_3PO_4). The silver ion is probably the mobile species in the membrane. The potential of this electrode should then follow the equation

$$E = E^0_{Ag} + 19.4 \log K_{so} - 19.4 \log a_P \quad (20\,^\circ C) \tag{1}$$

where K_{so} is the solubility product of silver orthophosphate, E^0_{Ag} is the standard potential, and a_P is the activity of the PO_4^{3-} species. When the values E^0_{Ag} = 804 mV (20 °C) and pK_{so} = 20.7 (at $\mu = 0$) [11] are inserted into eqn. (1), the value found for the electrode potential, measured against the SCE, and neglecting the diffusion potentials of liquid junctions, is

$$E = 156.4 - 19.4 \log a_P \tag{2}$$

The activity of PO_4^{3-} depends on the total phosphate concentration, P_T, and is influenced by pH and by the ionic strength of the solution. If necessary, the electrode can be calibrated in terms of total orthophosphate present in the solution. It should, however, always be kept in mind that the electrode is selective for the PO_4^{3-} species, so that in such a case measurements must be made at constant ionic strength and pH, and no metal—orthophosphate complexes should be present.

The limit of sensitivity of the electrode should depend primarily on the solubility of the membrane material itself. The literature [12] gives different values for the solubility product ranging from pK_{so} 15.84 to 20.8.

The Davies expression [13] was used to calculate activity coefficients for the different phosphate species. These activity coefficients can be inserted in the formula for the side-reaction coefficient, α_H: $\alpha_H \cdot a_p = P_T$, in which P_T is the total orthophosphate concentration, a_p is as defined above and α_H is the side-reaction coefficient depending on pH and ionic strength. Another way of handling the data is to use a medium of constant ionic strength, so that the pK values of phosphoric acid determined at the same ionic strength can be employed. This gives values for α'_H and the $[PO_4^{3-}]$ concentration.

Both methods include some uncertainties about the exact value of the different constants used. With the aid of a simple computer program, the appropriate value of α_H can easily be calculated on a good pocket calculator. Values of $p\alpha'_H$ and $p\alpha_H$ are given in Table 1.

The solubility of silver phosphate can then be calculated with the aid of the calculated α_H values, according to $(Ag^+)^3 P_T = 10^{-20.7} \cdot \alpha_H$. This has been done for $\mu = 0.1$ in terms of $pP_T = -\log P_T$ and $p(PO_4^{3-})$ and the results are also given in Table 1.

Table 1 shows that the solubility is lowest at high pH, but also that the activity of the orthophosphate which is in equilibrium with silver phosphate, decreases with decreasing pH. It should therefore be possible to measure 10^{-10}—10^{-12} M orthophosphate given a high enough P_T ($> 10^{-3}$) and low enough pH. The minimum P_T that can be measured will be in the range of 10^{-4}—10^{-5} M at pH 9. At higher pH there will be the risk of silver hydroxide formation at low P_T. In this context, it is necessary to emphasize that all species present in the system which influence the stability of silver orthophosphate (i.e. chlorides, sulfides, complexing species) also affect the sensitivity of the electrode.

TABLE 1

Calculated values of $p\alpha'_H$ (with dissociation constants [12] of orthophosphoric acid measured at $\mu = 0.1$, $pK_1 = 2.10$, $pK_2 = 6.72$, $pK_3 = 4.8$), and of $p\alpha_H$ (with activity constants [12] of orthophosphoric acid for $\mu = 0$, $pK_1 = 2.12$, $pK_2 = 7.20$, $pK_3 = 12.33$ and the activity coefficients for $\mu = 0.1$, $f_{H_2PO_4^-} = 0.79$, $f_{HPO_4^{2-}} = 0.38$ and $f_{PO_4^{3-}} = 0.11$) for different pH values of interest.
(Note that $(\log f_{PO_4^{3-}}) + p\alpha'_H$ should equal $p\alpha_H$. The calculated PO_4^{3-} activities and total phosphate concentrations in equilibrium with silver phosphate are also given at $\mu = 0.1$ in terms of the negative logarithm of these values.)

pH	$p\alpha'_H$ ($\mu = 0.1$)	$p\alpha_H$ ($\mu = 0.1$)	$p(PO_4^{3-})$	pP_T
5	−8.52	−9.64	12.7	3.1
5.5	−7.54	−8.65	12.0	3.3
6	−6.59	−7.68	11.3	3.6
6.5	−5.72	−6.79	10.6	3.8
7	−4.98	−6.00	10.0	4.0
7.5	−4.37	−5.34	9.5	4.2
8	−3.82	−4.78	9.1	4.3
8.5	−3.31	−4.26	8.7	4.4
9	−2.80	−3.75	8.3	4.6

RESULTS AND DISCUSSION

Basically, two methods can be used to test the functioning of the electrode. Either P_T is varied at a constant ionic strength and pH, or a_P is varied at a constant ionic strength by varying the pH at constant P_T. The latter procedure has the advantage that sufficiently low values of a_P, buffered by the relatively high P_T present, can be achieved. For the present purpose the pH value of a solution containing 10^{-3} M P_T in 0.1 M KNO_3 was changed by stepwise additions of rather concentrated sodium hydroxide and nitric acid solutions. The results of the measurements are given as points in Fig. 1. The straight line which has been drawn was computed according to eqn. (2).

The deviations of the measured values from the theoretical line at high a_P can probably be attributed to the inaccuracy in the calculated activity coefficients, as at high pH the contribution of $f_{PO_3^{3-}}$ to α_H is greater than at low pH.

The deviation at low a_P is caused by the contribution to the a_P in the solution made by the solubility of the active material itself. As the agreement between the measured and calculated values is seen to be fairly good, the value chosen for the solubility product is probably not far from the true value for the material used in these experiments. The same experiments were performed at $pP_T = 2.7$ and $\mu = 0.1$. These measurements coincided with those presented in Fig. 1. Thus, the electrode responds equally well to a diminution in P_T as to pH changes. The response time of the electrode was found to be about 2 min.

The stability of the electrode is very good: it remained stable within 0.5 mV over a three-day period at least. The lifetime of the electrode is sufficiently long; after some weeks the sensitivity was sometimes reduced to a slope of 16—17 mV/pPO_4^{3-}, which was accompanied by longer response times (about 6 min). It is, however, easy to renew the electrode surface. The calibration described above is of importance for thermodynamic measurements with the aid of this electrode (e.g. activity measurements, solubility product determination).

Another experiment consisted of varying P_T, at constant pH and ionic strength (0.05 M borax buffer pH 9.25), in the range 10^{-2}—10^{-5} M P_T. These results are given in Fig. 2.

Interfering ions

The response of the electrode was tested in the presence of sulfate, nitrate, chloride, polyphosphate and sodium trimetaphosphate. The concentration of the anion tested was varied from 10^{-5} to 10^{-2} M with $P_T = 10^{-2}$ at pH around 7. None of these anions interfered except chloride. Chloride interference is to be expected on the basis of the solubility product of silver chloride.

It can be concluded that the electrode behaves in accordance with the theoretical predictions, and that it can measure total phosphate down to 10^{-5} M P_T.

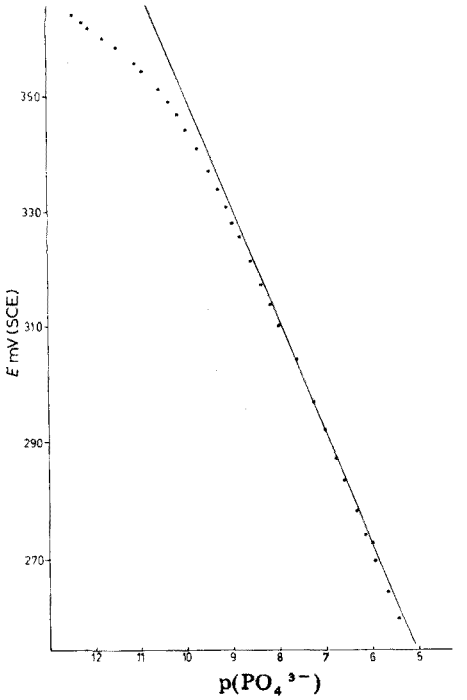

Fig. 1. (left) Negative logarithm of the PO_4^{3-} activities as a function of the measured potential (mV vs. SCE). The points are the data measured at $P_T = 10^{-3}$ at different pH values ($4.59 < pH < 9.32$). The $p\alpha_H$ values of Table 1 were used to convert total phosphate to a_p. The straight line is drawn according to eqn. (2).

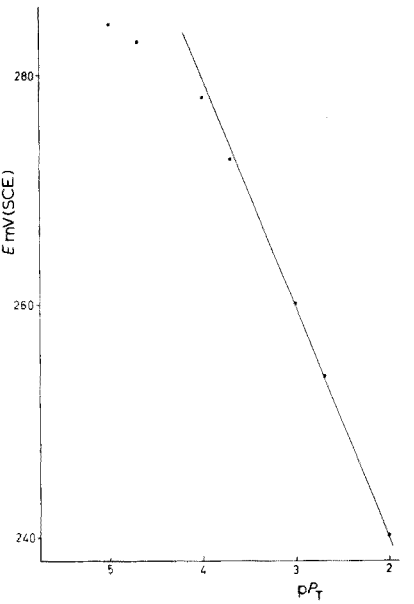

Fig. 2. (right) The negative logarithm of total phosphate as a function of the measured potential (mV vs. SCE). All solutions contained 0.05 M borax which resulted in a pH of 9.25. The straight-line portion has a slope of 19.6 mV/pP_T.

The authors thank E. van Loenen for the experimental work. One of us (W. H. v. R.) thanks the Commission on Manure and Odour Problems in Animal Husbandry for financial support.

REFERENCES

1 E. Pungor, K. Toth and J. Havas, Mikrochim. Acta, 4 (1966) 689.
2 G. Rechnitz, Z. F. Lin and S. B. Zamochnik, Anal. Lett., 1 (1967) 29.
3 G. G. Guilbault and P. J. Brignac, Jr., Anal. Chem., 41 (1969) 1136.
4 F. R. Shu and G. G. Guilbault, Anal. Lett., 5 (1972) 559.
5 M. Nanjo, T. J. Rohm and G. G. Guilbault, Anal. Chim. Acta, 77 (1975) 19.
6 G. G. Guilbault and M. Nanjo, Anal. Chim. Acta, 78 (1975) 69.
7 I. Novozamsky and W. H. van Riemsdijk, patent no. 75.15205 The Netherlands
8 A. K. Covington, in R. Durst (Ed.), Ion-selective Electrodes, N.B.S. Spec. Publ. 314, Washington, 1969, Chap. 4.
9 J. Růžička and C. G. Lamm, Anal. Chim. Acta, 54 (1971) 1.

10 J. Růžička, C. G. Lamm and J. Chr. Tjell, Anal. Chim. Acta, 62 (1972) 15.
11 R. Flatt and G. Brunisholz, Anal. Chim. Acta, 1 (1947) 124.
12 L.G. Sillen and A.C. Martell, Stability Constants of Metal–Ion Complexes, 2nd. edn, Chem. Soc. Spec. Publ. 17., London, 1964.
13 C. W. Davies, Ion Association, Butterworth, London, 1962, p. 41.

Analytica Chimica Acta, 85 (1976) 47—53

THE DETECTION LIMIT OF THE ORION IODIDE/SILVER ION-SELECTIVE ELECTRODE

J. KONTOYANNAKOS, G. J. MOODY and J. D. R. THOMAS

Chemistry Department, UWIST, King Edward VII Avenue, Cardiff CF1 3NU, Wales (Great Britain)

(Received 27th January 1976)

SUMMARY

The solid-state Orion 94-53A iodide/silver ion-selective electrode can be calibrated with a linear near-Nernstian response down to ca. 10^{-7} M with respect to iodide and silver ions by appropriate spiking of water that must be nitrogen-saturated for iodide ions. The data suggest that the detection limits for the two ions are dictated by the solubility of the membrane material rather than an alternative mechanism based on silver defects. Data in the region near the detection limit of this silver sulphide—silver iodide membrane electrode indicate a solubility product of ca. 10^{-15} M^2 l^{-2} for the silver iodide in these membranes.

The detection limits quoted for solid-state ion-selective electrodes vary according to the way they are defined [1] and depend ultimately on the solubility product, K_{so}, of the membrane sensor material [2—16]. However, factors such as the adsorption of primary ions on container walls [17], sensor surface contamination [13], interference from supporting electrolytes [3—5, 12, 13, 18], and solid-state defects [19] can also contribute to detection limits.

Ion-selective electrodes have been used to determine the solubility product of their own solid sensor membrane materials, either by potentiometric titration [3] or by direct calibration [2, 8, 11—15, 20] against standards. The ease with which the ultimate detection limit and data for such determinations can be assessed, depends largely on the chemical properties of the primary ion and on the actual linear detection limit of the ion-selective electrode which in most cases is around 10^{-6} to 10^{-5} M. This paper concerns the experimental problems associated with the direct determination of the ultimate detection limits of an Orion 94-53A iodide/silver ion-selective electrode and the solubility product of the silver iodide in the silver iodide—silver sulphide sensor disc.

EXPERIMENTAL

The response profile of the Orion 94-53A iodide-selective electrode was studied with an Orion 90-02 double-junction saturated calomel reference electrode, and a Beckman Research millivoltmeter reading to ±0.1 mV and coupled to a Servoscribe chart recorder. All measured solutions were contained in 250-cm^3 three-necked flasks. Deionized water or solutions (150 cm^3 at 25 ± 0.1 °C) were saturated and continuously stirred with either white-spot nitrogen previously scrubbed with alkaline pyrogallol, or carbon dioxide-free oxygen or air. Calibration standards were prepared by either serial dilution or spiking from an Agla micrometer syringe burette.

Solutions were prepared from AR ascorbic acid, potassium iodide, potassium nitrate or silver nitrate in deionized water.

RESULTS AND DISCUSSION

Calibration with iodide and silver ion standards

The potential response, E, of the Orion 94-53A ion-selective electrode to iodide of activity, a_I, is given by the Nernst expression

$$E = E' - S \log a_I \qquad (1)$$

where S for Nernstian response is $2.303RT/F$ and E' is a constant whose value is the cell potential at $a_I = 10^0$ M. All ion-selective electrodes exhibit a linear response on decreasing the activity of the primary ion until the linear detection limit is reached; the response then becomes increasingly sub-Nernstian, and eventually the potential becomes essentially constant at, and beyond, the ultimate detection limit regardless of dilution (Fig. 1).

It is usually quite easy to construct an E vs. a_i plot for ion-selective electrodes because the primary ions, i, are chemically stable and the linear detection limit frequently lies around 10^{-5}—10^{-4} M. In cases of low predicted detection limits, notably for the sulphide/silver ion-selective electrode [11] with a detection limit around 10^{-17} M, it is not physically feasible to prepare the sulphide, or indeed silver, standards by serial dilution techniques much below 10^{-6} M. The facile aerial oxidation of sulphide ion is another complicating factor although the use of antioxidants and saturation of solutions with scrubbed nitrogen is of considerable assistance.

For the silver/iodide ion-selective electrode, the ultimate detection limit is predicted from the frequently quoted solubility product of ca. 10^{-16} M^2 l^{-2}, to be ca. 10^{-8} M. The oxidation of iodide according to

$$2I^- + \tfrac{1}{2}O_2 + 2H_3O^+ \rightarrow I_2 + 3H_2O \qquad (2)$$

poses no serious problems regarding direct calibration with iodide standards down to 10^{-5} M but with ascorbic acid antioxidant or nitrogen saturation the linear calibration can be extended to 10^{-6} M.

The considerable potential increase (ca. 160 mV) observed by Morf et al.

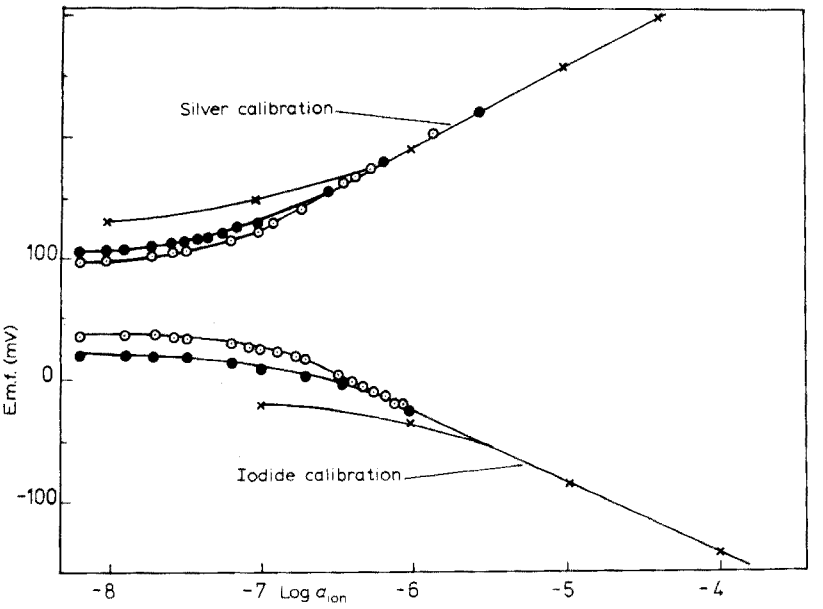

Fig. 1. The calibration of the Orion 94-53A iodide/silver ion-selective electrode below 10^{-4} M in silver and iodide solutions at 25 °C. ×, serial dilution; ○, spiking into water; •, spiking into 0.5 M KNO_3.

[19] with electrodes made from pressed discs of silver iodide on changing from 10^{-5} M to 10^{-6} M iodide standards was attributed to crystal defects, but the difference may indicate a simple oxidation effect (eqn. 2) which shifts the cell-e.m.f.s for iodide to more positive values [21].

In the present study, the steady —77-mV potential observed in 10^{-5} M iodide solution saturated with nitrogen changed to —62 mV within 45 min of switching to air, but in an identical run with ascorbic acid as antioxidant this oxygen—iodide reaction was effectively delayed for 60 min. Similar e.m.f. profiles have been reported [11] for the Orion 94-32A sulphide-selective electrode where the oxygen effect can lead to larger potential changes owing to the lower detection limit of the electrode and the greater sensitivity of sulphide to oxidation.

To extend the calibration investigation below 10^{-6}—10^{-5} M levels of iodide and silver ions, the electrode assembly was first immersed in deionized water, which for iodide calibrations was continuously saturated with pure nitrogen. Iodide or silver ion spikes (from 1 μl to 150 μl), as appropriate, were then introduced from an Agla syringe burette containing silver ion or nitrogen-saturated iodide solutions (10^{-1}, 10^{-2} or 10^{-3} M) and the potentials corresponding to each increment were plotted (Fig. 1). In this way the linear near-Nernstian detection limit for both silver and iodide ions can be extended to ca. 10^{-7} M, thus confirming the value of the spiking technique [11] as a

simple means of offsetting contamination and of preventing sample oxidation during dilution of calibration standards. Also, as for the sulphide electrode [11], the presence of silver defects in the membrane surface does not appear to play the extensive part in governing detection limits that has been suggested by other workers [19]. This effect could be due to excess of soluble silver ions remaining in the silver sulphide sensor material precipitated with excess silver nitrate [22].

Behaviour of the electrode in water

When the Orion 94-53A iodide/silver ion-selective electrode is immersed in nitrogen-saturated water, the equilibrium potential vs. the reference electrode reaches a mean e.m.f. of +75 mV but with a large standard deviation of ±46 mV. The mean e.m.f. of +75 mV is close to that which can be deduced from the intersection of the linear portions of the calibration curves for silver and iodide ions (Fig. 1) and is also similar to the ca. +80 mV corresponding to the calibration intersection for the iodide electrode in the work of Morf et al. [19], who used a reference electrode similar to that used here.

It is interesting to note the effect of oxygen and nitrogen on the e.m.f. when the electrode system is immersed in deionized water, and the only iodide in the system originates from the sensor dissolution processes. For example, when pure nitrogen was admitted to the water, a steady potential of +32.8 mV was recorded within 60 min (Fig. 2, point A), but within a few minutes of switching from nitrogen to oxygen (Fig. 2, point B), the mV—pH profile changes in accordance with eqn. (2). This Δ mV—ΔpH cycle of events can be qualitatively repeated by switching between oxygen and nitrogen, but as emphasized above by the large standard deviation of the equilibrium e.m.f., the initial potentials in nitrogen-saturated water in different experiments fall into a wide range.

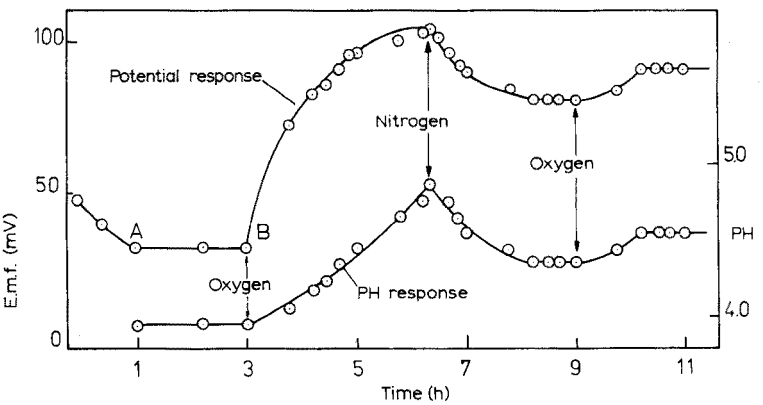

Fig. 2. The pH—potential response cycle of the Orion 94-53A iodide/silver ion-selective electrode in deionized water saturated with nitrogen or oxygen at 25 °C.

Solubility product of silver iodide

The e.m.f. vs. iodide and silver ion data can be variously treated to compute the solubility product of silver iodide. For example, the intersection of the linear portions of the calibration curves suggests detection limits of $2 \cdot 10^{-8}$ M for silver or iodide ions, which would indicate a K_{so} value of $4 \cdot 10^{-16}$ M^2 l^{-2} for silver iodide.

Alternatively, the K_{so} value for silver iodide can be calculated from the e.m.f. data in the region where the electrode begins to fail, i.e. where the response becomes non-linear because of the finite solubility of the membrane material.

The total iodide, T_I, sensed by the electrode is the sum [12] of the sample iodide, S_I, and that provided by the sensor membrane, M_I. In the linear calibration regions $S_I > M$, in the "fail" region $S_I \approx M_I$ and at, and beyond, the ultimate response region $S_I < M_I$. It can be easily shown [12] that when $S_I \approx M_I$,

$$T_I = S_I + \left(\frac{K_{so}}{\gamma_{Ag} \cdot \gamma_I}\right) \cdot \frac{1}{T_I} \tag{3}$$

where γ terms represent activity coefficients. In potassium iodide standards below ca. 10^{-3} M, $\gamma \approx 1$ and eqn. (3) simplifies to

$$T_I - S_I = \Delta T_I = K_{so}/T_I \tag{4}$$

which can be used to evaluate the solubility product of silver iodide graphically [12]. The appropriate T_I values can be established for any cell potential values (E) recorded for the corresponding S_I values of each standard solution from

$$-\log T_I = (E - E')/S \tag{5}$$

The fact that the ΔT_I vs. T_I^{-1} plots (Fig. 3) are linear for both neat potassium iodide (slope = $1.05 \cdot 10^{-15}$ M^2 l^{-2}, and $r = 0.998$) and potassium iodide in 0.5 M potassium nitrate (slope = $0.97 \cdot 10^{-15}$ M^2 l^{-2} and $r = 0.991$) possibly establishes the solubility of the sensor membrane material to be the principal, perhaps the sole, factor which fixes the ultimate detection limit for this particular electrode. Parthasarathy et al. found [12] that the Beckman solid-state chloride ion-selective electrode presented a similar linear ΔT_{Cl} vs. T_{Cl}^{-1} pattern in a 10^{-2} M sodium nitrate background but which did not pass through the origin when calibrated in 0.5 M sodium nitrate background solutions. This behaviour was interpreted in terms of either interference from, or chloride impurities in, the higher sodium nitrate background electrolyte, there being little difference in the evaluated solubility product.

A similar ΔT_{Ag} vs. T_{Ag}^{-1} plot was obtained on calibrating the Orion 94-53A electrode in pure silver nitrate and silver nitrate in 0.5 M potassium nitrate (Fig. 3). The slopes correspond to $K_{so} = 1.14 \cdot 10^{-15}$ and $1.02 \cdot 10^{-15}$ M^2 l^{-2}, respectively.

Differences in the solubility product values for freshly precipitated

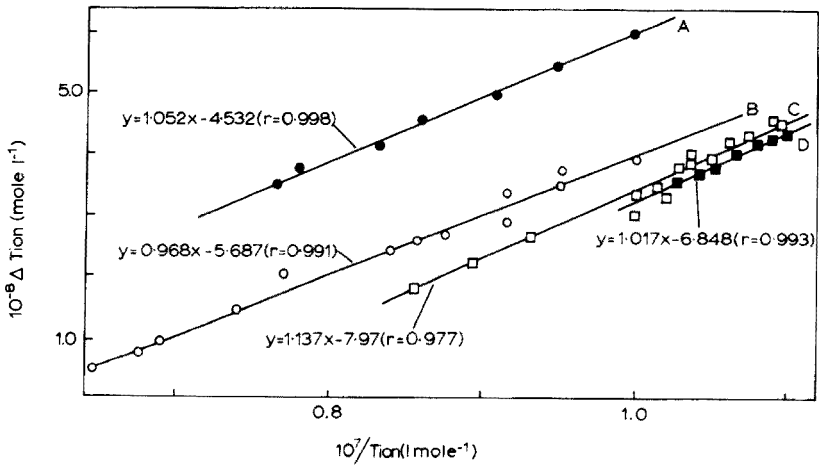

Fig. 3. Some ΔT_{ion} vs. T_{ion}^{-1} plots for the Orion 94-53A iodide/silver ion-selective electrode at 25 °C.
A. Aqueous iodide. $y = 1.052x - 4.532$ ($r = 0.998$).
B. Aqueous iodide—0.5 M KNO_3. $y = 0.968x - 5.687$ ($r = 0.991$).
C. Aqueous silver(I)—0.5 M KNO_3. $y =$ ~~1.017x − 6.848 (r = 0.993)~~. 1.137x − 7.97 (
D. Aqueous silver(I). $y =$ ~~1.137x − 7.97 (r = 0.977).~~
P. 3 Jan. 1977 → = 1.017x − 6.848 (r = 0.993)

lanthanum fluoride and the same material as the sensor membrane of the lanthanum fluoride ion-selective electrode are of the order of 10^{10} [8]. Differences encountered in the present study could be due to similar thermodynamic effects; moreover, the membrane also contains considerable silver sulphide in addition to silver iodide. Thus a literature value [23] for K_{so}(AgI) = $8.3 \cdot 10^{-17}$ M^2 l^{-2} is to be compared with values ranging from $0.97 \cdot 10^{-15}$ to $1.14 \cdot 10^{-15}$ M^2 l^{-2} in this work. This is also to be seen in the light of the work of Woodson and Liebhafsky [20] who reported differences of ca. 10^3 M^2 l^{-2} between the literature values and those calculated from extrapolated e.m.f. vs. iodide activity plots when the Orion 94-53A ion-selective electrode was used at 25° and 50 °C.

J. Kontoyannakos thanks the National Technical University of Athens for paid leave of absence.

REFERENCES

1 G. J. Moody and J. D. R. Thomas, Sel. Annu. Rev. Anal. Sci., 3 (1973) 59.
2 M. S. Frant and J. W. Ross, Science, 154 (1966) 1553.
3 J. J. Lingane, Anal. Chem., 39 (1967) 881.
4 E. W. Baumann, Anal. Chim. Acta, 54 (1971) 189.
5 J. Růžička and C. G. Lamm, Anal. Chim. Acta, 54 (1971) 1.
6 J. Buffle, N. Parthasarathy and D. Monnier, Anal. Chim. Acta, 59 (1972) 427.
7 E. Pungor, K. Tóth and J. Havas, Mikrochim. Acta, (1966) 689.
8 P. A. Evans, G. J. Moody and J. D. R. Thomas, Lab. Pract., 20 (1971) 644.

9 E. Pungor, K. Tóth and J. Havas, Acta Chim. Acad. Sci. Hung., 58 (1968) 16.
10 R. P. Buck, Anal. Chem., 40 (1968) 1432.
11 D. J. Crombie, G. J. Moody and J. D. R. Thomas, Anal. Chim. Acta, 80 (1975) 1.
12 N. Parthasarathy, J. Buffle and D. Monnier, Anal. Chim. Acta, 68 (1974) 185.
13 J. Buffle, N. Parthasarathy and W. Haerdi, Anal. Chim. Acta, 68 (1974) 253.
14 T. S. Hseu and G. A. Rechnitz, Anal. Chem., 40 (1968) 1054.
15 D. C. Müller, P. W. West and R. H. Müller, Anal. Chem., 41 (1969) 2038.
16 J. N. Butler, in R. A. Durst (Ed.), Ion-Selective Electrodes, National Bureau of Standards Special Publication No. 314, 1969.
17 R. A. Durst and B. T. Duhart, Anal. Chem., 42 (1970) 1002.
18 E. Mesmer, Anal. Chem., 40 (1968) 443.
19 W. E. Morf, G. Kahr and W. Simon, Anal. Chem., 46 (1974) 1538.
20 J. H. Woodson and H. A. Liebhafsky, Anal. Chem., 41 (1969) 1894.
21 M. N. Khayat, Ph.D. Thesis, University of Manchester, 1974.
22 R. P. Buck, Anal. Chem., in press.
23 Handbook of Chemistry and Physics, 52nd edn., Chemical Rubber Publishing Co., Cleveland, Ohio, 1970.

·= 0.977)

Analytica Chimica Acta, 85 (1976) 55—60

AN ENZYME REACTOR ELECTRODE FOR DETERMINATION OF AMINO ACIDS

GILLIS JOHANSSON, KERSTIN EDSTRÖM and LARS ÖGREN

Department of Analytical Chemistry, University of Umeå, S-90187 Umeå (Sweden)

(Received 11th February 1976)

SUMMARY

L-Leucine can be determined with an enzyme reactor electrode containing L-amino acid oxidase immobilized with glutaraldehyde to glass. The reactor also contains immobilized catalase which splits the hydrogen peroxide formed. Oxygen for the reaction is also supplied by adding hydrogen peroxide to the samples. The electrode is an ammonia gas sensor. The calibration curve is strictly linear with Nernstian slope between $3 \cdot 10^{-5}$ and 10^{-3} M leucine.

It was recently shown [1] that an enzyme reactor electrode for urea has various advantages over other types of enzyme electrodes. Urease is known to have a very high turnover rate and the kinetics are relatively simple. In order to test the reactor electrode concept further, an enzyme reaction with complicated kinetics and dependence on two substrates was selected. L-Amino acid oxidase has been used earlier in enzyme electrodes [2—5], and shows a very complex reaction pattern [6—8]

$$R{-}\underset{\underset{COOH}{|}}{CH}{-}NH_2 + E{-}(FAD)_2 \rightleftharpoons R{-}\underset{\underset{COOH}{|}}{C}{=}NH + E\begin{matrix}FAD\\ \diagup\\ \diagdown\\ FADH_2\end{matrix} \qquad (1)$$

$$R{-}\underset{\underset{COOH}{|}}{C}{=}NH + H_2O \rightleftharpoons R{-}\underset{\underset{COOH}{|}}{C}{=}O + NH_3 \qquad (2)$$

$$E\begin{matrix}FAD\\ \diagup\\ \diagdown\\ FADH_2\end{matrix} + O_2 \rightarrow E{-}(FAD)_2 + H_2O_2 \qquad (3)$$

$$R{-}\underset{\underset{COOH}{|}}{CH}{-}NH_2 + E\begin{matrix}FAD\\ \diagup\\ \diagdown\\ FADH_2\end{matrix} \rightarrow R{-}\underset{\underset{COOH}{|}}{C}{=}NH + E{-}(FADH_2)_2 \qquad (4)$$

The enzyme contains two moles of flavin adenine dinucleotide (FAD) per mole of enzyme. The first is readily reduced (eqn. 1) and reoxidized (eqn. 3). The second FAD molecule can also be reduced in the presence of excess of substrate (eqn. 4), but its reoxidation is slow. Consequently, the enzyme is severely inhibited by excess of substrate. If the normal reoxidation is retarded

by oxygen deficiency, conversion to the fully reduced enzyme complex will be favoured. High substrate concentrations as well as oxygen deficiency are therefore expected to be detrimental to the operation of an enzyme reactor column.

Three methods have been used to follow the enzymatic reaction: measuring the consumption of oxygen, the production of ammonia or the production of hydrogen peroxide. Monitoring the hydrogen peroxide has some drawbacks, as it may react with the α-ketoacid in a side-reaction.

$$R{-}\underset{\underset{O}{\|}}{C}{-}COOH + H_2O_2 \rightleftharpoons R\underset{\underset{O}{\|}}{C}OH + CO_2 + H_2O \qquad (5)$$

The amount of oxygen available can be increased by using catalase

$$H_2O_2 \xrightarrow{\text{catalase}} 1/2\ O_2 + H_2O \qquad (6)$$

Oxidation of one mole of amino acid requires one mole of oxygen. If immobilized catalase is added to the column, half a mole of oxygen per mole of amino acid can be recycled.

EXPERIMENTAL

Enzyme immobilization

Purified L-amino acid oxidase from snake venom (Sigma Chemical Co., A 9378, 3—6 units/mg) was immobilized on CPG-10 controlled-pore glass (Corning Glass, pore diam. 70 nm, 120-200 mesh) as described earlier [1]. Enzyme (5 mg) in 3 ml of buffer was coupled with glutaraldehyde to 0.5 g of alkylamino-activated glass.

Catalase (5 mg; Sigma Chemical Co., C-40, 10000—25000 Sigma units/mg) was immobilized to 0.5 g of activated glass by the same procedure.

Flow system (Fig. 1)

A three-channel peristaltic pump (Pharmacia Fine Chemicals, Model P3) was used with 2.1- and 1.0-mm tubing, so that the flow could be varied over the ranges 2—32 ml h^{-1} or 0.6—9 ml h^{-1} per channel. The buffer was 0.05 M sodium phosphate containing 1 mM EDTA (pH 7.0). The enzyme reactor consisted of a PVC tube (i.d. 3.2 mm, length 45 mm) threaded at the ends to fit Altex or Chromatronix couplings for teflon tubes. The enzyme-coated glass beads were tightly packed into the column and silver frits (1/8 in. diameter with 0.015-mm holes; Reeve Angel, Cat. No. LA 230) were fitted at the ends. The connecting tubing and the heat exchanger were made of teflon (i.d. 0.5 mm; Altex Scientific, Berkeley).

The heat exchanger and the ammonia flow-through electrode (E.I.L. ammonia probe, Model 8002) were immersed in a bath thermostated at 25.0 °C. The enzyme reactor was immersed in a bath which was kept at 37 ± 1 °C in most of the experiments. The electrode was connected to a digital pH meter provided with a strip chart recorder.

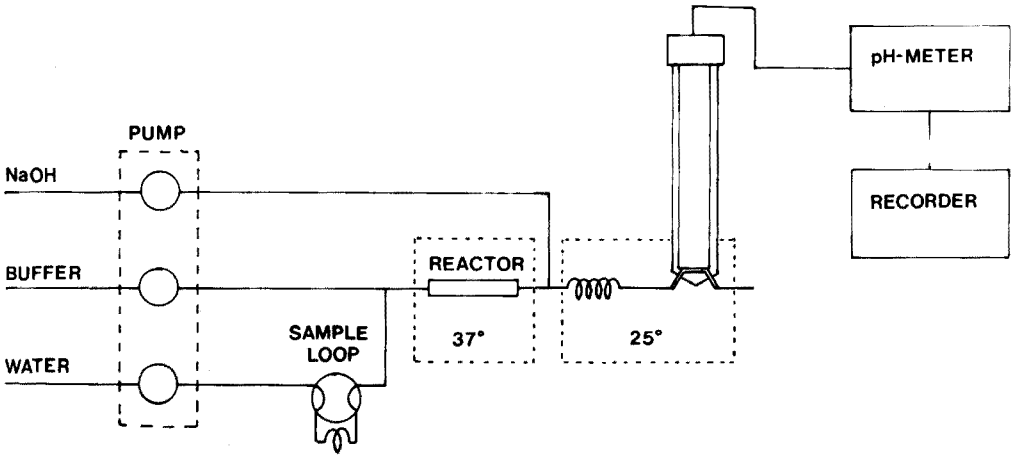

Fig. 1. Diagram of the flow system and the enzyme reactor electrode arrangement.

Samples were introduced via a sampling valve (Altex 4-way Rotary Valve, series 202) provided with a sample loop of about 2.3 ml.

Operation

A sample of amino acid was injected into the sample loop in the bypass position (see Fig. 1). In this position water was mixed with the buffer and the diluted buffer passed through the enzyme reactor to the T-joint, where it was mixed with 0.5 M sodium hydroxide solution. The alkaline solution then passed through the ammonia probe, giving a base-line on the recorder (corresponding to less than 10^{-6} M ammonia in the sample). When the flow was switched to pass through the sample loop, the sample was mixed with buffer and passed into the enzyme reactor. Under optimal conditions, an equivalent amount of ammonia was split off and measured. With samples of adequate size a steady state was attained, so that the ammonia concentration in the flow-through electrode was constant for a short time. The ammonia probe then attained equilibrium and the recorder trace was flat at the new level. The digital reading on the pH meter was noted, as it was more accurate than the recorder. When the sample had been eluted, it was followed by water, and the recorder then returned to the base-line.

RESULTS AND DISCUSSION

Tests were made with the purified as well as the crude enzyme from the venom of *Crotalus adamanteus*. The preparations made from the crude enzyme lost activity within a couple of days, whereas preparations from the purified enzyme retained adequate activity for more than two months. As there might have been some loss of FAD, an attempt was made to rejuvenate the column with FAD after a period of use, but no increase in activity could

be seen. The experiments reported below were all made with the purified enzyme.

Oxygen for reaction (3) is supplied from oxygen dissolved in the sample and the buffer. This puts an upper limit on the concentration of amino acid which can be oxidized. At equal flow rates in the sample and buffer channels, the upper limit was calculated to be $5 \cdot 10^{-4}$ M amino acid, and this was confirmed by experiment. By utilizing catalase it should be possible to extend the range to about $8 \cdot 10^{-4}$ M.

The immobilized catalase was first filled into a column and tested at room temperature. Samples of hydrogen peroxide mixed with buffer were run through the column, and the effluent was collected and analyzed spectrophotometrically at 240 nm; the amount of unreacted hydrogen peroxide was evaluated from a calibration curve. It was found that $7 \cdot 10^{-4}$ M hydrogen peroxide remained unreacted if 0.1 M hydrogen peroxide was pumped into the reactor at a flow rate of 21 ml h^{-1}. If 0.02 M hydrogen peroxide was run through the reactor, the absorption of the effluent was equal to the blank, i.e. less than 10^{-4} M hydrogen peroxide. The immobilized catalase was thus a very efficient catalyst for eqn. (6).

Immobilized L-amino acid oxidase and immobilized catalase were mixed in the proportion 3:1 and filled into the reactor. This reactor, operated at 37 ± 1 °C, was used in all experiments described below. The pH-optimum is known to depend on the substrate [7], and the range is quite wide for an amino acid such as L-leucine. Runs were made at pH 7.0, 7.6 and 8.0 which confirmed that the activity of the immobilized enzyme was practically independent of pH for L-leucine.

Table 1 shows the results obtained with samples of 1 mM L-leucine. Using an air-saturated buffer the conversion was found to be incomplete at the tested flow rates. The reason is that the oxygen concentration is so low that the enzyme becomes fully reduced, with a resulting decrease in its turnover rate. If oxygen is bubbled through the buffer, the efficiency of the reactor increases somewhat, but it is still low and depends on the flow rate. The

TABLE 1

Voltage reading of the enzyme reactor electrode when air or oxygen was flushed through the buffer

Sample	Concn. (mM)	Flow rate (ml h^{-1})	Gas	Reading (mV)
NH_4Cl	1	21	air	−2.0
L-Leucine	1	21	air	4.0
L-Leucine	1	13.5	air	0.3
L-Leucine	1	21	O_2	0.9
L-Leucine	1	13.5	O_2	−0.6
L-Leucine	0.1	21	O_2	57.5
L-Leucine	0.01	21	O_2	114.2

electrode response is 4 % lower than in the ammonia standard. Lower concentrations were also used; Table 1 shows that the response is almost Nernstian, being 58.1 mV/decade to 0.1 mM and 56.7 mV/decade between 0.1 and 0.01 mM leucine.

It is possible to increase the amount of oxygen by adding hydrogen peroxide to the sample or the buffer. If the hydrogen peroxide is added to the buffer, there will be an excess of oxygen in the absence of substrate. It was found that at most $2 \cdot 10^{-3}$ M hydrogen peroxide could be added before oxygen bubbles in the flow caused malfunction of the ammonia sensor. Hydrogen peroxide was therefore added to the samples.

A calibration curve for L-leucine was run at a flow rate of 13.5 ml h^{-1}, see Fig. 2. The samples contained hydrogen peroxide in the same concentration as the amino acid. It can be seen that the enzyme reactor electrode operates ideally between $3 \cdot 10^{-5}$ and 10^{-3} M leucine with an almost Nernstian slope, 57.7 mV/decade. The reproducibility in this range is better than 1 %. Ammonium standards are also shown, and the agreement between standard and sample is excellent at 10^{-3} and 10^{-4} M. At 10^{-5} M the rate of reaction is too low for complete conversion. As the hydrogen peroxide was added at the same concentration as the leucine the increase in oxygen pressure is very small at this concentration; a higher concentration of peroxide may increase the rate. At concentrations higher than 10^{-3} M substrate, inhibition occurs in the first part of the reactor, decreasing the overall efficiency. There are deviations from the straight line at $3 \cdot 10^{-3}$ M

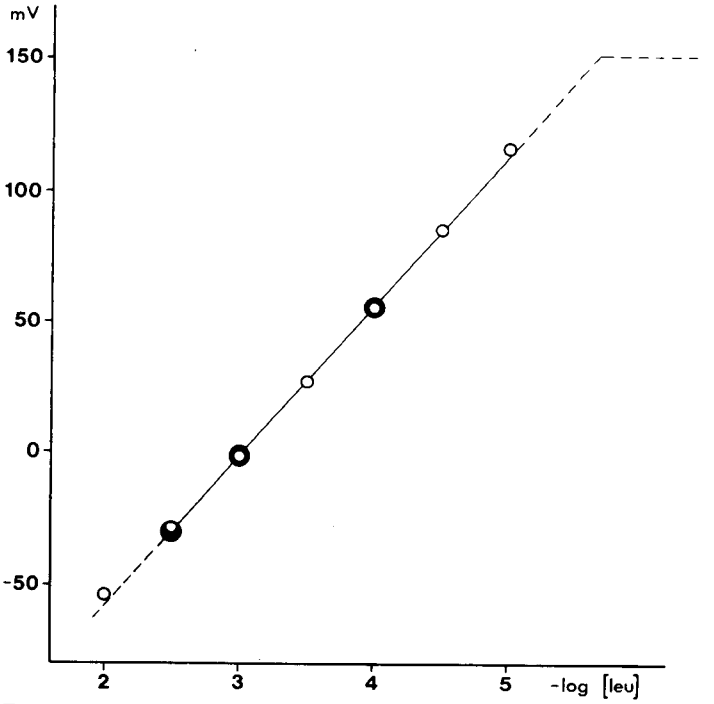

Fig. 2. Calibration curve for L-leucine(○) and for NH_4Cl standards (●).

leucine and higher. The results shown in Fig. 2 were obtained with an enzyme reactor 2.5-months old, the activity of which had decreased substantially. New columns give better performance.

The results presented above show that the enzyme reactor electrode can be used with enzymes which have a complex kinetic pattern. They also prove that by adding catalase and hydrogen peroxide an oxygen-dependent system can be used in the reactor. The device is linear in the concentration range of interest and the precision is high. When the flow is decreased sufficiently, the response is independent of flow fluctuations.

REFERENCES

1 G. Johansson and L. Ögren, Anal. Chim. Acta, 84 (1976) 23.
2 G. G. Guilbault and E. Hrabankova, Anal. Lett., 3 (1970) 53.
3 M. Nanjo and G. G. Guilbault, Anal. Chim. Acta, 73 (1974) 367.
4 G. G. Guilbault and G. Nagy, Anal. Lett., 6 (1973) 301.
5 G. G. Guilbault and G. J. Lubrano, Anal. Chim. Acta, 69 (1974) 183.
6 D. Wellner and A. Meister, J. Biol. Chem., 235 (1960) 2013; 236 (1961) 2357.
7 W. K. Paik and S. Kim, Biochim. Biophys. Acta, 96 (1965) 66.
8 T. P. Singer and E. B. Kearney, Arch. Biochem. Biophys., 29 (1950) 190.

Analytica Chimica Acta, 85 (1976) 61—68

AN IMPROVED CONDUCTIMETRIC MEASUREMENT OF CARBON DIOXIDE

PIETRO LANZA

Chemical Institute "G. Ciamician", University of Bologna, Bologna (Italy)

PIER LUIGI BULDINI

C.N.R., Lamel Laboratory, Bologna (Italy)

(Received 29th January 1976)

SUMMARY

An improved apparatus for measurement of carbon dioxide is described; it is based on the change in conductivity of a sodium hydroxide solution on absorption of carbon dioxide. The carrier gas purification unit, absorption—conductivity cell and metering system are discussed in detail. For calibration, coulometric generation of carbon dioxide from oxalic acid solution provides good precision at the low p.p.m. level. Application of the method to the analysis of gas mixtures and pure gases is described.

Increasing interest in the production of ultra-pure materials sometimes makes it imperative to determine accurately low carbon contents. Many papers have dealt with such determinations, and most of the available chemical procedures are based on the oxidation of carbon to carbon dioxide and its subsequent determination by techniques such as conductimetry [1—4], coulometry [5], gas chromatography [6], etc. Commercial equipment is available for each of these techniques, particularly for determinations by electrical conductivity measurements, but in general, they are not suitable for measuring carbon dioxide at the p.p.m. level. Only recently, a carefully elaborated apparatus [4] was described which permits conductimetric determinations of carbon in the low p.p.m. range.

The first commercial apparatus, developed by Wösthoff (Bochum), was based on the work of Koch and Malissa [2, 7], and was intended especially for metallurgical analyses. The various features of this technique have been widely examined. Holm-Jensen [8, 9] examined the cell design, correlating it to the efficiency of the carbon dioxide absorption in the alkaline solution. Schmidts and Bartscher [10] examined the conductivity-meter signal as a function of the amount of carbon dioxide absorbed and some other parameters, and later [11] studied the composition of the alkaline solution in relation to the efficiency and rapidity of carbon dioxide absorption. Waclawek [12] described a coulometric testing device for the equipment for the carbon

determination. This device, which is very practical and accurate, was considered by Pribyl [13], but seems to have been neglected by other authors who described methods of calibration. Usually, the analysis of known standard alloys [1, 4], the combustion of pure organic standards [1] or the use of gas mixtures having a known content of carbon dioxide, has been recommended for checking performance.

The problem is still of interest. The present paper describes a study of an apparatus based on electrical conductivity measurements which is relatively cheap, but sensitive and practical, especially with regard to rapid checking during routine analyses. In the method, trace quantities of carbon dioxide, arising from a combustion furnace or any other source, and present in a carrier gas, must be completely absorbed in a suitable alkaline solution; the resulting change in conductivity is correlated to the quantity of absorbed carbon dioxide by suitable calibration, as in other similar procedures.

EXPERIMENTAL

Figure 1 shows schematically the suggested equipment, which consists of four main parts: (a) purification unit, (b) calibration device, (c) absorption–conductivity cell and (d) recording set.

Gas purification

The carrier gas can be an inert gas (nitrogen or argon) or oxygen; if the sample has to be burnt in a furnace or similar device, the flow can be connected directly to the conductivity apparatus. In all cases, very efficient

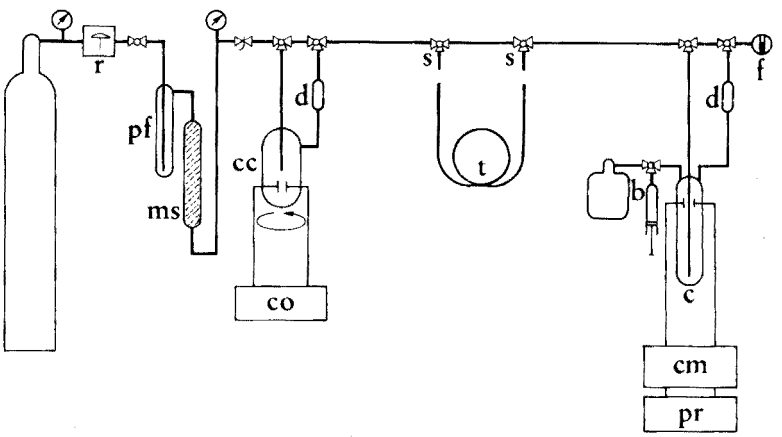

Fig. 1. Apparatus.
r — pressure regulator. pf — gas bubbler (filled with sulfuric acid). ms — molecular sieves. cc — calibration cell. co — coulometer. d — desiccant (silica gel). s — PTFE stopcocks. t — calibrated tube. b — motor-syringe buret. c — absorption-conductivity cell. cm — conductivity meter. pr — potentiometric recorder. f — flow meter.

purification is necessary to maintain the blank determinations at low levels. Apart from carbon dioxide itself, possible interfering impurities are any substances that give ionic species in alkaline solutions, e.g. sulfur dioxide, nitrogen oxides, halogens, etc., and any substances that can generate carbon dioxide (e.g. carbon monoxide or hydrocarbons) or sulfur dioxide on combustion in oxygen.

When an inert carrier gas is used, it is sufficient to pass it through a column filled with molecular sieve (Union Carbide; type 5A, 1/16 in. pellets), which removes carbon dioxide, hydrocarbons, etc.

If oxygen is used, an auxiliary furnace with a catalyst for burning impurities must be included before the molecular sieve column. There are many possible catalysts; in the present work, a 600-mm long quartz tube (i.d. 25—30 mm) filled with the conventional 5 % platinized asbestos (J. T. Baker) and heated at 700 °C, proved effective.

Even with the purest carrier gas, the base-line recorded at high sensitivity always shows a residual positive or even negative slope, denoting a decrease or increase in the conductivity of the alkaline solution. This effect, which has already been pointed out [1, 15], cannot be ascribed to residual impurities or to small temperature drifts. The positive residual slope may be caused by some action of the alkaline solution on the glass cell; the negative slope may arise from gradual concentration of the solution by evaporation during passage of a dry carrier gas, when this cannot be previously saturated.

This residual slope cannot be compensated easily; however, its magnitude corresponds to an apparent absorption of not more than ± 3 μg CO_2 per hour, and changes only very slowly, so that accurate definition of analytical steps or slopes is still possible.

Absorption-conductivity cell

The absorption cell must absorb completely all the carbon dioxide present even at very low concentrations in the carrier gas. The conventional principle of a long helical gas passage, connected to the electrode chamber, was used. The cell (Fig. 2) has the following features: from inlet A, the gas passes through sintered-glass disk B (20—40 μm), to ensure intimate contact with the absorption solution; the helix is about 170 cm long (4 mm i.d.), which suffices for complete absorption. To prove this, a second absorption cell was attached behind the first one; no change occurred in the second solution. From the upper reservoir, the solution runs into the electrode chamber into which is fitted the conductivity cell D (Philips PW 9512/01; cell constant 0.67 cm^{-1}). From this chamber, the solution is sucked to the lower part E of the cell by the pumping action of the gas bubbles in the helix.

About 45 ml of alkaline solution is required to fill the cell and the total amount is circulated through the cell about once every 30 s.

The cell is connected through joint C to a flow meter (Brooks Instruments; type B215AA, float sapphire) and to a motor-syringe buret (Metrohm E 415); the latter makes it easy to replace exhausted solution, which can be pumped

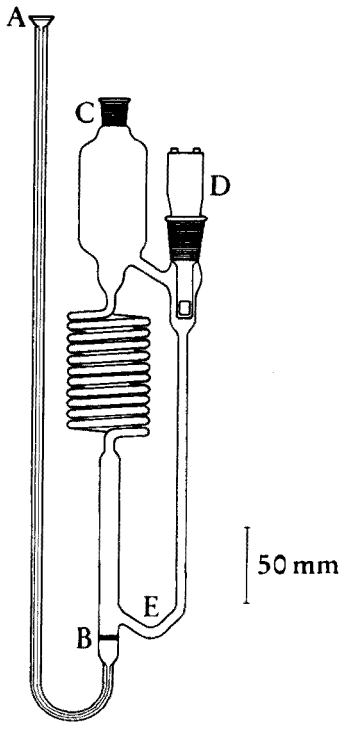

Fig. 2. Absorption—conductivity cell.
A. Gas inlet tube. B. Sintered glass disk. C. Connexion to flow meter and buret.
D. Conductivity cell.

out via tube A. A drying tube is inserted before the flowmeter, to prevent water condensation.

The cell is clamped at the top, so that the part containing the alkaline solution can be immersed in a thermostated water bath at about 30 °C. The temperature must be kept constant within ±0.01 °C, to avoid variations in the conductance of the solution. A temperature of about 30 °C was chosen because of the relatively slow absorption of carbon dioxide in the very dilute alkaline solution [11].

Water condensation on the wall of the cell above the thermostated bath was prevented by heating with a low infra-red lamp. This avoids the noise caused by drops falling into the solution and the consequent small sudden change in concentration.

Various absorption solutions, such as ammonia and aminoethanol, have been suggested in the literature but tests showed that the best absorbent is dilute sodium hydroxide solution. Its optimal concentration depends on the amount of carbon dioxide to be absorbed, with the consideration that the relative change in conductance is greater in dilute solutions. Theoretically a $2 \cdot 10^{-3}$ M sodium hydroxide solution can absorb, with an almost linear change

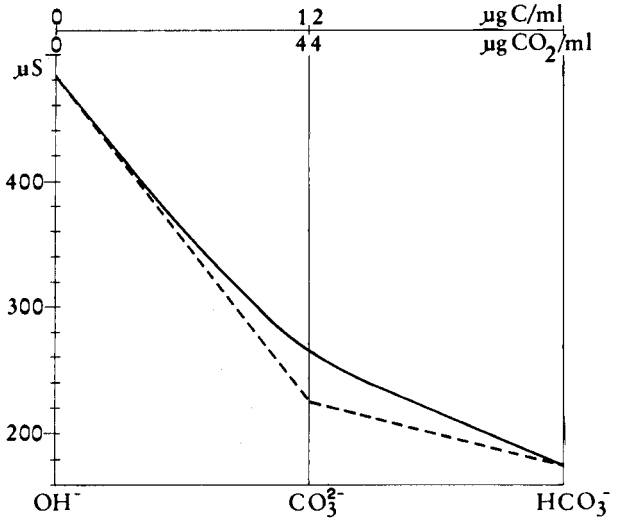

Fig. 3. Calculated change in a $2 \cdot 10^{-3}$ M sodium hydroxide solution on absorption of carbon dioxide (at 25 °C). – – – – not considering hydrolysis. ———— considering hydrolysis.

in conductance, about 20—25 µg CO_2 ml^{-1} (see Fig. 3). Practically, an initial carbon dioxide content in the alkaline solution can reduce the capacity to about half the calculated value. In the range of linear response, the absorption of 1 µg of carbon dioxide in 45 ml of the $2 \cdot 10^{-3}$ M sodium hydroxide solution decreases the conductivity by about 0.03 %.

Conductivity bridge

The bridge consists of a precision conductivity meter (Philips PW 9501/01) that permits measurement of very small conductivity changes when it is connected to an external reference resistance with a fixed suitable value (Hatfield 11,111-ohm decade box with a 0.1 % precision). Since the meter is based on an operational amplifier, the signal change is proportional to the conductivity variation and to the reference resistance.

In order to avoid the noise arising from imperfect compensation of two conductivity cells, which is difficult in the high-sensitivity range, a reference resistance box was preferred, and the measurements were made in an unbalanced bridge condition. Before recording is done, the output signal is brought to the end of the conductivity-meter scale, by adjusting the reference resistance, i.e. the bridge balance. The slight change towards the balancing condition caused by the carbon dioxide absorption, is then recorded with a potentiometric recorder (Amel model 867) at a 2-mV full-scale range.

All the external connections should be made with co-axial cables to reduce noise. For the same reason, a small earthing screen is set up in the thermostated bath around the electrode chamber of the cell.

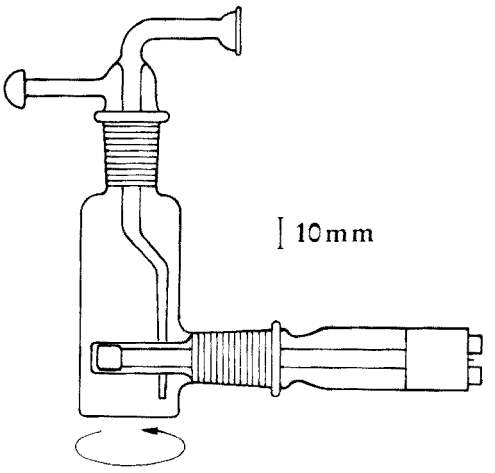

Fig. 4. Calibration cell.

Calibration device

The apparatus is calibrated by introducing into the conductance cell exactly known amounts of carbon dioxide. A practical procedure is based on coulometric generation of carbon dioxide from an oxalic acid solution, according to the well known reaction: $C_2H_2O_4 \rightarrow 2\ CO_2 + 2\ e^- + 2\ H^+$, which has been studied electrochemically [13, 16], and is quantitative in an acid medium.

The cell used as the calibration device (Fig. 4) permits the electrolysis of the oxalic acid solution with magnetic stirring while the carrier gas is flowing. The cell is provided with two platinized platinum electrodes (Philips PW 9512/01) and is filled with 0.1 M oxalic acid solution. Electrolysis is done at a suitable constant current, the current and time being measured with a coulometer (Amel model 831). A current of 0.804 mA was selected; this causes the oxidation of 0.10 μg C s^{-1} (i.e. 0.37 μg of carbon dioxide).

The output current of the coulometer was checked potentiometrically with a standard resistance, and was found to be accurate within ±0.1 %; the electrolysis time was measured with an accuracy of ±0.1 s.

A calibration curve obtained under the conditions described, was linear over the range 0—8 μg of carbon, which corresponded to chart measurements of 0—170 mm. The sensitivity of the method was 21.5 ± 0.74 (standard deviation) mm per μg of carbon, after about one hundred measurements had been made under the conditions described above.

The strength of the alkaline solution changes during a series of experiments, so that the sensitivity also varies (as shown in Fig. 3); for this reason, it is advisable to check the calibration during each set of measurements.

SOME ANALYTICAL APPLICATIONS

The apparatus was found to be particularly suitable for analyses of pure and ultra-pure gases.

Carbon dioxide was determined in air and in some pure gases supplied by I.G.T. (Industria Gas Tecnici, Pisa). Pure (PP) oxygen, pure and ultra-pure (UPP) nitrogen and pure argon were analyzed simply by connecting the tank to the carrier gas line; see Fig. 1, at (s). After the apparatus had reached equilibrium (constant slope of the recorded base-line), the response was checked with the calibration device. When all the coulometric carbon dioxide had been absorbed, and the step was fully developed, the previous slope of the base-line being reached in 5—10 min, the unknown gas was introduced, and its flow was regulated to the usual value of 100—150 ml min^{-1}. When the new slope, i.e. the sample slope, was clearly defined (normally, within 15—20 min), the flow was stopped and the calibration could be checked again.

Gas mixtures with a relatively high carbon dioxide content, e.g. air, can be analyzed by introducing into the carrier gas line a known volume of the gas, from a gas-tight syringe or, better by connecting a calibrated tube, as a by-pass, to the main gas line; see Fig. 1, at (t).

The results obtained are shown in Table 1.

TABLE 1

Analysis of pure and ultra-pure gases

Tank No.	I.G.T. gas	Residual slope (mm h^{-1})	Sample slope (mm h^{-1})	Flow (ml min^{-1})	Sens.[a] (mm μg^{-1})	CO_2 (p.p.m.)
06817	N_2 UPP	0	66	130	21.5	0.76
09200	N_2 UPP	12	33	100	21.0	0.32
01217	N_2 UPP	0	13	120	18.0	0.19
01217		24	38	110	21.5	0.20
29716	O_2 PP	6	384	130	17.5	5.41
29716		12	314	90	21.5	5.21
17834	Ar PP	0	18	120	18.5	0.26
17834		0	20	120	19.5	0.28

[a]The sensitivity, given as mm per μg C, depends on the exhaustion of the sodium hydroxide solution.

The carbon dioxide content of laboratory air was also determined; a calibrated PTFE tube (i.d. 4 mm) fitted with glass ball-joints was used, and its volume was determined previously by weighing the water content. The tube volume was 7.70 ml. This volume gave chart steps about 50 mm long which were completely developed in less than 5 min. The total acid impurity, given as carbon dioxide, was found to be 0.068 % (±0.0007).

The authors wish to thank Prof. Dario Nobili for his helpful discussions and suggestions and Prof. Giovanni Semerano, Director of the "G. Ciamician" Chemical Institute, for his encouraging remarks and friendly criticism.

REFERENCES

1 J. E. Still, L. A. Daucey and R. C. Chirnside, Analyst (London), 79 (1954) 4.
2 H. Malissa, Mikrochim. Acta (Wien), 1957 553.
3 W. Bartscher and D. Pel, Anal. Chim. Acta, 68 (1974) 197.
4 P. Schoch, E. Grallath, P. Tschöpel and G. Tölg, Z. Anal. Chem. 271 (1974) 12.
5 H. J. Boniface and R. H. Jenkins, Analyst (London), 96 (1971) 37.
6 D. L. Fanter and C. J. Wolf, Anal. Chem., 45 (1973) 565.
7 W. Koch and H. Malissa, Arch. Eisenhüttenwes., 27 (1956) 695.
8 Ib Holm-Jensen, Anal. Chim. Acta, 23 (1960) 13.
9 Ib Holm-Jensen, Anal. Chim. Acta, 29 (1963) 365.
10 W. Schmidts and W. Bartscher, Z. Anal. Chem., 181 (1961) 54.
11 W. Bartscher and W. Schmidts, Z. Anal. Chem., 203 (1964) 168.
12 J. Waclawek, Chim. Anal. (Paris), 40 (1958) 247.
13 M. Pribyl, Z. Anal. Chem., 217 (1966) 7.
14 E. J. Merkle and J. W. Graab, Anal. Chem., 38 (1966) 159.
15 R. S. Smith and W. Wilson, Lab. Pract., 16 (1967) 1377.
16 F. Salzer, Z. Elektrchem., 49 (1902) 122.

Analytica Chimica Acta, 85 (1976) 69—74

THE DETERMINATION OF CARBON IN SILICON BY WET OXIDATION AND ELECTRICAL CONDUCTIVITY MEASUREMENT*

PIETRO LANZA

Chemical Institute "G. Ciamician", University of Bologna, Bologna (Italy)

PIER LUIGI BULDINI

C.N.R., Lamel Laboratory, Bologna (Italy)

(Received 29th January 1976)

SUMMARY

A method for the determination of carbon in silicon based on wet oxidation of silicon in hydrofluoric acid solution with chromic acid, is described. The carbon dioxide formed is swept into a sodium hydroxide solution and determined by the change in electrical conductivity, with relatively simple apparatus. The importance of purifying the reagents and pre-treating the sample is emphasized. The method is applicable to carbon determinations in the p.p.m. range with a relative standard deviation of 3—9 %.

In recent years, considerable interest has been shown in the influence of various elements on the physical properties of silicon, and the effect of carbon on these properties has been the subject of several investigations [1, 14]. The carbon concentration in silicon has been evaluated by several techniques, e.g. i.r. spectrometry [3—7], mass spectrometry [5, 8], charged-particle activation analysis [9—13] and combustion [14, 15]. Unfortunately, when these different methods are applied to the same silicon types, the results obtained may be reproducible within themselves, but differ sometimes by orders of magnitude [2, 7, 11, 16]. Owing to this difficulty, no standards for carbon in silicon are yet commercially available.

Wet chemical methods of analysis generally give carbon contents substantially higher than those obtained with recent physical methods [15—17]. The reasons for these discrepancies are not completely clear [2, 18]. Martin et al. [17], however, in a clear and critical discussion, emphasize various reasons for the results obtained by different techniques. They concluded that perhaps the most general sources of error in the analysis are insufficient washing of the sample and the common practice of neglecting the powder, liquid or gas adsorbed on the fresh surface of the powdered silicon. Obviously, this factor is particularly important in the wet chemical methods. By keeping in mind these sources of error, Schnöller [15]

*Presented as a preliminary communication at Euroanalysis II, Budapest, August 1975.

succeeded in obtaining carbon values by a classical wet chemical method, which agreed with those obtained by recent physical methods.

Chemical methods cannot reach the high sensitivity of the more sophisticated physical methods, such as charged-particle activation analysis or mass spectrometry. However, within the limits of their sensitivity, the accuracy and reliability of the chemical methods and the advantages of working with inexpensive apparatus should be emphasized.

The development of an accurate and reliable determination of microgram quantities of carbon dioxide by conductimetric measurements [19] made it seem worthwhile to extend the method to a chemical determination of carbon in silicon. The method described in this paper is based on the wet oxidation of silicon with a chromic and hydrofluoric acid solution. The carbon is converted to carbon dioxide which is then determined by measuring the variation in conductivity of a sodium hydroxide solution.

This procedure eliminates the usual combustion of silicon in an oxygen flow by using a flux (Pb, PbO, Cu, $PbCrO_4$, Fe, etc.), which has often a carbon content even higher than that of the sample to be analyzed.

EXPERIMENTAL

Apparatus

The basic apparatus has been described [19]. It is modified for this particular problem with a sample treatment device, which consists of a reaction cell (rc) and a cold trap (t) (Fig. 1).

Reaction cell. This is a pyrex test tube (rc) (26 mm i.d., 100 mm long) with a PTFE cap (ca) connected by flexible PTFE tubing (6 mm o.d., 4 mm i.d.) to the main apparatus, to the chromic acid container (ar) and to the cold trap (t). The wall thickness of the tubing must be sufficient to prevent any carbon dioxide diffusion from the atmosphere [20]. Pyrex glass test tubes are preferable to PTFE tubes, because complete reaction of the sample can be observed. Even though the tubes, which are about 3 mm thick, become corroded by hydrofluoric acid, each tube can be used for 15—20 analyses. The excess of hydrofluoric acid used ensures complete sample dissolution.

A syringe microburet (s) permits the introduction into the reaction cell (rc) of known quantities of a pre-purified chromic acid solution, without opening the cap (ca) or stopping the gas flow.

At the gas outlet, a tube filled with silica gel (d) prevents liquid condensation along the tube walls.

Cold trap. This is a U-tube (t) cooled by a dry ice—acetone mixture, to condense water and hydrofluoric acid, in order to prevent their entering the conductivity cell.

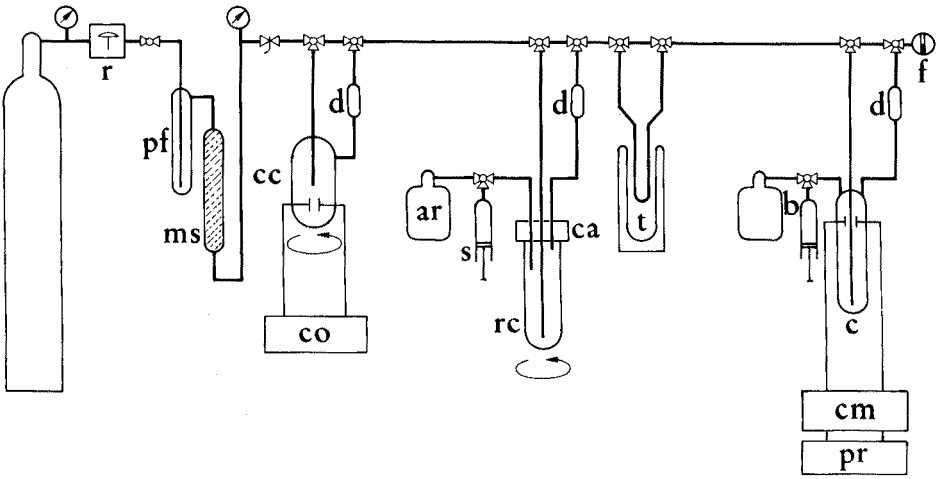

Fig. 1. Apparatus. r, pressure regulator; pf, gas bubbler (filled with sulphuric acid); ms, molecular sieves; cc, calibration cell; co, coulometer; d, drying tube (silica gel); ar, chromic acid reservoir; s, syringe; rc, reaction cell; ca, PTFE cap; t, cold trap; b, motor-syringe buret; c, absorption-conductivity cell; cm, conductivity meter; pr, potentiometric recorder; f, flow meter.

Reagents

The reagents used for silicon dissolution were 50 % (w/v) chromic anhydride solution (C. Erba, RPE) and 8 % (w/v) hydrofluoric acid solution (J. T. Baker, MOS type). These reagents were pre-purified of organic substances which could be oxidized to carbon dioxide.

The chromic acid, acidified with sulphuric acid (about 2 %), was boiled for several hours; nitrogen was then bubbled through the solution to remove any traces of carbon dioxide. The hydrofluoric acid was electrolyzed for about 6 h in a PTFE cell with platinum electrodes. The absorption solution was $2 \cdot 10^{-3}$ M sodium hydroxide. Trichloroethylene, acetone, methanol and nitric acid were J. T. Baker MOS-type reagents.

Pre-treatment of the silicon samples

The samples, generally as slices, were cleaned carefully by the following procedure.

Washing and degreasing. The silicon slices were washed in an ultrasonic bath filled with distilled water, for about 5 min. They were then rinsed in warm methanol in a quartz vessel, and dried in a nitrogen flow. The dried slices were kept for 5 min in boiling trichloroethylene (in a quartz vessel), for 5 min in boiling acetone, and for 5 min in boiling methanol. After this treatment, the samples were washed for 15—30 min in running distilled water and then dried in a nitrogen flow.

Etching and grinding. The dried slices were etched in a 1:1 hydrofluoric-nitric acid mixture in a PTFE vessel, rinsed with running distilled water and then dried in a nitrogen flow. These slices were placed in a 60-ml agate container and ground in a mill (Spex Model 8000 Mixer/Mill) for about 30 min. The agate container was previously cleaned by the same treatment as for the samples.

All the above steps were done on a laminar-flow clean bench. The importance of this treatment for the removal of surface impurities is emphasized by the results shown in Table 1.

Procedure

A sample of suitable size (10—100 mg of silicon, containing 1—10 μg of carbon) is placed in the reaction cell and 14 ml of 8 % hydrofluoric acid solution is added. Carrier gas is passed through the cell until all the carbon dioxide present in the apparatus, in the solution and possibly on the sample surface, has been expelled; this is shown by the recorder trace reaching the "residual slope" [19]. The gas flow through the cell is then switched off, and 2 ml of 50 % chromic acid solution is added. For complete dissolution of the sample, the solution is left under magnetic stirring. Meanwhile, the carrier gas is passed into the measuring cell (c) through the main line.

After 30—45 min, the carrier gas is again passed through the reaction cell to sweep the carbon dioxide formed to the conductivity cell (c); this takes about 15 min. The gas flow through the reaction cell is then stopped, and the

TABLE 1

Analysis of silicon samples
(The results are given in $\mu g\ g^{-1}$, with the standard deviation and the number of determinations in parentheses)

Silicon type	Sample form	C content	
		With pretreatment	Without sample pretreatment
Schuchardt SI 172	Powder		165 ± 5.0 (20)
B.D.H.	Powder		160 ± 9.6 (10)
Wacker (P type) 2—4 ohm cm	Slice	90 ± 2.7 (10)	110 ± 3.4 (10)
Wacker (P type) 2—4 ohm cm[a]	Slice	140 ± 5.6 (15)	190 ± 9.8 (15)
Montedison (polycrystalline)	Slice	50 ± 4.5 (20)	
Montedison (monocrystalline)	Slice	50 ± 4.5 (10)	

[a] A 50-μm epitaxial layer N was grown on the same substrate; after its removal, the slice resistivity was 4—6 ohm cm.

flow is switched to the coulometric cell (cc), for calibration of the apparatus.

During a series of experiments, errors may be caused by changes in the composition of the alkaline absorbent [19], so that calibration checks should be done after each sample analysis.

RESULTS AND DISCUSSION

The results obtained by analyzing commercial silicon samples are shown in Table 1. In order to evaluate the contribution of carbon dioxide adsorbed on the surface of the sample, some measurements were made by introducing the sample into the hydrofluoric acid solution, after carbon dioxide had been completely eliminated from the reagent, the sample and the cell, by means of purified nitrogen. For this purpose, the sample was placed in a small PTFE container fitted with a magnetic bar, which was held, by means of an external magnet, on the wall of the reaction cell (rc) during the deaeration of the hydrofluoric acid solution. After complete elimination of carbon dioxide, the sample was allowed to fall into the hydrofluoric acid solution.

The results showed that the contribution of carbon dioxide adsorption, can reach 20—60 $\mu g\ g^{-1}$, the actual value depending to some extent on the degree of grinding and on the preliminary treatment of the samples.

In principle, the method is quite simple and not too time-consuming. When the apparatus is in operation for series analysis, each sample can be analyzed in about 1 h. The method is, therefore, suitable for routine analysis. However, because of the high sensitivity of the method, skilled operators are essential if reliable results are to be obtained.

The authors thank Prof. Dario Nobili for his helpful discussions and suggestions, and Prof. Giovanni Semerano, Director of the "G. Ciamician" Chemical Institute, for his encouraging remarks and friendly criticism.

REFERENCES

1 T. Nozaki, Y. Yatsurugi and N. Akiyama, J. Electrochem. Soc., 117 (1970) 1566.
2 E. Spenke, in R. R. Haberecht and E. L. Kern (Eds.), Semiconductor Silicon, Electrochemical Society, New York, 1969, p. 1.
3 J. Eysymontt and B. Matecka, Euroanalysis II, Budapest (Hungary), August 1975, paper 1—76; Chem. Anal., Warsaw, in press.
4 R. C. Newman and J. B. Willis, J. Phys. Chem. Solids, 26 (1965) 373.
5 J. A. Baker, T. N. Tucker, N. E. Moyer and R. C. Buschert, J. Appl. Phys., 39 (1968) 4365.
6 Y. Endo, Y. Yatsurugi, N. Akiyama and T. Nozaki, Anal. Chem., 44 (1972) 2258.
7 C. Gross, G. Gaetano, T. N. Tucker and J. A. Baker, J. Electrochem. Soc., 119 (1972) 926.
8 A. M. Andreani, J. C. Brun, J. P. Mermoud and R. Stefani, Methodes Phys. Anal., 7 (1971) 269.
9 Ch. Engelmann and A. Marschal, Radiochem. Radioanal. Lett., 6 (1971) 189.
10 C. Vandecasteele, F. Adams and J. Hoste, Anal. Chim. Acta, 72 (1974) 269.

11 E. Schuster and K. Wohlleben, Z. Anal. Chem., 240 (1968) 175.
12 J. Martin and E. Haas, Z. Anal. Chem., 259 (1972) 97.
13 T. Nozaki, Y. Yatsurugi and N. Akiyama, J. Radioanal. Chem., 4 (1970) 87.
14 P. Rai-Choudhury, A. J. Noreika and M. L. Theodore, J. Electrochem. Soc., 116 (1969) 97.
15 M. Schnöller, Z. Anal. Chem., 259 (1972) 101.
16 W. Gebauhr and J. Martin, Le Dosage du Carbone et de l'Azote dans le Silicium et le Germanium, Bureau Eurisotop (n. 87), Bruxelles, 1974, p. 41.
17 J. Martin, M. Schnöller and E. Haas, Z. Anal. Chem., 259 (1972) 105.
18 W. Bonsel and J. L. Lambert in ref. 2, p. 89.
19 P. Lanza and P. L. Buldini, Anal. Chim. Acta, 85 (1976) 61.
20 E. Scarano and C. Calcagno, Anal. Chem., 47 (1975) 1055.

Analytica Chimica Acta, 85 (1976) 75—81

DETERMINATION OF IRON, MANGANESE, AND MAGNESIUM IN HIGH-PURITY MOLYBDENUM BY HIGH-FREQUENCY PLASMA TORCH EMISSION SPECTROMETRY

RYOZO NAKASHIMA and SHOZO SASAKI

Government Industrial Research Institute, Nagoya, Hirate-machi Kita-ku, Nagoya (Japan)

(Received 25th January 1976)

SUMMARY

The determination of impurities in molybdenum metals by high-frequency plasma torch emission spectrometry with direct introduction of sample solutions without prior separation has been studied. Iron, manganese and magnesium present in amounts greater than 0.005 % can be determined by means of the 248.8-nm, 279.5-nm and 279.6-nm lines, respectively. The lanthanum carrier technique, with 8-hydroxyquinoline as precipitant at pH 12—12.5 can be used when the content of these elements is less than 0.005 %. The effects of molybdenum and lanthanum on the spectral intensities of iron, manganese and magnesium are also discussed.

The determination of impurities in high-purity molybdenum and molybdates by emission spectrography is difficult, because of the volatility of molybdenum oxides and complexity of the spectrum. To overcome this difficulty, Dyck and Veleker [1], and Raginskaya and his co-workers [2] developed a highly sensitive technique in which the powdered sample was mixed with graphite powder so that the complex molybdenum spectrum was suppressed by the formation of molybdenum carbide and enhancement of the spectral intensity of the impurities was achieved. Unfortunately, the preparation of standard samples for this technique is difficult. An atomic absorption method was also utilized for iron, nickel, cobalt, manganese, chromium and calcium in tungsten and molybdenum metals [3, 4]. Although traces of iron [5] and manganese [6] in molybdenum metals were determined by the extraction—photometric method with PAN, troublesome procedures for each element had to be performed separately.

In this laboratory, high-frequency plasma torch emission spectrometry has been combined [7, 8] with the carrier precipitation concentration technique, which is particularly suitable for the pre-treatment of samples for this purpose. This report presents a simple analytical method for the determination of more than 0.005 % of iron, manganese and magnesium without separation of base material; when less than 0.005 % of these elements was present, the lanthanum carrier precipitation technique [9] was applied.

EXPERIMENTAL

Apparatus

A Hitachi UHF-plasma Spectrascan Model 300 [7] was used. The working conditions were: plasma gas, 3.0 l Ar min^{-1}; sheath gas, 3.5 l Ar min^{-1}; cooling water, 5 °C; heating chamber, 180 ± 10 °C; entrance slit, 30 μm; exit slit, 50 μm; pneumatic nebulizer, 3.5 ml min^{-1} with water at 3.0 l Ar min^{-1}; anode current, 300 mA; field current, 400 mA; photomultiplier, Hamamatsu TV R106 at 600 V.

Signal heights were recorded with monochromator scanning, sample solution being introduced continuously. When limited amounts of sample solution were available, the signal was recorded at the fixed wavelength of the element when a known amount of the sample solution was introduced. In all determinations, the mean values from five replicates were taken. Emission measurements were made in the outer region of the plasma torch to obtain maximum intensity.

Reagents

Stock solutions containing 100 μg ml^{-1} of iron, manganese, magnesium and other elements were made from the high-purity metals. Stock solutions (10^5 p.p.m.) of lanthanum and molybdenum were prepared from lanthanum oxide (99.999 %) (Shinetsu Chemicals) and molybdenum rod (Johnson Matthey Specpure), respectively. Analytical-grade hydrochloric and nitric acids (Wako Chemicals) were used.

Iron and manganese in the molybdenum rod were determined by the extraction—photometric method [5, 6] and magnesium was determined by an atomic absorption method in the aqueous phase after cupferron-chloroform extraction of the matrix element; 10.9 μg of iron, 9.3 μg of manganese and 2.6 μg of magnesium were detected in a 1.00-g sample. Although these amounts were all below the detection limits on 100-fold dilution of the stock solution, large amounts of molybdenum (ca. 10^4 p.p.m.) were used and the signal heights for added amounts of iron, manganese and magnesium were obtained by referring to the blank.

Optimization of experimental conditions

Optimal lines in the presence of molybdenum. In order to assess the practical utility of the emission technique for molybdenum metal analysis without prior separation, studies were made of the interference of molybdenum, at the 10^4 p.p.m. level, on the lines listed in Table 1, which shows the relative intensities for the different iron, manganese and magnesium lines. The emission lines selected on the basis of linear calibrations passing through the origin were 248.8 nm (iron), 257.6 nm and 279.5 nm (manganese), and 279.6 nm (magnesium). Although Table 1 shows that the 257.6-nm line gave the strongest intensity for manganese, the 279.5-nm line was used for the

TABLE 1

The spectral lines examined

Metal	Lines (nm)	Relative intensity	Metal	Lines (nm)
Fe	248.3 (I)	100	W	400.9 (I)
	259.9 (II)	97		407.4 (I)
	248.8 (I)	60		429.5 (I)
Mn	257.6 (II)	100	Sn	235.5 (I)
	259.4 (II)	92		242.9 (I)
	279.5 (I)	87		270.7 (I)
Mg	280.3 (II)	100		
	285.2 (I)	54		
	279.6 (II)	100		

reason described later. The calibration lines for iron, manganese and magnesium were all displaced from the origin by the interference from molybdenum. The detection limits of these three elements, on the basis of a signal-to-noise ratio of 2:1 were estimated to be 0.5 p.p.m.

In experiments with tungsten and tin solutions containing 10^4 p.p.m. of molybdenum, attempts to obtain linear calibration lines through the origin failed because of coincidence of the molybdenum lines with those of tungsten and tin. For 20 p.p.m. of tungsten and tin, more than 300—400 p.p.m. of molybdenum interfered with the 400.9-nm and 242.9-nm lines for tungsten and tin, respectively.

Effect of molybdenum concentration. The effects of molybdenum concentration on the spectral intensities of iron, manganese and magnesium are given in Fig. 1, where values measured in the absence of molybdenum are represented as 100. The intensity of the iron line decreased slightly up to 10^4 p.p.m. of molybdenum; beyond this concentration, it decreased abruptly. As the molybdenum concentration increased, the intensity of the 257.6-nm line for manganese decreased to a greater extent than the 279.5-nm line, which was slightly stronger than the 257.6-nm line in the presence of 10^4 p.p.m. of molybdenum.

Effect of molybdenum on the intensity of the lead line. The effect of molybdenum on the intensity of the lead line is shown in Fig. 2. The spectrum (a) was given by a solution containing 20 p.p.m. of lead when introduced into a clean nebulizer, heating chamber, and condenser. Introduction of a solution containing 20 p.p.m. of lead and 10^3 p.p.m. of molybdenum then gave (b). When the 20 p.p.m. lead solution was again introduced, (c) was given. After the system had been cleaned by the passage of distilled water for 10—20 min, 20 p.p.m. of lead gave (d). Similar absorption effects were also obtained for

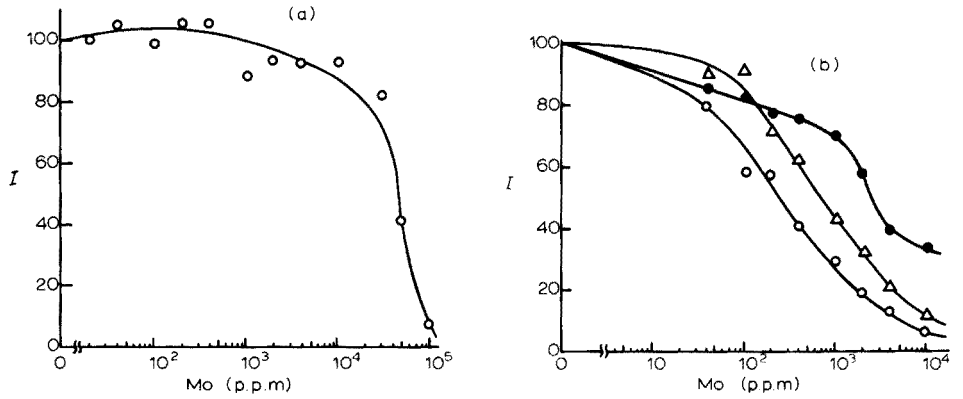

Fig. 1. Effect of molybdenum on the intensity of other lines. (a) 10 p.p.m. Fe at 248.8 nm. (b) (•) 20 p.p.m. Mn at 279.5 nm; (○) 20 p.p.m. Mn at 257.6 nm; (△) 20 p.p.m. Mg at 279.6 nm.

mercury and silver, which, like lead, form compounds with molybdenum oxide.

Procedure

Place the sample (1.00 g, powder or cuttings) in a 200-ml beaker surrounded by a waterjacket. Add 25 ml of hydrochloric acid and 30 % hydrogen peroxide or concentrated nitric acid until a violent reaction occurs. If necessary, cool the beaker with water to avoid the formation of an insoluble precipitate. Continue to add 30 % hydrogen peroxide or concentrated nitric acid occasionally until all the substance dissolves. Evaporate to dryness, add 5—10 mg of lanthanum, and adjust with 20 % sodium hydroxide solution to pH 12—12.5. Add 2.0 ml of 2 % 8-hydroxyquinoline (containing as little sodium hydroxide as possible), with stirring. Leave for 30 min on a water bath, transfer the contents to a 50-ml centrifuge tube, centrifuge, decant the supernatant solution, and rinse the beaker with redistilled water. Dissolve the precipitate with 0.5 ml of perchloric acid, and 0.5 ml of nitric acid, heat on a hot plate until the organic substance is decomposed and the perchloric acid is almost expelled. Add 0.5—1.0 ml of nitric acid to dissolve the residue and dilute to 5.00 or 10.00 ml.

RESULTS

Effect of lanthanum on the spectral intensities

This effect is shown in Fig. 3; spectral intensities of metals in the absence of molybdenum are expressed as 100. The intensities of the manganese, magnesium and iron lines increased 8.0, 3.5 and 1.5 times, respectively, in the presence of 10^3 p.p.m. of lanthanum. Of these, only the iron intensity decreased on the further addition of molybdenum. In practice, these effective

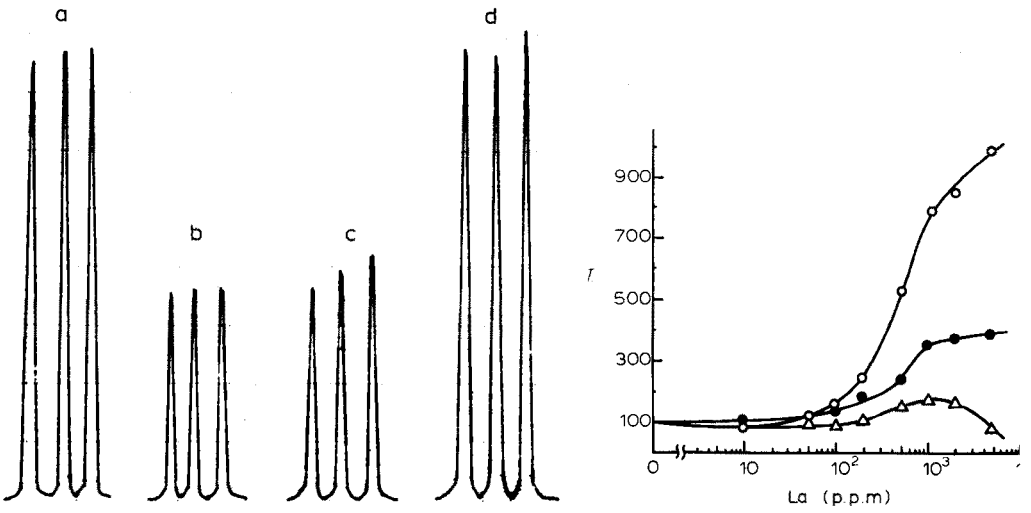

Fig. 2. Effect of molybdenum on the spectral line of lead at 368.3 nm. (a) 20 p.p.m. Pb, clean apparatus (b) 20 p.p.m. Pb, 1000 p.p.m. Mo (c) 20 p.p.m. Pb introduced (d) 20 p.p.m. Pb after passage of distilled water for 12 min.

Fig. 3. Effect of lanthanum. (△) 0.5 p.p.m. Fe; (•) 0.5 p.p.m. Mg; (○) 0.5 p.p.m. Mn.

enhancements were achieved when the final solution was diluted to 5.00 or 10.00 ml.

Coprecipitation by the use of lanthanum carrier

The lanthanum carrier precipitation (except for the addition of 8-hydroxyquinoline) was carried out as described above. Table 2 shows that low recoveries of magnesium were obtained at pH 12 with a slight improvement at pH 13. The recovery tests were also carried out on molybdenum powder for which the extraction—photometric [5, 6] and atomic absorption methods indicated the presence of iron (268 μg), manganese (6.00 μg) and magnesium (42.3 μg) in a 1.00-g sample. Very low recoveries (iron 181 μg; manganese 3.6 μg, magnesium 10.7 μg) were obtained.

Carrier precipitation enrichment techniques with organic reagents have been used in pre-treatments prior to conventional emission analyses to obtain improved analytical sensitivity. 8-Hydroxyquinoline, thionalide, and tannic acid have been used as precipitants under a variety of conditions [10, 11] and a large excess of PAN has been used [12] as a precipitant and carrier for several metals. 8-Hydroxyquinoline was used in this work since it precipitates iron, manganese, and magnesium, but not molybdenum at pH 12.

Analytical results

The results obtained for 99.94 % molybdenum powder containing 124 μg

TABLE 2

Recovery of iron, manganese and magnesium

Elements	Taken (μg)	Found (μg)	Recovery (%)
Iron	4.0	4,3,3.5	97
	20.0	14,18	79
Manganese	4.0	4.0,5.2	115
	20.0	24,21	113
Magnesium	4.0	1.2,1.1 1.1	29
	20.0	6.7,6.5 6,5	33
	4.0	2.9,2.8[a]	72
	20.0	15,14[a]	71

[a]pH 13.

TABLE 3

Results for iron, manganese and magnesium

Sample	Iron (μg)	Manganese (μg)	Magnesium (μg)
Mo powder[a] (99.94 %); 1.000 g	110,120 150,155 (Av. 134)	1.6,1.9 2.1,3.1 (Av. 2.2)	3.9,2.4,2.7 3.9,5.8,4.3 (Av. 3.8)
Mo powder (99.94 %); 1.000 g	120[b]		
Fe added; 100 μg	230,215 (Av. 223)		
Mn added; 5.0 μg		6.4,7.1 6.8,6.5 (Av. 6.7)	
Mg added; 5.0 μg			6.5,9.1,9.0 9.5 (Av. 8.5)

[a]Iron 124 μg (PAN extn—abs.); manganese 2.7 μg (cupferron extn.—PAN extn.—abs); magnesium, 3.6 μg (cupferron extn.—a.a.s.).
[b]No separation was done.

of iron, 2.7 μg of manganese and 3.6 μg of magnesium are shown in Table 3. The blank values originated mainly in the sodium hydroxide solution (20 % w/w) and this reagent must be as pure as possible. The blank values were 0.6 μg of iron, 0.1 μg of manganese and 0.07 μg of magnesium.

The standard deviations (0.65 and 1.22 for manganese and magnesium) obtained on a 1.00-g sample are somewhat large but the mean values found agree reasonably with those established by the extraction—photometric method.

The authors wish to thank Professor D. Ishii, Faculty of Engineering, Nagoya University, for helpful discussion.

REFERENCES

1 R. Dyck and T. J. Veleker, Anal. Chem., 31 (1959) 1640.
2 L. K. Raginskaya, T. G. Monova and V. N. Sotnikova, Zavod. Lab, 36 (1970) 1348.
3 G. M. Neumann, Z. Anal. Chem., 258 (1972) 180.
4 G. M. Neumann, Z. Anal. Chem., 259 (1972) 337.
5 R. Puschel, E. Lassner and K. Katzengruber, Chemist Analyst, 56 (1967) 63.
6 E. M. Donaldson and W. R. Inman, Talanta, 13 (1966) 489.
7 R. Nakashima, S. Sasaki and S. Shibata, Anal. Chim. Acta, 70 (1973) 265.
8 R. Nakashima, S. Sasaki and S. Shibata, Anal. Chim. Acta, 77 (1975) 65.
9 R. Ko and P. Anderson, Anal. Chem., 41 (1969) 177.
10 M. C. Farquhar, J. A. Hill and M. M. English, Anal. Chem., 38 (1966) 208.
11 E. F. Cruft and J. Husler, Anal. Chem., 41 (1969) 175.
12 R. Puschel and E. Lassner, J. Less—Common Met. 17 (1969) 313.

Analytica Chimica Acta, 85 (1976) 83—88

FLAMELESS ATOMIC ABSORPTION SPECTROMETRY OF GALLIUM WITH A METAL ATOMIZER

KIYOHISA OHTA and MASAMI SUZUKI*

Department of Chemistry, Faculty of Engineering, Mie University, Kamihama-cho, Tsu-shi, Mie-ken 514 (Japan)

(Received 1st December, 1975)

SUMMARY

The flameless atomic absorption spectrometry of gallium with a metal micro-tube atomizer is described. This atomizer provides better sensitivity than a metal strip atomizer; the 1 % absorption sensitivity for aqueous solution at the 294.364—294.418-nm line is $1.5 \cdot 10^{-11}$ g. Diverse metals interfere at 100-fold concentrations, so that preliminary separation by solvent extraction is recommended for complex matrices. Gallium in rock and aluminum samples can be determined satisfactorily.

Little information is available in the literature about the flameless atomic absorption spectrometry of gallium. Anderson et al. [1] found a detection limit of $5 \cdot 10^{-11}$ g for gallium with a carbon-filament atom reservoir. Langmyhr et al. [2] reported the direct atomization of gallium in bauxite, clay, etc. in a high-frequency induction heated graphite furnace. Several types of metal filament atomizer have been investigated [3—8]. With these atomizers, the residence time of atoms in a high-temperature environment is short, and the observation height above the filament is critical for good sensitivity. Ohta and Suzuki [9, 10] have developed a metal micro-tube atomizer to overcome the disadvantages of the filament, and have discussed the flameless atomic absorption spectrometry of copper, cobalt, aluminum, palladium and selenium.

This paper describes the flameless atomic absorption characteristics of gallium with a metal atomizer. The usefulness of the micro-tube atomizer for gallium determinations is also demonstrated, the results being compared with those obtained with the strip-type atomizer.

EXPERIMENTAL

Apparatus

The metal micro-tube atomizer (1.5 mm diameter and 25 mm long) and absorption chamber have been described [9, 10]. Radiation from a hollow-

*To whom correspondence should be addressed.

cathode lamp (Hamamatsu TV Co.) was passed through the micro-tube to a 0.5-m Ebert-type grating monochromator (Nippon Jarrell-Ash Co.) fitted with a R106 photomultiplier (Hamamatsu TV Co.). The signal from the photomultiplier was then amplified by a JEOL AA-HMA signal control unit, the response of which was faster by about two orders of magnitude than that of the conventional system and fed to a Hitachi 056-1001 recorder (0.4-s full-scale deflection). The signal was also monitored by a DS5016 dual-beam synchroscope (Iwatsu Electric Co.) which had a time constant of 1 μs. Background absorption was compensated with a deuterium lamp (Original Hanau D200F). The analytical wavelength was 294.364—294.418 nm and the slit width was chosen so as to give a spectral band pass of approximately 0.02 nm.

The tube temperature was measured as follows: the voltage signal from the atomizer and the absorption signal were recorded simultaneously with two beams of the synchroscope. Both signals were synchronized and the temperature was determined from the voltage signal which had previously been calibrated in terms of temperature with an optical pyrometer (Chino works).

Argon was used as purge gas at a flow rate of 450 ml min^{-1} with hydrogen at a flow rate of 20 ml min^{-1}. All samples were injected with glass micropipets. All extractions were done with an electric shaker (Iwaki KM). Uni-Seal decomposition vessels were used for the decomposition of rock samples.

Reagents

Gallium stock solutions were prepared by dissolving gallium oxide in hydrochloric acid; a gallium nitrate solution was prepared by heating gallium chloride with nitric acid. Titanium(III) chloride solution was prepared by dissolving titanium metal in hydrochloric acid in an atmosphere of carbon dioxide.

All reagents were of analytical-reagent grade, and deionized-distilled water was used in all dilutions.

RESULTS AND DISCUSSION

Atomization of gallium in the micro-tube atomizer

In order to compare the atomization characteristics of gallium, attempts were made to atomize gallium from various compounds and complexes. These included gallium chloride and nitrate; gallium oxinate, pyridylazonaphthol and rhodamine B complexes in chloroform; and the gallium chlorocomplex in isopropyl ether. The complexes were prepared as described in the literature. The effect of tube temperature for atomization of gallium from compounds and complexes is shown in Fig. 1. Inorganic compounds were dried at 100 °C before atomization, and decomposition at 200 °C was also applied for the organic complexes. Each absorption was obtained by atomizing for 1 s. It can be seen that the absorptions were somewhat different at the lower temperatures, whereas the differences were slight above 2000 °C. These characteristics differed from those of lead. As for lead [11], the temperatures for optimum atomization differed for different compounds and complexes.

The absorption signals were also monitored by feeding the output signals from the signal control unit to the synchroscope. Figure 2 shows the synchroscope traces; the micro-tube atomizer was heated for 1 s, reaching 2200 °C about 0.29—0.32 s after the power had been switched on. The absorption profiles were similar for chloride, nitrate and the rhodamine B complex, although there were small differences in the temperatures at which the absorption commenced and ended. Variations in absorption profiles were observed in the atomization of lead from various compounds and complexes [11]. The small absorption appearing before the gallium absorption for the rhodamine B complex is probably molecular absorption caused by organic material. The peak absorptions obtained from the synchroscope traces were considerably greater than those given by the strip chart recorder, probably because of mechanical limitations of the recording device. The synchroscope was preferred as the detection system for recording fast atomization responses.

Atomization with the strip-type atomizer

For comparison, atomization was carried out with a strip-type atomizer. The sample solution (1 μl) was placed on the molybdenum strip (1.5 mm wide and 20 mm long) and dehydrated slowly by applying low power (0.02 V, 3 A) to the strip for about 30 s. Then, gallium was atomized by applying high power (2.1 V, 14 A) within 1 s. The strip temperature was 2200 °C. Figure 3 shows the synchroscope traces of gallium absorption measured at heights of 0.75, 1.7 and 3.5 mm above the strip. The absorptions were poor, presumably

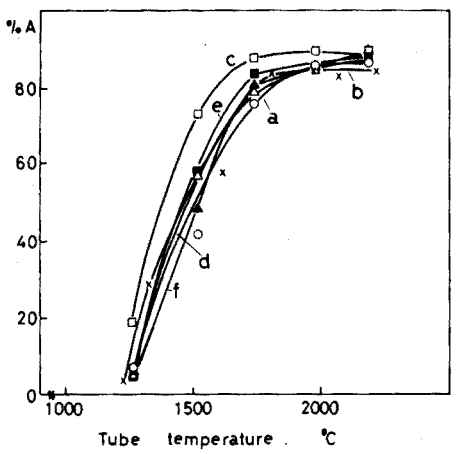

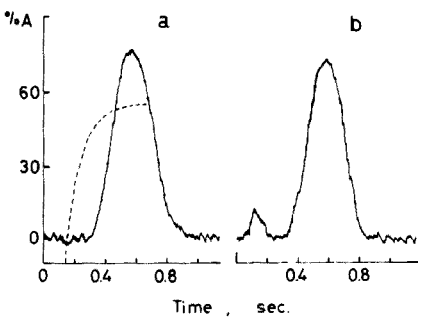

Fig. 1. Effect of tube temperature on atomization of gallium from various compounds and complexes. (a) Chloride (○); (b) nitrate (X); (c) pyridylazonaphthol complex (□); (d) oxinate complex (△); (e) rhodamine B complex (■); (f) chlorocomplex (▲). $1.1 \cdot 10^{-8}$ g Ga.

Fig. 2. Synchroscope traces for atomization of gallium from nitrate and rhodamine B complex. (a) Nitrate; (b) rhodamine B complex. $1.1 \cdot 10^{-9}$ g Ga. Dashed line shows the curve of temperature increase.

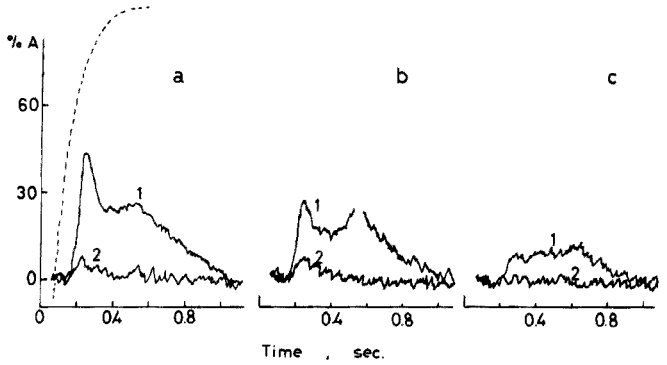

Fig. 3. Synchroscope traces for gallium absorption at various observation heights above a molybdenum strip. (a) 0.75 mm; (b) 1.7 mm; (c) 3.5 mm. (1) $1.1 \cdot 10^{-8}$ g Ga; (2) $1.1 \cdot 10^{-9}$ g Ga. Dashed line shows the curve of temperature increase.

because of the shorter residence time of atoms in the optical path. From these results, it may be concluded that the metal micro-tube atomizer provides a much more effective atomization of gallium.

Sensitivity and reproducibility

The sensitivity (for 1 % absorption) was measured by injecting 1-μl samples of standard gallium chloride solution into the micro-tube atomizer. The sensitivity obtained was $1.5 \cdot 10^{-11}$ g under the optimized conditions. A sensitivity of $2.4 \cdot 10^{-10}$ g was measured with the strip-type atomizer.

The relative standard deviation of 5 replicate determinations of $1.1 \cdot 10^{-9}$ g of gallium was 2 %.

Interferences

The effects of diverse metals on the gallium absorption signal were measured at 2200 °C. Solutions ($1 \cdot 10^{-9}$ g Ga) containing 10- or 100-fold amounts of different foreign ions were employed. The ions included Na(I), Ca(II), Al(III), Pb(II), Sb(III), Cu(II), Zn(II), Cr(III), Mn(II), Fe(III), Co(II) and Ni(II); all were added as chloride salts, except lead. Gallium absorption was depressed by 10-fold amounts of aluminum and calcium, but little affected by others. The measurement of gallium suffered multiple interferences (usually 20—90 % depression) from 100-fold amounts of various metals, particularly calcium, but copper and antimony did not interfere. The reproducibility of the gallium determination was poor in the presence of interfering ions. Anderson et al. [12] stated that interference effects from volatile matrix elements were generally more serious with the carbon filament device than in flame systems, whereas interference effects from elements forming refractory oxides were significantly less troublesome; they concluded that the interferences were most probably due to interelement effects in the vapor phase. However, interference from volatile elements tends to be less prominent in

atomization of gallium with a metal micro-tube atomizer. The tube temperature influenced the magnitude of interferences. Figure 4 shows the synchroscope traces obtained for gallium in the presence of aluminum at 2200 ° and 2400 °C; these results indicate that atomization at elevated temperatures is effective in eliminating interference. However, the severe interference from calcium was not improved at higher temperature. In the absorption profiles at 2400 °C, a negative peak appeared after the gallium absorption; the cause of this peak could not be fully elucidated.

Application to the determination of gallium in rocks and aluminum

The application of the flameless atomic absorption spectrometry of gallium to rocks and aluminum was examined. Preliminary separation of gallium was necessary for complex samples because of interferences.

Procedure for rocks. Decompose 0.5 g of rock sample with 4 ml of 14 M nitric acid and 7 ml of 40 % hydrofluoric acid in a Uni-Seal decomposition vessel by heating at 120 ° C in an electric oven for 2 h. After decomposition, transfer the solution to a Teflon beaker and evaporate to dryness on a water bath. Repeat the evaporation after addition of 3 ml of 12 M hydrochloric acid. Then, dissolve the residue in 10 ml of 6.5 M hydrochloric acid and dilute to 50 ml with 6.5 M hydrochloric acid. Transfer an aliquot of the solution to a separatory funnel. Reduce iron(III) by adding titanium(III) chloride solution dropwise, and extract the gallium chlorocomplex with 5 ml of isopropyl ether. Transfer 1 μl of the organic phase to the metal micro-tube atomizer, and atomizate gallium at 2200 °C.

Prepare a calibration curve by atomizing organic extracts obtained from standard solutions as above.

Procedure for aluminum. Dissolve 0.1—1 g of sample in 6 M hydrochloric acid. After dissolution, evaporate the resulting solution to dryness on a water bath. Dissolve the residue in 6.5 M hydrochloric acid and proceed as above with the extraction of gallium.

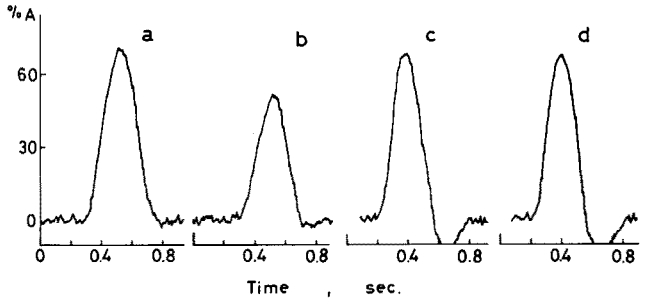

Fig. 4. Synchroscope traces for atomization of gallium in the presence of aluminum. (a) Ga alone (2200 °C); (b) Ga and Al (2200 °C); (c) Ga alone (2400 °C); (d) Ga and Al (2400 °C). $1.1 \cdot 10^{-9}$ g Ga (as chloride).

Results for the determination of gallium in standard rock and aluminum samples are shown in Table 1. The solvent extraction technique allowed the separation of gallium from the majority of interfering ions, and so contributed to satisfactory accuracy. This flameless atomic absorption technique should be suitable for biological samples.

TABLE 1

Determination of gallium in standard rock samples and aluminum samples

Sample	Ga (p.p.m.)	
	Found[a]	Independent result
JB-1 (basalt)	17 ± 1	17[b]
JG-1 (granodiorite)	18 ± 0.4	16,28[b]
GSP-1 (granodiorite)	22 ± 1	22[b]
Al No. 1	76.0 ± 9.0	80[c]
Al No. 2	9.4 ± 1.0	10[c]
Al No. 3	320 ± 10.0	300[c]

[a]Mean of 3—4 determinations.
[b]A. Ando et al., Geochemical J., 5 (1971) 151; F. J. Flanagan, Geochim. Cosmochim. Acta, 37 (1973) 1200.
[c]Obtained by another method.

The authors wish to thank Dr. A. Ando, Geological Survey of Japan, for the rock samples and Mr. K. Mukai, Nippon Light Metal Research Laboratory, Ltd. for the aluminum samples.

REFERENCES

1 R. G. Anderson, I. S. Maines and T. S. West, Anal. Chim. Acta, 51 (1970) 355.
2 F. J. Langmyhr and S. Rasmussen, Anal. Chim. Acta, 72 (1974) 79.
3 J. Y. Hwang, P. A. Ullucci, S.B. Smith and A.L. Malenfant, Anal. Chem., 43 (1971) 1319.
4 T. Takeuchi, M. Yanagisawa and M. Suzuki, Talanta, 19 (1972) 465.
5 J. V. Chauvin, M. P. Newton and D. G. Davis, Anal. Chim. Acta, 65 (1973) 291.
6 J. E. Cantle and T. S. West, Talanta, 29 (1973) 459.
7 N. S. McIntyre, N. G. Cook and D. G. Boase, Anal Chem., 46 (1974) 1983.
8 M. P. Newton and D. G. Davis, Anal. Chem., 47 (1975) 2003.
9 K. Ohta and M. Suzuki, Talanta, 22 (1975) 465.
10 K. Ohta and M. Suzuki, Anal. Chim. Acta, 77 (1975) 288.
11 K. Ohta and M. Suzuki, Anal. Chim. Acta, 83 (1976) 381.
12 R. G. Anderson, H. N. Johnson and T. S. West, Anal. Chim. Acta, 57 (1971) 281.

Analytica Chimica Acta, 85 (1976) 89—93

SENSITIVE INFRARED MEASUREMENT OF PILOCARPINE—ISOPILOCARPINE ISOMERIZATION

JAMES A. RYAN

Department of Pharmaceutical Research and Development, Merck Sharp and Dohme Research Laboratories, Division of Merck & Co., Inc., West Point, Pa. 19486 (U.S.A.)

(Received 16th December 1975)

SUMMARY

A sensitive and convenient method of measurement of the degree of isomerization of pilocarpine in 3-mg samples is described. The drug base is dissolved directly or is extracted from salts in basic buffer with chloroform. After evaporation the residue is dissolved in carbon disulfide and examined in a 3.0-mm pathlength infrared cell. The absorbance ratio $A^{1100cm^{-1}}/A^{1082cm^{-1}}$ is used to calculate the isopilocarpine content from a standard curve. Drug formulation excipients do not interfere if they are insoluble in carbon disulfide, but non-polar substances which cannot be removed by prior extraction interfere. Results from the application of the method to pilocarpine salts are presented. The relative standard deviation of 50—50 isomer mixture is ± 1.83 % for seven determinations.

Several authors [1—3] have studied the isomerization of pilocarpine(I) to isopilocarpine(II); the latter compound shows considerably less physiological activity [4]. The qualitative similarity and weaker activity have been mentioned in an extensive review of these jaborandi alkaloids [5]. Other substances formed in this process are pilocarpic acid(III) and isopilocarpic acid (IV). Repta and Higuchi [4] have shown that I and II can be separated quantitatively from the salts of III and IV by partition between slightly alkaline carbonate (pH 8.5) and chloroform.

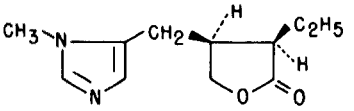

PILOCARPINE I

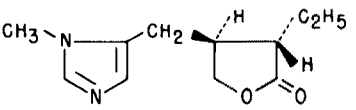

ISOPILOCARPINE II

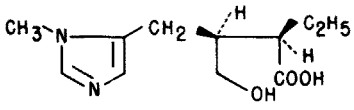

PILOCARPIC ACID III

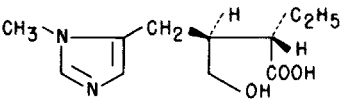

ISOPILOCARPIC ACID IV

A recent publication [6] has explained that the substance isolated by Pinner [7] (called metapilocarpine) is a racemic mixture of d- and l-isopilocarpine. Hill and Borcza [8] have established the relative and absolute configurations of these alkaloids. Other authors [4, 5] have published methods of analysis for pilocarpine, including measurement of optical rotation for assessing the interconversion. The optical rotation method [9] is not very selective and suffers from insensitivity; a typical sample requirement is 200 mg, or somewhat less, depending on the equipment used. Because drugs such as pilocarpine may require low dosage levels, a method of measuring the tendency of this miotic to isomerize in various products is required.

Long-path length i.r. cells have been utilized successfully for quantitative analysis at low concentration levels in relatively transparent infrared solvents, for many systems [10—13]. Larger, more conveniently sized glassware is utilized than would be necessary with conventional path-length infrared cells.

Results from the application of the method to pilocarpine nitrate (USP) are shown in Table 1, column A. Application of the method to products from random trial formulations on stability, and from a marketed product, gave the results shown in column B for storage times of up to 40 weeks with accelerated storage isotherms as high as 60 °C. A study at unknown higher temperatures and exposure times yielded the analysis values in column C; qualitative infrared evidence from the fingerprint region confirmed that large amounts of isopilocarpine were present. The data presented in Table 1 illustrate the practical application of the method.

EXPERIMENTAL

Equipment

A Perkin-Elmer 521 infrared spectrophotometer was employed with nominal 3-mm path-length liquid cells fitted with NaCl windows. Separatory

TABLE 1

Analytical results by infrared spectrometry

A Pilocarpine nitrate USP			B Application to products stressed below 60 °C			C Certain dosage forms stressed above 60 °C[a]		
	% I	% II		% I	% II		% I	% II
1.	100	0	1.	93.0	7.0	1.	85.5	14.5
2.	99.5	0.5	2.	100	0.0	2.	74.8	25.2
3.	100	0	3.	100	0.0	3.	86.7	13.3
4.	99.0	1.0	4.	95.0	5.0	4.	76.6	23,4
5.	100	0	5.	98.0	2.0			
6.	100	0	6.	97.0	3.0			
7.	98.5	1.5	7.	95.0	5.0			

[a]See text for detail.

funnels (60 ml) with Teflon or plastic stopcocks were employed. Stopcock grease was excluded. An efficient fume hood was used for the solvent evaporations and transfers.

Reagents

pH 9.7 carbonate buffer (0.4 M). Dissolve 17 g of $NaHCO_3$ and 21 g of Na_2CO_3 in distilled water, mix, dilute to 1l at room temperature, and adjust to pH 9.7 if necessary. Other solvents used were ACS or reagent grade.

Standard curve

A standard curve of absorbance ratios (1100 cm^{-1}/1082 cm^{-1}) was prepared (Fig. 1). Separate aqueous solutions were prepared from isopilocarpine nitrate (Aldrich) and pilocarpine nitrate (USP) to contain exactly 32.6 mg of each isomer in 50 ml (0.5 mg of base equivalent of each isomer per ml).

Aliquots of these pure isomer solutions were transferred immediately to clean 60-ml separatory funnels to prepare the standard mixtures indicated in Table 2. (All glassware should be clean, i.e., CS_2 placed in the glassware should not give a response above the reagent CS_2 baseline over the range 1300—900 cm^{-1} (see Fig. 2).)

Distilled water (20 ml) and 5 ml of pH 9.7 carbonate buffer were added to each funnel. After mixing, each flask was extracted with 3 × 2-ml portions of chloroform; the extracts were collected in 50-ml volumetric flasks. Inclusion of any aqueous phase in the extracts was avoided. The solutions were evaporated to complete dryness on a water bath at less than

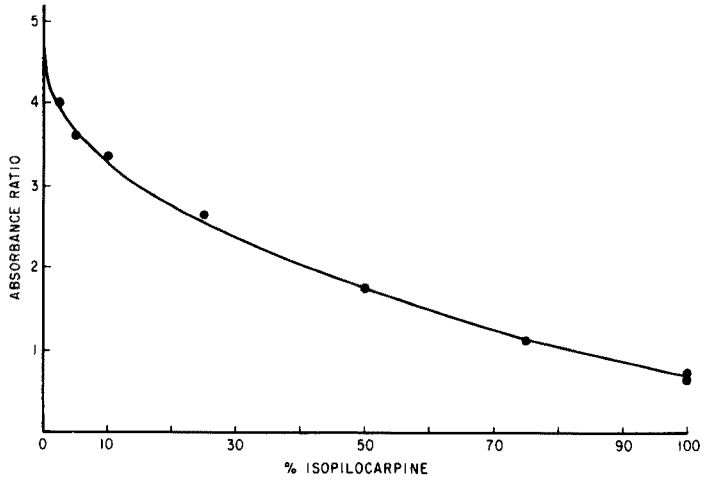

Fig. 1. Standard curve of absorbance ratios.

TABLE 2

Standard mixtures prepared

Separatory funnel	Isopilocarpine ml	(%)	Pilocarpine ml	(%)
A	0	0	6.00	100
B	0.15	2.5	5.85	97.5
C	0.30	5.0	5.70	95.0
D	0.60	10.0	5.40	90.0
E	1.50	25.0	4.50	75.0
F	3.00	50.0	3.00	50.0
G	4.50	75.0	1.50	25.0
H	6.00	100.0	0	0

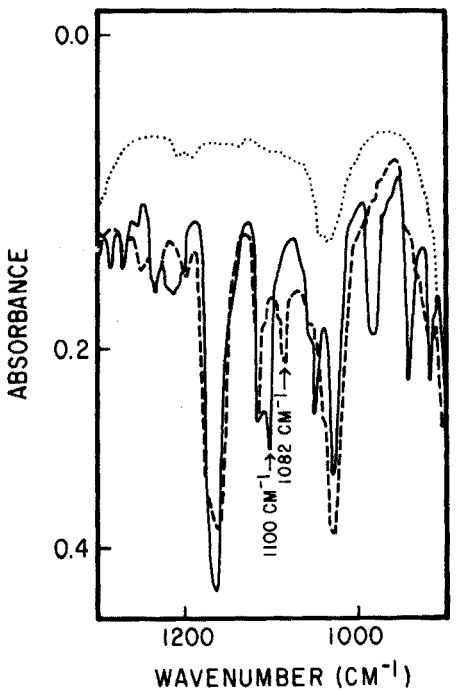

Fig. 2. Infrared spectra of extracted pilocarpine base (———), isopilocarpine base (- - - - - - - -) and solvent CS_2 baseline (·····).

65 °C. When no odor of chloroform remained, 3.0 ml of CS_2 was added immediately to each flask. The flasks were stoppered and agitated frequently until the bases dissolved completely. By means of qualitative parameters (see below) and a slow scan between 1300 and 900 cm^{-1}, a baseline for pure CS_2 in the tightly stoppered cell was obtained. Air was used as a reference. The solution under test was transferred to the cell by

Pasteur pipette. Without changing the parameters, each solution was scanned in turn over this frequency interval; finally pure CS_2 was scanned to check that baseline drift had not occurred. The sampling area of the spectrophotometer was left open and the cell was removed immediately from the instrument after each scan to prevent CS_2 vapour from any minor cell leaks being ignited by the instrument source.

The instrumental parameters used were: scan time, 32; slit program, 1000; attenuator speed, 1100; source, 0.78 A; gain, normal; initial frequency setting 1300 cm^{-1}. On other instruments good resolution and reasonable precision are a guide to parameter selection. The amplifier was balanced and the pen set carefully at 0% and 100 % T before use. Standard data were calculated as follow

$$\frac{A_{\text{std.}}^{1100} - A_{CS_2}^{1100}}{A_{\text{std.}}^{1082} - A_{CS_2}^{1082}} = R \text{ (Absorbance Ratio)}$$

All standard R values (ordinate) were plotted versus % isopilocarpine (abscissa).

Sample procedure and evaluation

An aliquot, equivalent to an estimated 3 mg of pilocarpine base, was withdrawn from the solution under test, evaporated to dryness, reconstituted with CS_2, and examined by the procedure described above. The "R" value was determined and the concentration read as % isopilocarpine directly from the standard curve. If extraneous organic contamination of the sample is suspected, the family of standard curves should be examined for spectral deviations.

REFERENCES

1 W. Dopke and G. d'Heureuse, Tetrahedron Lett., 15 (1968) 1807.
2 R. A. Anderson, Ph.D., Thesis, University of Sydney, Australia, 1967.
3 P. Chung, T. Chin and J. L. Lach, J. Pharm. Sci., 59 (1970) 1300.
4 A. Repta and T. Higuchi, J. Pharm. Sci., 60 (10) (1971) 1465.
5 A. R. Battersby and H. T. Openshaw, in R. H. F. Manske and H. L. Holmes (Eds.), The Alkaloids, Vol. III, Academic Press, New York, 1953, p. 213.
6 Y. Hassen Aboul-Enein, Acta Pharm. Suec., 11 (1974) 387.
7 A. Pinner, Chem. Ber., 38 (1905) 2560.
8 R. K. Hill and S. Borcza, Tetrahedron, 22 (1966) 2889.
9 The United States Pharmacopeia, 19th Rev., Mack Publishing, Easton, Pa., 1974, pp. 384, 385.
10 L. Hahn and L. Pauling, Anal. Chem., 40 (1948) 1283.
11 R. K. Ritchie and D. Kulowic, Anal. Chem., 42 (1970) 1080.
12 J. A. Ryan, L. J. Cali and E. McGonigle, Anal. Chim. Acta, 54 (1971) 105.
13 J. A. Ryan, E. McGonigle and J. M. Konieczny, Anal. Chim. Acta, 55 (1971) 83.

Analytica Chimica Acta, 85 (1976) 95—102

THE USE OF NEUTRON ACTIVATION FOR ROUTINE ANALYSIS OF PURE IRON AND CHROMIUM

Ch. LOOS-NESKOVIC, M. FEDOROFF and G. REVEL

Centre d'Etudes de Chimie Métallurgique 15, Rue Georges Urbain — 94400 Vitry-sur-Seine (France)

(Received 19th January 1976)

SUMMARY

A method is presented for the routine analysis of high-purity iron and chromium by neutron activation analysis. The impurities determined are those which are significant in the control of the purification processes. Nine elements are determined in iron without separation; Co, Cr and Mo can also be determined after an anion-exchange separation. In chromium, a single elution on an anion exchanger allows the detection of nine significant impurities. For the determination of nickel a special method is used. All these methods were chosen to obtain the most comprehensive analytical procedure at the lowest cost.

Iron represents a relatively favourable case for neutron activation analysis since the matrix is only moderately active after irradiation. Numerous schemes have been proposed for destructive determination of impurities by means of NaI(Tl) γ-ray spectrometry [1—11], but these methods need extensive radiochemical separations. The introduction of Ge(Li) detectors has allowed the simultaneous determination of trace elements and has greatly reduced the number of chemical separations [12—14]. Some elements may be detected without chemical separation [15].

Until now, chromium has received less attention since the matrix is very radioactive even after a short irradiation time. The separation schemes proposed for its analysis were established before the introduction of Ge(Li) detectors [16, 17].

Attempts to characterize the purity of iron and chromium samples by the determination of some significant elements have been undertaken to control their purification. The high resolution of Ge(Li) detectors and the high purity of the iron samples makes it possible to determine many elements by non-destructive analysis after a short irradiation.

After a long irradiation determinations are not possible because of the high radioactivity of the matrix, and a chemical separation is then necessary. The simplest chemical procedure which would just remove the matrix and allow counting with a Ge(Li) detector was sought, and division of the elements to be determined into many fractions, as in earlier separation schemes, was avoided.

Nuclear data and interferences

Table 1 shows the radioactive characteristics of the isotopes used for these analyses.

TABLE 1

Characteristics of nuclides used for analysis

Element	Nuclide	γ-ray (keV)	Half-life	Element	Nuclide	γ-ray (keV)	Half-life
As	^{76}As	559	26.4 h	La	^{140}La	1596	40.2 h
Au	^{198}Au	412	64.8 h	Mn	^{56}Mn	847	2.6 h
Co	^{60}Co	1173	5.2 y			1810	
		1332		Mo	^{99}Mo	142	66 h
Cr	^{51}Cr	320	27.8 d	Na	^{24}Na	1368	15 h
Cu	^{64}Cu	511	12.8 h	Ni	^{65}Ni	1481	2.6 h
Ga	^{72}Ga	630	14.1 h	Pt	^{199}Au	159	76.8 h
		834		Sb	^{122}Sb	564	67.2 h
Fe	^{59}Fe	1099	45 d		^{124}Sb	603	60 d
		1291		W	^{187}W	479	23.9 h
K	^{40}K	1525	12.4 h			686	

Iron gives in a neutron thermal flux only one isotope of significant activity: ^{59}Fe($t_{1/2}$ = 45 d). But in a fast neutron flux, interferences from the reactions ^{56}Fe(n,p)^{56}Mn and ^{54}Fe(n,α)^{51}Cr are involved in the determinations of manganese and chromium. The interference is calculated for a flux ratio of fast neutrons to thermal neutrons equal to 10^{-3} and leads to an apparent concentration of 0.05 μg g^{-1} for chromium and 0.02 μg g^{-1} for manganese. The same values were found by the double irradiation technique, with and without a cadmium cover.

In chromium, a thermal neutron flux produces the following reactions: ^{50}Cr(n,γ)^{51}Cr ($t_{1/2}$ = 27.8 d) and ^{54}Cr(n,γ)^{55}Cr ($t_{1/2}$ = 4 min). Interference from the reaction ^{54}Cr(n,γ)^{55}Cr $\xrightarrow{\beta^-}$ ^{55}Mn(n,γ)^{56}Mn must be considered. The amount of manganese produced by this interference depends on the irradiation time, but after 1 h the apparent concentration induced is less than 10^{-4} μg g^{-1} [17].

Study of chemical separations

Iron matrix. Some authors have described a separation scheme based on an ion-exchange procedure in hydrofluoric acid medium [6, 12, 13, 18], but teflon vessels and great care in manipulations are necessary. Recently, many elements have been separated from an iron matrix by cation exchange in dilute nitric acid [19], but this procedure requires a large volume of solution for an iron sample of 1 g. A Dowex 50 resin was also used with tartrate or oxalate solutions for iron and steel analysis but the separation scheme was not simple [20].

Iron is retained [21] on a cation exchange resin while cobalt and chromium

are eluted with concentrated hydrochloric acid. The adsorption characteristics were checked by means of tracer experiments. A known amount of a radioactive tracer was added to 0.5 g of iron before dissolution. After elution, the resin was extruded from the column and the activities of both resin and eluate were determined and referred to the original amount of added tracer.

Results showed that the elution of some elements needs a very large volume of eluant (Fig. 1). In a mixture of 25 % hydrochloric acid (0.5 M) and 75 % acetone, iron is eluted while cobalt, chromium and molybdenum are retained on the resin [22]. In our conditions, in the presence of an iron matrix some elements such as chromium are incompletely eluted (Fig. 2).

After these unsuccessful attempts, an anion exchange resin of the Dowex 1 type was used. Chromium is eluted quickly with concentrated hydrochloric acid; cobalt is eluted by 6 M HCl and iron is completely recovered by washing the column with 1 M HCl containing 1 % hydrogen peroxide. Molybdenum is retained on the resin (Fig. 3). A separation scheme, described in the analytical procedure (Fig. 4), was developed subsequently.

Chromium matrix. In a mixture of 9 M hydrochloric acid—1 % hydrogen peroxide a chromium matrix is completely eluted by 60 cm^3 of this solution (Fig. 5). The decontamination factor for chromium on the column is 10^4. The impurities arsenic, cobalt, copper, gallium, iron, antimony and tungsten are retained on the resin under these conditions. In the same medium, sodium may be fixed on a column of antimony pentoxide while chromium is eluted. This separation scheme was used for the analysis (Fig. 6).

Separation of nickel. This element with a short half-life (2.6 h) and a low γ-emission rate is not detectable with a good sensitivity by instrumental analysis. A separation scheme for this element [23] has been developed.

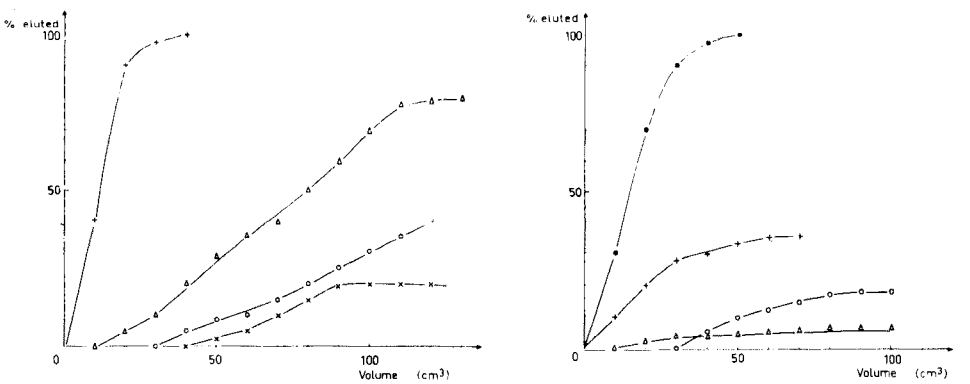

Fig. 1. Elution curves on Dowex 50-X8 resin in 12 M HCl in the presence of a 0.5-g iron matrix retained on the column. +, Cr; △, Co; ○, Mo; X, W.

Fig. 2. Elution curves on Dowex 50-X8 resin ina mixture of 25 % 0.5 M HCl—75 % acetone in the presence of a 0.5-g iron matrix. •, Fe; +, Cr; ○, Mo; △, Co.

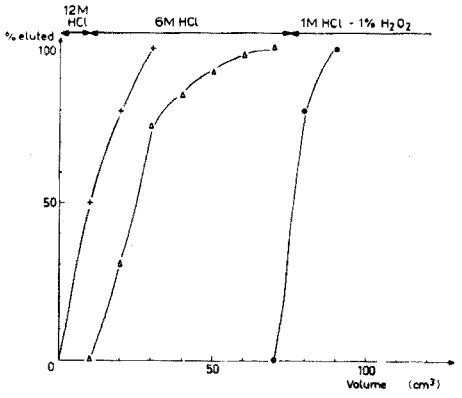

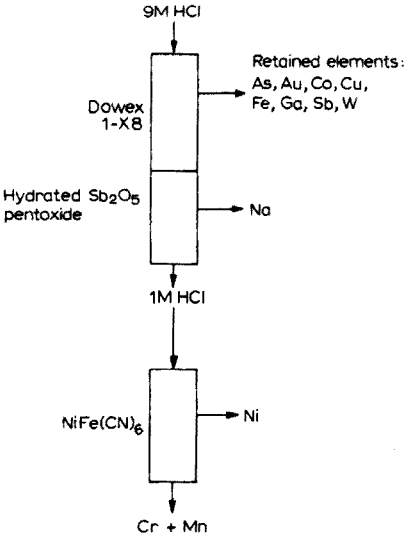

Fig. 3. Elution curves on Dowex 1-X8 resin. The column was charged with 10 cm³ of concentrated hydrochloric acid containing a 0.5-g iron matrix. +, Cr; △, Co; •, Fe.

Fig. 4. Separation scheme for radiochemical analysis of iron.

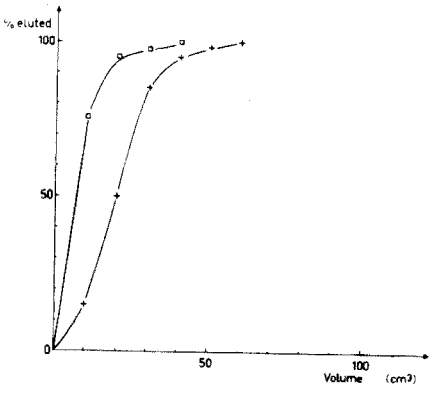

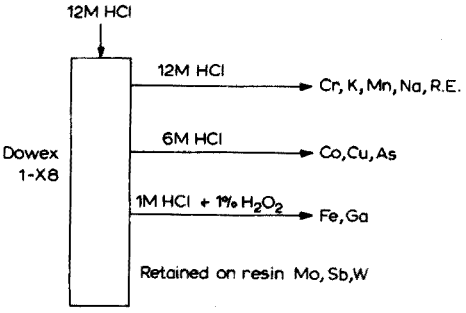

Fig. 5. Elution curves on Dowex 1-X8 in 9 M HCl. The column was charged with 10 cm³ of 9 M HCl containing a 0.5-g chromium matrix.

Fig. 6. Separation scheme for radiochemical analysis of chromium.

EXPERIMENTAL

Preparation of exchangers

Dowex resins and hydrated antimony pentoxide (Carlo Erba) and nickel hexacyanoferrate(II) (Applied Research) were used. The exchangers were sieved and the 75—125 μm fraction was used. After equilibration in 6 M hydrochloric

acid, the resin was placed in a glass-tube of 1-cm diameter. The height of the resin bed was adjusted to 10 cm.

Preparation of standards

For each irradiation, at least one standard for each impurity to be determined was placed in the rabbit with the sample. The standards were prepared in the following way. A known weight of the element (or one of its salts with a definite concentration) was dissolved. A known amount of this solution was deposited on filter paper and evaporated to dryness by means of an i.r. lamp. After irradiation, the paper was dissolved in nitric—sulfuric acids and the activity of the solution was measured under the same conditions as the samples. For nickel and iron standards, a piece of metal (5—10 mg) was used. Some checks on the standards were done by taking one of them as a flux monitor, and comparing the measured activity with the theoretical.

Irradiation conditions, etching and dissolution of samples

Samples (0.5—1 g) were irradiated in the EL_3 reactor, Saclay, in a thermal neutron flux of $5 \cdot 10^{12}$ n cm^{-2} s^{-1} for an irradiation time of 1—2 h or 65 h.

The surfaces of the samples were etched after irradiation to remove superficial contamination. Iron samples were etched with a mixture of 98 % hydrogen peroxide—2 % hydrofluoric acid, and then dissolved in a mixture of hydrochloric and nitric acids.

Chromium samples were etched in a hot solution of 1 M hydrochloric acid and dissolved in concentrated hydrochloric acid.

Counting and calculation equipment

All measurements were made with a Quartz and Silice Ge(Li) detector (volume 50 cm^3, resolution 2.25 keV for 1332 keV) connected to an Intertechnique DIDAC 4000 multichannel analyser. The activity of each fraction was measured with counting times varying from 30 min to 10 h. To correct errors [25] from pulse pile-up effects, a pulse generator [24, 25] was used. The correction was effective up to 30 % dead-time. After each measurement the spectrum was stored on punched tape and processed with a Hewlett-Packard 9810A desk-calculator [26].

Analysis without chemical separation

After irradiation for 1 h, it was possible to determine many elements in iron samples without chemical separation (Table 2). Direct measurement of the activity in the energy band over 600 keV gave a detection limit of 5 μg for nickel and 10^{-3} μg for manganese (calculations for this last element were based on the activity of the 1810-keV γ-peak) in chromium samples.

Analysis of iron with chemical separation

The separation scheme with the Dowex 1-X8 resin is shown in Fig. 4. After dissolution, the iron sample was poured on the column in 10 cm^3 of concen-

TABLE 2

Analysis of high-purity iron without chemical separation (Results in $\mu g\ g^{-1}$)

Sample	As	Au	Cu	Ga	K	Mn	Na	Sb	W
FM9	≤0.03	0.006	0.75	≤0.02	≤0.5	0.03	0.02	≤0.04	0.25
S3	≤0.03	≤0.002	0.15	≤0.04	—	0.02	≤0.01	≤0.06	≤0.04
J4	≤0.03	≤0.002	0.3	≤0.04	—	0.015	≤0.01	≤0.06	≤0.04
Ju4	≤0.03	≤0.002	0.5	≤0.03	≤0.5	0.04	0.015	≤0.05	≤0.04
Ju4Q	≤0.03	≤0.002	0.85	≤0.03	≤0.5	0.15	0.03	≤0.05	≤0.3
Ji4	≤0.03	≤0.002	0.8	≤0.03	≤0.3	0.25	0.015	≤0.05	≤0.04
S4Sp	≤0.03	≤0.002	0.7	≤0.03	≤0.5	0.025	≤0.01	≤0.05	≤0.04

trated hydrochloric acid at a flow rate of 1 $cm^3\ min^{-1}$. Chromium, manganese and alkaline earth elements were not retained. Cobalt, arsenic and copper were eluted by 60 cm^3 of 6 M hydrochloric acid. The activity of all these elements can be measured at the same time. The iron matrix was completely removed by washing the column with 100 cm^3 of a mixture of 99 % 1 M hydrochloric acid and 1 % of hydrogen peroxide. The resin containing molybdenum, antimony, and gold was extruded and counted.

Analysis of chromium with chemical separation

The scheme shown in Fig. 6 was applied. After dissolution, the chromium sample was poured on the Dowex 1-X8 resin in concentrated hydrochloric acid. The activity of chromium on the resin was very low after the passage of 50 cm^3 of 12 M hydrochloric acid. The activities of arsenic, cobalt, copper, gallium, iron, antimony, and tungsten were measured on the resin. The solution was passed through a column of antimony pentoxide on which sodium was retained. After partial neutralization of the acidity with ammonia, nickel could be retained on a nickel hexacyanoferrate(II) column at pH ~ 1.

RESULTS AND DISCUSSION

The methods were applied to the analysis of iron purified by zone melting (Tables 2 and 3). The elements determined are the most significant for the control of zone melting. Nine elements are determined routinely by non-destructive analysis, copper and manganese being the most important. The destructive method adds Co, Cr, and Mo to the analysis. Molybdenum has a 140-keV line which interferes with the 142.5-keV line of ^{59}Fe. The chemical scheme developed ensures good decontamination of iron and removes this interference.

With this method 12 elements in 7 samples can be determined simultaneously after irradiation for 72 h in a thermal neutron flux of $5 \cdot 10^{12}$ n $cm^{-2}\ s^{-1}$. One chemist can perform the chemical separations in 8 h. The fractions (2 for each sample) are counted three times, each for 1 h, on a Ge(Li) detector.

TABLE 3

Analysis of high-purity iron after chemical separation of the matrix (Results in $\mu g\ g^{-1}$)

Sample	As	Au	Co	Cr	Cu	La	Mn	Mo	Na	Pt	Sb	W
?M9	0.01	0.005	0.4	0.7	0.8	$<10^{-4}$	0.035	0.4	0.02	0.1	0.0005	0.23
33	0.0015	—	0.04	0.3	—	—	—	0.2	—	—	0.0005	0.01
14	0.01	—	0.03	0.4	—	—	—	0.2	—	—	0.0001	0.002
lu4	0.01	2.10^{-5}	0.07	1.5	0.55	$<10^{-4}$	0.05	0.5	0.01	0.01	0.0002	0.003
lu4Q	0.02	0.0003	0.2	2	0.95	$<10^{-4}$	0.2	0.7	0.05	0.07	0.0015	0.03
li4	0.01	10^{-4}	0.3	0.4	0.9	$<10^{-4}$	0.25	0.6	0.01	0.015	0.0015	0.01
34Sp	0.001	10^{-4}	0.03	0.3	0.8	$<10^{-4}$	0.03	0.2	0.001	0.05	$<10^{-4}$	0.01

TABLE 4

Detection limits ($\mu g\ g^{-1}$) of impurities in high-purity iron after irradiation in a thermal flux of $5 \cdot 10^{12}$ n $cm^{-2}\ s^{-1}$ for 1 h and 72 h

Time (h)	As	Au	Co	Cr	Cu	Ga	K	La
1	0.03	0.002	—	—	$5 \cdot 10^{-3}$	0.03	0.5	10^{-3}
72	10^{-3}	10^{-4}	10^{-2}	0.05	10^{-3}	—	—	$5 \cdot 10^{-5}$

	Mn	Mo	Na	Ni	Pt	Sb	W
1	$2 \cdot 10^{-4}$	—	0.01	0.1	0.01	0.04	0.04
72	10^{-4}	0.05	10^{-4}	—	10^{-3}	10^{-4}	$5 \cdot 10^{-4}$

TABLE 5

Analysis of electrolytic chromium after chemical separation of the matrix (Results in $\mu g\ g^{-1}$)

As	Au	Co	Cu	Ga	Fe	Na	Sb	W
0.03	0.002	0.01	0.1	0.005	3	0.2	0.1	0.005

Under these conditions, the detection limits are very low (Table 4). Up to 5 analyses of each sample were done. The precision, which varies from 5 to 10 %, depends on the element and its concentration: close to the detection limit, the precision is poorer.

Nine elements are determined routinely in chromium by destructive analysis. Other elements could also be determined after the same separation scheme, but are not included in the routine analysis. This method was applied to chromium purified by electrolytic deposition (Table 5). The precision and sensitivity are approximately the same as in an iron matrix (detection limit of iron in a chromium matrix, 0.1 $\mu g\ g^{-1}$).

The separation schemes developed are suitable for application to a matrix containing iron, chromium, and nickel. A slightly modified scheme could be used for the analysis of stainless steel.

Nickel was determined in both iron and chromium. Concentrations of 3 $\mu g\ g^{-1}$ in the FM9 iron sample and below the detection limit (0.5 $\mu g\ g^{-1}$) in electrolytic chromium were found. An irradiation in fast neutrons for 65 h in the Osiris reactor (thermal neutron flux, $2 \cdot 10^{14}$ n $cm^{-2}\ s^{-1}$) gave a concentration of 0.2 $\mu g\ g^{-1}$ in chromium with a limit of detection of 0.1 $\mu g\ g^{-1}$.

CONCLUSION

The simple procedure suggested allows the routine determination of up to 12 significant elements with good sensitivity and reproducibility in high-purity iron and chromium. Some simple chemical separations allow the simultaneous analysis of 7 samples irradiated at the same time. Neutron activation analysis is a suitable and competitive method for the routine control of the purification of these metals. The decrease in the cost of the analysis is mainly achieved by optimizing the choice of the elements determined and the separation procedure.

REFERENCES

1 G. Aubouin and J. Laverlochere, C.E.A., (1963) 2359.
2 W. J. Ross, Anal. Chem., 36 (1964) 1114.
3 J. W. MacMillan, Analyst (London), 89 (1964) 594.
4 D. A. Hilton and D. Reed, Analyst (London), 90 (1965) 541.
5 R. Malvano and P. Grosso, Anal. Chim. Acta, 34 (1966) 253.
6 L. Danielsson, Ark. Kemi, 27 (1967) 453, 467.
7 J. C. Ricq, J. Radioanal. Chem., 1 (1968) 443.
8 Ph. Albert, Colloq. Int. Fer très haute pureté, Paris 1966; Mem. Sci. Rev. Met., 65 (1968) 1.
9 B. A. Thompson and P. D. La Fleur, Anal. Chem., 41 (1969) 852.
10 A. Lesbats and R. Tardy, J. Radioanal. Chem., 17 (1973) 127.
11 N. Deschamps, Thesis, Paris, 1966.
12 C. de Wispelaere, J. P. op de Beek and J. Hoste, Anal. Chim. Acta, 70 (1974) 1.
13 E. Steinnes, Scand. J. Metall., 1 (1972) 137.
14 C. Cleyrergue and N. Deschamps, J. Radioanal. Chem., 17 (1973) 139.
15 C. de Wispelaere, J. P. op de Beek and J. Hoste, Anal. Chim. Acta, 64 (1973) 321; Anal. Chem., 45 (1973) 547.
16 F. Dugain, C. Castre and B. Beyssier, Anal. Chim. Acta, 42 (1968) 39.
17 J. L. Debrun, Thesis, Orsay, 1969.
18 L. Danielsson and T. Ekström, Acta Chem. Scand., 20 (1966) 2402, 2415.
19 J. M. Peters and G. del Fiore, Radiochem. Radioanal. Lett., 16 (1974) 109.
20 B. C. Lee, M. Y. Park and K. C. Park, Daehan Hwahak Hwoejee, 17(5) (1973) 346; through CA 74, 80, 55510 y.
21 F. Nelson, T. Murase and K. A. Kraus, J. Chromatogr., 13 (1964) 503.
22 I. Hazan and J. Korkisch, Anal. Chim. Acta, 32 (1965) 46.
23 C. Neskovic-Loos, M. Fedoroff and G. Revel, 8th Radiochem. Conf. Marianske Lazne, 1975, J. Radioanal. Chem., 30 (1976) 633.
24 O. U. Anders, Nucl. Instrum. Methods, 68 (1969) 205.
25 B. Maziere, A. Gaudry, W. Stanilewicz and D. Comar, J. Radioanal. Chem., 16 (1973) 281.
26 M. Fedoroff, J. Blouri and G. Revel, Nucl. Instrum. Methods, 113 (1973) 589.
27 L. A. Currie, Anal. Chem., 40 (1968) 586.

Analytica Chimica Acta, 85 (1976) 103—115

CHROMATOGRAPHY OF AROMATIC COMPOUNDS ON CATION-EXCHANGE RESINS OF THE SULPHONIC ACID TYPE

LUTFUL MAJID JAHANGIR and OLOF SAMUELSON

Department of Engineering Chemistry, Chalmers University of Technology, Fack, S-402 20 Göteborg (Sweden)

(Received 27th February 1976)

SUMMARY

In aqueous media, the distribution coefficients of aromatic compounds on sulphonated cation-exchange resins with a styrene—divinylbenzene matrix decrease with increasing degree of sulphonation and temperature. The sorption is mainly determined by non-polar interactions and by the molar volume of the solutes. Efficient chromatographic separations are obtained in dilute hydrochloric acid or in acetic acid on conventional resins in the free-acid form. In several systems improved separation factors are obtained with partially de-sulphonated resins.

In analyses of effluents from various industries, e.g. from the production of wood pulp, it is convenient to exchange the metal cations for hydrogen ions by means of a cation-exchange resin of the sulphonic acid type before the separation of the organic solutes. It is well known that aromatic non-electrolytes are retained by the cation exchanger. This may result in losses of aromatic compounds but can also be utilized in chromatographic separations [1—5]. The purpose of this paper is to elucidate the influence of various factors, including the structure of the solutes, on their sorption and chromatographic separation in aqueous eluents.

EXPERIMENTAL

Most of the experiments were made with a commercial sulphonic acid resin having a styrene—divinylbenzene matrix (Aminex A-5, 11—15 μm; Bio-Rad). The exchange capacity was 4.1 mmol g^{-1}. The non-ionic adsorption resin Amberlite XAD-2 (Rohm and Haas) was crushed and sieved. The 60—75-μm fraction was treated with water, ethanol, 1 M sodium hydroxide, 1 M hydrochloric acid and finally with water. Sulphonated samples of XAD-2 were prepared [6] by stirring the same fraction of the resin (swelled in toluene) with 97 % sulphuric acid (30 g per g of XAD-2). A resin with an exchange capacity (Q) of 2.5 mmol g^{-1} was obtained after 38 h at 90 °C. Low-sulphonated resins were obtained after 18 h at 40 °C (Q = 1.45) and 3.5 h at 2 °C (Q = 0.47). The solution was displaced with sulphuric acid of decreasing

concentration to avoid breakage of the resin particles and purified as described above.

In addition, experiments were made with a low-sulphonated styrene—divinylbenzene resin (Aquapac, 37—75 μm, Q = 0.65; Waters Associates) and with a sample of Aminex A-5 which was partially desulphonated [7]. The exchange capacity was 3.3 mmol g^{-1}. Unless otherwise mentioned, the cation-exchange resins were used in their free-acid form.

The chromatographic runs were made in jacketed columns (346 × 2.6 mm) maintained at constant temperature. The columns were preconditioned with the eluent before the aromatic solutes (0.1—2.4 μg) dissolved in the eluent were applied. The absorbance of the eluted aromatic solutes was determined at 254 nm. Cyclohexane was measured with a refractive-index detector.

The adjusted retention volume (retention volume minus interstitial volume) was calculated in column volumes. In the experiments with Aminex A-5 in its free-acid form, the values were independent of the nominal linear flow (1—5 cm min^{-1}) and of the amount applied except for the experiments with partially dissociated acids. With this exception the values reported for this resin are equilibrium distribution coefficients (D_v) valid for the linear part of the sorption isotherm. For XAD-2 and the low-sulphonated resins, the reported values should only be taken as an approximate measure of D_v.

SAMPLE SIZE AND ELUENT COMPOSITION

The hydrogen ion concentration in the free-acid form of a sulphonic acid resin is so high that the dissociation of the phenols and carboxylic acids is negligible in this phase. The ratio of the equilibrium concentration of a solute in the resin (c_r) to its analytical concentration in the external solution, c (molar scale) can therefore be calculated from the equation

$$\frac{c_r}{c} = K_D \frac{[H^+]}{K_a + [H^+]}$$

where the distribution constant K_D is the ratio of the concentration of undissociated solute in the resin phase (calculated per unit volume) to that in the external solution, and K_a is the acid dissociation constant. At low solute concentration, K_D and K_a should be constant.

Most solutes were weak acids ($K_a \ll [H^+]$) which means that their dissociation can be disregarded even in water and that the sorption isotherms should be linear. Theoretically, the peak positions of these compounds should be independent of the amount applied. This was confirmed by chromatography in water which showed that the positions of compounds like phenol and 3-chlorophenol (Fig. 1) were unchanged when the amount was increased by a factor 10. Under ideal conditions symmetric elution peaks should be obtained, but as can be seen some tailing was observed even for the lowest amount applied to the column.

For the carboxylic acids the hydrogen ion concentration in the mobile

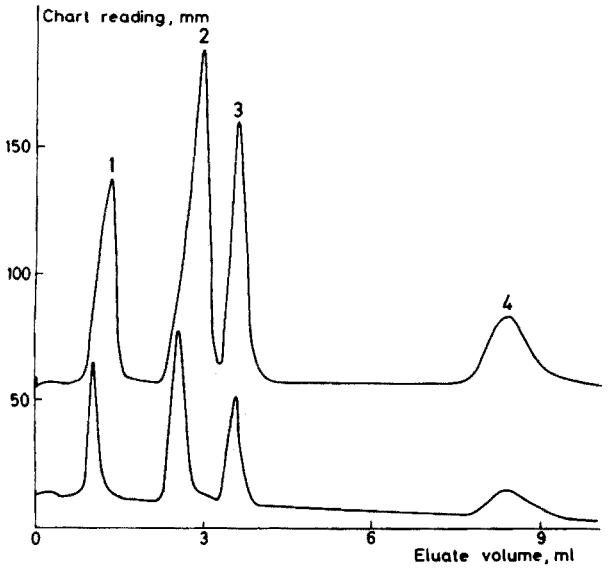

Fig. 1. Separation of (1) 2-chlorobenzoic acid, 1.6 μg; (2) benzoic acid, 2.4 μg; (3) phenol, 1.3 μg and (4) 3-chlorophenol, 2.4 μg, on Aminex A-5 (H^+; 346 × 2.6 mm) in water at 70 °C. In the run represented in the lower chromatogram the amounts applied were 10 % of those given above (referring to the upper chromatogram). Nominal linear flow: 7.2 cm min^{-1}.

phase is markedly affected by acid concentration when water is used as eluent and decreases during the passage of the chromatographic zone through the column. The equation predicts a concave sorption isotherm which means that the elution curves should be fronting and that the retention volume should increase for increasing amounts applied to the column. This was confirmed by the experiments given in Fig. 1. Similarly, the retention volumes of the polychlorinated phenols were markedly affected by the amount applied. Hence, pure water is unsuitable as eluent in chromatographic separations of the more acidic solutes but is well suited to a group separation of benzoic acids from phenolic compounds.

In agreement with the equation given above, it was observed (Table 2) that for the weakly acidic solutes the retention volume in 0.001 M hydrochloric acid was only slightly higher than that in water, while for the stronger acids (phenols containing two or more chloro groups and benzoic acids) the retention increased markedly in the presence of hydrochloric acid. As predicted the largest change was observed with the carboxylic acids.

Experiments in 0.01 M hydrochloric acid showed that the position of phenol was unchanged while the retention values of benzoic and 2-chlorobenzoic acids increased to 2.22 and 2.80, respectively. In this medium 2-chlorobenzoic acid was still dissociated to an appreciable extent while the dissociation of benzoic acid was negligible. Experiments were made in 0.1 M sulphuric acid to suppress the dissociation of 2-chlorobenzoic acid further.

TABLE 1

Adjusted retention volume calculated in column volumes for hydroxybenzenes on non-sulphonated and sulphonated resins (H^+) in water

	Phenol	1,2-Dihydroxy-benzene	1,3-Dihydroxy-benzene	1,4-Dihyd benzene
XAD-2, 30 °C	29	9.6	5.7	2.0
Sulphonated XAD-2, Q = 0.47; 30 °C	90	17	5.9	2.9
Sulphonated XAD-2, Q = 1.45; 30 °C	37	5.3	2.4	1.6
Sulphonated XAD-2, Q = 2.50; 30 °C	15	2.9	1.4	1.0
Aquapac, Q = 0.65; 30 °C	36	8.7	4.5	2.2
Aquapac, Q = 0.65; 70 °C	16	4.5	2.2	1.2
Aminex A-5, Q = 4.1; 30 °C	2.3	1.5	1.4	1.4
Aminex A-5, Q = 4.1; 70 °C	1.4	0.93	0.86	0.86

The following retention volumes were obtained: phenol 1.53, benzoic acid 2.44 and 2-chlorobenzoic acid 3.32. The increase observed for phenol and benzoic acid can be ascribed to salting-out. The larger effect for 2-chlorobenzoic acid can be attributed to the acid being virtually undissociated in this medium.

Except for 2-chlorobenzoic acid the D_v values for all solutes investigated (Table 2) decreased markedly when the elution was made in 1 M acetic acid instead of 0.001 M hydrochloric acid, although the hydrogen ion concentration was somewhat higher in the acetic acid. A change in solvent structure and the formation of association compounds with acetic acid explain the observed effect. The largest decrease in $\ln D_v$ was observed for the solutes which were held very strongly by the resin. For chlorobenzoic acid the depressed dissociation of the acid has the effect of increasing D_v. Almost symmetric elution curves were obtained in these media.

The effect of the acetic acid concentration over a wider range was studied for some phenols and chlorinated phenols. The D_v values decreased markedly with increasing concentration but the elution order was not affected (Fig. 2). The shape of the curves was similar for all solutes. For some compounds the separation factor was slightly lower at high acetic acid concentration than at low concentration. However, the decrease in D_v led to more rapid separations.

INFLUENCE OF THE DEGREE OF SULPHONATION AND COLUMN TEMPERATURE

Previous studies of desulphonated resins [8] and of gel-type resins sulphonated to obtain increasing concentrations of sulphonic acid groups [9] showed that the sorption of non-polar solutes decreased markedly with increased exchange capacity of the resin. More recently, non-sulphonated macroreticular resins prepared by copolymerization of styrene and divinylbenzene (e.g. Amberlite XAD-2) have been used for the sorption of aromatic compounds from aqueous solutions [10]. The effect of the sulphonic acid group concen-

TABLE 2

Retention data for Aminex A-5, H^+ (13 ± 2 μm) in various eluents at 70 °C

	Adjusted retention volume[a]			$\Delta \ln D_v$[b]
	Water[c]	0.001 M HCl	1 M HAc	
Benzene	2.6 (3.5)	2.70	2.02	0.29
Methoxybenzene	3.8 (4.0)	4.00	2.71	0.39
Benzaldehyde	3.0	3.23	2.09	0.43
Chlorobenzene	6.3	6.46	4.20	0.43
Phenol	1.4 (2.0)	1.48	1.13	0.27
2-Chlorophenol	3.3 (5.0)	3.45	2.30	0.40
3-Chlorophenol	4.0 (7.3)	4.10	2.67	0.43
4-Chlorophenol	3.8 (6.6)	4.10	2.69	0.42
2,3-Dichlorophenol	9.2	9.95	5.84	0.53
2,4-Dichlorophenol	8.5 (15)	9.12	5.51	0.50
2,5-Dichlorophenol	7.9 (14)	8.28	4.91	0.52
2,6-Dichlorophenol	6.2 (7.7)	6.85	4.06	0.52
2,4,5-Trichlorophenol	20	21.8	10.6	0.72
2,4,6-Trichlorophenol	13	15.3	8.14	0.63
3,4,5-Trichlorophenol	20	28	13.5	0.73
2,3,4,5-Tetrachlorophenol	40	52	21	0.91
2,3,4,6-Tetrachlorophenol	21	34	14.7	0.84
2,3,5,6-Tetrachlorophenol	20	32	15.0	0.76
3-Methylphenol	2.4	2.46	1.71	0.46
4-Chloro-3-methylphenol	7.2	7.76	4.52	0.54
Benzoic acid	0.8	2.1	1.58	
4-Hydroxy-3-methoxybenzoic acid	0.7	2.3	1.31	
2-Chlorobenzoic acid	0.5	1.8	1.81	

[a]Calculated in column volumes.
[b]$\Delta \ln D_v$ is the difference in $\ln D_v$ in 0.001 M HCl and 1 M acetic acid.
[c]The values in parentheses refer to experiments with the sodium form of the resin.

tration, over the range from the non-sulphonated resin to highly sulphonated cation exchanger, with the same resin matrix is illustrated in Table 1.

For all solutes the highest distribution coefficients were obtained with the cation exchanger with the lowest exchange capacity. The net result of an increasing concentration of sulphonic acid groups linked to the resin matrix can be interpreted as a salting-out effect. The fact that in experiments with a commercial resin (Table 2) larger retention volumes were obtained for all non-electrolytes on the sodium form than on the hydrogen form (cf. ref. 3) shows that the counter ions affect this salting-out.

The observation that non-sulphonated Amberlite XAD-2 gave lower retention volumes than the low-sulphonated resin indicates that for steric reasons not all parts of this resin were accessible to the aromatic compounds.

At 30 °C broad peaks were recorded with these resins. The peaks were much sharper at higher temperature. The separation factors for the solutes investigated were more favourable on the sulphonated XAD-2 than on

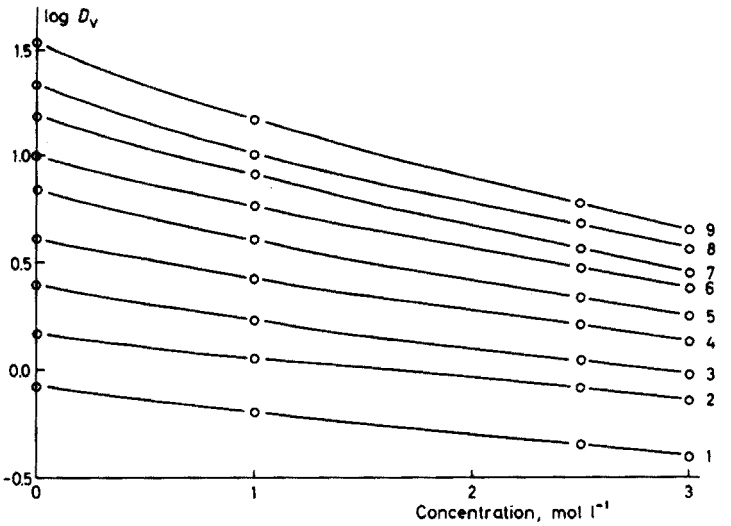

Fig. 2. Influence of acetic acid concentration on log D_v at 70 °C. Aminex A-5 (H^+). Zero concentration refers to 1 mM HCl. (1) 1,3-Dihydroxybenzene; (2) phenol; (3) 3-methylphenol; (4) 4-chlorophenol; (5) 2,6-dichlorophenol; (6) 2,3-dichlorophenol; (7) 2,4,6-trichlorophenol; (8) 2,4,5-trichlorophenol; (9) 2,3,4,6-tetrachlorophenol.

commercial resins of gel type (cf. Table 1 and ref. 2). Unfortunately, the sulphonated XAD-2 resins were compressed so severely under conditions suitable for rapid chromatographic separations that the columns had to be repacked after a few runs.

Improved separation factors and increased distribution coefficients without loss in stability of the packing and column efficiency were obtained with a sample of partially desulphonated Aminex A-5. Figure 3 shows the separation of eight compounds at 30 °C; 2 h were required. At 50 °C the height of a theoretical plate was decreased by 20—40 % for different compounds, but no further improvement was obtained at 70 °C. Similar observations were made with Aminex A-5 which had not been subjected to desulphonation. The separation factors of most solutes tended to decrease at high temperature. Hence, phenol and 3,4-dihydroxybenzaldehyde, which were separated almost completely at 30 °C, were eluted as a single peak at 50 °C.

In agreement with the results reported by Nomura et al. [2], it was found that the distribution coefficients of all compounds decreased markedly with increasing temperature (Fig. 4). The change in enthalpy ($-\Delta H^0$) was slightly higher for the partially desulphonated resin than for Aminex A-5 and considerably higher for the low-sulphonated XAD-2 resin. Separate experiments, not reported here, show that this also applied to non-sulphonated XAD-2. Evidently, the decrease in enthalpy contributes significantly to the decrease in free energy, which is linearly related to ln D_v.

The results show that low-sulphonated resins are preferred when aromatic

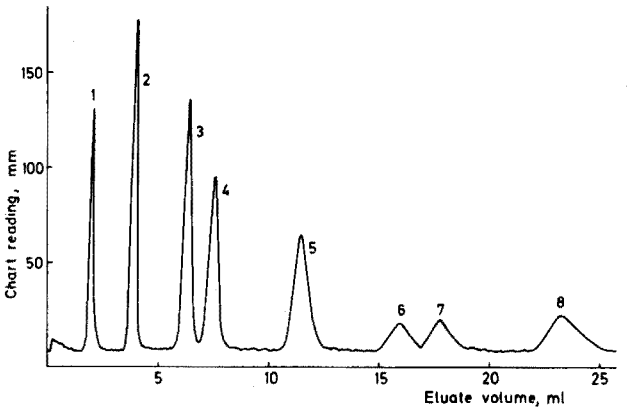

Fig. 3. Separation of eight phenolic compounds on partially desulphonated (Q = 3.3 mmol g^{-1}) Aminex A-5 (H^+; 337 × 2.55 mm) in 1 mM HCl at 30 °C. Nominal linear flow: 4.2 cm min^{-1}. (1) Guaiacylglycerol; (2) 1,3-dihydroxybenzene; (3) phenol; (4) 3,4-dihydroxybenzaldehyde; (5) 3-methylphenol; (6) 2,6-dimethoxyphenol; (7) 2-chlorophenol; (8) 3-chlorophenol.

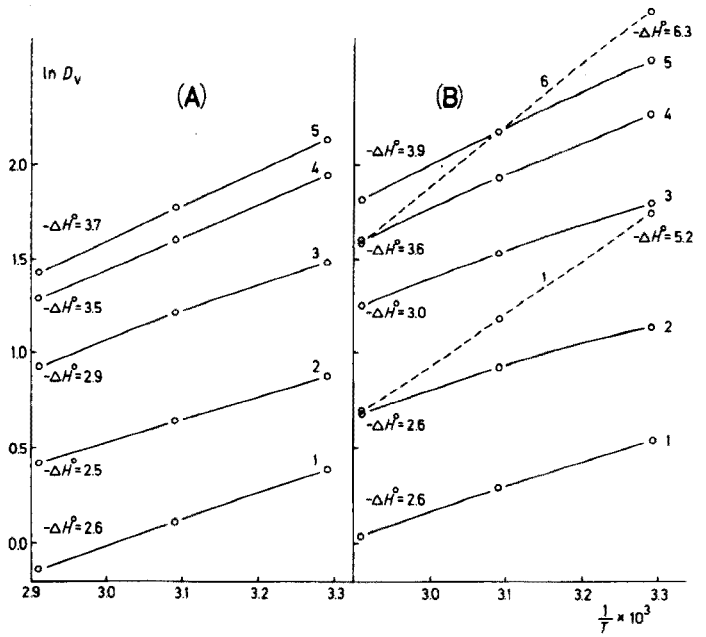

Fig. 4. Influence of the thermodynamic temperature (T) on the distribution coefficients in 1 mM hydrochloric acid on (A) Aminex A-5 (Q = 4.1), (B) partially desulphonated Aminex A-5 (Q = 3.3) (full line) and low-sulphonated XAD-2 (Q = 0.47) (dashed line). ($-\Delta H^\circ$ values are given in kcal mol^{-1} at 323 K). (1) 1,3-Dihydroxybenzene; (2) phenol; (3) 3-methylphenol; (4) 2-chlorophenol; (5) 3-chlorophenol; (6) 1,2-dihydroxybenzene.

solutes have to be removed from aqueous solutions and concentrated as a group. The solutes can then be eluted with organic solvents, e.g. ethanol. These operations can be carried out advantageously at ambient temperature.

Chromatographic separations on commercial fully sulphonated resins and on partially desulphonated resins can be carried out at room temperature provided that fine particles are used. Elevated temperature can be used to speed up the separation provided that the compounds are stable and have favourable separation factors. Careful temperature control is required to obtain reproducible results.

SORPTION MECHANISM AND ELUTION ORDER

A cation-exchange resin of the sulphonic acid type behaves like a concentrated solution of a sulphonic acid. Conventional resins (gel-type) contain no pores filled with external solution and for most purposes can be considered to approximate a homogeneous solution (resin phase) [11]. The distribution of non-electrolytes between an external aqueous solution and the resin phase can therefore be represented by the Gibbs—Donnan equation [12]

$\ln c_r/c = -\pi\bar{v}/RT - \ln \gamma_r/\gamma$, where π is the swelling pressure, $\bar{v}$ the partial molar volume of the non-electrolyte, and γ_r/γ the ratio of the activity coefficients in the two phases. Strongly polar solutes such as polyols exhibit a lower concentration in the resin phase than in the external solution. The concentration ratio decreases with increasing molecular size. Calculations have shown that the pressure—volume term predominates [13]. Conversely, apolar solutes are concentrated in the resin phase. This fact and the observation that the distribution coefficient tends to be higher for aromatic solutes of high molecular size than for smaller molecules shows that the activity coefficient term predominates.

With anion-exchange resins, hydrogen bonding of phenolic protons to ions in the resin phase, together with non-polar interactions are responsible for the sorption [14]. The latter include those due to differences in water structure in the resin phase and in the external solution. The facts that the sorption of phenolic compounds decreases with an increased degree of sulphonation of the cation exchanger, and that the elution order dihydroxybenzene < phenol < benzene is valid both for the H^+ and Na^+ forms of the resin, show that with cation-exchange resins the contribution from hydrogen bonding with the ions in the resin phase is of minor or no importance. The fact that 1,2-dihydroxybenzene with strong intramolecular hydrogen bonds is held more strongly than its isomers (Table 1 and ref. 3), and the elution order chlorophenols < chlorobenzene, support this conclusion. In addition, there is a tendency among the chlorinated phenols for isomeric compounds to be eluted in order of decreasing acid strength. With hydrogen bonding as a predominant sorption mechanism, the elution order would have been reversed.

As in the anion-exchange systems studied previously [14], the interactions between the π-electrons in the aromatic nucleus and the resin seem to be of

little importance. Hence cyclohexane (D_v = 6.6) was held much more strongly in water than benzene (D_v = 2.6). This indicates that hydrophobic interactions caused by differences in water structure between the resin and the external solution, and thus related to the solubility in water, are much more important. In addition to these solute—water interactions, the decrease in activity coefficients caused by interactions between solutes and the hydrocarbon skeleton of the resin will contribute, while the salting-out effect arising from the $-SO_3^-H^+$ groups will depress the sorption. Sorption decreases markedly with increasing temperature, showing that there are significant enthalpy contributions and that the mechanism is more complex than in those aqueous systems containing certain apolar solutes, where the gain in entropy is solely responsible for the sorption [15].

The results discussed above suggest that there will be a trend for solutes having low solubility in water to be held more strongly than those of higher solubility. The elution order dihydroxybenzenes < phenol < 3-methylphenol < benzene < methoxybenzene < chlorobenzene, and that for halobenzenes reported by Yamada et al. [3] (fluoro < chloro < bromo < iodo) are in agreement with this prediction. Similarly, the increase in the D_v values of phenols with an increasing number of chloro-substituents can be ascribed to a decreased solubility in water. The D_v value of pentachlorophenol was so high that it could not be determined reliably in 1 mM hydrochloric acid. In 3 M acetic acid, the D_v value was 6.6 compared to 6.2 for 2,3,4,5-tetrachlorophenol.

The D_v values of 2-methoxyphenol and other compounds related to lignin are given in Table 3. As expected, because of its lower solubility in water, D_v for 2-methoxyphenol was much higher than that of phenol. Similarly, 2,6-dimethoxyphenol, in which the hydroxyl group is shielded by two methoxyl groups which can serve as proton acceptors in intramolecular hydrogen bonding, was held more strongly than 2-methoxyphenol. As shown in Table 2, benzaldehyde was adsorbed more strongly than benzene. The elution sequences phenol < 4-hydroxybenzaldehyde, 1,2-dihydroxybenzene < 3,4-dihydroxybenzaldehyde, and 2-methoxyphenol < vanillin were therefore predictable.

The introduction of a glycerol side-chain in 2-methoxyphenol resulted in a striking decrease in D_v. In fact, the concentration of compound (8) in the resin phase was lower than in the external solution (c_r/c = 0.75 at 30 °C and 0.48 at 70 °C). The larger molar volume will, according to the equation given above, result in a decrease in ln D_v of about 0.5 while the observed decrease in ln D_v was 2.0 at 30 °C and 2.1 at 70 °C. Evidently, the weakening of the non-polar interactions by introduction of a strongly hydrophilic side-chain is a more important factor than the increase in molar volume.

The effect of the pressure—volume term will be lower for compound (9) with a hydroxymethyl substituent in the same position. Similarly, the weakening of the hydrophobic interactions will be less. As expected, this compound took an intermediate position between 2-methoxyphenol and compound (8).

Conversely, the propyl group in compound (10) led to a large increase in

TABLE 3

Volume distribution coefficients (D_v) for Aminex A-5, H^+ in 1 mM hydrochloric acid at 30 °C and 70 °C

	Compound[a]	30 °C	70 °C
1	Phenol	2.30	1.48
2	2-Methoxyphenol, R'H	3.81	2.18
3	2,6-Dimethoxyphenol	6.12	2.96
4	4-Hydroxybenzaldehyde	4.87	2.37
5	1,2-Dihydroxybenzene	1.52	0.93
6	3,4-Dihydroxybenzaldehyde	2.98	1.48
7	Vanillin, R'CHO	5.40	2.45
8	$R'CH(OH)CH(OH)CH_2OH$	0.46	0.29
9	$R'CH_2OH$	2.38	1.38
10	$R'CH_2CH_2CH_3$	16.5	8.36
11	$R'CH_2CH{=}CH_2$	12.4	6.05
12	$R'CH_2CH_2CH_2OH$	6.86	3.54
13	$R'CH(OH)CH(CH_2OH)OR''$	5.44	2.65
14	$R'CH(OH)CH_2OR''$	41	12.8
15	$R'''CH(OH)CH(CH_2OH)OR''$	12.4 (t)[b]	5.67
16	$R'COCH_2R'$	70	19.8
17	$R'CH(OH)CH(CH_2OH)R'$	1.65	0.88

[a]Key: R' = 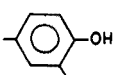 R'' = 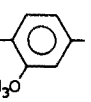 R''' = 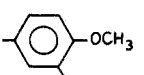

[b]t = severe tailing.

D_v. Evidently, non-polar interactions exert a much greater effect than the pressure—volume term. Unsaturated aliphatic hydrocarbons are less hydrophobic than the corresponding saturated compounds [16]. Thus the effect of an allyl substituent (compound 11) was less than that of a propyl group. A hydroxyl group at the end of the side chain (compound 12) resulted in a decrease in D_v compared to the propyl derivative, confirming that the influence of non-polar interactions predominates.

The experiments with compounds containing two benzene rings linked by an aliphatic chain support these results. Thus compound (13) with two hydroxyl groups in the aliphatic chain had a much lower D_v value than compound (14) with one aliphatic hydroxyl group. Similarly, the introduction of a methoxyl group in place of a phenolic hydroxyl group resulted in increased non-polar interactions. Therefore D_v for compound (15), which lacked phenolic hydroxyl groups was about twice that of compound (13) with an otherwise identical structure. The high D_v for compound (16) supports the conclu-

sion that carbonyl compounds are retained very strongly. The decrease in non-polar interactions caused by the introduction of hydroxyl groups in the aliphatic chain is responsible for the extremely low D_v of compound (17). It is noteworthy that this compound was held less strongly than compound (9). The effect of the pressure—volume term for compounds containing several polar substituents explains the elution order.

Evidently, the D_v values can give information about the probable structure of aromatic compounds and hence guidance as to the choice of methods for final identification. However, the contribution of a substituent to the change in free energy for the sorption (linearly related to ln D_v) depends both on the position of the substituent and on the structure of the solute into which the substituent is introduced. For final identification it is, therefore, necessary to apply additional methods.

APPLICATIONS IN CHROMATOGRAPHY

Conventional resins of high exchange capacity, commercially available as small beads, and partially desulphonated resins of this type gave excellent chromatographic separations of a large number of aromatic solutes. The free-acid form of the resins was employed, since in many practical analyses, e.g. of effluents, it is desirable to combine the chromatographic separation with the removal of metal cations present in the solution. Metal ions may otherwise complicate the determination of solutes such as carbohydrates and hydroxy acids which pass into the effluent. Pure water has previously been used as eluent [2, 3] but, as shown in Fig. 1, this eluent has great disadvantages when acidic aromatic compounds are to be separated. Even for weak acids such as phenol, a larger scattering in retention volumes was observed compared with experiments in 1 mM hydrochloric acid or 1—3 M acetic acid. With the latter eluents the peak positions were reproducible to ±1 % over a period of several weeks at 50 ± 0.1 °C. When a conventional resin had been used in 1 M acetic acid at 70 °C for 20 days the adjusted retention volumes of phenol, 3-methoxyphenol, 2-chlorophenol and 3-chlorophenol increased by approximately 4 %, probably because of a slight decrease in ion-exchange capacity.

A typical separation of nine different phenols (0.4—1.7 μg of each) in 2.5 M acetic acid at 70 °C is illustrated in Fig. 5. The last compound was eluted within 60 min. It can be seen that the separations were complete although slight tailing was obtained. The peak areas were reproducible within ±1.5 % or better for stable compounds. The results show that the method is suitable for quantitative analysis of complex mixtures of aromatic compounds. It should be stressed, however, that the field of application of the free-acid form of cation exchangers is limited to samples containing compounds stable in acid. Among compounds studied in the present work compound (17) (Table 3) decomposed at 70 °C whereas no severe decomposition occurred at 30 °C. In analysis of mixtures containing unknown compounds,

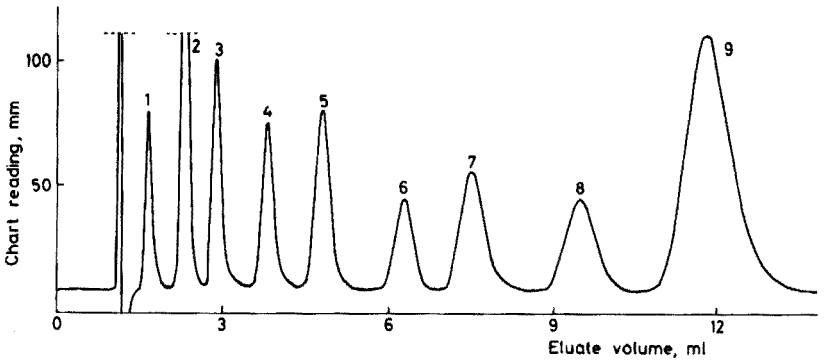

Fig. 5. Separation of nine phenolic compounds on Aminex A-5, (H^+; 346 × 2.6 mm) in 2.5 M acetic acid at 70 °C. Nominal linear flow: 4.4 cm min^{-1}. (1) 1,3-Dihydroxybenzene; (2) phenol; (3) 3-methylphenol; (4) 4-chlorophenol; (5) 2,6-dichlorophenol; (6) 2,3-dichlorophenol; (7) 2,4,6-trichlorophenol; (8) 2,4,5-trichlorophenol; (9) 2,3,4,6-tetrachlorophenol.

it is advisable therefore to check that no decomposition occurs, e.g. by chromatography at two widely different flow-rates. In routine analyses, time can be saved by elution at high temperature but in most analyses it is safer to use a lower temperature, e.g. 30 °C, both with regard to the improved separation factors and to the risk of decomposition.

Since the sorption mechanism for the cation exchanger differs from that responsible for the sorption onto anion-exchange resins and polyvinylpyrrolidone [17], it is obvious that chromatography on a cation exchanger is a valuable complement to chromatography on the other resins. As an example, 2,3-dichlorophenol and 2,5-dichlorophenol were not resolved on these resins but were well separated on a cation exchanger in 1 mM hydrochloric acid or 1 M acetic acid. For some other solutes, anion exchangers and polyvinylpyrrolidone are preferred. In analysis of complex mixtures such as effluents, it is advantageous to use both a cation exchanger and one of the other resin types to obtain a satisfactory resolution of the mixture before final identification of the solutes e.g. by g.c.—m.s.

The financial support of the Swedish Institute and the Swedish Board for Technical Development is gratefully acknowledged. The authors also wish to thank Dr Knut Lundquist for valuable discussions and for gifts of lignin model compounds.

REFERENCES

1 T. Seki, J. Chem. Soc. Japan, Pure Chem. Sect., 75 (1954) 1297.
2 N. Nomura, S. Hiraki, M. Yamada and D. Shiho, J. Chromatogr., 59 (1971) 373.
3 M. Yamada, N. Nomura and D. Shiho, J. Chromatogr., 64 (1972) 253.
4 H.-W. Lange and K. Hempel, J. Chromatogr., 59 (1971) 53.
5 J. Chmielowiec and W. Kemula, J. Chromatogr., 102 (1974) 197.

6 K. W. Pepper, J. Appl. Chem., 1 (1951) 124.
7 G. E. Boyd, B. A. Soldano and O. D. Bonner, J. Phys. Chem., 58 (1954) 456.
8 O. Samuelson, Sven. Kem. Tidskr., 54 (1942) 170.
9 A. Ehmann and R. S. Bandurski, J. Chromatogr., 72 (1962) 61.
10 J. S. Fritz and A. Tateda, Anal. Chem., 40 (1968) 2115.
11 O. Samuelson, Undersökningar angående jonbytande fasta ämnen, Esselte, Stockholm, 1944.
12 F. G. Donnan and E. A. Guggenheim, Z. Phys. Chem., Abt. A, 162 (1932) 346.
13 M. Mattisson and O. Samuelson, Acta Chem. Scand., 12 (1958) 1386.
14 L. M. Jahangir, L. Olsson and O. Samuelson, Talanta, 22 (1975) 973.
15 J. Feitelson, in J. A. Marinsky (Ed.), Ion Exchange, Vol. 2, Marcel Dekker, New York, 1969, pp. 135—165.
16 C. Tanford, The Hydrophobic Effect: Formation of Micelles and Biological Membranes, Wiley, New York, 1973.
17 L. Olsson, N. Renne and O. Samuelson, J. Chromatogr., in press.

Analytica Chimica Acta, 85 (1976) 117—126

CONDITIONS OF QUANTITATIVE PRECIPITATION, COMPLEXATION AND EXTRACTION

B. W. BUDESINSKY

Phelps Dodge Corporation, Morenci, Arizona 85540 (U.S.A.)

(Received 1st December 1975)

SUMMARY

A theory is described that allows the optimum conditions for quantitative precipitation, complexation, and extraction to be estimated by computer calculations. Theoretical conditions are compared with practical conditions for 8-hydroxyquinoline precipitation, EDTA complex formation, and dithizone, 8-hydroxyquinoline, cupferron, acetylacetone, and thenoyltrifluoroacetone extraction. The difficulties of a similar approach for redox reactions are discussed.

Each year, the number of papers dealing with the determination of stability and extraction constants seems to increase greatly. Undoubtedly, the computer technique of data evaluation has brought a tremendous improvement into that area. The utility of stability and extraction constants for a more precise characterization of individual methods is generally accepted. Ringbom [1] made the first systematic attempt to use stability and extraction constants for prediction of quantitative reactions, and recognized that the concept of effective (conditional) stability constants is central to the problem. His approach was based on simple mathematics so that no computer was necessary. Several years ago, another approach to establishing the conditions for optimum acidity of complexation [2] and extraction [3] was described, but that was also a non-computer approach based on inconvenient differential equations.

In this paper, a simple computer-based method for the estimation of optimal conditions of quantitative reactions is discussed.

THEORETICAL

Acidity Optimum

For a metal ion M, a ligand L, and a masking (or buffer) ligand Y, the formation of a compound $M_m Y_i H_j L_n$ (H is the hydrogen ion), that either precipitates or forms a soluble (sometimes extractable) complex in the solution, is governed by the side-reaction function

$$\phi_H = [H]^j \alpha_{Y(H)}^{-i} \alpha_{M(Y)}^{-m} \alpha_{L(H)}^{-n} \quad (1)$$

where the meaning of the individual side-reaction coefficients $\alpha_{u(v)}$ is described in Fig. 1. The acidity optimum of formation of that compound is given by the maximum value of ϕ_H for which we have

$$d\phi_H/d[H] = 0 \text{ and } d^2\phi_H/d[H]^2 < 0 \qquad (2a, b)$$

In practice, it is unnecessary to use eqns. (2a, b). Direct iteration with eqn. (1) is more convenient. If the sequence of values $pH_w = pH_0 + w\Delta pH$ (where $w = 1, 2, \ldots$ and ΔpH is the measure of precision)* is introduced, the corresponding increasing values of $\phi_{H(w)}$ and the first value for which $\phi_{H(w)} < \phi_{H(w-1)}$ indicates the maximum value $\phi_{H(w-1)}$, can be calculated.

The function ϕ_H is more convenient than the effective (conditional) constant since it contains only acidity-dependent quantities. Two simplifying assumptions are made: (1) $c_Y \gg c_M$ so that $c_Y = [Y]\alpha_{Y(H)}$; (2) the compound $M_mY_iH_jL_n$ is the only compound formed between M and L. For the meaning of c_Y, see below.

Quantitative precipitation

The relationship between the solubility product β_{mijn} and ϕ_H is described by the equation

$$(c_M - mc)^m (c_L - nc)^n \phi_H c_Y^i = \beta_{mijn} \qquad (3)$$

where c_M, c_L and c_Y are the starting concentrations of M, L and Y respectively; c is the concentration equivalent to the precipitated product of $M_mY_iH_jL_n$. If the condition of quantitative precipitation

$$(c_M - mc) = 0.001c_M \qquad (4)$$

so that $mc \approx c_M$ is introduced, the relationship presented in Fig. 1 is obtained. The designation of β_{mijn} for the solubility product was used to simplify the programming and, in practice, it cannot be confused with the overall stability constant (see below) because its logarithm is always a negative number.

Quantitative complex formation

The overall stability constant β_{mijn} and ϕ_H are in the following relationship

$$c(c_M - mc)^{-m} (c_L - nc)^{-n} = \beta_{mijn} c_Y^i \phi_H \qquad (5)$$

where c is the actual concentration of the complex $M_mY_iH_jL_n$ in the solution; c_M, c_L and c_Y are the total concentrations of M, L and Y, respectively. The condition for quantitative complex formation has the same form as eqn. (4). When eqn. (4) is introduced into eqn. (5), the equation described for complexation in Fig. 1 is obtained. The value of $\log \beta_{mijn}$ is always a positive number.

---

*pH_0 is the optional starting value of pH.

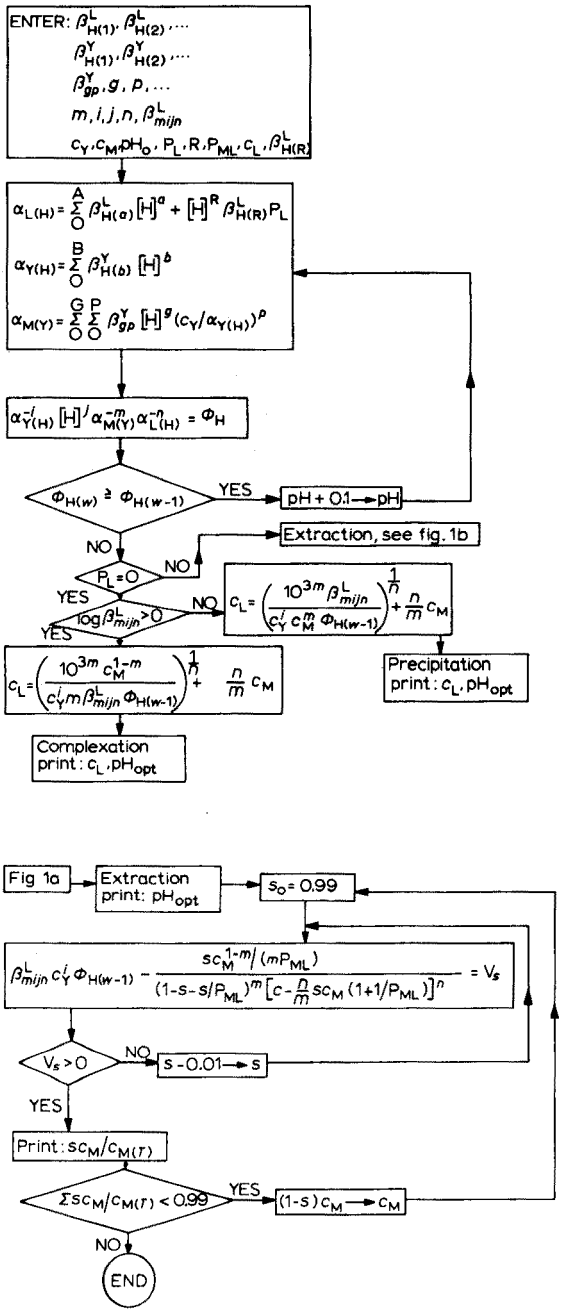

Fig. 1. Flow chart of the computer program for precipitation and complexation (1a) and extraction (1b). The overall stability constants β corresponding to particular ligands are designated with superscripts L and Y; $\beta^L_{H(x)} = [H_xL][H]^{-x}[L]^{-1}$, $\beta^Y_{gp} = [MH_gY_p][M]^{-1}[H]^{-g}[Y]^{-p}$, $\beta^L_{mijn} = [M_mY_iH_jL_n][M]^{-m}[Y]^{-i}[H]^{-j}[L]^{-n}$.

Quantitative extraction

In this case, β_{mijn} has again the meaning of the overall stability constant of the extractable complex $M_m Y_i H_j L_n$. However, ϕ_H has a different meaning because of the different meaning of $\alpha_{L(H)}$ (see Fig. 1), where $H_R L$ is the extractable species with a partition constant

$$P_L = [H_R L]_0/[H_R L] \tag{6}$$

where $[H_R L]_0$ and $[H_R L]$ are the actual concentrations of that species in the organic and aqueous phases, respectively. Equal volumes of both phases are assumed. Similarly, we can write

$$P_{ML} = c_0/c \tag{7}$$

where c_0 and c are the actual concentrations of the species $M_m Y_i H_j L_n$ in the organic and aqueous phases, respectively. Then, the relationship between β_{mijn} and ϕ_H is given by

$$c[c_M + mc(1 + P_{ML})]^{-m}\,[c_L - nc(1 + P_{ML})]^{-n} = \beta_{mijn} c_Y^i \phi_H \tag{8}$$

where c_M and c_L are the total concentrations of M and L in both phases. Since a single extraction does not necessarily lead to a quantitative transfer of the metal M to the organic phase, let us describe its effect by

$$mc_0/c_M = s \tag{9}$$

Quantitative transfer is then the result of multiple extractions that can be described by the condition

$$\sum_1^X mc_{0(x)}/c_{M(T)} = \sum_1^X s_x c_{M(x)}/c_{M(T)} \tag{10}$$

where X is the total number of extractions, and $c_{M(x)}$ and $c_{M(T)}$ are the total concentration of M is a single extract and in the total sum of extracts, respectively. Combination of eqns. (7)—(9) results in the final equation for extraction given in Fig. 1.

Redox reactions

The general equation assumed for the redox reactions is

$$a\,A + b\,B + h\,H \rightleftharpoons e\,E + f\,F + g\,H_2O \tag{11}$$

H always represents hydrogen ion, A is an oxidant, and B a reductant. If a buffering and complexing medium of ligand Y is present, and $c_Y \gg c_A^0$, c_B^0 (those are the total or starting concentrations of Y, A, and B, respectively), then, the side-reaction function ϕ_H has the form

$$\phi_H = [H]^h \alpha_{A(Y)}^{-a} \alpha_{B(Y)}^{-b} \alpha_{E(Y)}^{e} \alpha_{F(Y)}^{f} \tag{12}$$

where the meaning of the individual side-reaction functions $\alpha_{u(v)}$ is described in Fig. 2. The relationship between the overall equilibrium constant β of reaction (11) and the function ϕ_H is given by equation

$$(f/e)^f c_E^{e+f} (c_A^0 - c_E a/e)^{-a}\,(c_B^0 - c_E b/e)^{-b} = \beta\,\phi_H \tag{13}$$

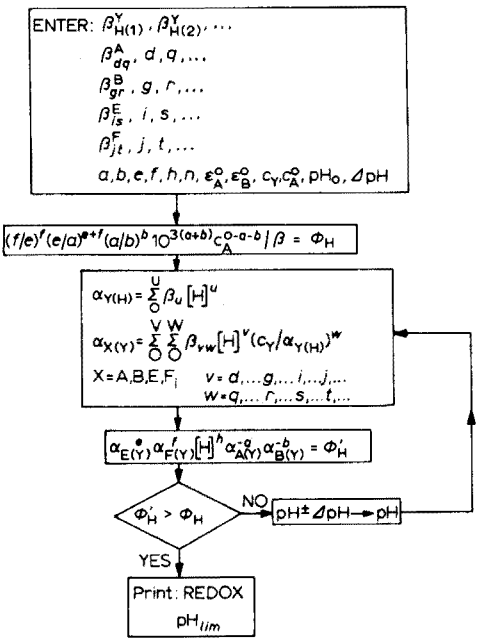

Fig. 2. Flow chart of the computer program for redox reactions. The superscripts Y and A, B, E, F designate the corresponding ligand and central cation, respectively; $\beta^{Y}_{H(x)} = [H_x Y][H]^{-x}[Y]^{-1}$, $\beta^{A}_{dq} = [A\,H_d Y_q][A]^{-1}[H]^{-d}[Y]^{-q}$, β^{B}_{gr}, β^{E}_{is} and β^{F}_{jt} have a similar meaning.

The superscripts ^{0} indicate the starting concentrations, and c_E is the final concentration of E. Since redox equilibria are usually characterized by standard redox potentials ϵ^0_x, the overall equilibrium constant is given by the well known equation

$$\log \beta = n(\epsilon^0_A - \epsilon^0_B)F/(2.303\,RT) = n(\epsilon^0_A - \epsilon^0_B)/0.0591 \qquad (14)$$

where the last term is valid for 25 °C; F is the Faraday constant (96, 487 coulomb), R is the gas constant (8.3143 J deg^{-1} mol^{-1}), T is the absolute temperature (K), and n the number of transferred electrons. ϵ^0_A designates the standard potential of the reaction involving the oxidant component A; ϵ^0_B is the standard potential of the reaction involving the reductant component B, and therefore has a negative sign in eqn. (14).

Furthermore, if it is assumed that the component A and B are always in a stoichiometric ratio

$$c^0_A/a = c^0_B/b \qquad (15)$$

and the reaction described by eqn. (11) is quantitatively shifted from left to right, then

$$c^0_A - c^0_E\, a/e = 0.001\, c^0_A \qquad (16)$$

When eqns. (15) and (16) are introduced into eqn. (13), the expression

$$(f/e)^f (e/a)^{e+f} (a/b)^b c_A^{0-(a+b)} = \beta \phi_H \qquad (17)$$

described in Fig. 2 is obtained. The limiting acidity, for which eqn. (16) is still valid, is calculated by combination of eqns. (12) and (17) as indicated in Fig. 2.

RESULTS AND DISCUSSION

Table 1 shows some results for the optimum conditions calculated for quantitative precipitation and complexation. Those conditions can be identical with the optimum conditions for spectrophotometry only if there is no absorbance interference by other components of the solution.

Results for quantitative extraction conditions, calculated for some common systems, are collected in Table 2. Since the stability constants for the 8-hydroxyquinoline complexes MH_aL_{n+a} are unknown, those complexes had to be omitted from practical examples, although they are quite common.

Optimum acidity as a mathematical limit is less distinct for redox reactions than for complex formation. Usually, the controlling effect on reaction rate is approached from only one side, either from strong acidity or strong alkalinity. Accordingly, the concept of acidity limit, determining the threshold of quantitative reaction, is more practical. A sufficiently general form of equations is another problem with redox reactions. There are still many of these reactions that do not obey the equations described. Lack of knowledge of all the involved equilibrium constants is also a serious drawback so that the theory cannot be used on a wider scale. A few examples of redox reactions are presented in Table 3; there is reasonable agreement between theory and practice.

Despite the tremendous amount of work done during the last two decades, the description of metal hydrolysis equilibria remains relatively poor, and the systems involving those equilibria therefore exhibit the poorest agreement with experiment.

The theory developed is based on considerable simplifications that may not always be justified; yet it is a useful tool in the search for optimum conditions for a reaction in a new system. The assumption that a single complex is formed between M and L, is not necessarily only a simplification, but is in agreement with the requirement of reaction uniformity that is essential for analytical purposes.

The theory can be extended to systems containing another metallic cation N and its complexes with L and Y and several complexes between M and L, provided that all complexes are mononuclear ($m = 1$) and no mixed M—N complexes are formed. In that case the function ϕ_H has the form

$$\phi_H = [H]^j \, \alpha_{Y(H)}^{-i} (\alpha_{M(L)} + \alpha_{M(Y)})^{-1} (\alpha_{L(H)} + \alpha_{L(M)} + \alpha_{L(N)})^{-n} \qquad (18)$$

where

$$\alpha_{M(L)} = \sum\sum\sum \beta_{xyz} (c_Y/\alpha_{Y(H)})^x \, [H]^y \, [L]^z \qquad (19)$$

TABLE 1

Optimum conditions for quantitative precipitation and complexation[a]

Species	c_Y	c_L	pH_{opt}		Ref.
			Calcd.	Found	
Precipitation					
$CuOx_2$	1.00(NH_3)	0.02	6.1	>2.6	5
$MgOx_2$	55.55(OH)	0.02	10.8	9.4—12.6	5
$NiOx_2$	1.00(NH_3)	0.02	7.4	>4.6	5
$AlOx_3$	0.10(EDTA)	0.03	10.4	10.0—11.0	6
$FeOx_3$	0.10(EDTA)	0.03	10.4	10.0—11.0	6
$GaOx_3$	0.10(EDTA)	0.032	10.4	10.0—11.0	6
UO_2HOx_3	55.55(OH)	1.11	7.4	5.5—9.7	5
	55.55(OH)	0.78[b]	7.4	5.5—9.7	5
$MnOx_2$	0.10(EDTA)	0.029	10.0	10.0—11.0	6
$BaSO_4$	0.10(EDTA)	0.01	4.0	3.5—4.5	1, 7
$PbSO_4$	0.10(EDTA)	0.032	1.2	1.2—1.5	1
$(UO_2)_3(PO_4)_2$	0.05(EDTA)	0.007	4.2	4.0—4.5	1
Complexation					
InL[c]	55.55(OH)	0.01	5.3	2.3—8.0	8
$Fe^{II}L$	55.55(OH)	0.01	9.1	9.0—10.0	8
$Fe^{III}L$	55.55(OH)	0.01	5.1	2.0—5.0	8
NiL	55.55(OH)	0.01	9.6	5.0—10.0	8
$Mn^{II}L$	55.55(OH)	0.01	10.4	9.0—10.5	8
$Tl^{III}L$	55.55(OH)	0.01	4.6	4.0—5.0	8
$V^{V}L$	55.55(OH)	0.01	2.8	2.0—5.0	8
ZnL	55.55(OH)	0.01	8.4	6.0—11.0	8
ZrL	55.55(OH)	0.01	1.9	1.3—2.0	8
CdL	55.55(OH)	0.01	9.8	5.0—10.0	8
$Cr^{III}L$	55.55(OH)	0.01	6.4	4.0—6.0	8
$Cu^{II}L$	55.55(OH)	0.01	7.3	4.0—10.0	8
GaL	55.55(OH)	0.01	4.9	3.0—5.0	8
$Co^{II}L$	1.00(NH_3)	0.01	7.9	6.0—11.0	8
$Cu^{II}L$	1.00(NH_3)	0.01	6.0	4.0—11.2	8
NiL	1.00(NH_3)	0.01	7.3	5.0—11.2	8
CdL	1.00(NH_3)	0.01	7.2	5.0—11.0	8
ZnL	1.00(NH_3)	0.01	6.8	6.0—11.0	8
CaL	55.55(OH)	0.01	11.0	9.0—12.0	8
MgL	55.55(OH)	0.01	10.5	10.0—11.0	8
BiI_4	0.10(EDTA)	0.04	−1.1	<0.5	9

[a]For the values of stability constants and solubility products used, see ref. 4; Ox is the ligand of 8-hydroxyquinoline; OH means that no buffer or masking reagent were taken into the account so that the hydrolysis could take place. c_M = 0.01 M throughout.
[b]c_M = 0.05 M.
[c]The ligand L refers to EDTA.

TABLE 2

Optimum conditions for quantitative extraction[a]
(All examples are taken from Stary [10])

Species	c_M	c_L	c_Y	pH_{opt} (% extraction)	
				Calcd.	Found
8-Hydroxyquinoline (in chloroform)					
$BeOx_2$	10^{-5}	0.01	55.55(OH)	10.9(99)	6.0—10.0(87)
$CuOx_2$	10^{-5}	0.01	1.00(NH_3)	6.0(99)	2.8—14.0(99)
$FeOx_3$	10^{-5}	0.01	55.55(OH)	8.8(99)	2.5—12.6(99)
$GaOx_3$	10^{-5}	0.01	55.55(OH)	7.8(99)	2.2—12.0(99)
$LaOx_3$	10^{-5}	0.01	55.55(OH)	12.7(99)	7.0—10.0(99)
$MgOx_2$	10^{-5}	0.01	55.55(OH)	12.5(99)	10.7—13.6(99)
$MnOx_2$	10^{-5}	0.01	55.55(OH)	11.7(99)	6.5—10.0(99)
$NiOx_2$	10^{-5}	0.01	1.00(NH_3)	7.4(99)	4.0—10.0(99)
$PbOx_2$	10^{-5}	0.01	55.55(OH)	10.7(99)	6.0—10.0(99)
Dithizone (in carbon tetrachloride)					
AgDz	10^{-5}	$2 \cdot 10^{-3}$	1.00(NH_3)	5.8(99)	0.2—7.0(99)
AgDz	10^{-5}	$2 \cdot 10^{-3}$	0.01(EDTA)	5.9(99)	
$BiDz_3$	10^{-5}	$2 \cdot 10^{-3}$	55.55(OH)	6.7(99)	3.0—10.0(99)
$CdDz_2$	10^{-5}	$2 \cdot 10^{-3}$	1.00(NH_3)	7.5(99)	6.5—14.0(99)
$CoDz_2$	10^{-5}	$2 \cdot 10^{-3}$	1.00(NH_3)	7.9(99)	5.5—8.5(99)
$CuDz_2$	10^{-5}	$2 \cdot 10^{-3}$	1.00(NH_3)	5.9(99)	2.0—7.0(99)
$HgDz_2$	10^{-5}	$2 \cdot 10^{-3}$	1.00(NH_3)	4.4(99)	6M[b]—4.0(99)
$HgDz_2$	10^{-5}	$2 \cdot 10^{-3}$	0.01(EDTA)	0.7(99)	
$NiDz_2$	10^{-5}	$2 \cdot 10^{-3}$	1.00(NH_3)	7.3(99)	6.0—9.0(99)
$PbDz_2$	10^{-5}	$2 \cdot 10^{-3}$	55.55(OH)	8.6(99)	8.0—10.0(99)
$PdDz_2$	10^{-5}	$2 \cdot 10^{-3}$	0.01(EDTA)	1.5(99)	6M[b]—4.0(99)
$SnDz_2$	10^{-5}	$2 \cdot 10^{-3}$	55.55(OH)	8.6(99)	5.0—9.0(99)
$ZnDz_2$	10^{-5}	$2 \cdot 10^{-3}$	1.00(NH_3)	7.0(99)	6.0—9.5(99)
Cupferron (in chloroform)					
$AlCf_3$	10^{-3}	0.02	55.55(OH)	6.1(99)	3.5—9.5(99)
$BeCf_2$	10^{-3}	0.02	55.55(OH)	6.4(99)	3.2—8.0(99)
$BiCf_3$	10^{-3}	0.02	55.55(OH)	6.4(99)	2.0—12.0(99)
$CoCf_2$	10^{-3}	0.02	1.00(NH_3)	7.0(99)	4.6—10.0(99)
$CuCf_2$	10^{-3}	0.02	1.00(NH_3)	5.8(99)	2.0—10.0(99)
$FeCf_3$	10^{-3}	0.02	55.55(OH)	5.7(99)	0.0—12.0(99)
$GaCf_3$	10^{-3}	0.02	55.55(OH)	6.1(99)	1.5—12.0(99)
$HgCf_2$	10^{-3}	0.02	1.00(NH_3)	3.4(60, 90)	2.0—5.0(98)
$InCf_3$	10^{-3}	0.02	55.55(OH)	6.1(99)	3.0—8.0(99)
$LaCf_3$	10^{-3}	0.02	55.55(OH)	8.9(99)	4.0—10.0(90)
$PbCf_2$	10^{-3}	0.02	55.55(OH)	6.7(99)	3.0—9.0(99)
$ScCf_3$	10^{-3}	0.02	55.55(OH)	6.8(99)	3.0—12.0(95)
$ThCf_3$	10^{-3}	0.02	55.55(OH)	6.9(99)	2.5—8.5(99)
Acetylacetone (in benzene)					
$CuAa_2$	0.01	0.10	1.00(NH_3)	6.0(95, 99)	4.0—10.0(90, 99)
$FeAa_3$	0.01	0.10	55.55(OH)	7.0(99)	2.5—7.0(99)
$AlAa_3$	0.01	0.10	55.55(OH)	6.3(95, 99)	3.0—6.0(90, 99)

TABLE 2 (continued)

Species	c_M	c_L	c_Y	pH_{opt} (% extraction)	
				Calcd.	Found
Thenoyltrifluoroacetone (in benzene)					
$BeTt_2$	0.01	0.10	55.55(OH)	7.9(99)	7.0—8.0(99)
$CoTt_2$	0.01	0.10	1.00(NH_3)	7.7(99)	7.6—8.8(99)
$CuTt_2$	0.01	0.10	1.00(NH_3)	6.0(99)	3.0—6.0(99)
$HfTt_4$	0.01	0.50	55.55(OH)	4.4(99)	2M[c]—5.0(99)
UO_2Tt_2	0.01	0.15	55.55(OH)	4.5(99)	3.5—8.0(99)
$ZrTt_4$	0.01	0.10	55.55(OH)	4.0(99)	2M[c]—5.0(99)

[a]The overall stability constants of cupferron complexes were determined by stoichiometric dilution [11], their logarithmic values are as follows: 12.5 ($AlCf_3$), 8.1 ($BeCf_2$), 21.1 ($BiCf_3$), 6.1 ($CoCf_2$), 12.3($CuCf_2$), 25.8 ($FeCf_3$), 20.9 ($GaCf_3$), 10.6 ($HgCf_2$), 18.4 ($InCf_3$), 9.8 ($LaCf_3$), 8.2 ($PbCf_2$), 19.3 ($ScCf_3$), 26.8 ($ThCf_4$). For other information see Table 1, footnote a.
[b]Molarity of sulfuric acid.
[c]Molarity of perchloric acid.

TABLE 3

Quantitative conditions for some redox reactions[a]

Reaction	c_A	c_Y	pH_{lim}		Ref.
			Calcd.	Found	
$UO_2^{2+} + 2\,Fe^{2+} + 4\,H^+ \rightleftharpoons$	0.01	0.1	6.8	8—11	12
$U^{4+} + 2\,Fe^{3+} + 2\,H_2O$			8.8[b]		
(Y = Tiron)			11.8[c]		
$VO_2^+ + Fe^{2+} + 2\,H^+ \rightleftharpoons$					
$VO^{2+} + Fe^{3+} + H_2O$	0.01	0.1	6.7	3—7	8, 13
(Y = EDTA)					14
$Cr_2O_7^{2-} + 6\,Fe^{2+} + 14\,H^+ \rightleftharpoons$	0.01	3.0	3.6	0.1—3	8, 15
$2\,Cr^{3+} + 6\,Fe^{3+} + 7\,H_2O$					
($Y = PO_4^{3-}$)					

[a]For other information, see Table 1, footnote a.
[b]For 99.99 % accuracy.
[c]For 99.999 % accuracy.

$$\alpha_{L(M)} = \frac{c_M \sum\sum\sum z\beta_{xyz}(c_Y/\alpha_{Y(H)})^x [H]^y [L]^{z-1}}{\beta_{ijn}(c_Y/\alpha_{Y(H)})^i [H]^j [L]^n + \alpha_{M(L)} + \alpha_{M(Y)}} \tag{20}$$

$$\alpha_{L(N)} = \frac{c_N \sum\sum\sum p\beta_{hkp}(c_Y/\alpha_{Y(H)})^h [H]^k [L]^{p-1}}{\sum\sum\sum\beta_{hkp}(c_Y/\alpha_{Y(H)})^h [H]^k [L]^p} \tag{21}$$

To calculate the value of [L], the values of c_L and pH must be made optional. Then the value of [L] is calculated by iterations with the equation

$$c_L = \frac{c_M \beta_{ijn} (c_Y/\alpha_{Y(H)})^i [H]^j [L]^n}{\beta_{ijn} (c_Y/\alpha_{Y(H)})^i [H]^j [L]^n + \alpha_{M(L)} + \alpha_{M(Y)}} + [L](\alpha_{L(H)} + \alpha_{L(M)} + \alpha_{L(N)}) \quad (22)$$

Those iterations should be performed for all necessary values of pH until the condition of optimum acidity, $\phi_{H(w)} < \phi_{H(w-1)}$, is reached.

It can be seen that the present state of computerized chemistry offers wide possibilities in the estimation of optimum conditions for quantitative reactions. The limitations are mostly due to the present lack of knowledge of the true equilibria involved.

REFERENCES

1 A. Ringbom, Complexation in Analytical Chemistry, Interscience, New York, 1963.
2 B. W. Budesinsky, Anal. Chem., 42 (1970) 928.
3 B. W. Budesinsky in D. Dyrssen, J. O. Liljenzin and J. Rydberg, (Eds.), Solvent Extraction Chemistry, North Holland, Amsterdam, 1967, p. 660.
4 L. G. Sillén and A. E. Martell, Stability Constants of Metal-Ion Complexes, The Chemical Society, Spec. Publ. 17, London, 1964; 2nd edn. Supplement No. 1, Spec. Publ. 25, 1971.
5 I. M. Kolthoff, E. B. Sandell, E. J. Meehan and S. Bruckenstein, Quantitative Chemical Analysis, Macmillan, New York, 1969, p. 279.
6 A. Claassen, L. Bastings and J. Visser, Analyst (London), 92 (1967) 618.
7 M. Nishimura, M. Saito and Y. Uzumasa, Japan Analyst, 13 (1964) 544.
8 G. Schwarzenbach and H. Flaschka, Complexometric Titrations, Methuen, London, 1969.
9 B. W. Budesinsky and J. Körbl, Collect. Czech. Chem. Commun., 24 (1959) 1791.
10 J. Stary, Solvent Extraction of Metal Chelates, Pergamon, London, 1964.
11 B.W. Budesinsky, Z. Anal. Chem., 258 (1972) 186.
12 J.W. Miller, Talanta, 4 (1960) 292.
13 G.G. Rao, G. Aravamudan and N.C. Venkatama, Z. Anal. Chem., 146 (1955) 161.
14 V.S. Syrokomskii and L.I. Antropov, Zavod. Lab., 9 (1940) 818.
15 A. Sarver and I.M. Kolthoff, J. Am. Chem., Soc., 53 (1931) 2902, 2906.

Analytica Chimica Acta, 85 (1976) 127—134

EXTRACTION DU TITANE(IV) D'UNE PHASE AQUEUSE CHLORHYDRIQUE PAR L'OXYDE DE TRI-*n*-OCTYLPHOSPHINE EN SOLUTION DILUÉE DANS LE TÉTRACHLORURE DE CARBONE

G. ROLAND, M. C. BLANDIAUX et G. DUYCKAERTS

Laboratoire de Chimie Analytique, Université de Liège au Sart Tilman, B-4000, Liège (Belgique)

(Reçu le 12 février 1976)

RÉSUMÉ

L'extraction du Ti(IV) d'une solution chlorhydrique par la TOPO en solution diluée dans le tétrachlorure de carbone est décrite. L'analyse chimique et les spectres Raman de la phase organique montrent que le Ti(IV) s'extrait en formant des complexes de stoechiométrie 2:1 ([TOPO]/[Ti(IV)]). Le rapport $[Cl^-]/[Ti(IV)]$ engagé dans le complexe dépend de l'acidité dans la phase aqueuse: pour 5,5 à 12 M HCl, le complexe $(TOPO)_2TiCl_4$ est toujours présent, mais pour des molarités en HCl inférieures à 10, il faut envisager la formation d'un autre complexe, probablement $(TOPO)_2TiOCl_2$. Pour des molarités en HCl supérieures à 10, le complexe $(TOPO)_2TiCl_4$ fixe des molécules de HCl pour donner le complexe $(TOPO)_2TiCl_4.nHCl$. Les variations des spectres UV de la phase organique en fonction de la molarité en HCl dans la phase aqueuse ne permettent pas le dosage spectrophotométrique direct du Ti(IV) dans la phase organique.

SUMMARY

The extraction of Ti(IV) from hydrochloric acid solutions by solutions of TOPO in carbon tetrachloride has been studied. Chemical analysis and Raman spectra of the organic phase indicate that Ti(IV) is extracted with the formation of complexes of 2:1 stoichiometry ([TOPO]/[Ti(IV)]). The $[Cl^-]/[Ti(IV)]$ ratio in the complexes depends on the acid concentrations in the aqueous phase: for 5.5—12 M HCl, the $(TOPO)_2TiCl_4$ complex is always present, but for HCl molarities below 10, the formation of another complex, probably $(TOPO)_2TiOCl_2$, must be considered. Above 10 M HCl the $(TOPO)_2TiCl_4$ complex associates with HCl molecules to form $(TOPO)_2TiCl_4.nHCl$. The variations of the UV spectra of the organic phase with the aqueous HCl molarities do not allow the direct spectrophotometric determination of Ti(IV) in the organic phases.

Dans une publication antérieure [1], nous avons examiné l'extraction du titane(IV) d'une phase aqueuse chlorhydrique par une solution diluée de tributylphosphate (TBP) dans le tétrachlorure de carbone. Par dosages des ions Ti(IV) et Cl^- extraits en phase organique et par spectroscopie Raman, nous avons montré que la stoechiométrie des complexes formés dépend des concentrations en TBP et en acide chlorhydrique, respectivement dans les phases organique et aqueuse. La présence de ces différents complexes, qui

se traduit par une modification importante des spectres ultraviolets, exclut toute possibilité de dosage spectrophotométrique direct et aisé du Ti(IV) dans la phase organique.

Nous avons poursuivi cette étude en utilisant l'oxyde de tri-*n*-octylphosphine (TOPO), base nettement plus forte que le TBP. Les seuls renseignements que nous possédons concernant l'extraction du Ti(IV) d'une phase aqueuse chlorhydrique par cette base sont donnés par Cerrai et Testa [2] et par White et Ross [3] qui ont établi les courbes d'extraction de ce cation en fonction de la concentration en acide chlorhydrique de la phase aqueuse. Les graphiques obtenus par White et Ross montrent que l'extraction du Ti(IV) augmente lorsque l'activité en acide dans la phase aqueuse croît, mais ne nous donnent aucun renseignement quant à la stoechiométrie et la stabilité des complexes formés. Ce sont ces points que nous avons essayé d'éclaircir dans ce travail.

PARTIE EXPÉRIMENTALE

Le tétrachlorure de carbone de qualité "pour analyse" a été distillé avant l'emploi. La TOPO (Merck) a été utilisée sans purification préalable. Les solutions de Ti(IV) ont été obtenues à partir d'une solution concentrée de Ti(IV) préparée par attaque de titane métallique par HCl 10 M puis oxydation quantitative du Ti(III) par HNO_3 6 M.

L'extraction du Ti(IV) a été effectuée en agitant vigoureusement 5.0 ml de phase organique pendant 10 min à la température ambiante (23 ± 1 °C). Après agitation, les solutions ont été centrifugées quelques minutes.

Les concentrations en Ti(IV) en phase aqueuse ont été déterminées par colorimétrie en mesurant l'absorbance à 410 nm du complexe Ti(IV)—H_2O_2 en milieu H_2SO_4 1 M. Le spectromètre est un Cary 17. Le Ti(IV) en phase organique a été dosé après réextraction du Ti(IV) dans le réactif colorimétrique.

Les spectres infrarouges ont été enregistrés à l'aide d'un spectromètre Perkin-Elmer 125, la fente spectrale étant de l'ordre de 1,5 cm^{-1}; les cellules utilisées étaient équipées d'une armature en téflon pour éviter tout contact entre les solutions acides et l'acier des porte-cellules.

Les spectres Raman ont été enregistrés par un spectromètre Cary 81 équipé d'un laser hélium—néon de la firme O.I.P. [4]. Les mesures de dépolarisation ont été effectuées par simple rotation d'une lame demi-onde dans le trajet du faisceau laser.

RESULTATS EXPÉRIMENTAUX

Influence de la concentration en acide chlorhydrique sur les courbes d'extraction

Les courbes d'extraction du Ti(IV) établies en fonction de la molarité en acide chlorhydrique de la phase aqueuse (Fig. 1) montrent que l'extraction du Ti(IV) augmente en fonction de l'acidité de la phase aqueuse. Elle est pratiquement totale pour une solution de TOPO 0,1 M lorsque l'acidité est supérieure à 9 M.

L'influence de la concentration en acide sur les courbes d'extraction s'interprète facilement si l'on tient compte que le Ti(IV) en phase aqueuse peut exister sous plusieurs entités dont les formations sont influencées d'une manière différente par l'acidité de la solution. Dans le cas des complexes TOPO—Ti(IV), ce serait donc l'espèce formée en milieu très acide qui s'associerait le plus facilement à la TOPO.

Cette interprétation semble d'ailleurs se vérifier si on compare les résultats obtenus avec la TOPO et le TBP dans des conditions expérimentales semblables: en portant $\log E$ en fonction de $\log a_{HCl}$, où E et a_{HCl} représentent respectivement le coefficient de partage et l'activité de l'acide chlorhydrique en phase aqueuse, on obtient, pour ces deux bases, des courbes d'allure voisine (Fig. 2). Etant donné que l'acide chlorhydrique n'influence pas directement la formation du complexe $(TBP)_2TiCl_4$, on peut penser qu'il en est de même pour les complexes TOPO—Ti(IV). Dans ces conditions, l'allure des courbes d'extraction dépendrait essentiellement des réactions en phase aqueuse.

Courbes d'extraction obtenues en maintenant les concentrations en acide chlorhydrique et en Ti(IV) initiales constantes, mais en faisant varier la concentration totale en TOPO dans la phase organique

Nous avons réalisé sept séries d'expériences à différentes molarités en acide chlorhydrique en maintenant pour chaque série les concentrations initiales en Ti(IV) et en acide chlorhydrique constantes et nous avons fait varier la concentration en TOPO en phase organique de 0,003 à 0,1 M. Après équilibration des deux phases, nous avons dosé les ions Ti(IV) et Cl^- dans la phase organique et les ions Ti(IV) en phase aqueuse. Les résultats expérimentaux sont rassemblés sur la Fig. 3.

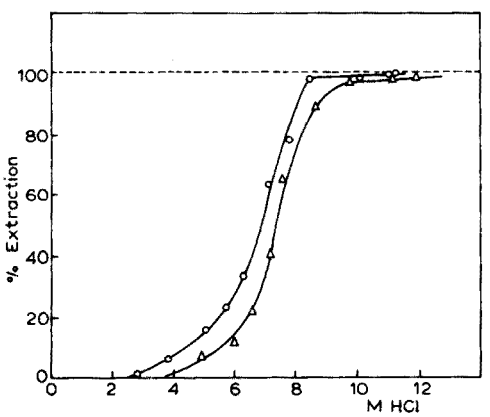

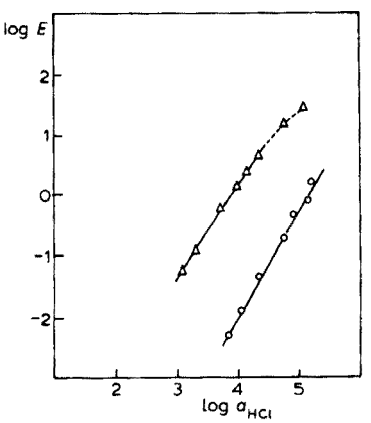

Fig. 1. Extraction du Ti(IV) en fonction de la molarité en acide chlorhydrique dans la phase aqueuse. $[Ti(IV)]_{aq}$ = 0,025 M. (○) $[TOPO]_{t\ org}$ = 0,1 M. (△) $[TOPO]_{t\ org}$ = 0,02 M.

Fig. 2. Extraction du Ti(IV) en fonction de l'activité en acide chlorhydrique. $[Ti(IV)]_{init}$ = 2.10^{-2} M. Solvant 1,2-dichloroéthane (△) $[TOPO]_{t\ org}$ = 0,1 M. (○) $[TBP]_{t\ org}$ = 0,1 M.

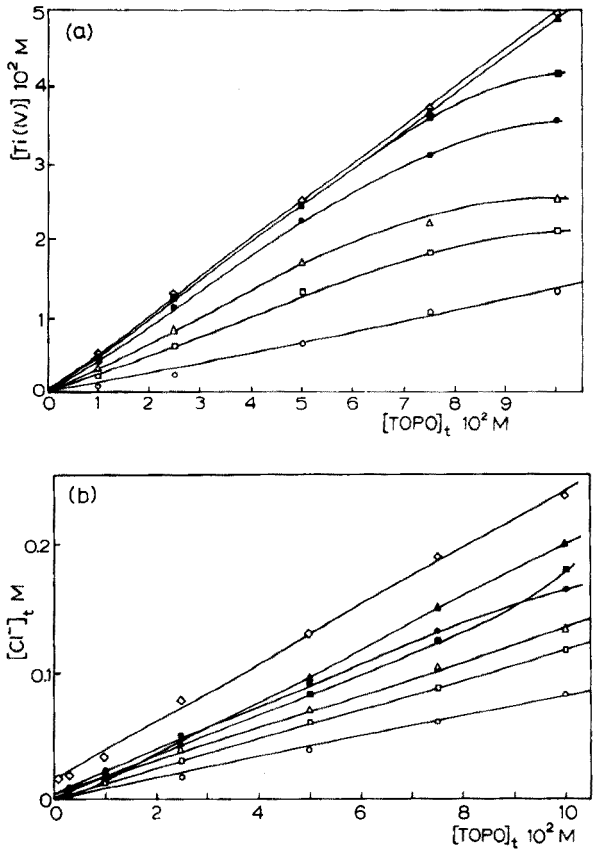

Fig. 3. Variation de la concentration en Ti(IV) (a), en Cl^- (b) en phase organique en fonction de la concentration totale en TOPO pour différentes acidités en HCl dans la phase aqueuse. Concentration initiale en Ti(IV) dans la phase aqueuse, 5.10^{-2} M. HCl = 5,61 (○); 6,56 (□); 6,90 (△); 7,80 (●); 8,45 (■); 9,87 (▲); 11,2 (◇) M.

DISCUSSION

En présence d'une phase aqueuse chlorhydrique, la TOPO en phase organique est complètement neutralisée par l'acide. Les différents travaux consacrés à ces associations [5, 6] montrent que, toute chose égale, la concentration en acide extrait en phase organique augmente quand l'activité de l'acide en phase aqueuse croît. La valeur du rapport [HCl]/[TOPO] en phase organique pouvant être supérieure à 2 prouve, qu'en plus du complexe de stoechiométrie 2:1 identifié par Bucher et al. [7], il existe d'autres complexes TOPO—HCl. Dans ces conditions, la concentration en TOPO libre ne peut être calculée et la détermination de la stoechiométrie des complexes TOPO—Ti(IV) ne peut s'effectuer par mesure de la droite obtenue en portant log E en fonction de log $[TOPO]_{libre}$ en phase organique.

Nous avons établi la stoechiométrie des complexes formés par spectroscopie Raman laser: nous avons enregistré le spectre Raman des phases organiques dans la région des raies Ti—Cl après extraction du Ti(IV) de phases aqueuses de molarités en HCl variables et nous avons comparé les spectres obtenus avec celui du complexe $(TOPO)_2TiCl_4$ préparé par addition à la TOPO d'un volume adéquat d'une solution de $TiCl_4$ dans le sulfure de carbone anhydre. La Fig. 4 montre que les différents spectres sont identiques et présentent tous une raie Raman intense à 291 cm^{-1}. On pourrait donc être tenté de conclure que le Ti(IV) s'extrait en phase organique uniquement sous la forme de complexe $(TOPO)_2TiCl_4$.

L'analyse chimique de la phase organique infirme partiellement ces conclusions. En effet, la stoechiométrie de ce complexe peut s'obtenir de la manière suivante:

(a) on détermine la concentration en [TOPO] en phase organique susceptible de former des complexes avec l'acide; cette concentration est égale à $[TOPO]_t - 2\,[Ti(IV)]_{org}$;

(b) on trace une courbe d'extraction de l'acide chlorhydrique en fonction de la concentration totale en TOPO en choisissant une concentration en acide dans la phase aqueuse aussi voisine que possible de celle contenant les ions Ti(IV);

(c) la concentration en Cl^- engagée dans les complexes TOPO—Ti(IV) ($[Cl^-]_c$) s'obtient immédiatement par la relation $[Cl^-]_{c\,org} = [Cl^-]_{t\,org} - [TOPO—HCl]_{org} - [HCl]_s$, où $[HCl]_s$ et $[TOPO—HCl]$ représentent respectivement la concentration en HCl dans le solvant en l'absence de TOPO et la concentration en HCl engagée dans les complexes avec la TOPO;

(d) en portant $[Cl^-]_{c\,org}$ en fonction de $[Ti(IV)]_{org}$ on obtient directement les rapports $[Cl^-]_c/[Ti(IV)]_{org}$ (Fig. 5 et Tableau 1).

On constate immédiatement que le rapport $[Cl^-]_c/[Ti(IV)]_{org}$ n'est pas constant, ce qui prouve que le complexe $(TOPO)_2TiCl_4$ identifié par spectrométrie Raman n'est pas seul en solution.

Complexes formés en milieu fortement chlorhydrique

Pour les concentrations élevées en acide chlorhydrique dans la phase aqueuse, l'extraction du Ti(IV) est totale et le rapport [Ti(IV)]/[TOPO] égal à 0,5 confirme la seule présence d'un complexe de stoechiométrie 2:1, même en présence d'un net excès de Ti(IV) en phase aqueuse.

Le rapport $[Cl^-]_c/[Ti(IV)]_{org}$ supérieur à 4.0 ne peut s'expliquer par la présence de complexes formés par paires d'ions tels $(TOPOH^+)_2TiCl_6^{2-}$ ou encore $(TOPOH_3O^+)_2TiCl_6^{2-}$ car on n'observe ni les trois raies Raman du groupement $TiCl_6^{2-}$ (situées d'après Van Bronwyk et al. [8] à 320 cm^{-1} 271 cm^{-1} et 173 cm^{-1}) ni les bandes d'absorption dans l'infra-rouge de l'ion H_3O^+.

L'excès d'ions Cl^- en solution pourrait provenir de la fixation de molécules de HCl sur le complexe extrait par la réaction

$$n\text{HCl} + (TOPO)_2TiCl_4 \rightleftharpoons (TOPO)_2TiCl_4.n\text{HCl}$$

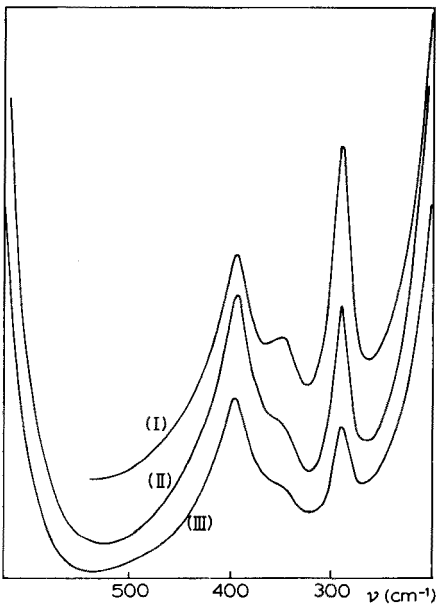

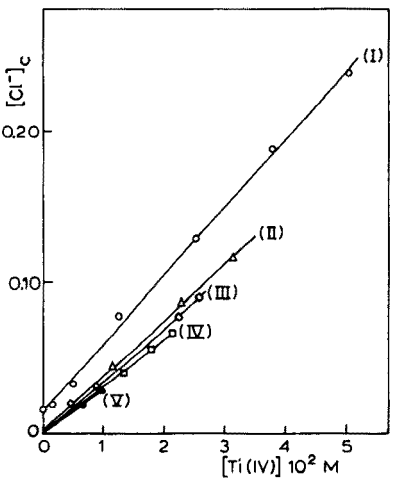

Fig. 4. (I) et (III): Spectres Raman des complexes TOPO—Ti(IV) après extraction du Ti(IV) par une solution 0,1 M en TOPO dans le CS_2. (II): $[TOPO)_2TiCl_4$ = 2.10^{-2} M dans le CS_2 anhydre. (I) $[Ti(IV)]_{org}$ = $3{,}96.10^{-2}$ M; $[HCl]_{aq} \approx 9$ M. (III) $[Ti(IV)]_{org}$ = 0,027 M; $[HCl]_{aq} \approx 7$ M.

Fig. 5. Variation de la concentration en Cl^- engagé dans les complexes TOPO—Ti(IV) en fonction de la concentration en Ti(IV) en phase organique pour différentes molarités en HCl dans la phase aqueuse. (I) 11,3 M. (II) 7,89 M. (III) 6,90 M. (IV) 6,56 M. (V) 5,60 M.

TABLEAU 1

Rapports $[Cl^-]_c/[Ti(IV)]_{org}$ pour différentes molarités en HCl

HCl (M)	5,60	6,56	6,90	7,80	10,1	11,3
$[Cl^-]_c/[Ti(IV)]$	3,15	3,20	3,5	3,78	4,0	4,46

Cette interprétation est étayée par la présence, dans les spectres infra-rouges d'une bande très large située à 2550 cm^{-1} que l'on peut attribuer à la molécule de HCl associée au complexe. Remarquons que cette bande n'est pas due aux complexes TOPO—HCl car la TOPO est complexée quantitativement par le Ti(IV) et, en outre, la fréquence νH—Cl des complexes TOPO—HCl se situe en dessous de 2200 cm^{-1} [9].

Complexes formés à partir de phases aqueuses d'HCl < 10 M

Pour des concentrations en acide chlorhydrique en phase aqueuse inférieures à 10 M, l'analyse chimique de la solution montre qu'il y a formation de complexes caractérisés par un rapport $[Cl^-]_c/[Ti(IV)]_{org}$ inférieur à 4.0.

Le tétrachlorure de carbone ne permettant pas l'étude des spectres Raman de solutions diluées dans la région des raies Ti—Cl, nous avons enregistré les spectres de ces complexes dans le sulfure de carbone, dépourvu de raies Raman intenses en dessous de 500 cm^{-1}. La Fig. 4 montre que les spectres présentent tous, quelle que soit la normalité en HCl en phase aqueuse, les seules raies du complexe $(TOPO)_2TiCl_4$.

Nous avons déterminé la concentration de cette entité en mesurant le rapport d'intensité entre la raie Raman du complexe située à 291 cm^{-1} (I_c) et la raie 397 cm^{-1} du CS_2 (I_r) dont la concentration peut être considérée comme constante en solution diluée. La théorie de l'effet Raman nous permet d'écrire

$$I_c/I_r = k.[(TOPO)_2TiCl_4]_{org}$$

où la valeur de k égale à 37 $(M/l)^{-1}$ a été déterminée à partir du spectre du complexe $(TOPO)_2TiCl_4$ formé en milieu anhydre. Dans le Tableau 2, nous avons rassemblé les résultats des mesures effectuées pour différentes molarités en acide dans la phase aqueuse.

La Tableau 2 montre que la concentration en $(TOPO)_2TiCl_4$ en phase organique est inférieure à la concentration en Ti(IV) et que le pourcentage de ce complexe augmente lorsque l'acidité de la solution croît. Ces résultats prouvent que le complexe $(TOPO)_2TiCl_4$ existe toujours en solution, quelle que soit la molarité de l'acide en phase aqueuse et que le rapport $[Cl^-]_c/[Ti(IV)]_{org}$ voisin de 3.0 dans le tétrachlorure de carbone pour les faibles acidités en HCl, ne peut s'expliquer par la présence d'un seul complexe, mais proviendrait de l'existence simultanée de $(TOPO)_2TiCl_4$ et d'un autre complexe renfermant moins de 3 atomes de chlore.

En tenant compte du rapport $[Cl^-]_c/[Ti(IV)]$ et de la concentration en Ti(IV) en phase organique, nous avons calculé le pourcentage de la forme $(TOPO)_2TiCl_4$ dans le CCl_4 à différentes molarités en acide, en supposant l'existence du complexe $(TOPO)_2TiOCl_2$. L'accord entre ces calculs et les valeurs enregistrées par spectrométrie Raman dans le CS_2 peut être considéré comme satisfaisant si on tient compte du chevauchement des bandes qui rend les mesures d'intensités des raies Raman peu précises dans cette région du spectre et de la différence de solvants.

TABLEAU 2

Concentration de $(TOPO)_2TiCl_4$ pour différentes molarité en acide

HCl (M)	$[(TOPO)_2TiCl_4]$ ($\cdot 10^{-2}$ M)	$[Ti(IV)]_{org}$ ($\cdot 10^{-2}$M)	$[TOPO)_2TiCl_4]$ (%)
6,48	1,13	2,45	46
6,92	1,49	2,67	56
8,01	3,49	3,96	88

Spectres ultraviolets de la phase organique

La présence de différents complexes en solution se traduit par une modification importante des spectres ultraviolets. Sur la Fig. 6, nous avons porté le coefficient d'extinction molaire du Ti(IV) en phase organique pour différentes normalités en HCl en phase aqueuse. Ces courbes montrent clairement l'évolution des spectres en fonction de l'acidité de la phase aqueuse. D'une manière générale, le coefficient d'extinction des complexes diminue lorsque l'acidité de la phase aqueuse décroît.

En conclusion, si la TOPO extrait plus facilement le Ti(IV) que le TBP dans des conditions expérimentales identiques, elle ne permet pas le dosage spectrophotométrique direct du Ti(IV). En effet, la reproductibilité des mesures ne pourrait être obtenue que dans des conditions expérimentales très précises qui enlèveraient toute souplesse à la méthode.

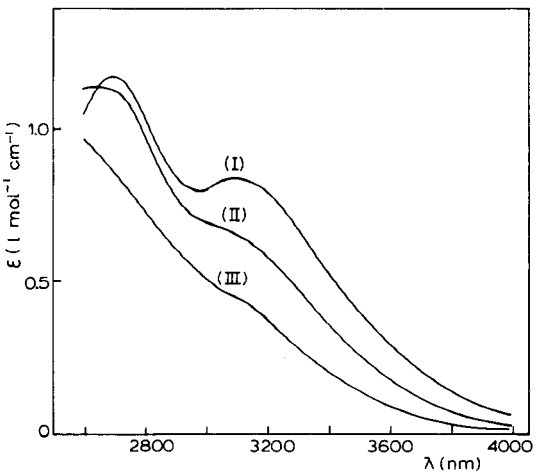

Fig. 6. Variation du coefficient d'extinction molaire des complexes TOPO—Ti(IV) en fonction de la molarité de l'acide chlorhydrique dans la phase aqueuse. $[TOPO]_t$ = 0,1 M dans CCl_4. $[HCl]_{aq}$ = 11,6 M (I); 8,0 M (II); 6,7 M (III).

BIBLIOGRAPHIE

1 G. Roland et B. Gilbert, Anal. Chim. Acta, 60 (1972) 57.
2 E. Cerrai et C. Testa, J. Chromatogr., 7 (1962) 112.
3 J. C. White et W. J. Ross, Nat. Acad. Sci. Nucl. Sci. N.A.S.-NS., (1961) 3102.
4 B. Gilbert et G. Duyckaerts, Spectrochim. Acta, Part A, 26 (1970) 197.
5 A. I. Mikhailichenko, Radiokhimiya, 12 (1970) 594.
6 B. Marin, Bull. Soc. Chim. Fr., (1974) 389.
7 J. J. Bucher, T. J. Conocchioli, E.R. Held, J.A. Labinger, B.A. Sudbury et R.M. Diamond, J. Inorg. Nucl. Chem., 37 (1975) 221.
8 W. Van Bronwyk, R. J. H. Clark et L. Maresca, Inorg. Chem., 8 (1969) 1395.
9 J. Sladkovska, V. Jedinakova et M. Mrnka, Proceedings International Solvent Extraction Conference, 1974, Vol. 1, 487.

Analytica Chimica Acta, 85 (1976) 135—148

EINE DIREKTE FLUORIMETRISCHE BESTIMMUNG DES URANS IN MINERALEN

J. C. VESELSKY und A. WÖLFL

International Atomic Energy Agency, Laboratory Seibersdorf, A-2444 Seibersdorf (Österreich)

(Eingegangen den 15 December 1975)

ZUSAMMENFASSUNG

Im ersten Teil des Artikels wird ein Überblick über das Gesamtgebiet der fluorimetrischen Bestimmung des Urans gegeben, ihre Fehlerquellen und deren Vermeidung diskutiert sowie auch kurz auf die für diese Methodik notwendigen Messgeräte eingegangen. Der zweite Teil enthält die Beschreibung einer sehr vereinfachten Technik ("Direktmethode") zur Bestimmung von Uran in Mineralen geringen Gehalts.

SUMMARY

The determination of uranium by fluorimetry is reviewed; sources of error and their elimination are discussed, and the equipment necessary for the measurements is described briefly. A simplified technique ("direct method") suitable for the determination of uranium in low-grade ores is then outlined; particular attention is given to the effects of particle size and spike concentrations.

GRUNDLAGEN UND PROBLEME DER FLUORIMETRIE

Im Jahre 1926 veröffentlichten Nicholls und Slattery [1] eine Arbeit über die durch Uranspuren aktivierte Fluoreszenz verschiedener Stoffe ($NaPO_3$, NaF, Borax u.a.) bei Anregung mit UV-Licht oder Kathodenstrahlen. Hierbei wurde die besonders intensive Fluoreszenz des Systems U—NaF entdeckt, welche bei einem molekularen Verhältnis von $1:10^7$ als noch "leicht messbar" beschrieben wurde. Die Hauptbande der Fluoreszenz lag bei ca. 555 nm, also im gelbgrünen Bereich des Spektrums, dessen Zusammensetzung später noch mehrfach nachgemessen und bestätigt wurde (Tab. 1). Auf Grund dieses Effekts entwickelten Papish und Hoag [2] einen ausserordentlich empfindlichen qualitativen Urannachweis und konstruierten den ersten Vorläufer der heutigen Fluorimeter, als Lichtquelle diente ein Eisenfunken die Proben wurden in NaF—Perlen eingeschmolzen. Eine qualitative Uranbestimmung auf derselben Basis wurde auch von Hernegger ausgearbeitet [3] und zu einem quantitativen Verfahren weiterentwickelt [4]. Mit Hilfe der von Hernegger und Karlik angegebenen Methodik [4] war es erstmals

TABELLE 1

Fluoreszenzmaxima von Uran in Fluoridschmelzen

Autoren	Wellenlängen (in nm)
Nichols u. Slattery (1926) [1]	634, 606, 577, 557
Hernegger u. Karlik (1935) [4]	626, 602, 577, 555
Price u.a. (1953) [5]	628,4, 601,6, 577,1, 554,6, 535,6
Fred (1953) [6]	602,2, 577,7, 555,0, 535,8
Widua u.a. (1974) [7]	siehe Spektrum in [7]

möglich, den geochemisch interessanten Urangehalt des Meerwassers zu bestimmen, wegen seines relativ hohen Salzgehalts war eine komplizierte chemische Aufarbeitung nötig; die ersten gefundenen Werte lagen zwischen $3{,}6 \cdot 10^{-7}$ und $3{,}37 \cdot 10^{-6}$ g U l^{-1}.

Fehlermöglichkeiten der fluorimetrischen Uranbestimmung und ihre Beseitigung

Fluoreszenzlöschung durch Begleitstoffe. Bereits Papish und Hoag [2] beschrieben die löschende Wirkung mancher Substanzen wie TiO_2, SiO_2 u.a. auf die Fluoreszenz von U—NaF Schmelzen, sie führten diese auf den starken F^--Verbrauch der betreffenden Stoffe durch Bildung komplexer Fluorverbindungen, etc. zurück. Das Uran liegt in der Schmelze als Uranyl-Ion vor [8].

Die Fluoreszenzreduktion durch verunreinigende Fremdstoffe wurde für verschiedene Schmelzflusszusammensetzungen untersucht, sie wird als unabhängig von der vorhandenen Uranmenge beschrieben, welche nach Price u.a. [5] bis zu einem Faktor von 10^3 oder mehr variieren kann [9] und verstärkt sich mit der Menge des vorhandenen "Löschers", wobei sich die spektrale Zusammensetzung des Fluoreszenzlichts verschieben kann. Der "Auslöschungsgrad" Q ist durch folgende Beziehungen gegeben:

$$Q = 100 \times \left(1 - \frac{F}{F_0}\right) = 100 \times (1 - \phi)$$

wo F = Fluoreszenz der Schmelze, welche Uran und Löscher enthält; F_0 = Fluoreszenz derselben Uranmenge in der Schmelze ohne Löscher; $F/F_0 = \phi$ wird als "relative Auslöschungswirksamkeit" bezeichnet. Alle Fluoreszenzwerte müssen für die "Blankfluoreszenz" korrigiert werden.

Für den viel verwendeten, von Centanni u.a. [10] eingeführten NaF—LiF Schmelzfluss (98 % NaF, 2 % LiF) haben Schönfeld u.a. [11] die Löscheffekte verschiedener Metallionen bestimmt und die Tatsache festgestellt, dass für die untersuchten Elemente (Fe, Ni, Co, Cr, Mn) eine Grenzkonzentration in der Probe existiert, oberhalb welcher die Löschung anscheinend konstant bleibt; die erhaltenen Resultate wurden kürzlich für Fe und Cr von Widua u.a. [7] nachgeprüft und bestätigt. Vozzella u.a. [12] untersuchten in demselben

Schmelzgemisch die Löschwirkung des Zirkon. Auch für den Fall des reinen NaF liegen Untersuchungen vor: Price u.a. [5] bestimmten das Löschvermögen verschiedener Stoffe wie Fe, Cr und Th, Osipov besonders dasjenige des Eisens [13] (vergl. auch [9]).

Der Karbonat—Fluorid-Fluss (45,5 % Na_2CO_3 und K_2CO_3, 9 % NaF) [14] war Gegenstand einer Arbeit von Cuttitta und Daniels [15], besonders in Hinblick auf die Löschwirkung des Zirkons, eine ausführliche Untersuchung der gleichen Schmelzflusszusammensetzung bezüglich der Fluoreszenzlöschung durch eine ganze Reihe von Elementen stammt von Singer und Cifkova [16], wo auch eine Klassifizierung der Elemente nach ihrem Löschvermögen erfolgt, als "sehr starke Auslöschmittel" etwa gelten Co und Cr. Daten über die Löschverhältnisse in einem $NaKCO_3$—KF-Schmelzfluss (97,5 % $NaKCO_3$, 2,5 % KF) finden sich in [17], betreffend eine Mischung von 95 % $NaKCO_3$ und 5 % NaF in [9]. Über mögliche Mechanismen des Löscheffekts vergl. [18].

Zur Umgehung der Verfälschung von Messergebnissen durch die Löschwirkung verschiedener Stoffe sind im Prinzip drei Möglichkeiten gegeben: 1. das "Hinwegverdünnen" der Verunreinigungen; 2. die Befreiung des Urans von den Störelementen; 3. die Anwendung des "Zugabe" ("Spike") — Verfahrens, d.h. die Benutzung eines internen Standards.

Die Möglichkeit der Beseitigung von Löschwirkungen durch Verdünnen [5, 19] beruht einerseits auf der Tatsache, dass bei dieser Massnahme Löscheffekte schneller abnehmen als die Uranfluoreszenz (nach Fioletova [20] 10× rascher), andererseits auf der grossen Empfindlichkeit der Methode überhaupt: man verdünnt so lange, bis zwei aufeinanderfolgende Verdünnungen auf denselben Uranwert führen. Wie leicht einzusehen, ist die Methodik unbrauchbar, sobald in der Endverdünnung die Empfindlichkeitsgrenze des fluorimetrischen Verfahrens unterschritten wird, d.h. das Verhältnis Löscher: Uran ein allzu grosses ist.

Für die Reinigung des Urans, d.h. seine Befreiung von löschenden Begleitsubstanzen, sind verschiedene Verfahren in Anwendung gekommen, welche in der Hauptsache auf Ionenaustausch, Papierchromatographie und Lösungsmittelextraktion beruhen. Die früher benutzten Mitfällungsmethoden [4] werden heutzutage kaum mehr verwendet; über die Mitfällung des Urans an $Fe(OH)_3$ siehe die eingehende Untersuchung von Upor und Nagy [21], sowie die Arbeit von Thatcher und Barker [22].

Als Beispiel für die Abtrennung des Urans aus einer Matrixlösung mittels Anionenaustausch zum Zwecke seiner fluorimetrischen Bestimmung in Seewasser, Meeressedimenten, etc. sei die von Hazan u.a. entwickelte Methode genannt [23]; der Reinigungsprozess erfolgt hiebei in einem Salzsäure—Methylglykol Medium. In Weiterentwicklung dieser Methodik führten Korkisch und Steffan das System Tetrahydrofuran—Methylglykol—Salzsäure ein; über dessen Anwendung bei der Bestimmung von Uran in geologischen Proben und Urin siehe [24] betreffend die Urinanalyse vergl. auch Welford u.a. [25].

Eine Reihe von Verfahren zur Separierung des Urans bedient sich der

Papierchromatographie. Berthollet [26] chromatographiert auf Whatman-1 Papier unter Verwendung von verdünntem Tributylphosphat und benutzt die Methodik zur fluorimetrischen Bestimmung des Urans in Gesteinen, Wässern und dergl.; eine ähnliche Methode wurde von Agrinier beschrieben [27] (siehe auch [28, 29]).

Am häufigsten wird zur Reinabtrennung von Uranspuren die Lösungsmittelextraktion benutzt, die wichtigsten verwendeten Klassen von Extraktionsmitteln sind Äther, Ester, Ketone und Organophosphorverbindungen.

Smith u.a. [30] bestimmten 0,3—5 $\mu g\ g^{-1}$ Uran in 1-g Proben von Zirkon und Zircaloy unter Verwendung einer Diaethylaether-Extraktion aus Aluminiumnitrat-Lösung (vergl. auch [31]).

Grimaldi und Levine [32] führten die Extraktion des Urans aus Aluminiumnitrat-Lösungen (auch Kalziumnitrat wurde verwendet [33]) mittels Äthylazetat ein, welche mehrfach verbessert bzw. näher untersucht wurde und weite Anwendung gefunden hat [10—12, 19, 33—39]. Nachteile dieses Extraktionssytems sind die nicht ganz quantitative Uranextraktion sowie die Koextraktion einiger anderer Stoffe [29]. Schönfeld u.a. [11] fanden bei Anwendung der Methodik auf Kohlenasche-Aufschlusslösungen eine Extraktion von ">97 %", die bestimmten Verteilungskoeffizienten verschiedener Löschsubstanzen wie Cr^{3+} ($3 \cdot 10^{-4}$), Mn^{2+} ($1{,}5 \cdot 10^{-3}$), Fe^{3+} ($1{,}5 \cdot 10^{-3}$) u.a. zeigen, dass u.U. eine Reduktion der Uranfluoreszenz durch mitextrahierte Fremdstoffe im Bereich des Möglichen liegt. Ein Vergleich [40] verschiedener Uranextraktionssysteme ergab für die Kombination Aluminiumnitrat—Äthylazetat eine Uranausbeute von 97,1 % verbunden mit Koextraktion von Ce, Ru und wahrscheinlich auch Sb. Nach Adams und Maeck [19] ist die Ausbeute ">90 %", wegen seiner weiten Verbreitung wird Eisen als das "gefährlichste" Störelement angesehen, vergl. auch [36]. Ein teilweise mitextrahiertes, störendes Element ist das Thorium [35], es kann durch eine TBP-Vorextraktion entfernt werden [39]. Sehr unangenehm können sich auch manche Anionen bemerkbar machen, die mit dem Uran unter Komplexbildung reagieren und es so der Extraktion entziehen; vor allem ist hier die Schwefelsäure zu erwähnen, welche mit Uran die Komplexverbindungen $UO_2(SO_4)_2^{2-}$, bzw. $UO_2(SO_4)_3^{4-}$ bildet. Sie kann durch Fällen mit Ba^{2+} entfernt werden; sorgt man für die Gegenwart geringer Mengen dreiwertiger Ionen (Fe^{3+}, Al^{3+}), erfolgt praktisch keine Adsorption von Uran an dem $BaSO_4$-Niederschlag [11]. Fluorid-Ionen werden durch das Al^{3+} komplexiert.

Höhere Ausbeuten als Äthylazetat liefert das Methylisobutylketon (MIBK). Bei der Extraktion von Uran aus $Al(NO_3)_3$-Medium erhielten Nietzel und DeSesa [41] im Durchschnitt eine Extraktionsausbeute von 99,2 %; Schneider und Harmon [9] extrahierten aus $Al(NO_3)_3$ oder NH_4NO_3 mit ähnlich gutem Resultat. Der Hauptnachteil des MIBK besteht in seiner Unverwendbarkeit beim Vorliegen stark salpetersaurer Lösungen; bei HNO_3-Konzentrationen $>3\ M$ können explosionsartige Reaktionen auftreten; vorteilhaft sind seine geringe Löslichkeit in wässrigen Phasen und sein relativ hoher Siedepunkt. Gewöhnlich verwendet man das Uran in einer gesättigten Aluminiumoxynitrat-

lösung (acid-deficient aluminium nitrate), koextrahiert werden teilweise Hg, Tc, Ru, Pu und Th; da viele Uranminerale Th enthalten, muss dieses Element ausgeschaltet werden, dies kann durch die Anwendung eines $Ca(NO_3)_2$—EDTA Extraktionsmediums erfolgen, wodurch die starke Th-Extraktion aus $Al(NO_3)_3$ Lösungen praktisch vollkommen unterdrückt wird [42]. Bei der oben erwähnten MIBK-Extraktion nach Nietzel und DeSesa [41] sind Chlorid, Karbonat, Sulfat, Phosphat u. Tartrat tolerierbar, hingegen stören grössere Mengen von V, Hg, Zr und Ti; Maeck u.a. [40] extrahieren mit MIBK aus $Al(NO_3)_3$—Tetrapropylammoniumnitrat und erhalten Ausbeuten von >99,8 %, die Mitextraktion von V(V) und Zr(IV) ist <0,01 %, über weitere Dekontaminierungsfaktoren siehe [40], betreffend die mögliche Störung der Extraktion durch Ce(IV) und Th [43].

Von den Organophosphorverbindungen bedient man sich in der Hauptsache des Tributylphosphats (TBP) und des Trioctylphosphinoxids (TOPO), bzw. Tridecylphosphinoxids (TDPO). Die Extraktion des Urans aus hoch nitrathaltigen Lösungen mit TBP geht mit dem Quadrat der TBP-Konzentration, wobei zahlreiche Elemente mitextrahiert werden [29], eine ganze Reihe von ihnen sind mit EDTA maskierbar, so z.B. Fe, Ni, Co, Th, Cr, Mn und andere. Extrahiert man das Uran aus gesättigter $Al(NO_3)_3$-Lösung, erhält man bei Verwendung einer 10 %igen TBP—Hexan Mischung eine Extraktionsausbeute von 99,8 % [40]. Über die Extraktion des Urans mittels TBP—MIBK vergl. [44, 45], zur Verwendung eines Systems TBP—Kohlenwasserstoff [46], über die Bestimmung des Urans in Urin mittels TBP-Extraktion [16]. In Betreff der Anwendung von TOPO bzw. TDPO zur Uranextraktion mit anschliessender fluorimetrischer Bestimmung ist berichtet worden [47]. Mit diesen Extraktionsmitteln ist es möglich, das Uran auch in Anwesenheit gewisser Komplexbildner (Zitrat, Oxalat und Tartrat) sowie aus stark saurem Milieu (bis 12 *M*) quantitativ zu extrahieren (vergl. auch [48]), jedoch gehen einige "Löscher" ("quencher") wie Th, Cr(VI), Fe(III) u.a. teilweise mit [49]. Über die Extraktion von Uran mit Aminen vergl. [50, 51].

Das "Zugabe" ("spike") Verfahren beruht auf der Tatsache, dass die relative Fluoreszenzverminderung des Urans in Anwesenheit von "Löschern" in weiten Grenzen von der Urankonzentration unabhängig ist. Es ist also möglich, Messung der "gelöschten" Uranprobe dieser eine bekannte Menge Urans zuzusetzen und nach erneutem Durchschmelzen wieder zu messen: da die Fluoreszenz der zugefügten Uranquantität in demselben Ausmass reduziert wird wie die der Probe, lässt sich aus den beiden Messwerten der Urangehalt des Untersuchungsmaterials berechnen [52]. Es wird auch empfohlen, die Zugabe an einer separaten Probe vorzunehmen und die beiden Schmelzen parallel auszuführen [17].

In Betreff der zuzusetzenden Menge an "spike" — Uran werden verschiedene Angaben gemacht, die vom 2—5 fachen und 10 fachen der ursprünglichen Uranmenge [52] bis zum >10 fachen [5] reichen. Die vor dem Zusatz auf der Schmelzpille vorhanden gewesene Menge Uran kann nach folgender Gleichung errechnet werden [52]:

$$x = \frac{F \times U}{S - F}$$

wo x = Unbekannte Menge Uran (μg); F = Fluoreszenzintensität der Probe; U = Zugesetzte Menge U (μg); S = Fluoreszenzintensität nach dem Zusatz. Die Fluoreszenzwerte sind auf den Blankwert einer Leerpille zu korrigieren.

Zum Abschluss des Kapitels über die Fluoreszenzlöschung und die gebräuchlichen Massnahmen, die dadurch verursachten Analysenfehler zu eliminieren, mögen noch einige Worte zu einer evtl. Fluoreszenzverstärkung durch Fremdsubstanzen gesagt werden. Ein möglicher Effekt dieser Art, hervorgerufen durch Nb und Ta, ist wahrscheinlich irreal. Die beiden Elemente wurden zusammen mit dem Nd durch Price u.a. [53] in dieser Hinsicht untersucht, aber keine Fluoreszenz gefunden. Das Cadmium fluoresziert in hoch karbonathaltigen Schmelzen. Geringe Mengen von Stoffen, die in grösserer Menge Löschung bewirken (Ca, Mg, Te, Be, Al, V, Mo, Sb) können u.U. eine Erhöhung der Uranfluoreszenz bewirken [9]. Über die Untersuchung der Fluoreszenz von Nb, Nd, Er, Zr, Ce in NaF sowie Nb, Ta, Ti, Zr und Cd in Fluorid—Karbonat—Mischungen vergl. [5]; bezüglich einen derartigen Effekt des Cers etc. [54].

Schmelzflüsse, Schmelzen und Abkühlen. Die Zusammensetzung einiger durch Uran aktivierbarer Schmelzflüsse wurde oben bereits verschiedentlich erwähnt, in der Hauptsache kann man sie in solche auf Karbonat- und auf Fluoridbasis einteilen; erstere bestehen vorwiegend aus Gemischen von K_2CO_3 und Na_2CO_3, welche bis zu etwa 10 % NaF enthalten können. Ihr Hauptvorteil ist der relativ niedrige Schmelzpunkt (ca. 600 °C), wodurch der Gebrauch von Platinschälchen zur Aufnahme der Schmelzen vermeidbar erscheint. Nachteile sind einerseits seine hygroskopischen Eigenschaften, die sich in der Praxis manchmal als recht hinderlich erweisen, der höhere Blankwert, seine für die gegebene Menge Uran geringere Fluoreszenz (verglichen mit Fluoridschmelzen) sowie stärkere Löscheffekte und schlechtere Reproduzierbarkeit der Resultate im Vergleich zu Fluoriden [10].

Das reine NaF war historisch der erste für quantitative Fluorimetrie verwendete Schmelzfluss [4]. Sein hoher Schmelzpunkt (ca. 1000 °C) macht die Verwendung von Platinschälchen unvermeidbar, jedoch besitzen Fluoridschmelzen eine Reihe von vorteilhaften Eigenschaften, die sie gegenüber Karbonatmischungen auszeichnen (s. oben). Die Empfindlichkeit kann durch Zusatz von LiF noch etwas gesteigert werden, das Optimum liegt bei 2 % LiF [10], ein starker Angriff des Platins durch LiF, wie er berichtet wurde [5], ist in diesem Konzentrationsbereich nicht zu befürchten, auch liegt der Schmelzpunkt einer Mischung von 98 % NaF und 2 % LiF wesentlich tiefer als der des reinen NaF (850—900 °C gegen 1000 °C), ausserdem können, falls erforderlich, die Schmelzen leicht aus den Schälchen entfernt werden. Über eine Abhängigkeit der Messwerte vom Schälchenzustand ist berichtet worden [10].

Zum Durchschmelzen der Proben sind die verschiedensten Heizeinrichtungen verwendet worden wie einfache Gasbrenner [11], Mehrfachbrenner [5, 10, 46] und elektrische Öfen [7, 16, 22, 34], auch Rühreinrichtungen sind beschrieben worden [22]. Die Zusammensetzung der Atmosphäre, in welcher das Schmelzen erfolgt, scheint im Gegensatz zur Meinung mancher Autoren [9] belanglos zu sein [18], nur sollte ein Schmelzen der Fluoride in Sauerstoff vermieden werden, weil dabei eine Erhöhung der Platinkonzentration in der Schmelze eintritt, wodurch Löscheffekte hervorgerufen werden. Ähnliches tritt bei Verwendung sehr sauerstoffreicher Flammen auf.

Das Gewicht der verwendeten Schmelzpillen muss nicht exakt definiert sein, nach Schönfeld u.a. [11] fallen Gewichtsschwankungen der in dieser Arbeit benutzten NaF—LiF Pillen von ± 10% nicht ins Gewicht; diese können mittels einer kleinen Handpillenpresse mit genügender Genauigkeit selbst hergestellt werden [10], sind aber auch im Handel erhältlich.

Nach unserer Erfahrung ist einer der kritischsten Parameter der fluorimetrischen Uranbestimmung die Behandlung der Proben nach dem Schmelzen, es kommt hiebei sehr auf die genaue Einhaltung der einmal gewählten optimalen Abkühlungsbedingungen an [10, 11, 17, 22]. In unserem Laboratorium werden die Pillen nach dem Durchschmelzen im Muffelofen wie folgt behandelt: nachdem das vollständige Schmelzen eingetreten ist, wird der Deckel des Ofens abgehoben und gleichzeitig eine Stopuhr in Gang gesetzt, nach einer Minute wird der Probenhalter mit den Schälchen herausgenommen, 30 Sekunden in der Luft schwebend gehalten und dann auf eine Asbestplatte gesetzt. Nach weiteren zwei Minuten werden die Schälchen in einen Exsikkator übergeführt und sind nach 15—20 Minuten messbereit. Ein schnelleres Abkühlen führt zu unreproduzierbaren Messergebnissen.

Über die zur Stabilisierung der Probenfluoreszenz nötige Zeit existieren sehr verschiedene Angaben. Nach Getoff (Karbonat—Fluoridschmelze) ist die Fluoreszenzintensität erst nach 10—12 Stunden konstant [34], Centanni u.a. (Fluoridschmelze) berichten von einem Ansteigen der Fluoreszenz in den ersten 15 Minuten nach dem Schmelzen, gefolgt von einem Konstanzbereich über eine Stunde [10]. Adams und Maeck (Karbonat—Fluoridschmelze) erwärmen die Schmelzkuchen 10 Minuten unter der Lampe "zur Stabilisierung der Fluoreszenz" [19], Cuttitta und Daniels (Karbonat—Fluoridschmelze) lassen vor der Messung 20 Minuten im Exsikkator abkühlen [15], Singer und Cifkova messen "nach dem vollständigen Abkühlen der Tabletten" [16], ebenso Widua u.a. [7]. Über die in diesem Laboratorium erarbeiteten Bedingungen wurde oben schon kurz gesprochen; es hat sich auch herausgestellt, dass die Schmelzkuchen ohne Änderung ihrer Fluoreszenz über Nacht aufbewahrt werden können, vielleicht auch länger. Auf jeden Fall soll dies im Exsikkator geschehen, um Staub, Feuchtigkeit, etc. fernzuhalten. Nach Sommer bleiben die Fluoreszenzwerte über eine Woche stabil [52].

Fluorimeter

Zum Abschluss dieses Teils der vorliegenden Arbeit soll noch etwas zum Aufbau der für die fluorimetrische Uranbestimmung notwendigen Messinstrumente gesagt werden. Im Prinzip handelt es sich dabei um Geräte, welche imstande sein sollen, die zur Erregung der Fluoreszenz nötige Ultraviolettstrahlung zu liefern, das Fluoreszenzlicht passend auszufiltern und seine Intensität zu registrieren. Es werden heute praktisch ausschliesslich Reflexionsfluorimeter verwendet, d.h. das von der Probe reflektierte Fluoreszenzlicht gelangt zur Messung, vereinzelt wurden aber auch Transmissionsgeräte gebaut, als Beispiel sei das von Fletcher u.a. beschriebene Gerät genannt [55]. Als typisch für ein Reflexionsgerät möge dasjenige von Sommer [52] erwähnt werden: es benutzt eine Quecksilberhochdrucklampe als UV-Quelle, filtert den sichtbaren Teil des Spektrums aus und entfernt das reflektierte UV-Licht durch ein weiteres Filtersystem; das Fluoreszenzlicht wird mittels Sekundärelektronenvervielfacher und Galvanometer gemessen. Einen prinzipiell ähnlichen Aufbau besitzt der Apparat von Price u.a. [5]; ein weit verbreitetes Instrument ist das im Handel erhältliche "Galvanek—Morrison"-Fluorimeter der Jarrell—Ash [10, 11, 24], welches sich durch sehr kompakten Aufbau auszeichnet, die Quecksilberlampe ist hier durch zwei Schwarzstrahler ersetzt, deren UV-Maximum bei 355.0 nm liegt.

Eine interessante Konstruktion wurde kürzlich von Widua u.a. [7] beschrieben: ein Zusatzgerät zu den bekannten Zeiss'schen Spektralphotometern PMQ II/PMQ 3, welches diese Apparate als Reflexionsfluorimeter verwendbar macht; als UV-Quelle dient ein Hg-Brenner, das UV wird mit einer besonderen Farbstoff-Folie, welche am Sekundärelektronenvervielfacher angebracht ist, vom Fluoreszenzlicht getrennt.

DIE FLUORIMETRISCHE DIREKTBESTIMMUNG DES URANS IN MINERALSTOFFEN

Zu den Aufgaben unseres Laboratoriums zählt häufig die Bestimmung des Urans in mineralischen Stoffen verschiedensten, meist geringen Gehalts, hiefür wird unter anderem auch die Fluorimetrie herangezogen. Da in der Regel in dem Untersuchungsmaterial neben dem Uran auch mehr oder minder grosse Mengen an Löschern vorliegen, muss deren Einfluss eliminiert werden, was nach den im ersten Teil dieser Arbeit genannten Methoden erfolgen kann. Gewöhnlich gelangte ein Äthylazetatextraktionsverfahren zur Anwendung, welches auf der von Schönfeld u.a. angegebenen Methodik aufgebaut war [11], gelegentlich wurde auch die MIBK-Methode von Pakalns [42] benutzt.

Nahezu alle diese Analysenverfahren erfordern die Auflösung des Untersuchungsmaterials, was manchmal keine ganz einfache Aufgabe darstellt, wozu noch der oft nicht unbeträchtliche Zeitbedarf einer solchen Methodik kommt. Häufig wird zur Lösung der HNO_3—HF—$HClO_4$-Aufschluss angewandt [42, 56] welcher üblicherweise in Teflongefässen vor sich geht; evtl. Rückstände müssen u.U. energischer behandelt werden, zu welchem Zweck gewöhnlich eine Schmelze mit Soda, Natriumfluoborat [56] oder dergleichen ausgeführt

wird. Pakalns hat einen Aufschluss von Mineralen in Teflondruckgefässen bei erhöhter Temperatur (150 °C) beschrieben [57], wobei als Aufschlussmittel Fluorwasserstoffsäure und Königswasser benutzt werden. Es erschien uns naheliegend, letztgenannte Methode insofern zu vereinfachen, dass der Aufschluss der Probe direkt durch die geschmolzenen Alkalifluoride der Fluorimetriemischung erfolgt. Bei der hohen Schmelztemperatur des von uns verwendeten NaF—LiF Gemischs war ein weit effektiverer Aufschluss zu erwarten als etwa der beschriebene im Teflondruckgefäss, ein Extraktionsprozess für das Uran fällt weg und der Aufschluss ist mit dem ersten Schmelzen der Probe identisch. Für anwesende Löscher sollte nach dem "spike"-Verfahren korrigiert werden.

Eine Direktmethode, bei welcher 3,75 mg-Proben von 100-mesh Korngrösse in einen Karbonatschmelzfluss von 3 g eingeschmolzen werden, haben Grimaldi u.a. [54] zur Analyse von silikatischem, phosphatischem und anderem Material verwendet; das Verhältnis Probe:Fluss war dem unseren ähnlich (s. unten), es wurden keinerlei Löscheffekte gefunden und daher auch keine "spikes" angewendet, was bei den uns vorliegenden Proben stets nötig war. Zur Diskussion der Direktmethode vergl. auch Price u.a. [5] und Vozzella u.a. [12]. Eigene Experimente mit einer Direktmethode unter Verwendung eines Karbonatschmelzflusses und internen Standards führten zu keinen brauchbaren Ergebnissen.

Das Zugabe ("spike")-Verfahren

Da eine Analyse nach dem Zugabe-Verfahren gewöhnlich zwei Schmelzvorgänge einschliesst und hierbei die eingewogene Probe zweimal durchgeschmolzen wird, war nachzuprüfen, ob deren Uranfluoreszenz unter diesen Bedingungen unverändert bleibt. Es wurden daher 10 Mineralproben (300—400 μg) auf die in Platinschälchen befindlichen 400 mg Fluoridpillen gewogen und diese im elektrischen Muffelofen zweimal durchgeschmolzen. Aus den Resultaten war abzulesen, dass bei diesem Prozess keine wesentliche Fluoreszenzänderung erfolgt.

Als nächster Schritt wurde eine Serie von uranhaltigen Mineralstoffen verschiedenen Gehalts nach der oben angedeuteten Methode analysiert. Hierzu wurden 300—400 μg Probe auf die Pille gewogen, durchgeschmolzen, gemessen, dann mittels Mikropipette die Uranzugabe aufgesetzt, getrocknet, erneut durchgeschmolzen und gemessen; die Berechnung der Resultate erfolgte mit der obenerwähnten Formel. Es ist von Bedeutung, dass das Mineralpulver stets auf die Pille gebracht wird und nicht umgekehrt, die Resultate sind in letzterem Fall häufig völlig unbrauchbar; am besten hat sich ein "Vorschmelzen" der Pillen bewährt (siehe unten). Der "spike" wurde so bemessen, dass die Gesamtfluoreszenz etwa das 2—5fache der Probenfluoreszenz betrug; einige typische Beispiele zeigt Tab. 2.

Die Ergebnisse einer Reihe von Mineralanalysen, die nach diesem Prinzip durchgeführt wurden, zeigt Tab. 3. Man sieht deutlich das unbefriedigende Funktionieren der Methodik: die erhaltenen Resultate zeigen z.T. grosse,

TABELLE 2

Die Fluoreszenz (in relativen Einheiten) von Proben ohne und mit Uranzugabe für das Direktverfahren

Probe Nr.	1	2	3	4	5	6
Fluoreszenz						
vor Zugabe	22,5	20,5	15	23	43	32
nach Zugabe	71	67	63	62	100	94

TABELLE 3

Analyse einiger uranhaltiger Minerale nach der Direktmethode

Probe	% U	% U gef.	Relative Abweichung (%)
P3	0,21	0,18	−14
P4	0,079	0,106	+34
		0,071[a]	−10
P5	0,28	0,25	−11
		0,28	
		0,26	−7,1
		0,25[a]	−11
P6	0,034	0,024	−29
		0,027[a]	−21

[a] 3 Einzelbestimmungen, alle anderen 4.

meist negative Abweichungen vom Sollwert; es kommen Differenzen von 20—30 % vor. Die Referenzwerte wurden durch Analyse desselben Stoffes mit verschiedenen anderen Methoden erhalten; hauptsächlich Röntgenfluoreszenz, γ-Spektroskopie und Neutronenaktivierung (NAA). Wurde das Untersuchungsmaterial mittels Auflösung und Äthylazetatextraktion aufgearbeitet, zeigte sich gute Übereinstimmung mit den Soll-Werten (Tab. 4). Zur Aufklärung der mit der Direktmethode erhaltenen grossen Abweichungen wurden nun verschiedene Parameter der Methodik näher untersucht.

Detailuntersuchungen zur Direktmethode

Wie Tab. 3 zeigt, ergeben sich bei der Anwendung der Direktmethode auf uranhaltige Minerale starke Unterschiede gegenüber dem Sollwert. Eine

TABELLE 4

Analyse stark manganhaltiger Grasaschen mittels NAA und Fluorimetrie (Äthylazetatextraktion)

Probe Nr.	U II	U V	U VI
NAA (μg U g^{-1})	14	131	108
Fluorimetrie (μg U g^{-1})	14	132	116

Möglichkeit ihres Zustandekommens wäre durch einen eventuell unvollständigen Probenaufschluss gegeben, es wurden daher 7 Mineralproben (siehe oben) dreimal durchgeschmolzen; bei diesem Prozess erfolgt wieder keine wesentliche Fluoreszenzänderung. Es kann aus diesen Resultaten ohne weiteres abgeleitet werden, dass die Schmelz- und Aufschlussprozesse als wesentliche Störfaktoren ausgeschlossen werden können.

Wegen der für die beschriebene Methode erforderlichen kleinen Substanzmengen erschien es von grossem Interesse, den Einfluss der Probenhomogenität auf die Analysenergebnisse zu untersuchen. Wie ein in jüngerer Zeit unternommener Interlaboratoriumsvergleich von Uranmineralanalysen zeigte, spielt sie eine bedeutende Rolle; Florence u.a. empfehlen [58] das Mahlen der Proben auf einen Feinheitsgrad von 400 mesh, bei 200—300 mesh war noch keine vollständige Gleichförmigkeit gegeben.

Zum Zwecke unserer Untersuchung wurde daher ein relativ grobkörniges Mineralpulver bekannten durchschnittlichen Urangehalts (0,27 %) auf vier verschiedene Feinheitsgrade vermahlen und analysiert (Tab. 5). Aus diesen Resultaten kann ersehen werden, dass mit abnehmender Korngrösse sich nicht nur der gefundene Urangehalt dem Sollwert annähert, sondern auch die Standardabweichung der Mittelwerte immer geringer wird; es schien also empfehlenswert, bei Anwendung der Direktmethode zur Uranbestimmung in Mineralen diese möglichst fein zu pulvern. Zur Bestätigung dieser Annahme wurde eine Reihe von Proben derartig vorbehandelt und dann analysiert (Tab. 6). Vergleicht man die in dieser Tabelle zusammengestellten Werte mit denen von Tab. 3, lässt sich deutlich die starke Verbesserung der Übereinstimmung zwischen gefundenen und Sollwerten erkennen.

Es wurde auch die Möglichkeit der Abhängigkeit des Analysenresultats vom zugegebenen spike-Uran untersucht, wobei Uranzusätze entsprechend dem etwa ein- bis fünffachen der ursprünglichen Uranfluoreszenz angewendet

TABELLE 5

Die Abhängigkeit der Resultate der Direktmethode von der Proben-Korngrösse

Probe Nr.	% U (80—250 mesh)	% U (250—325 mesh)	% U (325—400 mesh)	% U (<400 mesh)
1	0,44	0,11	0,20	0,25
2	0,026	0,13	0,24	0,27
3	0,18	0,27	0,23	0,24
4	0,37	0,14	0,22	0,23
5	0,16	0,18	0,31	0,28
6	0,21	0,18	0,29	0,27
7	0,11	0,28	0,36	0,27
8	0,11	0,16	0,27	0,27
9	0,11	0,29	0,37	0,27
Mittel	0,19 ± 0,04	0,19 ± 0,02	0,28 ± 0,020	0,26 ± 0,006

TABELLE 6

Resultate der Direktmethode bei Verwendung gut homogenisierter Proben

Probe	% U	% U gefunden	Rel. Abweichung (%)
S1 (IAEA-Standard, Torbernit)	0,399	0,409; 0,389	+2,5; −2,5
S2 (IAEA-Standard, Torbernit)	0,265	0,262; 0,262	−1,1
S4 (IAEA-Standard, Uraninit)	0,318	0,308	−3,1
P66	0,115	0,114; 0,114	−0,9
P67	0,123	0,119; 0,120	−3,2; −2,4
P68	0,125	0,118	−5,6
P	0,070	0,073[a]	+4,3
P37	0,003[b]	0,0034	
P38	0,003[b]	0,0038	
1	0,06	0,0558	−7,0
2	0,0071	0,0073	+2,8
3	0,0019	0,0021	+10,5
4	0,0102	0,0111	+8,8

[a] 8 Bestimmungen. [b] Vierte Dezimale unsicher, 7 Bestimmungen. Alle anderen Proben 4 Bestimmungen.

TABELLE 7

Der Einfluss der spike-Konzentration auf die Analysenresultate

Spike (μg U)	Gefunden % U[a]
0,005	0,0038 ± 0,0007
0,010	0,0034 ± 0,0003
0,015	0,0034 ± 0,0003
0,020	0,0032 ± 0,0003
0,025	0,0030 ± 0,0003

[a] Je 8 Bestimmungen.

wurden (Tab. 7). Ob die anscheinende Tendenz zur Abnahme der Uranwerte mit steigender spike-Menge tatsächlich real ist, kann derzeit noch nicht gesagt werden.

Möglichkeiten und Grenzen der Direktmethode

Das direkte Einschmelzen des Probenmaterials in das Flussmittel, gefolgt von der Bestimmung des Urans mittels einen internen Standards ("spike") gibt die Möglichkeit, Mineralproben ohne grossen Zeit- und Arbeitsaufwand mit einer empfindlichen Methode zu analysieren; zur Gewinnung eines zuverlässigen Wertes sind feines Pulvern und gutes Durchmischen des Probenmaterials Voraussetzung. Proben mit einem sehr hohen relativen Gehalt an Löschern, bei welchen das Messgerät keinen gut beobachtbaren Ausschlag mehr liefert, können diesem Verfahren nicht unterzogen werden; sie sind jedoch

selten, ebenso auch solche, welche dem Angriff der Alkalifluoridschmelze widerstehen und nicht komplett aufgeschlossen werden, in letzteren Fällen muss ein anderer Aufschluss herangezogen werden (s. oben). Die Einwaagen wähle man nicht zu hoch (etwa 300—400 μg); bei Substanzmengen im mg-Bereich sind die Analysenresultate oft gänzlich unverwendbar. Ebenso ist es günstig, das Mineralpulver auf vorgeschmolzene Pillen zu wägen und so den Kontakt des Probenmaterials mit dem heissen Platin zu vermeiden; entsprechende Versuche haben ergeben, dass in derartigen Fällen die erhaltenen Werte oft viel zu tief ausfallen. Die Arbeit an der Weiterentwicklung der Methodik wird fortgesetzt.

Dem Leiter der LOWRA (low-level radioactivity) Abteilung, Herrn Dr. O. Suschny, sei an dieser Stelle für sein Interesse an vorliegender Arbeit herzlichst gedankt.

LITERATUR

1 E. L. Nichols und M. K. Slattery, J. Opt. Soc. Amer., 12 (1926) 449.
2 J. Papish und L. E. Hoag, Proc. Nat. Acad. Sci., 13 (1927) 726.
3 F. Hernegger, Anz. Wien. Akad. Wiss., 19. Jänner 1933.
4 F. Hernegger und B. Karlik, Mitt. Inst. Radiumforschg. Österr. Akad. Wiss., Nr. 360 (1935).
5 G. R. Price, R. J. Ferretti und S. Schwartz, Anal. Chem., 25 (1953) 322.
6 M. Fred zitiert in ref. 5.
7 L. Widua, H. Schieferdecker und U. Hezel, Z. Anal. Chem., 270 (1974) 12.
8 A. W. Evans, Report BR-363 (Dec. 1943).
9 R. A. Schneider und K. M. Harmon, HW-53368 (1961).
10 F. A. Centanni, A. M. Ross und M. A. DeSesa, Anal. Chem., 28 (1956) 1651.
11 T. Schönfeld, M. Elgarhy, C. Friedmann und J. Veselsky, Mikrochim. Acta, (1960) 883.
12 P. A. Vozzella, A. S. Powell, R. H. Gale und J. E. Kelly, Anal. Chem., 32 (1960) 1430.
13 B. S. Osipov, Zh. Anal. Khim., 21 (1966) 70.
14 F. S. Grimaldi, I. May und M. H. Fletcher, US Geol. Survey fluorimetric methods of Uranium Analysis, US Geol. Survey Circ., 199 (1952).
15 F. Cuttitta und G. J. Daniels, Anal. Chim. Acta, 20 (1959) 430.
16 E. Singer und D. Cifkova, Z. Anal. Chem., 202 (1964) 401.
17 C. J. Rodden, Analytical Chemistry of the Manhattan Project, McGraw-Hill, 1950.
18 I. M. Kolthoff, P. J. Elving und E. B. Sandell, Treatise on Analytical Chemistry, Part II, Vol. 9, Wiley—Interscience, New York, (1962) p. 102.
19 J. A. S. Adams und W. J. Maeck, Anal. Chem., 26 (1954) 1635.
20 A. F. Fioletova, Zh. Anal. Khim., 12 (1957) 718.
21 E. Upor und Gy. Nagy, Acta Chim. Acad. Sci. Hung., T.50 (1966) 5.
22 L. L. Thatcher und F. B. Barker, Anal. Chem., 29 (1957) 1575.
23 I. Hazan, J. Korkisch und G. Arrhenius, Z. Anal. Chem., 213 (1965) 182.
24 J. Korkisch und I. Steffan, Mikrochim. Acta, (1972) 837; (1973) 273.
25 G. A. Welford, R. S. Morse und J. S. Alercio, Ind. Hyg. J., (Feb. 1960) 68.
26 P. Berthollet, Rapport CEA-R-3557 (1968).
27 H. Agrinier, Rapport CEA-R-2791 (1966).
28 F. H. Burstall, G. R. Davies, R. P. Linstead und R. A. Wells, J. Chem. Soc., (1950) 516.
29 J. Korkisch, Modern Methods for the Separation of Rarer Metal Ions., Pergamon Press, Oxford, 1969.
30 D. L. Smith, H. R. Wilson und G. W. Goward, WAPD-CTA, GLA-431(Rev. 2), 1959.

31 C. J. Rodden, Anal. Chem., 21 (1949) 327.
32 F. S. Grimaldi und H. Levine, AECD-2824 (1948).
33 C. J. Rodden, Anal. Chem., 25 (1953) 1598.
34 N. Getoff, Atompraxis, 6 (1960) 41.
35 R. J. Guest und J. B. Zimmerman, Anal. Chem., 27 (1955) 931.
36 M. D. Hassialis und R. C. Musa, Proc. Int. Conf. Peaceful Uses of Atom. En., Geneva, 1955, VIII, 216.
37 H. Jacobs, Atompraxis, 13 (1967) H. 4/5 Direct. Inf.
38 L. A. König und H. Schieferdecker, Atomic Energy Rev., 12, No. 2, 1974, pp. 343 ff.
39 C. J. Rodden, Selected Measurement Methods for Plutonium and Uranium in the Nuclear Fuel Cycle, Sec. Ed., Office of Information Series USAEC, 1972, 232.
40 W. J. Maeck, G. L. Booman, M. C. Elliott und J. E. Rein, Anal. Chem., 30 (1958) 1902.
41 O. A. Nietzel und M. A. DeSesa, Anal. Chem., 29 (1957) 756.
42 P. Pakalns, AAEC/TM 552 (1970).
43 W. J. Maeck, G. L. Booman, M. C. Elliott und J. E. Rein, Anal. Chem., 31 (1959) 1130.
44 J. Gomez-Pantoja, Qa 0705/N-20 (1967).
45 J. V. Palomino, F. P. Delgado und J. C. Petrement Eguiluz, JEN 136-DQ/I 40 (1964).
46 TID-7015 (Sect. 1), 1 219240-1 (1958).
47 J. C. White, ORNL-2161 (1956).
48 T. Sato und T. Nishida, J. Inorg. Nucl. Chem., 36 (1974) 2087.
49 C. A. Horton und J. C. White, Anal. Chem., 30 (1958) 1779.
50 J. C. Veselsky, Pak Chan Kirl und N. Sezginer, J. Radioanal. Chem., 21 (1974) 97.
51 J. C. Veselsky, M. Nedbalek und O. Suschny, Allg. Prakt. Chem., 22 (1971) 2.
52 J. Sommer, Chem. Tech., 15 H.1 (Jan. 1963) 38.
53 G. R. Price, R. J. Ferretti und S. Schwartz, Report CC-2985 (1945).
54 F. S. Grimaldi, F. N. Ward und R. Kreher, AECD-2825 (1949).
55 M. H. Fletcher, I. May und J. W. Anderson, TEI-133 (1950).
56 T. M. Florence und Y. J. Farrar, Anal. Chem., 42 (1970) 271.
57 P. Pakalns, Anal. Chim. Acta, 69 (1974) 211.
58 T. M. Florence, P. Pakalns und L. S. Dale, AAEC/E 237 (1972).

Analytica Chimica Acta, 85 (1976) 149—159

EXPLOITATION NUMÉRIQUE DE LA MÉTHODE DES VARIATIONS CONTINUES: LE COMPLEXE SALICYLATO—FER(III)

JEAN MARC PISLOT et SERGE COMBET

Université de Provence, Laboratoire de Physicochimie ionique et Macromoléculaire, 3 place V. Hugo, 13331 Marseille Cedex 3 (France)

(Reçu le 9 février 1976)

RÉSUMÉ

Lorsqu'elle a été employée pour étudier la quantitativité de la formation des complexes, la méthode des variations continues n'a en général utilisé que peu des données expérimentales qu'elle peut fournir. On propose une exploitation numérique de mesures faites sur la totalité du domaine de variation du rapport de mélange de solution équimolaire de ligand et espèce complexée. Dans l'hypothèse de mesures spectrophotométriques, le cas particulier du complexe unique est résolu exactement en utilisant les notions de densité optique réduite apparente de mélange et de constante conditionnelle. Par ajustement non linéaire pondéré, sont simultanément déterminés, constante de dissociation et coefficient d'extinction moléculaire du complexe, la stoechiométrie étant vérifiée dans une étape séparée. On étudie le complexe salicylato—fer(III) en milieu aqueux acide, et compare constante de dissociation et spectre d'absorption entre 420 nm et 640 nm ainsi obtenus avec les données de la littérature.

SUMMARY

The method of continuous variations can be used to study quantitative aspects of complex formation, but in general the experimental data that it can give have not been utilized fully. The use of measurements over the entire range of equimolar mixtures of ligand and complexed species is proposed. By spectrophotometric measurements, the special case of a single complex can be characterized by means of the reduced apparent absorbance of the mixture and the conditional constant. By non-linear weighting, the dissociation constant and the molar absorptivity of the complex can be determined simultaneously, if the stoichiometry is established separately. The iron(III)—salicylate complex has been studied in aqueous acidic media; the dissociation constant and absorption characteristics in the 420—640-nm range are compared with literature values.

Ostromisslenski [1] et Denison [2] posèrent les premières bases de la méthode des variations continues. Job [3] en fit la mise au point afin de caractériser un complexe par l'étude du mélange en proportions complémentaires, x et $(1 - x)$, de solutions d'abord équimoléculaires puis non équimoléculaires de ligand L et d'espèce M ce qui permet l'obtention de courbes représentant les variations d'une propriété du mélange liée à la seule concentration du complexe ou qui soit additive par rapport aux deux constituants simples lorsqu'en dépend la propriété: nous aurons, de ce fait,

une grandeur apparente de mélange *Y*. Job [3] a démontré que, pour le mélange de solutions équimoléculaires, l'abscisse de l'extremum des courbes était indépendante de la constante de stabilité et donnait une relation entre les coefficients stoechiométriques et, pour celui de solutions non-équimoléculaires, fonction des concentrations analytiques et de la constante de stabilité qui est donc calculable après détermination de la stoechiométrie.

Longtemps il fut admis, y compris par Job [4], que la méthode des variations continues n'était généralement pas applicable à la formation de plus d'un complexe et, ce, jusqu'aux travaux de Vosburgh et Cooper [5]. Par la suite, un certain nombre d'auteurs, ne retenant de la méthode originale que le cas des solutions équimoléculaires, ont proposé son extension; nous pouvons distinguer deux périodes séparées par les années 1960—63.

Durant la première la méthode fut appliquée à l'étude de plusieurs complexes [5—8] en se limitant au problème du maximum en vue de la détermination des coefficients stoechiométriques: sur ce plan Katzin et Gebert [8] ont donné le développement le plus général. Parallèlement on s'est préoccupé, dans le cas de complexe unique, de la constante de stabilité mais dans des conditions d'applications particulières. La méthode d'Hagenmuller [9] est surtout applicable aux complexes 1:1 car elle nécessite la résolution d'équations à plusieurs inconnues et de degré $m + n$ (m et n étant les coefficients stoechiométriques du complexe). Schaeppi et Treadwell [10] ainsi que Budesinsky [11] ont exploité graphiquement les variations continues par le tracé des tangentes (supposées représenter la formation quantitative de complexe) aux points d'abscisses $x = 0$ et 1. Leur intersection était utilisée pour déterminer les coefficients stoechiométriques ainsi que la constante de stabilité, la différence entre les ordonnées de l'intersection et du maximum de la courbe étant supposée mesurer l'écart à la quantitativité à la stoechiométrie. Gilbert [12] et Klausen et Langmyhr [13] ont montré que cette méthode des tangentes pouvait conduire à des conclusions erronées tant pour la localisation du maximum si la courbe n'est pas symétrique que pour le calcul de la constante de stabilité; toutefois, elle donne des résultats satisfaisants dans le cas particulier de complexes 1:1 très stables. Dans cette période Woldbye [6], comparant la méthode des variations continues à celle des solutions correspondantes [14] de Bjerrum, concluait que la première était essentiellement "indicative".

Depuis les années 1960 certains travaux [13, 15] ont montré que l'on pouvait avoir une exploitation quantitative satisfaisante. Cette deuxième période, durant laquelle l'effort pour généraliser le problème à plusieurs complexes a été poursuivi [16], est marquée à la fois par l'étude théorique [12, 13, 17] complète du graphe des variations continues et des essais pour traiter [13, 15, 17a], avec plus ou moins de rigueur, les courbes obtenues à partir de solutions équimoléculaires de concentration C afin de déterminer la constante de stabilité. C'est ainsi que Klausen et Langmyhr [13] utilisent les valeurs calculées des concentrations maximales de complexe par rapport aux concentrations molaires totales: ce procédé nécessite le report sur des abaques

théoriques diminuant la précision. Likussar et Boltz [17] emploient le concept d'échelle de densité optique "normalisée", rapport de la densité expérimentale à celle d'une solution où l'ion M à la concentration $C/(m + n)$ serait totalement complexé par un excès de ligand, et déterminent la constante de stabilité en n'utilisant que le cas particulier du maximum. La méthode d'Ernst et Menashi [15] fait appel à un traitement itératif conduisant à obtenir les paramètres recherchés par extrapolations ou par approximations successives. Toutefois il est à noter que la fonction, du type $Y = f[(1-x)x/Y]$, établie [15] pour un complexe 1:1 et facilement extrapolable dans ce cas, n'est pas susceptible d'être étendue à d'autres types de complexes car elle ne serait plus linéaire: cependant elle peut servir à vérifier la symétrie d'une courbe de variations continues.

Nous pouvons observer que, sauf dans le cas d'utilisation d'abaques [13] ou de complexation particulièrement simple [15], en règle générale, l'exploitation quantitative des résultats expérimentaux de la méthode des variations continues ne fait appel qu'à un petit nombre de points remarquables de la courbe complète. Nous nous proposons de montrer, sur un exemple, qu'il est possible d'exploiter le contenu d'information de l'ensemble des points d'un graphe complet de variations continues.

PRINCIPE DE LA DÉTERMINATION GLOBALE DES PARAMÈTRES DE COMPLEXATION

Nous nous proposons de reformuler, en l'appliquant à des mesures spectrophotométriques, une fonction [13] des grandeurs expérimentales et des paramètre recherchés et de la traiter numériquement par la méthode des moindres carrés pondérés [18, 19]. Considérons le mélange de deux solutions contenant respectivement un ion métallique M et un ligand L à une même concentration analytique C de telle sorte que

$$[M]_t + [L]_t = C \quad \text{avec } [M]_t = xC \text{ et } [L]_t = (1-x)C \tag{1}$$

et que des complexes, du type $M_m L_j$, se forment (m ayant une valeur unique et j pouvant varier de 1 à n).

Si nous nous plaçons dans un cas souvent rencontré interviendront les équilibres suivants, les constantes étant exprimées en fonction des concentrations et les charges des ions n'étant pas indiquées dans un souci de simplification

$$H_i L \rightleftarrows H_{i-1} L + H \qquad K_{a_i} = [H_{i-1} L]\,[H]/[H_i L] \tag{2}$$

$$M_m L_j \rightleftarrows M_m L_{j-1} + L \qquad K'_j = [M_m L_{j-1}]\,[L]/[M_m L_j] \tag{3}$$

$$M + H_2O \rightleftarrows MOH + H \qquad K_h = [MOH]\,[H]/[M] \tag{4}$$

$$MA \rightleftarrows M + A \qquad K_c = [M]\,[A]/[MA] \tag{5}$$

$$HA \rightleftarrows A + H \qquad K_a = [A]\,[H]/[HA] \tag{6}$$

Le système A/HA est un tampon, à la concentration analytique $[A]_t$, destiné à maintenir le pH constant. Nous avons

$$xC = [M] + [MOH] + [MA] + m \sum_{j=1}^{j=n} [M_m\ L_j] \tag{7}$$

$$(1-x)C = [L] + \sum_{i=1}^{i=q} [H_iL] + \sum_{j=1}^{j=n} j[M_m\ L_j] \tag{8}$$

Appelons $[M]^*$ et $[L]^*$ les concentrations apparentes des ions, libres et complexes autres que $M_m L_j$. On a

$$xC = [M]^* + m \sum_{1}^{n} [M_m\ L_j] \tag{9}$$

$$(1-x)C = [L]^* + \sum_{1}^{n} j[M_m\ L_j] \tag{10}$$

avec

$$[M]^* = [M]\left[1 + \frac{[MOH]}{[M]} + \frac{[MA]}{[M]}\right] = [M]\left[1 + \frac{K_h}{[H]} + \frac{[A]_t - [MA]}{K_c(1 + K_a/[H])}\right] = \alpha[M] \tag{11}$$

$$[L]^* = [L]\left[1 + \sum_{i=1}^{i=q} \frac{[H]^i}{\prod_{1}^{i} K_{a_i}}\right] = \beta[L] \tag{12}$$

Considérons l'équilibre global

$$M_m\ L_n \rightleftarrows mM + nL \quad \text{avec } K'_n = \prod_{1}^{n} K'_j = \frac{[M]^m\,[L]^n}{[M_m\ L_n]} \tag{13}$$

et dont la constante conditionnelle K^*_n, au sens de Ringbom [20], s'écrit

$$K^*_n = \frac{[M]^{*m}\,[L]^{*n}}{[M_m\ L_n]} = K'_n\ \alpha^m\ \beta^n \tag{14}$$

Soient ϵ_M, ϵ_L, ϵ_A, ϵ_{HA}, ϵ_{MA}, ϵ_h, ϵ_i, ϵ_j les coefficients d'extinctions molaires respectivement des espèces M, L, A, HA, MA, MOH, H_iL et $M_m L_j$.

La densité optique réduite, mesurée à une longueur d'onde donnée et pour un trajet optique de 1 cm, sera

$$D = \epsilon_A[A] + \epsilon_{HA}[HA] + \epsilon_M[M] + \epsilon_{MA}[MA] + \epsilon_h[MOH] + \epsilon_L[L] + \sum_{1}^{q} \epsilon_i[H_iL] + \sum_{1}^{n} \epsilon_j[M_m\ L_j] \tag{15}$$

$$D = \epsilon_A[A] + \epsilon_{HA}[HA] + [M]\left[\epsilon_M + \frac{[A]_t - [MA]}{K_c\left[1 + \frac{K_a}{[H]}\right]}\epsilon_{MA} + \frac{K_h}{[H]}\epsilon_h\right]$$

$$+ [L] \left[\epsilon_L + \sum_1^q \frac{[H]^i}{\prod_1^i K_{a_i}} \epsilon_i \right] + \sum_1^n \epsilon_j [M_m L_j] \tag{16}$$

Posons

$$\epsilon'_M = \epsilon_M + \frac{[A]_t - [MA]}{K_c \left[1 + \frac{K_a}{[H]}\right]} \epsilon_{MA} + \frac{K_h}{[H]} \epsilon_h \tag{17}$$

$$\epsilon'_L = \epsilon_L + \sum_1^q \left(\frac{[H]^i}{\prod_1^i K_{a_i}} \right) \epsilon_i \tag{18}$$

En substituant les relations (11), (12), (17), (18) dans l'éqn. (16) on a

$$D = \epsilon_A [A] + \epsilon_{HA} [HA] + \frac{[M]^*}{\alpha} \epsilon'_M + \frac{[L]^*}{\beta} \epsilon'_L + \sum_1^n \epsilon_j (M_m L_j) \tag{19}$$

Le système A/HA ayant pour but de maintenir le pH constant [21] on peut considérer, s'il en est bien ainsi, que ϵ'_L et ϵ'_M sont, tout comme α et β, des termes constants; pour ϵ'_M il est nécessaire que [MA] soit négligeable devant $[A]_t$ ce qui est réalisé en prenant $[A]_t$ suffisamment supérieur à C. On voit donc que, pour toute valeur de x, on aura

$K^*_n = K'_n \cdot$ constante

Posons

$$\epsilon_{M^*} = \epsilon'_M/\alpha \quad \text{et} \quad \epsilon_{L^*} = \epsilon'_L/\beta \tag{20}$$

ϵ_{L^*} est constant et il en sera de même pour ϵ_{M^*} en choisissant un système A/HA n'absorbant pas aux longueurs d'onde utilisées. On aura alors

$$D = [M]^* \epsilon_{M^*} + [L]^* \epsilon_{L^*} + \sum_1^n \epsilon_j [M_m L_j] \tag{21}$$

Définissons la densité optique apparente de mélange selon

$$Y = D - x C \epsilon_{M^*} - (1 - x) C \epsilon_{L^*} \tag{22}$$

En substituant les relations (21) puis (9) et (10) dans l'éqn. (22) on obtient

$$Y = \sum_1^n [[M_m L_j] (\epsilon_j - \epsilon_{M^*} - j \epsilon_{L^*})] \tag{23}$$

Posons

$$\epsilon'_j = \epsilon_j - \epsilon_{M^*} - j \epsilon_{L^*} \quad \text{et} \quad D'_j = \epsilon'_j C \tag{24}$$

On aura

$$Y C = \sum_1^n D'_j [M_m L_j] \tag{25}$$

Considérons le cas d'un complexe unique (dont la stoechiométrie est déterminée d'après le maximum de Y) on aura

$$Y C = D'_n [M_m L_n] \quad (26)$$

L'éqn. (26) et les relations (9) et (10) permettent d'exprimer la constante K^*_n(éqn. 14) et d'obtenir la condition suivante

$$F = (K^*_n D'^{(m+n)}_n Y) - (xD'_n - mY)^m [(1-x)D'_n - nY]^n C^{(m+n)} = 0 \quad (27)$$

A partir d'une courbe des variations continues, les coefficients m et n étant déterminés par ailleurs, nous obtiendrons les paramètres K^*_n et D'_n par ajustement simultané avec pondération adéquate dans la fonction F. Il sera possible ensuite de calculer K'_n, au moyen des relations (11), (12) et (14), et le coefficient d'extinction molaire ϵ_n du complexe (au moyen de l'éqn. (24): soit directement si $\epsilon_{M^*} = \epsilon_{L^*} = 0$ soit combinée avec les relations (11), (12), (17), (18) et (20)).

APPLICATION EXPÉRIMENTALE

Partie expérimentale

Nous avons choisi comme exemple le premier complexe formé entre l'ion fer(III) et le ligand salicylate (l'acide salicylique étant représenté par H_2L) qui, maintes fois étudié, a donné lieu à la publication de résultats fort disparates comme on le verra plus loin. Nous avons déterminé une série de courbes de variations continues en solutions équimoléculaires de perchlorate de fer(III) (Koch-Light) et d'acide salicylique (Merck, R.P.), C variant de 10^{-4} à 10^{-3} M et les longueurs d'ondes étant choisies dans le domaine 420—640 mm. Les mélanges, x variant de 0,05 à 0,95, ont été faits au moyen de deux burettes de 25 et 50 ml dans des fioles jaugées de 50 ml: les incertitudes sur les divers volumes ont été utilisées pour calculer l'écart-type σ_x, variable, sur x. Les densités optiques D ont été mesurées, à 25,0 ± 0,1 °C, avec un spectrophotomètre Cary 14 (cuves de 2 et 5 cm en quartz) étalonné par des solutions alcalines de chromate de potassium (réf. 22; procédé A2) ce qui nous a permis de calculer, dans le domaine D = 0,1 à 1, un écart-type $\sigma_D = 2{,}56.10^{-3}$ par régression linéaire. Nous avons utilisé σ^2_D, lors des divers ajustements, comme estimation initiale, σ^2_0, de la variance externe $\sigma^2_{ext.}$. Le pH a été fixé entre 2,60 et 2,74, selon la valeur de C, au moyen d'acide acétique, HA, introduit à la concentration 10^{-1} M, bien supérieure à C, et d'acide perchlorique $2{,}5.10^{-3}$ M. Les mesures de pH ont été faites au moyen d'un pH-mètre "recherche" Beckman avec électrodes au calomel et de verre.

Paramètres de calcul

En ce qui concerne l'hydrolyse de l'ion fer(III) nous n'avons considéré que l'espèce $FeOH^{2+}$ car aux concentrations C aux pH et aux forces ioniques utilisées [16] les espèces $Fe(OH)^+_2$ et $(FeOH)^{4+}_2$ peuvent être négligées [23—25]: nous l'avons, d'ailleurs, vérifié à posteriori par un calcul en retour.

Pour les constantes des éqns. (2), (4), (5), (6), nous avons utilisé les

valeurs: $pK_{a_1} = 3{,}00 + 0{,}01$ [26] et $pK_{a_2} = 13{,}65 \pm 0{,}06$ [26] (force ionique $\mu = 0$), $pK_c = 3{,}23 \pm 0{,}03$ [27] ($\mu = 3$ M), $K_a = (1{,}753 \pm 0{,}004).10^{-5}$ [28] ($\mu = 0$), $K_h = 4{,}11.10^{-3}$ [29] ($\mu = 0{,}09$).

Ces constantes ont été recalculées en tenant compte de la force ionique, relativement faible (3 à 6.10^{-3} mol l^{-1}), des diverses solutions au moyen de la relation de Davies [30] permettant le calcul des coefficients d'activité

$$-\log \gamma = 0{,}5\, Z_i^2 \left[\frac{\sqrt{\mu}}{1 + \sqrt{\mu}} - 0{,}3\mu \right]$$

RÉSULTATS ET DISCUSSION

La régression non-linéaire pondérée sur la fonction F (éqn. 27) permet d'atteindre d'une part les paramètres recherchés, comme expliqué plus haut, ainsi que leur écart-type et d'autre part de calculer les écarts Δx et ΔY de la courbe expérimentale par rapport à la courbe théorique et la variance externe σ^2_{ext} qui permet de tester globalement l'importance de ceux-ci.

Le maximum de $Y = F(x)$ indique un rapport $m/n = 1$, et on a vérifié la solution particulière $m = n = 1$ au moyen du tracé de Y en fonction de $x(1 - x)/Y$ qui n'est linéaire sur toute l'étendue de variation de x que dans ce cas précis.

Nous avons contrôlé que le complexe est bien unique par:

- l'invariabilité de la longueur d'onde du maximum des spectres [5];
- la constance de K'_1 pour différentes longueurs d'ondes (Tableau 1) et pour différentes concentrations analytiques C (Tableau 2);
- la constance du paramètre ϵ_1 à une même longueur d'onde et différentes concentrations C (Tableau 3);
- la répartition aléatoire des Δx et ΔY;
- le fait que les σ^2_{ext}, des divers ajustements, ne sont pas significativement différents de σ^2_0.

Nous avons d'autre part rassemblé dans le Tableau 4 des résultats trouvés

TABLEAU 1

La constance de K'_1 pour différentes longueurs d'ondes ($C = 5.10^{-4}$; $\sigma_0 = 2{,}56.10^{-3}$ obtenu avec 14 degrés de liberté)

λ (nm)	$K'_1 \pm \sigma_{K'_1}$ ($.10^{-18}$)	$\epsilon_1 \pm \sigma_{\epsilon_1}$ (l mol^{-1} cm^{-1})	(σ_{ext}) ($.10^{-3}$)
640	4,855 ± 0,491	731 ± 4,5	1,512
600	4,647 ± 0,468	1136 ± 7,1	2,085
560	4,372 ± 0,402	1508 ± 6,9	2,029
530	4,319 ± 0,379	1613 ± 7,1	2,102
500	4,539 ± 0,411	1527 ± 7,3	2,113
460	4,508 ± 0,428	1036 ± 5,7	1,714
420	4,879 ± 0,619	519 ± 5,2	1,536

TABLEAU 2

La constance de $\overline{K'_1}$ pour différentes concentrations analytiques

$C(.10^{-4}$ M)	$(\overline{K'_1} \pm \sigma\overline{K'_1})\ (.10^{-18})^a$
10	4,26 ± 0,08
8,155	4,16 ± 0,06
5	4,54 ± 0,08
2.5	4,86 ± 0,12
1	4,24 ± 0,08
Moyenne pondéreé générale	4,33 ± 0,07

[a]Pour chaque concentration C donnée $\overline{K'_1}$ est une moyenne pondérée des résultats obtenus à différentes longueurs d'onde.

TABLEAU 3

La constance de ϵ_1 à 530 nm pour différentes concentrations analytiques

$C\ (.10^{-4}$ M)	$\epsilon_1 \pm \sigma_{\epsilon_1}$ (l mol^{-1} cm^{-1})
10	1605 ± 8
8,155	1612 ± 6,3
5	1613 ± 7,1
2,5	1624 ± 8,6
1	1598 ± 19

dans la littérature.

La comparaison des coefficients d'extinctions molaires ϵ_1 (Tableau 5) que nous avons trouvés est relativement aisée, essentiellement à 530 nm, avec ceux qui ont été publiés.

Celle des constantes de dissociation s'avère être délicate vu la disparité des conditions dans lesquelles les valeurs publiées ont été obtenues et la non-indication, parfois, de certains éléments, comme on peut le constater dans le Tableau 4: constantes de l'acide salicylique choisies, prise en compte ou non de l'hydrolyse des ions fer(III), constante apparente ou thermodynamique etc. . . . Nous avons, toutefois, essayé de normaliser les valeurs publiées en recalculant les constantes thermodynamiques (Tableau 4, colonne 11) à partir des données des auteurs à savoir k = [FeL] [H]/[Fe] [HL] (Tableau 4, colonne 9) aussi bien que K'_1 (Tableau 4, colonne 10) obtenu soit par la relation K_{a_1}/k soit par l'intermédiaire de constantes conditionnelles. Pour cela nous avons fait intervenir, chaque fois que c'était possible, la première constante d'hydrolyse des ions fer(III) et les constantes de l'acide salicylique utilisées dans nos propres calculs (si l'auteur utilisait un ou plusieurs de ces éléments nous avons substitué nos valeurs aux siennes). Quand l'auteur donnait une constante de complexation ou de dissociation apparente nous

TABLEAU 4

Résumé des résultats dans la littérature

t(°C)	μ	pH	K_{a_1} (.10^{-3})	K_{a_2} (.10^{-14})	K_{h_1}(.10^{-3})	λ (nm)	$-(\epsilon_1)_\lambda$ (l mol^{-1} cm^{-1})	k	K'_1(.10^{-17})	K_1 (.10^{-18})[a]	Réf.
				3,60		530		1000	4[a]	24,9	31
15 ± 1	3,6.10^{-3}	3 ± 0,05	1	3,60	2,512[b]	530	1630		4,47[a]	10,14	32
25	3,0	1,40 à				530	1350	500		—[f]	33
25	3,0	1,95	0,138[c]	3,60	—[d]			470[e]			
18	0,25	3,30 ± 0,02	1	3.981	2,512	532		316,2	12,59	1,3044	34
20			1,047	2,455	—[d]			550	4,47		35
20 ± 1	0,25	0,6 à 1,7	1	3,981	2,512	530	1490[g]	832		0,736	36
20	0,15								4,46[e]		37
	0,1		0,7244	3,981				1010		3,20	38
			1,064	2,56	6,7	530	1619		0,366[a]	3,66	15
25 ± 0,01	0,1		1,513		2,9[h]			1202[e]		1,02	39
20 à 25	0,05	2,04	1,071	7,586	—[d]	530	2000[i]		4,464[g]	5,206	40
		2,81				530	1720[j]				
25	0,5				1,6	530	1530	710		2,766	41
		2,50				530	1630				42
25 ± 0,1	0,1		1,513		1,62			1200		0,87	43
25	3.2.10^{-3} à 5,0.10^{-3}	2,5 à 3	1,07		—[d]	500	1527 ± 7[k]	1620[a] ± 30		4,00	44
						500	1529 ± 5[k]				
						500	1523 ± 5[k]				
25 ± 0,1	3.10^{-3} à 6.10^{-3}	2,60 à 2,74	1	2,239	4,11	530	1612 ± 10,5[l]		0,43 ± 0,07[l]	1,851	Ce trav.
						500	1518 ± 10,5[l]				

[a]Constante thermodynamique.
[b]Cet auteur tient compte aussi de la 2[e]. Cte. d'hydrolyse $K_{h_2} = [H^+]\,[Fe(OH)_2^+]/[FeOH^{2+}] = 1{,}995 \cdot 10^{-5}$.
[c]Pour $\mu = 3$.
[d]L'auteur ne tient pas compte de cet élement.
[e]Potentiométrie.
[f]Non calculé vu l'importance de la force ionique ($\mu = 3$).
[g]Valeur moyenne.
[h]L'auteur tient compte aussi de la 2[e]. Cte. d'hydrolyse $K_{h_2} = 9{,}65.10^{-4}$ ainsi que de la dimérisation $K_d = [Fe_2(OH)_2^{4+}]/[FeOH^{2+}]^2 = 1{,}4.10^{-3}$.
[i]Pour pH = 2,04.
[j]Pour pH = 2,81.
[k]ϵ_1 déterminé, respectivement, en milieu eau—éthanol (45.34 % en poids d'éthanol), eau—méthanol (50 % en poids de méthanol), et eau—isopropanol (50 % en poids d'isopropanol).
[l]Moyennes pondérées.

TABLEAU 5

Les coefficients d'extinctions molaires pour différentes longueurs d'ondes

λ (nm)	$\bar{\epsilon}_1 \pm \sigma_{\bar{\epsilon}_1}$ [a] (l mol^{-1} cm^{-1})	λ (nm)	$\bar{\epsilon}_1 \pm \sigma_{\bar{\epsilon}_1}$ [a] (l mol^{-1} cm^{-1})
640	719 ± 15	500	1518 ± 10,5
600	1126 ± 17,5	460	1031 ± 10,5
560	1505 ± 20	420	514 ± 25,5
530	1612 ± 10,5		

[a] $\bar{\epsilon}$ est une moyenne pondérée de résultats obtenus à différentes concentrations.

avons calculé la constante thermodynamique en utilisant la relation de Davies [30] pour les coefficients d'activité (sauf pour les constantes données par Agren [33], vu la force ionique à laquelle les mesures ont été faites).

CONCLUSION

Nous avons utilisé l'ensemble du domaine expérimental sans privilégier, outre mesure, le point particulier qu'est le maximum: ceci nous a permis d'avoir des arguments supplémentaires pour affirmer l'unicité du complexe.

Nous obtenons une estimation du coefficient ϵ_1 d'absorption molaire, pour chaque longueur d'onde considérée, bien plus sûre, car résultant d'un accord interne entre un grand nombre de mesures que ne le permettent des mesures relativement isolées bien que directes. Nos valeurs sont en bon accord avec celles des réfs. 15, 32 et 42 à 530 nm et réf. 44 à 500 nm. Par contre les coefficients donnés dans les réfs. 33, 36, 40 et 41 nous apparaissent sous ou sur estimées: il est à remarquer que ces valeurs résultent de mesures directes.

La constante de dissociation que nous avons déterminée correspond bien à l'ordre de grandeur de celles déjà publiées. Elle présente une très bonne fiabilité de par les précautions prises pour vérifier l'unicité du complexe ainsi que du fait que c'est une moyenne pondérée issue d'un ensemble de 35 courbes de variations continues qui nous fournirent 30 valeurs de K'_1 (5 ayant été rejetées à la suite de l'application du test de Fisher à $P = 0{,}05$) relativement peu dispersées et, de plus, réparties de manière aléatoire. Chacune des valeurs de K'_1 a été obtenue en parcourant la totalité du domaine expérimental qui, rappelons-le, couvre une variation de 1/20 à 20 du rapport des concentrations en ligand et en ion métallique.

Nous envisageons de tenter de généraliser la méthode d'exploitation numérique, appuyée sur la possibilité de simuler préalablement les résultats de mesure pour des complexes intermédiairement identifiés, au cas beaucoup plus délicat de la formation de plusieurs complexes.

BIBLIOGRAPHIE

1 L. Ostromisslenski, Ber. Deut. Chim. Ger., 44 (1911) 268.
2 R. B. Denison, Trans. Faraday Soc., 8 (1912) 20, 35.
3 P. Job, Ann. Chim. (Paris), (1928) 113.
4 P. Job, Ann. Chim. (Paris), (1936) 97.
5 W. C. Vosburgh et G. R. Cooper, J. Am. Chem. Soc., 63 (1941) 437.
6 F. Woldbye, Acta Chem. Scand., 9 (1955) 299.
7 L. Sommer et M. Hniličkova, Bull. Soc. Chim., (1959) 36.
8 L. I. Katzin et E. Gebert, J. Amer. Chem. Soc., 72 (1950) 5455.
9 P. Hagenmuller, C. R. Acad. Sci. (Paris), 230 (1950) 2190; Ann. Chim. (Paris), (1951) 5.
10 Y. Schaeppi et W. D. Treadwell, Helv. Chim. Acta, 31 (1948) 577.
11 B. W. Budesinsky, Collect. Czech. Chem. Commun., 32 (1967) 235.
12 T. W. Gilbert, J. Phys. Chem., 63 (1959) 1788.
13 K. S. Klausen et F. J. Langmyhr, Anal. Chim. Acta, 28 (1963) 167; 40 (1968) 335; K. S. Klausen, Anal. Chim. Acta, 44 (1969) 377.
14 J. Bjerrum, Kgl. Danske Videnskab Selskab., Mat.-fys. Medd., 21 (1944) no. 4, cité dans réf. 6.
15 Z. L. Ernst et J. Menashi, Trans. Faraday Soc., 59 (1963) 1794.
16 P. S. Ramanathan, J. Inorg. Nucl. Chem., 35 (1973) 3358.
17 W. Likussar et D. F. Boltz, Anal. Chem., 43 (1971) 1265.
17a G.F. Atkinson, J. Chem. Educ., 51 (1974) 792.
18 W. E. Deming, Statistical adjustment of data, Dover, New York, 1964.
19 W. E. Wentworth, J. Chem. Educ., 42 (1965) 96.
20 A. Ringbom, Les complexes en chimie analytique, Dunod, Paris, 1967.
21 M. M. Jones, J. Am. Chem. Soc., 81 (1959) 4485.
22 G. W. Haupt, J. Res. Nat. Bur. Stand., 48 (1952) 414.
23 L. N. Mulay et P. W. Selwood, J. Amer. Chem. Soc., 77 (1955) 2693.
24 R. N. Milburn et W. C. Vosburgh, J. Am. Chem. Soc., 77 (1955) 1352.
25 R. N. Milburn, J. Am. Chem. Soc., 79 (1957) 537; 56 (1934) 1889.
26 J. M. Pislot et S. Combet, C. R. Acad. Sci., 276 (1973) 491.
27 L. Ciavatta, G. Nunziata et L. G. Sillen, Acta Chem. Scand., 23 (1969) 1637.
28 A. Katchalsky, H. Eisenberg et S. Lifson, J. Am. Chem. Soc., 73 (1951) 5889.
29 V. V. Pal'chevskii et Kh. M. Yakubov, Dokl. Akad. Nauk. Tadzh. SSR, 6 (1963) 17; C. A., 59 (1963) 8175 d.
30 C.W. Davies, Ion association, Butterworths, London, 1962, p. 41.
31 A. K. Babko, J. Gen. Chem. Russ., 15 (1945) 745; C. A., 40 (1946) 7041.
32 C. Bertin-Batsch, Ann. Chim. (Paris), (1952) 481.
33 A. Agren, Acta. Chem. Scand., 8 (1954) 1059.
34 L. Vareille, Bull. Soc. Chim. Fr., (1955) 1493.
35 D. D. Perrin, Nature, 182 (1958) 741.
36 P. Romain et J. C. Colleter, Bull. Soc. Chim. Fr., (1958) 867; J. C. Colleter, Ann. Chim. (Paris), (1960) 415.
37 M. B. Shchigol, J. Inorg. Chem. Russ., 6 (1961) 664.
38 Tsin-Jao Ching, L. Sommer et A. Okac, Spisy Prirodovedecke Fak. Univ. Brno, (1961) no. 420, 93; C. A., 56 (1962) 11181 i.
39 M. V. Park, Nature, 197 (1963) 283; J. Chem. Soc. A, (1966) 816.
40 K. Ogawa et N. Tobe, Bull. Chem. Soc. Jap., 39 (1966) 227.
41 W. A. E. MacBryde, J. L. Rohr, J. S. Penciner et J. A. Page, Can. J. Chem., 48 (1970) 2574.
42 G. Ackermann et D. Hesse, Z. Anorg. Allg. Chem., 375 (1970) 77.
43 P. G. T. Fogg et R. J. Hall, J. Chem. Soc. A, 9 (1971) 1365.
44 S. K. Pal et S. C. Lahiri, Z. Phys. Chem. (Leipzig), 252 (1973) 177.

Analytica Chimica Acta, 85 (1976) 161—168

KINETIC DETERMINATION OF ADRENALINE, L-DOPA AND THEIR MIXTURES WITH A STOPPED-FLOW SPECTROPHOTOMETRIC TECHNIQUE

EZIO PELIZZETTI,* EDOARDO MENTASTI, EDMONDO PRAMAURO and GIANFRANCO GIRAUDI

Istituto di Chimica Analitica, Università di Torino, Via P. Giuria, 5, 10125 Torino (Italy)

(Received 19th January 1976)

SUMMARY

Catecholamines (adrenaline and L-Dopa) can be determined by a stopped-flow spectrophotometric technique. For individual determinations, catecholamines are oxidized to the corresponding *o*-benzoquinones by hexachloroiridate(IV). Concentrations in the range $2 \cdot 10^{-4}$—$2 \cdot 10^{-3}$ M can be determined with errors of about 2 %. For evaluation of mixtures, aminochromes are formed. The method allows a catecholamine concentration of about $5 \cdot 10^{-6}$ M to be determined in the presence of a ten-fold amount of another catecholamine, with a maximum error of about 10 %.

Adrenaline and L-Dopa (Levodopa; (-)-3-(3,4-dihydroxyphenyl)-L-alanine) can be determined by various methods; most of the chemical methods involve oxidation to the corresponding aminochromes, which can be evaluated by direct colorimetry or, after suitable conversion, by fluorimetry [1]. Polarographic methods have also been proposed [2].

The present paper gives kinetic methods for the determination of adrenaline, L-Dopa and their mixtures, and their accuracy and precision have been estimated. The methods are based on the kinetic behavior of adrenaline and L-Dopa with oxidizing agents (sodium hexachloroiridate(IV) and periodic acid) under different pH conditions, and a spectrophotometric stopped-flow technique is used.

PRINCIPLES OF THE METHODS

Individual determination of adrenaline or L-Dopa

In aqueous acidic perchlorate media, adrenaline and L-Dopa (represented as H_2Cat) are oxidized to the corresponding open-chain *o*-benzoquinones (qno) (see scheme; the successive cyclization to aminochromes is inhibited below pH 3) by means of sodium hexachloroiridate(IV), according to the equation

*To whom correspondence should be addressed.

$$H_2Cat + 2\ Ir(IV) \rightarrow qno + 2\ Ir(III) + 2\ H^+ \quad (1)$$

This reaction follows the simple relationship

$$d[qno]/dt = k[H_2Cat][Ir(IV)] \quad (2)$$

and with a large deficiency of iridium(IV)

$$-d[Ir(IV)]/dt = k'[Ir(IV)] \quad (3)$$

$$\text{where } k' = 2\,k[H_2Cat]. \quad (4)$$

The choice of iridium(IV) as oxidant was suggested by the following findings. (i) The experimentally determined rate constants are linearly dependent, according to eqn. (4), on $[H_2Cat]$ in a satisfactory range of concentration ($2 \cdot 10^{-4}$—$2 \cdot 10^{-3}$ M); at the higher concentration investigated the half-life of the reaction is about 20 ms. (ii) The specific rate constants for adrenaline and L-Dopa show a larger difference with iridium(IV) than with various other oxidizing agents (Co(III), Tl(III), Mn(III), I(VII), etc.) [3]; this point has no relevance in individual determinations, but is useful when this method is coupled with the following in the evaluation of mixture components. (iii) The rates show very small dependence on acidity and temperature.

Determination of adrenaline—L-Dopa mixtures by the single-point method of Lee and Kolthoff

By working at pH above 4, open-chain *o*-benzoquinones undergo cyclization to aminochromes [1], according to the following scheme

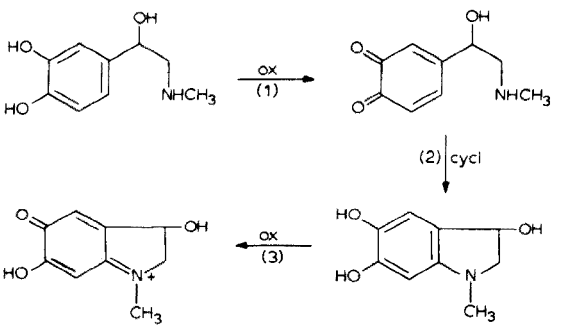

In a large excess of oxidizing agent (for example, periodic acid), step (2) becomes rate-determining [4] and the reaction rate follows the relationship

$$d[\text{Aminochrome}]/dt = k^{cycl}[H_2Cat] \quad (5)$$

For a binary mixture undergoing simple first-order reactions and giving the same final product (in the present case, the two aminochromes exhibit the same molar absorptivity), Lee and Kolthoff developed a method based on the determination of the total concentration of the mixture after a fixed time [5].

The following expression has been derived for mixtures of components A and B

$$\frac{C_\infty - C_t}{C_\infty} = (e^{-k_A t} - e^{-k_B t}) \frac{[A]_0}{[A]_0 + [B]_0} + e^{-k_B t} \quad (6)$$

and by plotting the left-hand side of eqn. (6) vs. the intial molar fraction of A, a straight line is obtained with slope $(e^{-k_A t} - e^{-k_B t})$ and intercepts $e^{-k_B t}$ and $e^{-k_A t}$ at molar fraction of A of 0 and 1, respectively. The optimum time (indicated as t^*) was chosen according to

$$t^* = \frac{\ln (k_{adr}^{cycl}/k_{Dopa}^{cycl})}{k_{adr}^{cycl} - k_{Dopa}^{cycl}} \quad (7)$$

A calibration plot can be drawn if the specific rate constants for each compound are known, i.e. k_{adr}^{cycl} and k_{Dopa}^{cycl}. The total concentration of the mixture can be determined spectrophotometrically. Alternatively, other kinetic measurements with a different reagent, i.e. iridium(IV), could be used.

EXPERIMENTAL

Apparatus

A Durrum-Gibson stopped-flow spectrophotometer (2.00-cm cells) was used for the kinetic runs. The reaction traces stored on a Tektronix 564 oscilloscope were photographed. The pH measurements were made with a Metrohm potentiometer (E 388), and spectra were recorded with an Hitachi-Perkin-Elmer spectrophotometer (EPS 3T).

Reagents

All reagents were analytical grade (Erba or Merck). The solutions of catecholamines and sodium hexachloroiridate(IV) were prepared daily. Twice-distilled water was used.

Evaluation of the rate constants

The rate constants were evaluated by a weighted least-squares method [6]. The standard deviation for each run was 1—3 %. For the determination of the kinetic parameters (average of several measurements) weighting was done on the basis of the standard deviations of the observed rate constants.

Procedures

Method A. The disappearance of iridium(IV) was followed at 487 nm (ϵ = 4070 l mol^{-1} cm^{-1}) [7]. By operating with [Ir(IV)] = $2 \cdot 10^{-5}$ M and [H_2Cat] > $5 \cdot 10^{-4}$ M, a plot of $\ln(A_t - A_\infty)$ (where A_t and A_∞ are the absorbances at time t and at equilibrium) vs. time was linear for at least 80 % of the reaction progress. The kinetic runs were performed at [$HClO_4$] = 1.00 M, μ = 1.0 M and 25.0 °C.

The specific rate constants $k^{ox}_{adr} = (6.4 \pm 0.15) \cdot 10^3$ and $k^{ox}_{Dopa} = (1.01 \pm 0.02) \cdot 10^4$ l mol^{-1} s^{-1} were obtained from ten independent measurements performed in the range $4 \cdot 10^{-4}$—$2 \cdot 10^{-3}$ M of catecholamine. In order to reduce the error, the averages of at least three separate kinetic runs were taken.

Method B. The formation of the aminochromes was followed at 25.0 °C and 480 nm with [H_2Cat] in the range 5—$7 \cdot 10^{-5}$ M and [periodic acid] = $1 \cdot 10^{-2}$ M at pH 5.98 ± 0.02 (acetate buffer, 0.10 M). The specific rate constants $k^{cycl}_{adr} = 18.8 \pm 0.3$ and $k^{cycl}_{Dopa} = 0.258 \pm 0.009$ s^{-1} were the average of five separate measurements.

RESULTS

Spectrophotometric data

By operating with an excess of oxidizing agent (i.e. periodic acid) with respect to different amounts of catecholamine, the values of ϵ at λ_{max} were determined for the open-chain *o*-benzoquinones ([$HClO_4$] = 1.00 M, μ = 1.0 M, 25.0 °C) and the aminochromes (pH 5.98, acetate buffer, 0.10 M, 25.0 °C) corresponding to adrenaline and L-Dopa:

$$\epsilon^{adr}_{390} = (1.32 \pm 0.04) \cdot 10^3 \text{ l mol}^{-1} \text{ cm}^{-1}$$

o-benzoquinones:

$$\epsilon^{Dopa}_{390} = (1.25 \pm 0.05) \cdot 10^3 \text{ l mol}^{-1} \text{ cm}^{-1}$$

$$\epsilon^{adr}_{390} = (4.05 \pm 0.15) \cdot 10^3 \text{ l mol}^{-1} \text{ cm}^{-1}$$

aminochromes:

$$\epsilon^{Dopa}_{490} = (4.00 \pm 0.21) \cdot 10^3 \text{ l mol}^{-1} \text{ cm}^{-1}$$

Individual determinations (Method A)

Figure 1 shows the working curves for the determination of adrenaline and L-Dopa. Table 1 shows the results obtained; the accuracy, expressed as the mean relative error, was around 2 %.

Analysis of mixtures (Method B)

For the mixture adrenaline—L-Dopa, the optimum reaction period, calculated from eqn. (7) with the specific rate constants reported, was 0.231 s. The equation of the straight-line calibration plot according to Lee and Kolthoff [5] was

$$Y = 0.0129 + 9.292 \cdot 10^{-3} X \qquad (8)$$

where Y is $(A_\infty - A_t)/A_\infty$ and X is the percent molar fraction of L-Dopa. Table 2 shows the results obtained for different molar fractions and a total concentration of $6.0 \cdot 10^{-5}$ M. Other measurements were performed at total concentrations of 4.0 and $8.0 \cdot 10^{-5}$ M, and satisfactory agreement was

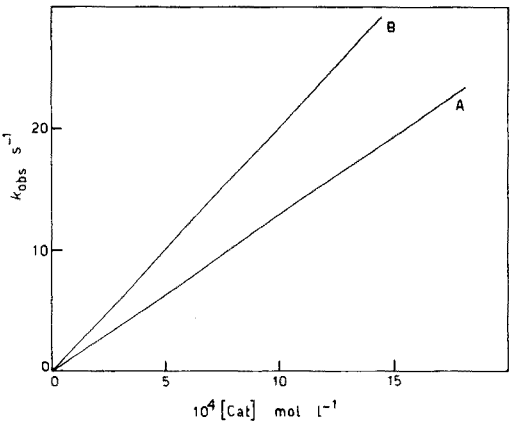

Fig. 1. Working curves for the individual determination of adrenaline (A) and L-Dopa (B); [Ir(IV)] = $2 \cdot 10^{-5}$ M, [$HClO_4$] = 1.0 M, 25.0 °C.

TABLE 1

Kinetic individual determination of adrenaline and L-Dopa

Sample	Taken[a] ($\cdot 10^{-4}$ M)	Found ($\cdot 10^{-4}$ M)	Error (%)
Adrenaline			
	4.00	4.14	+3.50
	5.00	4.96	−0.80
	6.00	6.18	+3.00
	8.00	7.97	−0.37
	10.00	10.06	+0.60
	12.00	11.83	−1.43
	16.00	15.74	−1.62
	20.00	19.70	−1.50
L-Dopa			
	4.00	4.15	+3.75
	5.00	5.16	+3.20
	6.00	5.98	−0.33
	8.00	8.03	+0.37
	10.00	9.88	−1.20
	12.00	12.18	+1.50
	16.00	15.72	−1.75
	20.00	19.52	−2.40

obtained, particularly for higher concentrations (see following section). The method allows a concentration of $5 \cdot 10^{-6}$ M of one catecholamine to be estimated in a ten-fold excess of another with an accuracy of 5—10 %. Obviously the error decreases for intermediate percentages (20—80 %).

TABLE 2

Kinetic determination of adrenaline and L-Dopa in mixtures
(Total concentration [Adr] + [Dopa] = $6.0 \cdot 10^{-5}$ M)

Percent molar fraction of L-Dopa		Error (Δ[Dopa]/[Dopa])%
Taken	Found	
90.0	88.3	−0.78
80.0	78.9	−1.38
70.0	69.2	−1.14
60.0	59.4	−1.00
50.0	49.8	−0.40
40.0	39.2	−2.00
30.0	29.9	−0.33
20.0	19.6	−2.00
10.0	10.4	−4.00

Criteria for selecting the optimum conditions in the determination of mixtures with stopped-flow spectrophotometry

A detailed review of the effect of errors in the parameters utilized in the method of proportional equations (of which the single-point method can be considered a particular case) has been published [8]. The use of the stopped-flow spectrophotometer for the evaluation of $(C_\infty - C_t)/C_\infty$, i.e. in the present case, $(A_\infty - A_t)/A_\infty$, allows the most suitable conditions for the analytical determination to be investigated. In this measurement two readings of transmittance are required (T_∞ and T_{t^*}) and then the problem is to choose the condition which causes least error in concentration, by assuming a constant uncertainty (ΔT) in the measurement of transmittance. Then

$$\Delta^2\left(\frac{A_\infty - A_{t^*}}{A_\infty}\right) = \alpha^2(\Delta T)^2 \tag{9}$$

where $\alpha = \dfrac{\mathrm{d}}{\mathrm{d}T_\infty}\left(\dfrac{A_\infty - A_{t^*}}{A_\infty}\right)$

From eqn. (6),

$$T_{t^*} = T_\infty^{\,L_k(k_A, k_B, t^*)} \tag{10}$$

and

$$L_k(k_A, k_B, t^*) = [1 - e^{-k_A \cdot t^*} + K(1 - e^{-k_B \cdot t^*})]/(1 + K) \tag{11}$$

where $K = [B]_0/[A]_0$.

Then

$$\alpha = \frac{0.4343}{-\log T_\infty}\left(\frac{L_k^2}{T_\infty^2} + \frac{1}{T_{t^*}^2}\right)^{\frac{1}{2}} \tag{12}$$

Hence

$$\left(\frac{\Delta[A]_0}{[A]_0}\right)^2 = \left[\frac{\alpha}{[A]_0\,(e^{-k_A \cdot t^*} - e^{-k_B \cdot t^*})}\right]^2 (\Delta T)^2 \qquad (13)$$

The value of T_∞ which minimizes α, for a given composition of the mixture (i.e. for a fixed K) is given by

$$\frac{L_k^2}{T_\infty^{2(1-L_k)}} + \frac{L_k \log T_\infty + 0.4343}{\log T_\infty + 0.4343} = 0 \qquad (14)$$

Figure 2 shows the relative error $\Delta[A]_0/[A]_0$ as a function of T_∞ for different values of K, by assuming $\Delta T = 0.005$. In Fig. 3, the values of T_∞ and T_{t^*} which minimize the error are reported as a function of the composition of the mixture. Thus preliminary experiments should be made to define the composition of the mixture, and then the optimum final transmittance for minimum error can be selected.

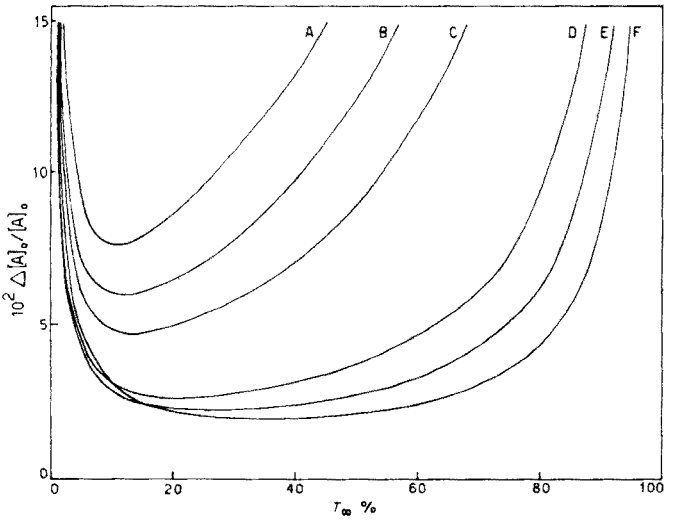

Fig. 2. Variation of relative error, arising from the uncertainty in transmittance measurements (assumed to be 0.005 units), as a function of T_∞ for the determination of adrenaline. Per cent mole fractions of adrenaline are: A, 5 %; B, 7 %; C, 10 %; D, 30 %; E, 50 %; F, 90 %.

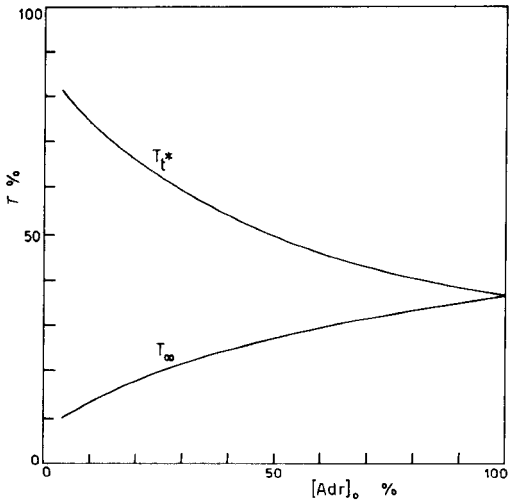

Fig. 3. Values of T_∞ (and consequently T_{t^*}) which minimize the error (arising from the uncertainty in transmittance measurements), as a function of the composition of the mixture (molar fraction of adrenaline).

REFERENCES

1 For a review, see R. A. Heacock, Chem. Rev., 59 (1959) 181; Adv. Heterocycl. Chem., 5 (1965) 205.
2 D. Cantin, J. Alary and A. Coem., Analusis, 3 (1975) 241.
3 E. Pelizzetti, E. Mentasti and E. Pramauro, J. Chem. Soc. Dalton Trans., (1976) 23. E. Mentasti, E. Pelizzetti and G. Giraudi, Zeit. Phys. Chem. (Frankfurt am Main), in press.
4 E. Pelizzetti, E. Mentasti and E. Pramauro, J. Chem. Soc. Perkin Trans. 2, in press.
5 T. S. Lee and I. M. Kolthoff, Ann. N.Y. Acad. Sci., 53 (1951) 1093.
6 G. Giraudi, E. Mentasti and E. Pelizzetti, Atti Accad. Sci. Torino, Cl. Sci. Fis. Mat, Nat., 108 (1974) 825.
7 I. A. Poulson and C. S. Garner, J. Am. Chem. Soc., 84 (1962) 2032.
8 H. B. Mark, Jr. and G. A. Rechnitz, Kinetics in Analytical Chemistry, Interscience, New York, 1968, Ch. 7.

Analytica Chimica Acta, 85 (1976) 169—174

THE KINETIC CATALYTIC ULTRAMICRO DETERMINATION OF SOME 8-HYDROXYQUINOLINE DERIVATIVES

T. J. JANJIĆ and G. A. MILOVANOVIĆ

Chemical Institute, Faculty of Sciences, University of Belgrade (Yugoslavia)

(Received 12th January 1976)

SUMMARY

A kinetic catalytic method for the determination of ultramicro quantities of some 8-hydroxyquinoline derivatives is proposed, and consideration is given to the effect of non-catalytic reactions on this type of determination. The oxidation of alizarin S by hydrogen peroxide in the presence of ammonium carbonate, with manganese as a catalyst, is applied as the indicator reaction for the determination of 8-hydroxyquinoline sulphate, 5,7-diiodo-8-hydroxyquinoline, 5-chloro-7-iodo-8-hydroxyquinoline and 7-iodo-8-hydroxyquinoline-5-sulphonic acid by the tangent method; the reaction rate is followed spectrophotometrically. The concentrations determined range from $2.85 \cdot 10^{-6}$ M to $11.3 \cdot 10^{-6}$ M, with standard deviations of 3.4—10.0 %.

A kinetic catalytic method has been proposed for the determination of ultramicro quantities of amino acids [1] and antihistamines [2] on the basis of the change in catalytic activity of a metal ion which complexes with the substance to be determined. The change in catalytic activity affects the indicator reaction rate, which is followed spectrophotometrically.

This paper gives general consideration to this kind of kinetic determination and a method for the determination of some 8-hydroxyquinoline derivatives which act as bacteriostatic and fungicidal agents, is described.

GENERAL CONSIDERATIONS

Previously it was assumed [1, 2] that the catalytic indicator reaction is not accompanied by a corresponding non-catalytic one, but this is often not the case. From an analytical point of view, it was important to establish whether the linear relation between tan α (see below) and the total concentration of the organic substance to be determined should be expected when the catalytic reaction and a non-catalytic reaction proceed simultaneously. Furthermore, it was of practical interest to find a way of estimating the "region of analytical application" i.e. the concentration range over which this linear relationship holds.

When the organic substance to be determined is present in a subequivalent quantity with respect to the metal catalyst, and when the 1:1 complex

formed is catalytically active, two reactions proceed [1] in parallel in the solution — the reaction catalyzed by the metal and the reaction catalyzed by the complex — and tan α of the total reaction consists of two parts, tan $\alpha_{(M)}$ and tan $\alpha_{(ML)}$. If the 1:1 complex formed is sufficiently stable and the experimental conditions such that both reactions are of pseudo-first order with respect to the indicator dye the following relation is valid:

$$\tan \alpha = \underbrace{-0.434\, k_1\, [M]_0 P_c' + 0.434\, k_1\, [L]_0 P_c'}_{\tan \alpha_{(M)}} \underbrace{- 0.434\, k_2\, [L]_0 P_c''}_{\tan \alpha_{(ML)}} \qquad (1)$$

where $[M]_0$, $[L]_0$ are the stoichiometric concentrations of the metal catalyst and the organic substance respectively; [M], [L] and [ML] are the equilibrium concentrations of the metal catalyst, the organic substance and the 1:1 complex formed, respectively; k_0, k_1 and k_2 are the rate constants of the non-catalytic reaction and of the reactions catalyzed by the metal ions and the complex, respectively; P_c^0, P_c' and P_c'' are the products or more complex functions of the concentrations of all the components involved in the non-catalytic reaction, in the reaction catalyzed by the metal ions and compl respectively; K is the apparent stability constant of the complex; and tan α is the slope of the linear function $\log A = f(t)$.

When the non-catalytic reaction of pseudo-first order also takes place, the term, tan α_0, has also to be introduced, giving

$$\tan \alpha = \underbrace{-0.434\, k_1\, [M]_0 P_c' + 0.434\, k_1\, [L]_0 P_c'}_{\tan \alpha_{(M)}} \underbrace{- 0.434\, k_2 [L]_0 P_c''}_{\tan \alpha_{(ML)}} \underbrace{- 0.434\, k_0 P_c^0}_{\tan \alpha_0} \qquad (2)$$

When the catalytic reaction is accompanied by the corresponding non-catalytic reaction, tan α will be a linear function of the total concentration of the organic substance $[L]_0$, and the dependence of tan α on $[L]_0$ is given in Fig. 1 for the cases: (a) when the complex is catalytically inactive, (b) when the complex is catalytically less active, and (c) when the complex is catalytically more active than the metal catalyst. The relationships given by eqns. (1) and (2) and by Fig. 1 are strictly valid only when the total quantity of the organic substance to be determined is coordinated with the metal. As this requirement cannot be completely satisfied in practice the expression "region of analytical application" was introduced [1], and this can be determined by means of the equation

$$[ML]^2 - [ML]\left\{[M]_0 + [L]_0 + K^{-1}\right\} + [M]_0[L]_0 = 0 \qquad (3)$$

Equation (3) allows the mole fraction (x) of the organic substance coordinated with a metal to be calculated for different values of K and $[L]_0$; Table 1 shows that, where $K^{-1} \leqslant [M]_0 \times 10^{-2}$, the "region of analytical application" lies within the interval $0 < [L]_0 \leqslant 0.8\, [M]_0$, since the error of about 4 % from incomplete coordination lies within the limits of the relative standard deviation of the results obtained. Table 1 enables the "region of analytical application" to be calculated for different mole fractions and for various other conditions with respect to K^{-1}, $[M]_0$ and $[L]_0$.

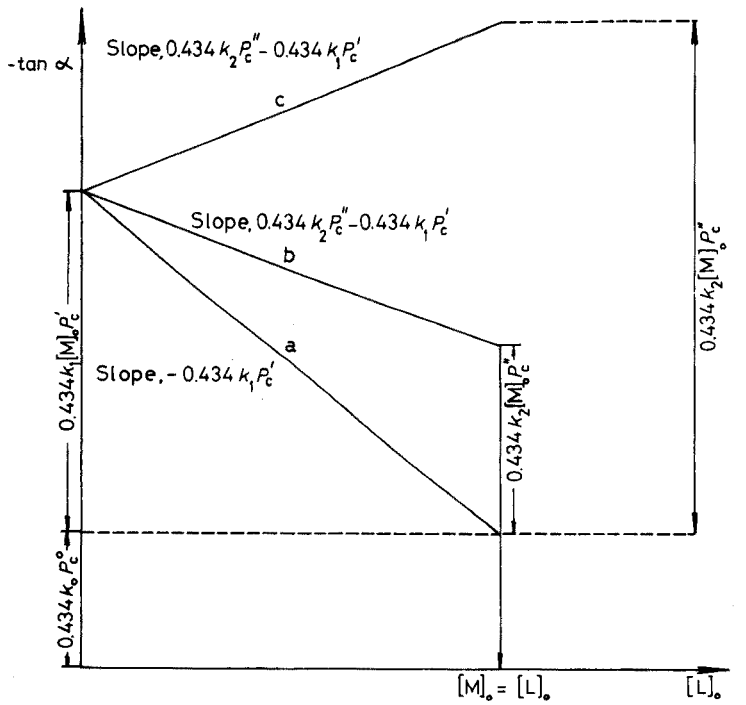

Fig. 1. Dependence of tan α on $[L]_0$ when complex ML is (a) catalytically inactive, (b) catalytically less active and (c) more active than catalyst M.

RESULTS AND DISCUSSION

For the determination of 8-hydroxyquinoline derivatives, the oxidation of alizarin S by hydrogen peroxide in the presence of manganese(II) ions was applied as an indicator reaction; the kinetics of this and the corresponding non-catalytic reaction have been studied [3].

The effect of some 8-hydroxyquinoline derivatives (8-hydroxyquinoline sulphate, 5,7-diiodo-8-hydroxyquinoline, 5-chloro-7-iodo-8-hydroxyquinoline

TABLE 1

Mole fractions of the organic substance coordinated with a metal, for some K^{-1} and $[L]_0$ values

K^{-1}	$[L]_0$				
	0.2 $[M]_0$	0.4 $[M]_0$	0.6 $[M]_0$	0.8 $[M]_0$	1.0 $[M]_0$
$[M]_0$	0.475	0.450	0.427	0.404	0.382
$[M]_0 \cdot 10^{-1}$	0.892	0.867	0.833	0.787	0.730
$[M]_0 \cdot 10^{-2}$	0.988	0.984	0.976	0.959	0.905
$[M]_0 \cdot 10^{-3}$	0.999	0.998	0.998	0.995	0.969

and 7-iodo-8-hydroxyquinoline-5-sulphonic acid) on the rate of the indicator reaction was studied; these substances lead to a decrease in the reaction rate. A linear dependence of tan α on the concentration of these substances when present in the subequivalent quantities with respect to manganese ions was given, when high concentrations of all the other components involved in the reaction were present (Fig. 2). Since these 8-hydroxyquinoline derivatives exhibit pronounced bacteriostatic and fungicidal effects, the possibility of applying the proposed indicator reaction for their determination was examined. To find the optimal experimental conditions it was necessary to investigate the kinetics of the indicator reactions catalyzed by manganese monocomplexes by the methods used previously [1—3]. The results obtained are summarized in Table 2; it may be concluded that the kinetic equation for the oxidation of alizarin S by hydrogen peroxide in the presence of manganese(II) ions is analogous to that for the same reaction catalyzed by manganese monocomplexes. On the basis of the rate constants, these monocomplexes are catalytically less active than manganese(II) ions.

Figure 1 shows that the sensitivity of the proposed kinetic method will be dependent on the slope of the straight line in the calibration plot. This slope is given by the expression $\pm\ 0.434\ (k_2P_c'' - k_1P_c')$, and since the kinetic equations for the reactions catalyzed by manganese(II) ions and by manganese monocomplexes are analogous ($P_c' = P_c''$), a change in experimental conditions cannot directly affect the sensitivity of the method. Since the sensitivity of such methods can be increased indirectly by a decrease in the

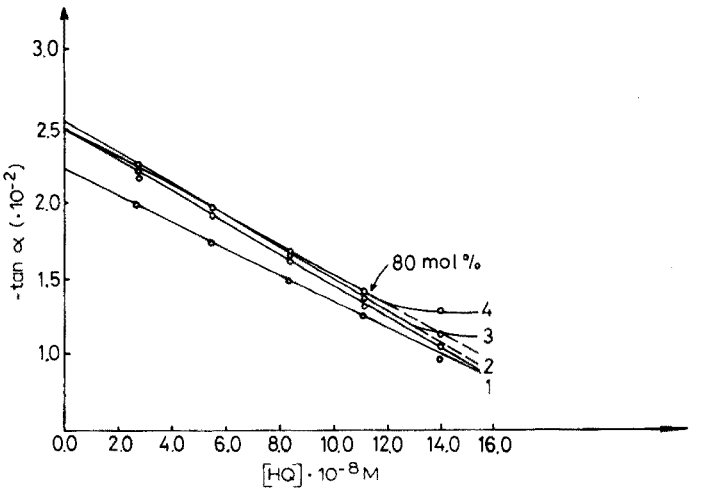

Fig. 2. Dependence of tan α on the concentration of 8-hydroxyquinoline derivatives in the oxidation of alizarin S by hydrogen peroxide. Initial concentrations: alizarin S, $6.2 \cdot 10^{-5}$ M; hydrogen peroxide, $9.8 \cdot 10^{-2}$ M; ammonium carbonate, 0.18 M; manganese(II) sulphate, $14.0 \cdot 10^{-8}$ M; pH = 9.35; I = 1 ($NaClO_4$); t = 20 ± 0.1 °C. (1) 8-hydroxyquinoline sulphate, (2) 5,7-diiodo-8-hydroxyquinoline, (3) 5-chloro-7-iodo-8-hydroxyquinoline, (4) 7-iodo-8-hydroxyquinoline-5-sulphonic acid.

TABLE 2

The kinetics of oxidation of alizarin S by hydrogen peroxide (buffer solution: ammonium carbonate; pH 9.35; I = 1 ($NaClO_4$); t = 20 ± 0.1 °C)

Sample	Reaction order[a] for			Rate constants[b]
	Mn	Mn 1:1 complex	H_2O_2	
—	—	—	0	$0.68 \pm 0.05 \cdot 10^{-1}$ (4)[c]
—	+1	—	−1	$2.32 \pm 0.15 \cdot 10^{5}$ (8)[c]
8-Hydroxyquinoline sulphate	—	+1	−1	$0.90 \pm 0.03 \cdot 10^{5}$ (9)
5,7-Diiodo-8-hydroxyquinoline	—	+1	−1	$0.96 \pm 0.04 \cdot 10^{5}$ (9)
5-Chloro-7-iodo-8-hydroxyquinoline	—	+1	−1	$0.92 \pm 0.05 \cdot 10^{5}$ (9)
7-Iodo-8-hydroxy-quinoline-5-sulphonic acid	—	+1	−1	$0.91 \pm 0.05 \cdot 10^{5}$ (9)

[a]First order with respect to alizarin S and buffer solution.
[b]Number of determinations is given in parentheses.
[c]Data taken from [3].

non-catalytic reaction rate relative to the catalytic one, the optimal conditions for the work will involve lower hydrogen peroxide concentrations. However, the concentration of hydrogen peroxide cannot be decreased below a definite limit, since the linear dependence of log A on time would disappear. The experimental conditions for the determination of manganese were therefore retained (i.e. $6.2 \cdot 10^{-5}$ M alizarin S, $9.8 \cdot 10^{-2}$ M hydrogen peroxide, 0.18 M ammonium carbonate and $14.0 \cdot 10^{-8}$ M manganese(II) sulphate). The determinations were performed by the tangent method. The calibration curves are given in Fig. 2; the results are presented in Table 3. These results prove that the derivatives can be determined in the 10^{-7}—10^{-8} mol l^{-1} range with very reasonable accuracy.

EXPERIMENTAL

Reagents and solutions

Re-distilled water was used for all solutions. The solutions of manganese(II) sulphate ($1.8 \cdot 10^{-4}$ M) and alizarin S ($1.5 \cdot 10^{-3}$ M) were prepared from recrystallized analytical-grade reagents. The solution of ammonium carbonate (Merck) was 1.8 M (pH 9.35). The hydrogen peroxide solution was 9.8 M; its concentration was determined by the permanganate method. Stock solutions of the organic substances to be determined were $1.78 \cdot 10^{-3}$ M, prepared by dissolving the appropriate amounts of 8-hydroxyquinoline sulphate, (Schuchardt), 5,7-diiodo-8-hydroxyquinoline, (Merck), 5-chloro-7-iodo-8-hydroxyquinoline, (Merck) and 7-iodo-8-hydroxyquinoline-5-sulphonic acid (Fluka).

TABLE 3

Determination of ultramicro quantities of some 8-hydroxyquinoline derivatives by the tangent method

Compound	Amount ($\cdot 10^{-8}$ mol l^{-1})		No. of detns.	s_r (%)
	Taken	Found		
8-Hydroxy-quinoline sulphate	2.85	3.17 ± 0.32	10	10.0
	5.70	5.86 ± 0.28	3	4.7
	8.50	7.98 ± 0.45	3	5.6
	11.3	11.6 ± 0.40	10	3.4
5.7-Diiodo-8-hydroxy-quinoline	2.85	2.61 ± 0.16	10	6.1
	5.70	5.30 ± 0.43	3	8.1
	8.50	8.64 ± 0.34	3	4.1
	11.3	11.8 ± 0.73	10	6.1
5-Chloro-7-iodo-8-hydroxy-quinoline	2.85	3.12 ± 0.29	10	9.2
	5.70	5.67 ± 0.28	3	4.9
	8.50	9.26 ± 0.30	3	3.6
	11.3	11.8 ± 0.51	10	4.3
7-Iodo-8-hydroxy-quinoline-5-sulphonic acid	2.85	2.79 ± 0.20	10	7.1
	5.70	5.67 ± 0.28	3	8.2
	8.50	8.02 ± 0.52	3	6.4
	11.3	10.6 ± ± 0.37	10	3.5

Apparatus

Absorbance measurements were made with a Beckman DU quartz spectrophotometer (1-cm cells). A Radiometer 4c pH-meter was used, and an "Ultra-Thermostat nach Höppler" type NBE (VEB Prüfgeräte-Werk, Medingen) was used for thermostatting the solutions.

Procedure

A reaction vessel with three compartments was used. The solution of alizarin S, manganese(II) sulphate and the 8-hydroxyquinoline derivative were measured into one compartment, ammonium carbonate into the second, and hydrogen peroxide and water (to a total volume of 25 ml) into the third compartment. The vessel was thermostatted at 20 ± 0.1 °C, and the reaction was initiated by vigorous mixing. During the oxidation of alizarin S the solution progressively loses its colour; the progress of the reaction was followed spectrophotometrically by measuring the absorbance at 335 nm every min, for 10 min from the start of the reaction.

REFERENCES

1 T. J. Janjić and G. Milovanović, Anal. Chem., 45 (1973) 390.
2 T. J. Janjić, G. Milovanović, Glas. Hem. Drus., Beograd, 40 (1975) 329.
3 T. J. Janjić, G. Milovanović and M. B. Ćelap, Anal. Chem., 42 (1970) 27.

Analytica Chimica Acta, 85 (1976) 175—178

Short Communication

USE OF THE IONOPHORE ANTIBIOTIC A23187 IN LIQUID ION-EXCHANGE ION-SELECTIVE ELECTRODES

ARTHUR K. COVINGTON and NARESH KUMAR

Department of Physical Chemistry, University of Newcastle upon Tyne, Newcastle upon Tyne NE1 7RU (England)

(Received 9th February 1976)

The carboxylic acid antibiotic A23187 [1] is an ionophore for divalent cations with a selectivity order $Mn^{2+} \gg Ca^{2+} \simeq Mg^{2+} \gg Sr^{2+} > Ba^{+}$, and little selectivity for monovalent cations at physiological pH [2]. A23187 is obtained by crystallization from broths of *Streptomyces chartreusensis* as the mixed magnesium—calcium salt which can be converted to, and crystallized as, the free acid. Elemental analysis gave $C_{29}H_{37}N_3O_6$ with a molecular weight of 523. The structure of the free acid was determined by ^{1}H- and ^{13}C-n.m.r. and x-ray methods by Chany et al. [3] and shown to exist in the crystal as the closed configuration shown below. The structure of the calcium salt has not been determined, but it is likely that the Ca^{2+} ions lie in a cavity of oxygen atoms provided by two molecules of A23187.

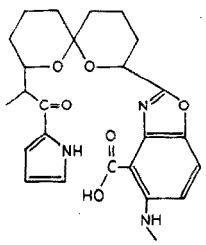

In view of the use of antibiotics such as valinomycin [4] in liquid ion-exchange ion-selective electrodes for the determination of monovalent ions such as potassium, it is of interest to examine other antibiotics with known selectivity properties for common ions in the search for ion-selective electrodes with improved selectivities over those commonly available. Such studies may also aid in the understanding of the role of ionophores in the transport of ions across biological membranes.

In the present work, A23187 dissolved in nitrobenzene and supported on cellulose ester membranes was examined as a liquid ion-exchange electrode for calcium.

Experimental

A23187 (Eli Lilly and Co.) was dissolved (2.5 % w/w) in nitrobenzene (BDH AnalaR). In view of the small total amount of material available and insufficient information on which to base selection of a suitable solvent, no study of the effect of solvent was possible, and the first solvent tried that gave adequate solubility was used.

Aqueous solutions of the alkaline earth and alkali metal chlorides were prepared from AnalaR-grade salts dissolved in triple distilled water. The former were analysed by titration with EDTA to eriochrome black T end-points.

The Orion Research 92 Series liquid ion-exchanger electrode body was used for all studies. Again because of the small quantity of material available, the suggested method [5] of making up the electrode was modified. The cellulose ester membrane (Orion 92-81 or Millipore Type VF) was placed on the membrane spacer assembly, and a small drop of liquid ion exchanger was placed on its shiny outer surface and left to soak in. Then another drop was placed on the inside of the membrane from a syringe with a long needle inserted through the outer vent of the electrode body. By this method an electrode can be prepared with only 5 μl of exchanger and about 40 electrodes could be made from the available 20 mg of A23187. A solution of the chloride of the primary cation (2 ml of a 0.02 mol l^{-1} solution) was injected into the central tube of the body, care being taken that no air bubbles were present. The electrode assembly was completed and the electrode left to equilibrate in a 10^{-6} mol l^{-1} solution of the primary cation for at least 2 h before calibration tests were commenced.

The E.I.L. Type 33-1320-710 sealed calomel reference electrode with an additional outer porous ceramic chamber containing 3 mol l^{-1} tetramethylammonium chloride to form a double junction, was used to prevent potassium ions reaching the test solutions. Cell potential differences were measured by means of an interfacing device, constructed from an electrometer amplifier (MF1-3, Computing Techniques, Billinghurst, Sussex), to a digital voltmeter (Fenlow Electronics Type 701). Measurements were made in a screened cabinet air thermostat to 25.0 ± 0.1 °C.

Calibration measurements for a selected primary cation were made over the range 10^{-6} to 10^{-1} mol l^{-1} starting with the most dilute solution. Steady potential differences were obtained, in most cases within a minute of placing the electrodes in the solution. After the calibration test, the electrode was left in 10^{-6} mol l^{-1} solution for 30 min before the selectivity tests were commenced. Selectivity constants were measured by the mixed solution method [6] at constant concentration of the interferent ion chosen to give a measurable remaining level of primary ion response. The selectivity constants were calculated from the equation $K_{ij} = c_{i(j)}/c_j$, where c_j is the constant level of interferent ion j and $c_{i(j)}$ is obtained from the abscissa value of c_i where the horizontal interferent and primary response curves intersect.

Results

Calibration and selectivity results are shown in Table 1. For comparison some results with the Orion 92-20 Calcium electrode are included. The calibration results with A23187 are linear over the range 10^{-1}—10^{-4} mol l^{-1}, with slightly lower slopes than given by the Orion material. It is known, however, from other work in this laboratory, that the double junction involving tetramethylammonium chloride leads to apparently slightly super-Nernstian calibration slopes. Selectivities and the levels of interferent ion employed are also given in the Table. These indicate a selectivity order $Ba^{2+}>Sr^{2+}>Ca^{2+}>Mg^{2+}$. It was noted that once an electrode has been employed in barium(II) solutions it shows no response to calcium(II) as primary cation, which suggests that the barium (II) complex is very stable. Interference from Na^+ and K^+ ions was found and may be attributed to the solvent since nitrobenzene is known to extract potassium from aqueous solutions [7]. Interference from hydrogen ion was not unexpected from the nature of A23187. All the results were obtained at the unadjusted salt solution pH (4.5—5.5) and this may account for the slightly low calibration slopes. An attempt was made to buffer the solutions to higher pH with tricine but this impaired the electrode response. Search for a buffer substance compatible with A23187 required more material than available. TRIS has been used in extraction studies [2]. Little difference in electrode performance could be attributed to the use of the two different types of cellulose ester membrane support materials.

TABLE 1

Electrode results for A23187 in nitrobenzene at 25 °C

Ion (i)	Range (mol l^{-1})	Membrane	Slope (mV/decade) in the presence of i only	Ion (j)	c_j (mol l^{-1})	K_{ij}
Ca^{2+}	10^{-1}—10^{-4}	92-81	26, 26, 29, 29	Mg^{2+}	0.45	0.051
				Na^+	$0.45 \cdot 10^{-3}$	0.23
		VF	25, 28, 25	Mg^{2+}	0.45	0.045
				Sr^{2+}	$4.5 \cdot 10^{-5}$	97
				K^+	$4.5 \cdot 10^{-4}$	16
				H^+	$2.2 \cdot 10^{-4}$	$2.5 \cdot 10^4$
Ba^{2+}	10^{-1}—10^{-4}	92-81	29, 29	Mg^{2+}	0.45	$0.8 \cdot 10^{-3}$
		VF	28, 28	Ca^{2+}	0.45	$1.4 \cdot 10^{-3}$
						$1.2 \cdot 10^{-2}$
				Mg^{2+}	0.45	$1.3 \cdot 10^{-3}$
						$1.4 \cdot 10^{-3}$
Mg^{2+}	10^{-1}—10^{-4}	92-81	26, 25	Ca^{2+}	10^{-3}	7.9
Ca^{2+}	10^{-1}—10^{-4}	92-20[a]	30, 33	Mg^{2+}	$9 \cdot 10^{-3}$	$8.6 \cdot 10^{-2}$
						$9.6 \cdot 10^{-2}$
				Ba^{2+}	$9 \cdot 10^{-3}$	0.17, 0.14

[a]92-20 Orion exchanger.

Discussion

The selectivity order found for the alkaline earth cations differs from that obtained when extraction and spectrophotometric techniques are used, but in those studies the solvents were dimethylformamide and ethanol. The high level of interference from barium and hydrogen ions would preclude the use of ion-selective electrodes from A23187 as calcium sensors in some applications. The high selectivity of A23187 for barium(II) may be attributable to the cavity size, with 6 oxygen atoms available for its coordination from each of two molecules of A23187 since barium(II) may prefer 12 coordination but calcium(II) six [8]. Only three oxygen atoms in A23187 are suitably positioned, according to Chaney et al. [3] based on models of its structure. A detailed study of the solution conformation of the calcium complex has now been published [10].

Conclusions. The selectivity order for A23187 as determined from its use in ion-selective electrodes is $Ba^{2+} > Sr^{2+} > Ca^{2+} > Mg^{2+}$, which is almost the reverse order of that determined by phase extraction studies [1]. Since barium and strontium ions are usually absent from solutions of physiological interest, electrodes based on A23187 could be of practical use, as has been shown by Band and Kratchovil [9] for PVC-based electrodes.

We thank Dr. D.E. Minnikin for drawing our attention to the properties of A23187, and Eli Lilly and Co. for the gift of a 20-mg sample.

REFERENCES

1 P. R. Reed and H. A. Lardy, J. Biological Chemistry, 247 (1972) 6970.
2 D. R. Pfeiffer, P. W. Reed and H. A. Lardy, Biochemistry, 13 (1974) 4007.
3 M. O. Chaney, P. V. Demarco, N. D. Jones and J. L. Occolowitz, J. Am. Chem. Soc., 96 (1974) 1932.
4 M. F. Frant and J. W. Ross, Science, 167 (1970) 987.
5 Orion Research Incorporated (Cambridge, Mass, U.S.A.), Handbooks for 92 Series Electrodes.
6 A. K. Covington, Crit. Rev. Anal. Chem., 3 (1974) 357.
7 T. Iwachido, Bull. Chem. Soc. Jpn., 44 (1971) 1835.
8 W. Simon, W. E. Morf and P. C. Meier, Struct. and Bonding (Berlin), 16 (1973) 113.
9 D. M. Band and J. Kratchovil, private communication, Feb. 1975.
10 C.M. Deber and D.R. Pfeiffer, Biochemistry, 15 (1976) 132.

Analytica Chimica Acta, 85 (1976) 179—183

Short Communication

RAPID DETERMINATION OF TRACE AMOUNTS OF HYDROGEN PEROXIDE

K. G. BOTO* and L. F. G. WILLIAMS

Department of Defence, Australian Defence Scientific Service, Materials Research Laboratories, P.O. Box 50, Ascot Vale, 3032 (Australia)

(Received 22nd December 1975)

Accurate hydrogen peroxide determination is needed for studies of oxygen reduction mechanisms on electrodes such as sulphides [1], glassy carbon [2] and silver [3], and on corroding metals [4], but a sufficiently simple, accurate and rapid technique does not appear to be available. The classical titrimetric technique [5] is accurate only for peroxide concentrations above $5 \cdot 10^{-4}$ mol l^{-1}, whereas, for the applications mentioned above, accurate analyses for concentrations of $1 \cdot 10^{-6}$ mol l^{-1} would normally be required. Azaz et al. [6] have developed a suitably sensitive method involving spectrophotometric monitoring of the kinetics of iodine disappearance but it is fairly time-consuming. Gohda et al. [7] describe an accurate method for peroxide down to ca. $2 \cdot 10^{-6}$ mol l^{-1} based on the peroxide—luminol chemiluminescence reaction, but this technique lacks simplicity. Other techniques such as fluorimetry [8], thermometric titrations [9] and colorimetry with titanyl sulphate [10] lack sufficient sensitivity.

This communication describes two simple and accurate techniques for the determination of trace quantities of hydrogen peroxide. The first is an extension of the standard permanganate titration to lower concentrations by using a potentiometric end-point. The second method employs direct differential pulse polarography.

Experimental

Reagents. All chemicals were of analytical reagent-grade purity and the water was singly or doubly distilled through all-glass apparatus. High-purity nitrogen was used to de-oxygenate the solutions for polarography. Peroxide solutions were prepared by dilution of a standardized concentrated solution. The concentrations of the peroxide stock solution and of the standard $1.00 \cdot 10^{-3}$ mol l^{-1} potassium permanganate solution were frequently checked, as neither solution is very stable.

*Present Address: Australian Institute of Marine Science, P.O. Box 1104, Townsville, 4810, Australia.

Potentiometric titrations. A 5-ml burette graduated in 0.01 ml divisions was used. Unknown solutions of 50—100 ml volume containing as little as $1 \cdot 10^{-7}$ mol of peroxide were titrated directly, while stirring, after addition of 10 ml of (1 + 9) sulphuric acid solution and a small crystal of manganese(II) sulphate. The titration was followed potentiometrically with a platinum wire indicator electrode and a Pye saturated calomel electrode (SCE); all potentials quoted here are with respect to the SCE. With care, volume increments of 0.01 ml could be easily achieved. Potentials were measured with a Tacussel type S70/AS potentiometer. To obtain the titration curve shown in Fig. 1, the potential was read 30 s after each volume increment had been added. From this curve, a standard end-point potential of 0.80 V was chosen, and subsequent titrations were carried out much more rapidly to this end-point potential. A point worth noting to facilitate the ease of titration is that, before the end-point is reached, the addition of each increment of titrant produces a rapid increase in potential, followed by a drop as reaction occurs. Near the end-point this drop is much slower and, at the end-point, the potential shows the initial rapid rise, followed by a further very slow rise past 0.80 V.

Differential pulse polarography. For solutions in which the blank titration is excessively high, i.e., another oxidizable species is present, the analysis can be performed by differential pulse polarography. A Princeton Applied Research (PAR) model 174A Polarographic analyser was used with the model

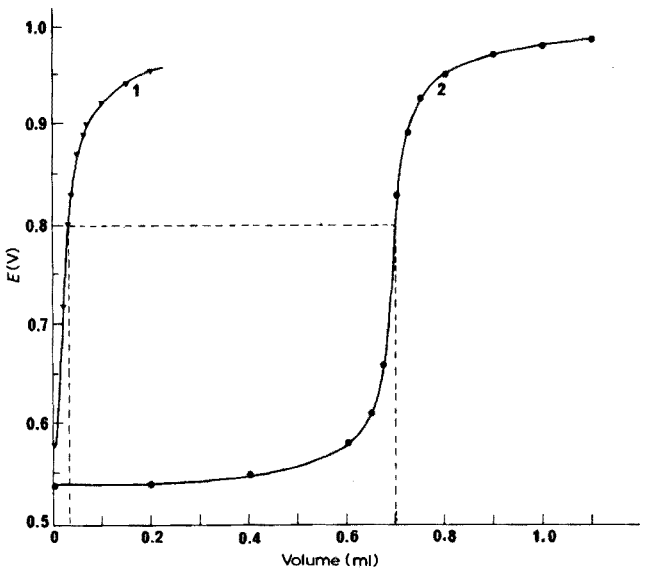

Fig. 1. A potentiometric titration curve (2) for a solution containing $1.69 \cdot 10^{-6}$ mol of H_2O_2 titrated with 10^{-3} mol l^{-1} $KMnO_4$. Curve 1 shows a blank titration.

174/70 drop-timer assembly. The polarographic cell was simply a 30-ml beaker fitted with a rubber stopper with suitable holes for the dropping mercury electrode (DME), platinum wire auxiliary electrode, reference electrode salt bridge connection, and nitrogen bubbler; the SCE was connected to the solution via a salt bridge filled with sodium sulphate solution. Polarograms were run on about 20 ml of the unknown solution after first degassing for 7—8 min with nitrogen. The control settings on the PAR were as follows: initial potential, —0.750 V; scan rate, 5 mV s^{-1}; pulse amplitude, 25 mV; pulse rate and drop time, 1 s. For calibration, the solution was "spiked" with 50-μl additions of standardized stock solution. Interference from metal ions such as nickel or zinc could be easily removed by addition of 2.0 ml of 0.1 M EDTA solution. The reduction peak potentials for these metals are then shifted to much more negative potentials and away from the peroxide reduction potential.

Results and discussion

Figure 1 shows the potentiometric titration curve obtained for a solution containing $1.69 \cdot 10^{-6}$ mol of hydrogen peroxide. The "blank" titration for a 100-ml volume of solution containing no peroxide is also shown. An excellent potentiometric end-point is achieved and the blank value of 0.035 ml is quite reasonable. When the 0.80-V end-point criterion is used, it is estimated that the titration errors are $\leqslant$ 0.01 ml. Table 1 shows some results obtained for addition of known amounts of peroxide to a 0.1 mol l^{-1} ammonium sulphate solution; the amounts found are in excellent agreement with the amounts added and in almost all cases the error was less than that calculated for a ± 0.01 ml titration error. The average titration takes about 2 min. The results indicate that as little as $1 \cdot 10^{-7}$ mol of peroxide can be determined with a maximum expected error of ± 15 %, while a solution containing $1 \cdot 10^{-6}$ mol of peroxide can be analysed to within ± 2 %.

This method has been used in these laboratories in a recent study of the role of oxygen reduction in zinc corrosion, where various solutions were used, e.g., acetate—acetic acid and succinate—succinic acid buffers, phosphate

TABLE 1

Potentiometric titration of hydrogen peroxide added to a 0.1 mol l^{-1} ammonium sulphate solution

H_2O_2 added ($\cdot 10^{-7}$ mol)	Blank (ml)	H_2O_2 found ($\cdot 10^{-7}$ mol)	Error (%)	Max. expected error (%)
1.69	0.07_4	1.85	+ 9.6	± 14.2
3.38	0.14_3	3.58	+ 5.9	± 7.1
7.76	0.26_5	7.6	— 1.9	± 3.7
15.5	0.53_5	15.3	— 0.9	± 1.9
19.4	0.68	19.5	+ 0.8	± 1.5

buffers and unbuffered sulphate solutions. No differences between solution types were found, although, for the buffer solutions, up to 50 ml of (1 + 9) sulphuric acid was added to ensure adequate acidity for the permanganate titration.

The differential pulse polarographic method is somewhat less sensitive, although solutions as low as ca. $2 \cdot 10^{-6}$ mol l^{-1} in peroxide can be analysed. Samples of the actual polarograms obtained for a sulphate solution with various known additions of peroxide are shown in Fig. 2. Although the peak obtained is fairly broad, the peak height (i_p) can be measured by extrapolation of the baseline as shown in Fig. 2. The blank current for the same solution with no added peroxide is subtracted from the measured peak current (i_p) to give the corrected peak height (i_c). The relationship between i_c and peroxide concentration was found to be linear over the range $5—20 \cdot 10^{-6}$ mol l^{-1} hydrogen peroxide (i_c = 19—79 nA) by the standard addition method. The polarographic method was found to be especially useful for determinations of peroxide in electrolyte solutions containing EDTA [4].

The direct potentiometric titration with permanganate provides a simple, rapid and sensitive method for determination of trace amounts of peroxide. This method should be especially useful for corrosion studies and basic electrochemical studies of oxygen reduction. The differential pulse

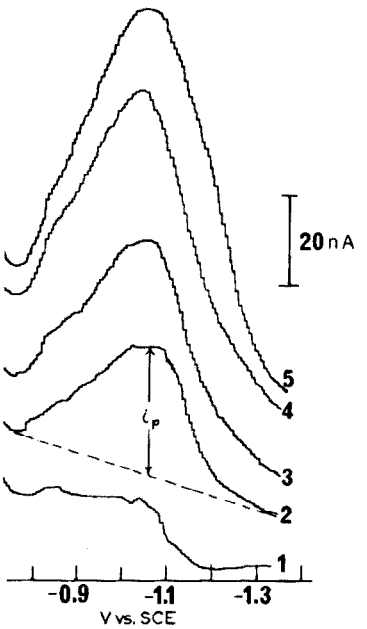

Fig. 2. Differential pulse polarograms of 24 ml of a 0.01 mol l^{-1} EDTA, 0.2 mol l^{-1} $(NH_4)_2SO_4$ and 0.3 mol l^{-1} NH_3 solution with additions of (1) 0 µl, (2) 200 µl, (3) 350 µl, (4) 500 µl and (5) 650 µl of a $6.03 \cdot 10^{-4}$ mol l^{-1} H_2O_2 solution.

polarographic method should have wider applicability. In the recent study of zinc corrosion [4], results obtained by both methods, where applicable, compared favourably (to within 2 %) and agreed with an indirect method involving integration of ring currents with a ring-disc electrode system.

REFERENCES

1 T. Biegler, D. A. J. Rand and R. Woods, J. Electroanal. Chem. Interfacial Electrochem., 60 (1975) 151.
2 R. J. Taylor and A. A. Humffray, J. Electroanal. Chem. Interfacial Electrochem., 64 (1975) 63.
3 I. Moraas, J. Electrochem. Soc., 122 (1975) 1008.
4 K. G. Boto and L. F. G. Williams, paper submitted for publication.
5 C. H. Lea, Proc. Roy. Soc., 108B (1931) 175; J. Soc. Chem. Ind., London, Trans., Commun., 65 (1946) 286.
6 E. Azaz, M. Donbrow and R. Hamburger, Analyst (London), 98 (1973) 663.
7 S. Gohda, Y. Yamashita, Y. Nishikawa and T. Shigematsu, Bunseki Kagaku 22 (1973) 1180.
8 W. Goedlicke and I. Goedick, East Ger. Patent 103, 059 (1974).
9 J. Brandstetr and P. Sapakova, Collect. Czech. Chem. Commun., 38 (1973) 2249.
10 M. Tanada, H. Uchida and K. Sawa, Shokuhin Eiseigaku Zasshi, 14 (1973) 431.

Analytica Chimica Acta, 85 (1976) 185—188

Short Communication

THE AMPEROMETRIC TITRATION OF PHOSPHATE WITH IRON(III)

J. W. BIXLER and L. F. COLWELL*

Department of Chemistry, State University College at Brockport, Brockport, New York 14420 (U.S.A.)

(Received 8th January 1976)

Current interest in the ecological effects of phosphate makes improved methods for determining low concentrations of phosphate of interest. The conventional amperometric titration with iron(III) at a dropping mercury electrode was therefore re-examined, with the goal of establishing stoichiometric reaction conditions. Previous workers using this method [1, 2] have employed mixed acetate—chloride supporting electrolytes of pH 3—4. However, attempts to use this electrolyte system gave distinctly late, non-stoichiometric end-points, as has been reported by Saikina and Toropova [1].

A study of $FePO_4$ precipitation is complicated by several pH-dependent side-reactions; these include formation of hydrated iron(III) oxide species, the $FeHPO_4^+$ complex [3] and complexes of iron(III) with the buffer-electrolyte. Chloroacetate was preferred to acetate as the supporting electrolyte in the work described here, because it has a good buffer capacity near pH 3 and is a weaker ligand than acetate for iron(III).

A dropping mercury indicator electrode (DME) was chosen, because the constantly renewed surface minimizes fouling problems in turbid systems. Cox and Cheng [4] have recently described a novel method for determining phosphate by cathodic stripping of iron(III) phosphate which has been concentrated electrochemically on a glassy carbon electrode.

Experimental

A modified Heath Model EUA-19-6 polarographic assembly was used. The commercial cell cover was replaced by a solid Teflon cover, which had holes for the DME, a salt bridge, a miniature glass pH electrode and a microburet. The cell was the bottom of a 45/12 weighing bottle, thermostated at 25 ± 0.02 °C. A salt bridge, containing supporting electrolyte with the same concentration and pH used in the cell, was interposed between the saturated calomel reference electrode and the cell. Limiting currents were monitored with a Beckman Electroscan 30 and pH was measured with a Corning Model 7

*Present Address: Department of Chemistry, Northeastern University, Boston, Massachusetts 02115.

pH meter. The DME had a 5.0-s open-circuit drop-life in 0.080 M chloroacetic acid.

Glass-distilled deionized water was used. The stock solution of iron(III) perchlorate in 0.01 M perchloric acid was standardized titrimetrically and verified coulometrically. The stock phosphoric acid solution was standardized alkalimetrically. Chloroacetic acid (Eastman) was recrystallized from water and dried over concentrated sulfuric acid in a vacuum desiccator.

Procedure. A 25.00-ml portion of phosphate test solution, containing the desired concentration of chloroacetic acid, was pipetted into a clean, dry polarographic cell. The pH was adjusted to 3.0—3.4 with very small additions of near-saturated NaOH solution. Uniform portions of 0.0902 M iron(III) titrant were added from a microburet. The size of the aliquots was chosen to insure that 6—9 additions were made in the region between 50 and 150 % titrated. After each addition of titrant, the solution was deaerated for 5 min and after 1 min the limiting current was measured at —0.4 V vs. SCE. The pH was checked frequently during each titration to verify adequate pH control by the chloroacetate buffer.

Results and discussion

The titration curves are of the reversed-L form (Fig. 1a) with a distinct change in slope near the stoichiometric point for the formation of $FePO_4$. The end-point was located by intersecting linear extrapolations of the data before and after the end-point; no more than the single data point nearest the intersection was discounted. The end-point was considered to be indeterminate if either line could not be easily defined by three or more linear points. Attempts to extrapolate data very early or very late in the titrations gave inconsistent and irrational results.

The effect of pH on the titration curves is shown in Fig. 1(a). As the pH is decreased, the current before the end-point increases. This undoubtedly reflects the presence of more of the soluble, electro-reducible $FeHPO_4^+$

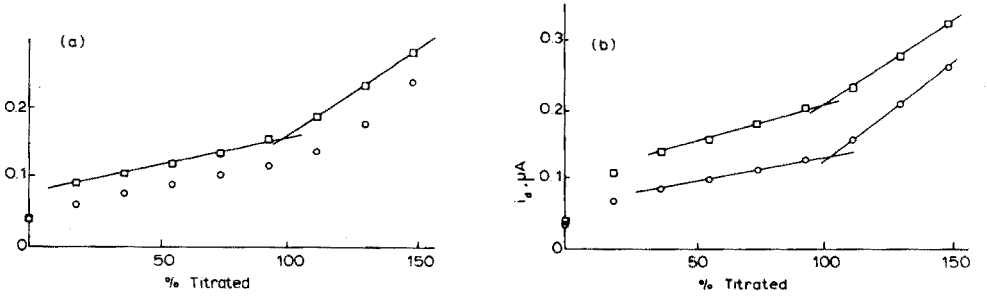

Fig. 1. Titration of 25.00 ml of $1.94 \cdot 10^{-4}$ M H_3PO_4 in chloroacetate buffer with 0.0902 M Fe(III). (a) Effect of pH (□) pH 3.1, (○) pH 3.3 in 0.050 M buffer. (b) Effect of total chloroacetate concentration at pH 3.2 (□) 0.125 M, (○) 0.050 M.

complex. The location of the end-point is not significantly altered, however, because the complex and precipitate have the same stoichiometry; the $FeHPO_4^+$: $FePO_4$ ratio must be essentially constant up to the end-point. The lower practical limit of pH is about 3.05, below which the line slopes are too similar to permit confident end-point location. At or above pH 3.30, the end-points are late because of hydrated iron(III) oxide interference. At pH 3.40, the normally white precipitate has a distinctly yellow color, and the linearity of response after the end-point is poor. Therefore, all measurements were made at pH 3.1—3.2.

The effect of total chloroacetate concentration on the titration curves is shown in Fig. 1(b). While the chloroacetate concentration need not be regulated as closely as the pH, its effect on the results depends somewhat on the amount of phosphate present. High chloroacetate concentration leads to the same curve shape as seen at low pH. When a titration was made in a medium containing 0.030 M chloroacetate and 0.0250 M sodium nitrate at pH 3.20, the current values before the end-point lay slightly below the values found for 0.030 M chloroacetate at pH 3.20. This indicates that the current enhancement with increasing chloroacetate concentration is due to increased formation of an electroactive iron(III) chloroacetate complex, rather than simply the diverse ion effect on the $FePO_4$ precipitate. The location of the end-point is independent of the chloroacetate concentration (Fig. 1b). This suggests that the fraction of total iron(III) present as the chloroacetate complex does not vary significantly in the linear region before the end-point, and shows that this complex has the same 1:1 $Fe:PO_4^{3-}$ stoichiometry as the precipitate [5].

The useful chloroacetate concentration range depends on the concentration of phosphate, being 0.05—0.125 M for $2 \cdot 10^{-4}$ M phosphate, 0.05—0.10 M for $1 \cdot 10^{-4}$ M phosphate, 0.03—0.05 M for $8 \cdot 10^{-5}$ M phosphate, and about 0.01 M for $4 \cdot 10^{-5}$ M phosphate. In each case, the upper limit is governed by the decreasing end-point sharpness with increasing chloroacetate concentration. The lower limit results from inadequate buffer capacity, as the titration reaction releases protons. In general applications, a trial titration should be made in approximately 0.05 M chloroacetate at pH 3.2. If the end-point is indistinct, the chloroacetate concentration should be reduced by a factor of 2—3 in further titrations.

The useful analyte concentration range is about 2—55 p.p.m. phosphate. The upper limit is governed by current instability caused by the effects of copious amounts of colloidal precipitate on the drop surface. The lower limit is determined by a combination of detector response and inadequate buffering by chloracetate solutions less concentrated than 0.01 M.

Twenty-four titrations of 2—55 p.p.m. phosphate were performed under the recommended conditions. The errors ranged from −7 % to +8 %, with an average error of 4 %, and there was no trend with regard to sign or magnitude. While the amperometric method is less sensitive than the stripping technique [4], it is at least as accurate and has the distinct advantages of being experimentally simple, and of being based on a stoichiometric reaction.

In a preliminary study of interferences, samples of $1.0 \cdot 10^{-4}$ M phosphate in 0.050 M chloroacetate were made $5.0 \cdot 10^{-5}$ M in sodium fluoride, sodium oxalate, sodium chloride or calcium nitrate. Only calcium nitrate altered the shape of the titration curve and caused a titration error. The reverse titration of $9.0 \cdot 10^{-5}$ M iron(III) with 0.097 M H_3PO_4 gave a sharp L-shaped titration curve with a stoichiometric end-point.

This work was supported in part by the Undergraduate Research Participation Program of the National Science Foundation. We thank C. W. Sansocie, A. L. Shobert and K. A. Schroeder for helping with the early stages of this work.

REFERENCES

1 M. K. Saikina and V. F. Toropova, Tr. Kom. Anal. Khim. Akad. Nauk SSSR, Otd. Khim. Nauk. 4, No. 7 (1952) 141; through Chem. Abstr., 48 (1954) 1889h.
2 Anal. Research Group, Dept. of Chemical Engineering, Chengtu Institute of Technology, Hua Hsueh Shih Chieh, 13 (1958) 451; through Chem. Abstr., 53 (1959) 5963e.
3 O. E. Lanford and S. J. Kiehl, J. Am. Chem. Soc., 64 (1942) 291.
4 J. A. Cox and K. H. Cheng, Anal. Lett., 7 (10) (1974) 659.
5 L. G. Sillen and A. Martell, Stability Constants of Metal Ion—Complexes, Section II, Special Publication, No. 17, The Chemical Society, London, 1964, p. 375.

Analytica Chimica Acta, 85 (1976) 189—194

Short Communication

SPECTROPHOTOMETRIC DETERMINATION OF MICROGRAM AMOUNTS OF AMINES WITH CHLORANIL

T. S. AL-GHABSHA and S. A. RAHIM

Chemistry Department, University of Mosul, Mosul (Iraq)

A. TOWNSHEND

Chemistry Department, Birmingham University, P.O. Box 363, Birmingham, B15 2TT (England)

(Received 20th February 1976)

The formation of molecular or charge-transfer complexes has been used for the spectrophotometric determination of sulphur dioxide, oxygen, nitrate ions, Vitamin A, etc. [1]. In particular, the compounds formed by primary aromatic amines [2] and amino acids [3] with chloranil can be used for the determination of traces of these species. This communication describes an investigation of the reaction of chloranil with a wide range of amines; sensitive methods for the determination of many of these compounds are proposed.

Experimental

Chloranil was purified by recrystallization from redistilled benzene and was used as a saturated ($1 \cdot 10^{-3}$ M) solution in ethanol.

Investigation of reactions with various amines. Solutions were made up with the amino compounds given in Table 1, as described for the benzylamine calibration solutions below. The amine concentrations used are given in Table 1.

Determination of benzylamine (0—160 μg). For calibration, add 0.0, 0.4, 0.8, 1.2 and 1.6 ml of aqueous 100 p.p.m. benzylamine solution to a series of 25-ml volumetric flasks; add exactly 5 ml of chloranil solution and 2 ml of a pH 9 borate buffer solution ($5 \cdot 10^{-2}$ M sodium borate). Dilute to volume with water, and heat in a water bath at 65 ± 1 °C for 15 min. Measure the absorbance against the blank solution, preferably in a double-beam spectrophotometer, in 1-cm cells at 349 nm. Plot the absorbance vs. benzylamine concentration.

For a determination take an approximately neutral sample ($\leqslant$ 18 ml) through the above procedure. Read the concentration from the calibration graph.

TABLE 1

Effect of development time (t) and temperature on the approximate molar absorptivities (ϵ)
(ϵ values are given as $x \cdot 10^3$ l mol^{-1} cm^{-1})

Compound	Concn.[a] (p.p.m.)	λ_{max} (nm)	28 °C		55 °C		60 °C		65 °C	
			t (min)	x	t (min)	x	t (min)	x	t (min)	x
n-Propylamine	2	348	>5	17	45	17	45	19	20	14
n-Butylamine	2.5	350	5	18	45	18	30	19	15	17
2-Aminobutane	2.5	350	>5	18	30	16	20	17	15	15
1-Amino-2-methylpropane	5	349	>5	13	60	11	30	11	15	10
n-Amylamine	4	350	>5	19	30	18	20	18	20	18
Isoamylamine	5	350	>5	15	30	17	15	18	10	15
Ethanolamine	2	347	4	19	30	15	20	15	15	14
4-Amino-n-butyric acid	6	348	4.5	2	40	18	40	17	35	16
Allylamine	2	348	4.5	17	30	13	20	15	10	16
Benzylamine	3	349	3	23	30	22	30	22	15	23
Ethylenediamine	2	350	1.5	13	20	12	15	12	10	12
Diethylenetriamine	4	350	3	21	45	17	20	13	10	15
Tetraethylenepentamine	4	350	3	25	15	21	15	22	15	20
Benzylmethylamine	20	351	>5	3	90	2	45	2	45	2
Adrenalin	10	354	0.7	7	15	7		D[b]		D[b]
Noradrenalin	20	354	1	2	25	3	15	3	15	3
N,N-diethylethylenediamine	6	350	4	15	30	14	20	13	15	12
Aniline	10	354	2.5	10	60	6	35	5	25	5
o-Tolidine	16	344	>5	8	90	3	60	2	30	2
o-Tolidine	10	354	3	10	60	9	30	7	30	7
p-Anisidine	10	352	0.8	6	10	5	10	6	10	5
p-Chloroaniline	20	354	2.5	9	60	5	35	4	25	4
p-Bromoaniline	12	355	>5	6	60	4	30	3	20	3
m-Aminophenol	20	354	3	5	30	4	15	4	15	3
m-Aminobenzoic acid	20	353	4.5	8	60	4	50	3	35	3
p-Aminobenzoic acid	10	356	6	13	60	4	45	4	30	3

8-Amino-1-napthol	20	354	1.8	3		D[b]		D[b]		D[b]
8-Amino-1-napthol-3,6-disulphonic acid (Na salt)	36	360	1	8	5	10	5	10	2	7
Sulpha-acetamide	40	352	>5	5	60	1.0	45	0.7	30	0.6
Benzidine	10	350	>5	14	30	9	30	8	20	7
Hydroxylammonium chloride	20	345	0.6	D(1[c])[b]		D[b]		D[b]		D[b]
Hydrazinium sulphate	20	350		D(3[c])[b]		D[b]		D[b]		D[b]
Phenylhydrazinium chloride	40	350		D(1[c])[b]		D[b]		D[b]		D[b]
Semicarbazide hydrochloride	40	364	2	1.3	15	0.6	5	0.6	5	0.8
Ammonium fluoride	20	340	3.8	0.2	50	0.2	25	0.1	15	0.2
Ammonium oxalate	20	335	3.8	0.3	35	0.3	20	0.3	15	0.3

[a]In the final solution.
[b]D: continually decreases with time.
[c]Value at time t = 0 min.

Determination of other amines (see Table 3). Use the procedure described for benzylamine, except for the reaction times and wavelengths given in Table 1.

Determination of stability constants. These were estimated by comparing the absorbance of a solution containing stoichiometric amounts of amine and chloranil, to one containing a five-fold excess of chloranil, under the optimal reaction conditions.

Results and discussion

As the reaction of primary aromatic amines [2] and amino acids [3] with chloranil is known to be slow, the effect of time and temperature on the development of the coloured reaction products of a large number of amines and related compounds was investigated. The reactions were carried out at pH 9, which was optimal for benzylamine, and had previously been found to be optimal for amino acids [3]. The results (Table 1) show that the reactions are generally too slow at room temperature to be analytically useful, but that at 60—65 °C, maximal absorbance is usually achieved within 15—30 min.

Table 1 also shows that sensitivities, as measured by the apparent molar absorptivities, are greatest for primary aliphatic amines, and are suitable for the determination of microgram amounts of these compounds. The molar sensitivities of the aromatic amines and the secondary amines studied were 2—7 times less. Most of the compounds gave absorbances which were unchanged on standing overnight at 28 °C, but the stable periods for *p*-anisidine (2.3 h), 8-amino-1-napthol (1.0 h), 8-amino-1-napthol-3,6-disulphonic acid (3.0 h) and the ammonium salts (1.0 h) were rather brief. Hydroxylamine, and hydrazine and its derivatives, also gave unstable colours, of poor sensitivity.

A more detailed examination was made of the most sensitive amine, benzylamine. The rate of formation of the coloured species at various temperatures is described in Table 2, which shows that colour development is fastest, and the maximal absorbance is marginally greatest, at 65 °C; 15 min sufficed to give maximal absorbance at 65 °C, the value remaining constant for a further 35 min. This temperature was used for all further investigations of benzylamine and other amines.

The effects of reagent concentrations were also investigated. The amount of pH 9 buffer solution added was not critical between 1 and 5 ml per 25 ml of final solution, but 2 ml gave marginally the greatest absorbance. The optimal amount of chloranil was found to be 5 ml of $1 \cdot 10^{-3}$ M solution; smaller amounts gave smaller absorbances. The order of addition of reagents was of no consequence. Under these optimal conditions, a linear correlation was obtained between absorbance and benzylamine concentration over the range 5—160 μg in a final volume of 25 ml. On extrapolation to zero concentration, the graph had a slight positive intercept on the absorbance axis.

TABLE 2

Effect of temperature and time on the absorbance at 349 nm of the benzylamine—chloranil system
(0.8 ml of $0.9 \cdot 10^{-3}$ M benzylamine solution and 5 ml of $1 \cdot 10^{-3}$ M chloranil solution diluted to 25 ml at pH 9.)

		Absorbance at								
Temp. (°C)	Time (min)	5	10	15	20	30	40	50	60	180
28		0.06	0.12	0.16	—	0.24	—	0.38	0.41	0.51[a]
55 ± 1		0.24	0.41	0.46	0.47	0.48	0.48	0.48	0.47	
60 ± 1		0.34	0.46	0.49	0.49	0.49	0.49	0.48	0.46	
65 ± 1		0.37	0.50	0.51	0.51	0.51	0.51	0.51	0.48	

[a]The absorbance then became 0.50 after 360 min, and remained constant for at least another 10 h.

The slope of the graph decreased above 160 μg of benzylamine. The relative standard deviation for the determination of 154 μg of benzylamine was 1.7 %. The composition of the benzylamine—chloranil compound was established by the methods of continuous variations, mole ratio and slope ratio, to be 1:1. Its stability constant was $4 \cdot 10^4$ l mol^{-1}, and its molar absorptivity was $2.0 \cdot 10^4$ l mol^{-1} cm^{-1}.

Some other amines were also investigated; these are listed in Table 3. All gave linear calibration plots over the ranges given in Table 3, when the procedure recommended for benzylamine was used, but at the wavelengths and reaction times at 65 °C given for the particular amine in Table 1. Precisions were similar to those for benzylamine. The compositions of the coloured compounds and their stability constants were determined as for benzylamine. These are also given in Table 3. Because each amine gives a product with a different molar absorptivity, a separate calibration graph is necessary for each amine. The accuracy of determination of the amines was better than ±2 % over the ranges given in Table 3.

The greater molar absorptivities of the primary aliphatic amine complexes than those of the aromatic amines parallels the greater basicity of the aliphatic compounds; this indicates that the molar absorptivity increases with increasing ability of the nitrogen atom to donate its lone pair of electrons. The stability constants of the complexes, however, are greater for the less basic, aromatic amines, which may indicate that the formation of a stronger bond between amine and chloranil decreases the possibility of excited state n—π charge transfer. The slow formation of the complexes and their relatively high stability are unusual for molecular complexes, and may indicate another mechanism of chromophore formation. Tashima et al. [2] assume that the colour is due to Schiff's base formation. It could be, therefore, that the rapid, initial colour development is charge-transfer complex

TABLE 3

Composition, stability constants, molar absorptivities and working range for some amine—chlorinal complexes

Amine	Amine: chloranil ratio	Stability constant ($l\ mol^{-1}$ or $l^2\ mol^{-2}$)	ϵ ($l\ mol^{-1}\ cm^{-1}$)[a]	Working range (μg)
Benzylamine	1:1	$4 \cdot 10^4$	20,000	5—160
Allylamine	1:1	$2 \cdot 10^4$	14,300	10—110
2-Aminobutane	1:1	$1 \cdot 10^4$	10,600	10—110
Diethylenetriamine	1:2	$2 \cdot 10^9$	19,000	5—150
Ethylenediamine	1:2	$3 \cdot 10^9$	14,100	10—110
p-Tolidine	1:1	$4 \cdot 10^5$	8,300	20—200
p-Chloroaniline	1:1	$3 \cdot 10^5$	3,250	100—1000
p-Aminobenzoic acid	1:1	$1 \cdot 10^5$	800	400—3200

[a]Calculated from the calibration graphs.

formation followed by slow conversion to the Schiff's base. In this respect, it is interesting that diethylenetriamine and ethylenediamine form complexes with two molecules of chloranil, indicating reaction with their two primary amino groups. However, it should be noted that secondary amines give coloured products with molar absorptivities as great as those of the aromatic amines; these compounds cannot be Schiff's bases. It is possible, therefore, that molecular complex formation occurs, but perhaps with a reaction product of chloranil [3].

Few interferences would be expected. Amino acids would give responses similar to the amines, and proteins also give sensitive responses [3]. Other nitrogen compounds, such as urea, do not give a complex, and ammonia forms only a slightly absorbing species.

REFERENCES

1 A. Townshend, Proc. Soc. Anal. Chem., 10 (1973) 39; 13 (1976) 64, and refs. therein.
2 Y. Tashima, H. Hasegawa, H. Yuki and K. Takiura, Jpn. Analyst, 19 (1970) 43.
3 F. Al-Sulimany and A. Townshend, Anal. Chim. Acta, 66 (1973) 195.

Analytica Chimica Acta, 85 (1976) 195—198

Short Communication

DETERMINATION OF ALUMINIUM IN BIOLOGICAL TISSUE BY FLAMELESS ATOMIC ABSORPTION SPECTROMETRY

J. R. McDERMOTT and I. WHITEHILL

MRC Demyelinating Diseases Unit, Newcastle General Hospital, Westgate Road, Newcastle-upon-Tyne NE4 6BE (England)

(Received 5th March 1976)

There has been renewed interest in the rôle of aluminium in the pathology of the human central nervous system since elevated aluminium concentrations were found in various areas of the brains of patients suffering from Alzheimer's presenile dementia [1]. A major pathological feature of presenile and also senile dementia is the widespread neurofibrillary degeneration [2] which takes the form of proliferating tangles located in the cytoplasm of neurons [3]. Injection of aluminium salts into the cerebrospinal fluid (CSF) of certain animals also induces neurofibrillary degeneration [4], although of a form morphologically distinct from that seen in human brains. The rôle of aluminium is not known; thus the elucidation of the cellular and subcellular localization of aluminium in experimental models and in human demented brain is obviously important. Since the availability of some tissue fractions is limited, a sensitive analytical method for aluminium is needed.

Flame atomic absorption spectrometry has been used to analyze human and animal brain for aluminium [5]. This paper reports the use of the more sensitive heated graphite atomizer for the determination of aluminium in rabbit and human tissues; sample preparation by dry ashing was preferable to an acid digestion method.

Experimental

Apparatus. A Perkin-Elmer HGA74 graphite tube furnace and model 360 atomic absorption spectrometer were used. The signal was recorded on a Servoscribe RE511 recorder (20-mV full-scale deflection). Expansion of the signal was obtained with the concentration mode of the spectrometer. The aluminium hollow-cathode lamp was operated at 10 mA; measurements were made at 309.3 nm; the slit-width was 0.7 nm. The atomizer was purged with argon (Air Products, ultrapure) during operation.

PTFE crucibles and test tubes (Xlon Products Ltd., London) were used. All apparatus was washed thoroughly in 10 % nitric acid, followed by water.

Reagents. Concentrated acids (Aristar), water (AnalaR) and aluminium nitrate standard solution (1 mg Al ml^{-1}) were obtained from BDH.

Biological material. Human brain was obtained post mortem from local hospitals. Brain, liver, kidney and muscle were removed from New Zealand white rabbit (age 6 months) under conditions designed to exclude contamination by dust.

Procedure for dry ashing. Weigh 0.5—1 g of wet tissue into a 10-ml vitreosil crucible, fitted with a lid; dry at 60—80 °C under vacuum. Ash the sample in an electric furnace at 2—300 °C with the muffle open for 18 h, and at 600 °C for 30 h with muffle closed. The crucibles are covered throughout to prevent dust contamination. Take up the ash in 1 ml of water and 0.1 ml of nitric acid at room temperature.

Procedure for wet ashing. Weigh 0.5—1 g of wet tissue into a PTFE test tube and dry as above. Cautiously add nitric and perchloric acids (each 2 ml g^{-1}) and warm the tubes gently in an oil bath; when frothing creases, raise the temperature to 170—180 °C. Evaporate the clear solution obtained after 24 h to dryness in a PTFE crucible on a hot plate at 180 °C. Dissolve the pale yellow residue in water (2 ml).

Determination. Place the sample (25 μl) in the furnace. The heating programme is: drying at 102 °C for 30 s; charring at 1300 °C for 25 s; atomization at 2660 °C for 30 s. Operate the spectrometer in the "miniflow" mode (gas flow reduced for 8 s during atomization), but the gas flow is not reduced during atomization for some samples. Dilute samples containing more than 0.8 μg Al ml^{-1}.

Results and discussion

The characteristics of the instrument were determined with standard aluminium nitrate solutions. Ten consecutive aliquots gave relative standard deviations of 1.3 % (for 10 ng Al) and 3.6 % (for 2.5 ng Al). The sensitivity (i.e. for 0.044 absorbance units) was 0.07 ng (miniflow) or 0.028 ng (gas-stop); a signal-to-noise ratio of 2:1 was obtained with 0.025 ng (gas-stop). Because of the high instrumental precision, the mean value from three aliquots of each sample was taken. The spectrometer gave a linear response up to 20 ng Al with full gas flow during atomization, and up to 10 ng in the miniflow mode (see Fig. 1). The 9 % nitric acid used to dissolve the dry-ashed samples increased the response obtained with 10 ng of aluminium standard by 15 % when full gas flow was used; under miniflow conditions, the signal was decreased by 5 %. The recovery of aluminium from the wet and dry ashing procedures was checked by adding aluminium nitrate and aluminium hydroxide standards to 0.25 g of a preparation of freeze-dried homogenized

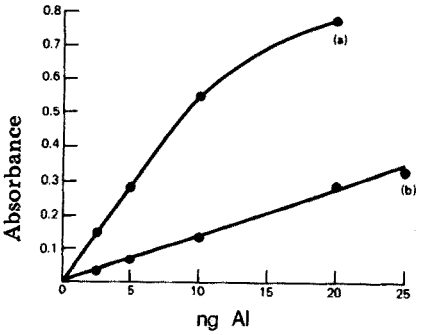

Fig. 1. Absorption signal obtained with standard amounts of aluminium: (a) gas flow interrupted for 8 s during atomization (b) uninterrupted gas flow.

rabbit liver of known aluminium content. Recoveries of 92—102 % were obtained for aluminium additions of 0.1—0.8 μg (nitrate) and up to 300 μg (hydroxide).

The digestion procedure of Krishnan et al. [5] (H_2SO_4, $HClO_4$ and HNO_3 in pyrex glassware at 160 °C) gave high blank values to which the high aluminium content of Aristar sulphuric acid and the glass apparatus contributed. However, PTFE apparatus offers a good alternative. With the omission of sulphuric acid, tissue could still be digested satisfactorily if the acids were not evaporated too rapidly; only the lower part of the tube should dip into the oil bath with the upper half acting as a condenser. Blank values between 0.05 and 0.10 μg Al per determination were obtained. The aluminium contents found for tissue samples are shown in Table 1.

The blank values from dry ashing were consistently lower than those obtained with the wet ashing method. The nitric acid used to dissolve the ash contained 0.011 μg Al ml^{-1} and blanks of 0.01—0.05 μg Al per determination were obtained. Airborne contamination can be the main source of aluminium in blank determinations, and care must be taken to exclude it. The results obtained with the dry ashing method (Table 1) do not differ significantly from those obtained by wet ashing. The results obtained for human brain compare well with those reported previously. The mean aluminium concentration (± standard deviation) of 25 human brain samples is 1.3 (±0.8) $\mu g\ g^{-1}$ of dried tissue. Tipton et al. (see ref. 6) report a value of 1.25 $\mu g\ g^{-1}$ (dry weight) for samples from normal human brains, while Crapper et al. found a mean value of 1.1 $\mu g\ g^{-1}$ with a range of 0.23—2.7 $\mu g\ g^{-1}$ (both dry weight) in two normal brains [1].

The dry ashing method was chosen for future work because of the lower background and ease of operation. The above results were obtained with 0.5—1 g samples. The wet weight of brain samples can be reduced to 50 mg and satisfactory analyses still obtained. The ash, taken up in 0.1 ml of 9 % nitric acid, is sufficient for three determinations. Platinum crucibles are preferable; there is a slight contribution to the blank value from vitreosil.

TABLE 1

Aluminium content of rabbit and human tissues

Tissue	μg Al/g wet tissue (± s.d.)[a]	
	Wet ash	Dry ash
Rabbit liver	0.32 ± 0.02 (4)	0.41 ± 0.06 (5)
Rabbit kidney	0.28 ± 0.08 (4)	0.36 ± 0.08 (5)
Rabbit cortex	0.44 ± 0.08 (4)	0.66 ± 0.50 (9)
Rabbit muscle	—	0.56 ± 0.10 (6)
Human grey matter (frontal cortex)	—	0.37 ± 0.22 (15)
Human white matter (corpus callosum)	—	0.34 ± 0.22 (12)

[a]Number of samples analysed is shown in parentheses.

Further reduction in sample size would require a lower concentration of aluminium in the reagents; this has not yet been explored.

Inhibition of atomic absorption signals can be caused by ions formed from the biological matrix. The standard method of additions was used to investigate this point. Known amounts of aluminium were added to the ash from 1 g of rabbit liver, and grey and white matter from human brain. The results showed that absorption is affected only slightly by the matrix. The aluminium absorption signal was essentially linear for serial dilutions (down to 1/16) of solutions of liver and brain ashes.

Aluminium can therefore be determined in small samples of brain, liver, kidney and muscle by a dry ashing technique; this method should be applicable to the determination of aluminium in other biological tissues.

REFERENCES

1 D. R. Crapper, S. S. Krishnan and A. J. Dalton, Science, 180 (1973) 511.
2 R. D. Terry, N. K. Gonatas and M. A. Weiss, Am. J. Pathol., 44 (1964) 269.
3 H. M. Wisniewski, R. D. Terry and A. Hirano, J. Neuropathol. Exp. Neurol., 29 (1970) 163.
4 I. Klatzo, H. M. Wisniewski and E. Streicher, J. Neuropathol. Exp. Neurol., 23 (1965) 187.
5 S. S. Krishnan, K. A. Gillespie and D. R. Crapper, Anal. Chem., 44 (1972) 1469.
6 D. R. Crapper, in P. Seeman and G. M. Brown (Eds.), Frontiers in Neurology and Neurosciences Research, University of Toronto Press, 1974, p. 97.

Analytica Chimica Acta, 85 (1976) 199—202

Short Communication

DETERMINATION OF CADMIUM IN A SULFIDE ORE AND ITS BENEFICIATION PRODUCTS BY EPITHERMAL NEUTRON ACTIVATION ANALYSIS

E. STEINNES

Institutt for Atomenergi, Isotope Laboratories, 2007 Kjeller (Norway)

(Received 4th February 1976)

Instrumental neutron activation analysis with Ge(Li) solid-state detectors has been frequently used in recent years for the determination of minor and trace elements in a wide variety of geological materials, but there have been few applications to sulfide ores [1, 2]. This may be associated partly with the fact that certain major elements in the ore give rise to high radioactivity (^{64}Cu, ^{65}Zn, etc.) which tends to overshadow the contribution from other elements in the γ-spectra.

In previous work from this laboratory [2] on trace element determinations in a sulfide ore and some beneficiation products, the feasibility of instrumental activation analysis with epithermal neutrons was discussed, and it was concluded that this technique might be advantageous compared to the ordinary version, which involves irradiation with the entire reactor neutron spectrum, for the elements As, Sb, Se, Ag, and Au. Another element for which available neutron cross-section data would indicate the advantage of epithermal activation, is cadmium. Cohen [3] used this technique for cadmium and indium in zinc blendes, employing the 49-min ^{111m}Cd isotope for the determination of cadmium in the 0.1—0.5 % range. When lower concentrations are involved, better results might be expected from the 53.5-h ^{115}Cd isotope. In a well thermalized neutron flux the sensitivity for cadmium with this isotope is rather poor, because of the low thermal neutron cross-section (0.30 b) and isotopic abundance (28.9 %) involved. If the neutron flux has an appreciable epithermal component, the situation is significantly improved, because the I/σ_0 ratio of ^{114}Cd is much higher than that of some of the isotopes which give rise to major activities in ore samples. A further relative improvement would be expected by using irradiation in a cadmium cover, which eliminates the thermal component of the neutron spectrum.

In the case of cadmium determinations in a pyritic lead—zinc ore and some of its beneficiation products by instrumental activation analysis, irradiation with the entire neutron spectrum did not yield adequate sensitivity, and a procedure based on epi-cadmium irradiation was introduced.

In order to assess the accuracy of that method, the same samples were also analyzed by a radiochemical activation method after an ordinary reactor irradiation.

Experimental

Samples of about 100 mg were wrapped in 30 × 30-mm sheets of aluminium foil for irradiation. Standards were prepared by evaporating 100-μl aliquots of 100-p.p.m. Cd solution on the same sort of aluminium sheets, and folding. The irradiations were carried out for 20 h in the JEEP-II reactor (Kjeller, Norway) in a position where the thermal neutron flux was about $1.5 \cdot 10^{13}$ n cm^{-2} s^{-1} and the cadmium ratio of ^{197}Au was 2.9. For the epithermal irradiation, a 1-mm thick cylindrical cadmium box (14 mm internal diameter and 10 mm internal height) was used. In order to avoid transfer of cadmium activity from the internal surface of the box to the samples, they were wrapped in an extra aluminium foil. Furthermore, the rock powder was removed from the foil wrappings before counting.

Activity was measured with a Ge(Li) detector connected to a multichannel analyzer. The resolution of the detector was 2.5 keV (FWHM) for the 1332-keV peak of ^{60}Co. Measurements were carried out for 20 min, and the total count rate was kept below 10^4 cps. Samples subjected to epithermal activation were measured 7 d after the end of the irradiation.

Samples irradiated with thermal neutrons, after 7 d of delay for the decay of ^{64}Cu and ^{24}Na, were treated by the following radiochemical procedure. The sample was transferred to a teflon beaker containing 10 ml of concentrated hydrofluoric acid and 2 mg of Cd carrier. The mixture was evaporated to dryness on a hot plate. Then 5 ml of concentrated hydrochloric acid and 5 ml of concentrated nitric acid were added, and the mixture was again evaporated to dryness. The residue was dissolved in 30 ml of 2 M HCl and subsequently fed to an anion-exchange column (Dowex 1-X8, 100—200 mesh, chloride form, 8-cm high resin bed, pre-equilibrated with 1M HCl). The column was washed with three 10-ml portions of 1 M HCl to remove ^{59}Fe, and cadmium was eluted with three 10-ml portions of 1 M ammonium nitrate. The combined eluate was collected in a 100-ml polyethylene screw-cap bottle. The activity measurement was postponed for 24 h to facilitate establishment of the equilibrium ^{115}Cd—^{115m} In. The chemical yield for cadmium was higher than 98 %, as shown by radiotracer experiments.

Results and discussion

Results of application of the two methods to a pyritic lead—zinc ore and its beneficiation products are given in Table 1; duplicate determinations were performed. The good agreement between the two sets of data indicates that the epithermal activation procedure is not associated with appreciable systematic error, except for possible errors affecting both methods to a

TABLE 1

Determination of cadmium in a sulfide ore and its beneficiation products (p.p.m.)

Sample	Instrumental activation analysis with epithermal neutrons	Method based on radiochemical separation
Crude ore	55	52.9
	55	50.8
Cu concentrate	170	169.1
	180	167.6
Zn concentrate	1990	1860
	2010	2030
Pyrite concentrate	5.0	5.5
	4.0	5.7
Pyrite tailings	3.3	3.8
	3.2	3.7

similar degree. The detection limit for the epithermal method is of the order of 1—2 p.p.m. for the samples concerned, except for the copper and zinc concentrates, where the detection limit depends on the Zn/Cd ratios.

The radiochemical method used for the thermal neutron-irradiated samples does not separate zinc and cadmium. At the Zn/Cd ratios involved in this work (about 250) the presence of ^{65}Zn activity did not interfere significantly in the activity measurements.

The 336.2-keV peak of ^{115m}In was preferred to the 527.9-keV peak of ^{115}Cd for quantitative measurements, because of a three-fold higher count-rate. The Compton-contribution from higher-energy γ-emitters was similar for both energies, except in the case of the pyrite concentrate where bremsstrahlung from fast neutron-induced ^{32}P from sulfur contributed to a somewhat higher base level for the ^{115m}In peak. Several γ-lines might be expected to interfere with the measurement of ^{115m}In in the epithermal method. No such interferences were found to be significant, however, except in the case of the pyrite concentrate, where the contribution from the 334.7-keV peak of ^{59}Fe had to be corrected for by means of the 1099-keV peak. Possible interference from ^{239}Np (334.4 keV) or ^{233}Pa (340.5 keV) may be corrected for by means of more prominent peaks of these nuclides.

Thermal neutron shielding effects were estimated to be insignificant in the samples investigated. Concerning the possibility of resonance neutron shielding in the samples, ^{114}Cd has its major resonance at an energy of 120 eV [4]. As none of the major elements in the samples show appreciable neutron absorption in that energy range, this source of error seems to be excluded.

In an irradiation position with an R_{Cd}^{Au} value of 2.9, the cadmium ratio of ^{114}Cd with respect to the production of 53.5-h ^{115}Cd is calculated [5] to be 1.45 on the basis of recommended cross-section data [6, 7]. However, the actual cadmium ratio observed in the present work was 6.0, indicating an I/σ_0 ratio of 6.0 rather than the value of 67 calculated from the recommended

cross-section values. Van der Linden et al. [8], using 1.0 mm Cd, found an I/σ_0 value of 11.4 for the production of ^{115}Cd. The apparently confusing values may indicate that a very considerable absorption of neutrons in the energy region about 120 eV takes place in the cadmium cover surrounding the samples. The effective flux of resonance neutrons would then depend critically on the size and configuration of the cadmium container. The apparent shielding effect in the cover, should, however, not introduce systematic error provided that each sample or standard inside the cover receives the same transmitted flux. The good agreement between the radiochemical and epithermal activation values indicates that this was the case in the present work.

Although a substantially lower epithermal activation of ^{114}Cd was obtained than initially expected, the sensitivity compared with that obtained in the same position without a cadmium cover is still considerable. The following "advantage factors" were calculated for ^{115}Cd relative to some major interfering nuclides: ^{24}Na, 9.4; ^{64}Cu, 4.8; ^{65}Zn, 3.0; ^{59}Fe, 5.0; ^{60}Co, 2.6; ^{46}Sc, 11.9. Compared with irradiation in a well thermalized flux, the advantage factors would be about 3 times higher, if the recommended value [7] of 20 for the infinite dilution resonance integral of the reaction ^{114}Cd (n,γ) ^{115g}Cd is correct. Thus the use of epi-cadmium irradiation for the determination of cadmium in sulfide ores by instrumental activation analysis is likely to give an improved sensitivity of a factor of 10 or more compared with thermal neutron irradiation. If the above interpretation of the unexpectedly high cadmium ratio of ^{114}Cd observed in the present work is valid, it may be assumed that the use of a thinner cadmium cover might bring a considerable further improvement.

REFERENCES

1 J. F. Lamb, S. G. Prussin, J. A. Harris and J. M. Hollander, Anal. Chem., 38 (1966) 813.
2 E. Steinnes and A. D. Mukherjee, J. Radioanal. Chem., 14 (1973) 129.
3 I. M. Cohen, Radiochem. Radioanal. Lett., 15 (1973) 379.
4 M. D. Goldberg, S. F. Mughabghab, S. N. Purohit, B. A. Magurno and V. M. May, USAEC Report BNL-325, 2nd edn., Suppl. 2 (1966).
5 E. Steinnes, in A. O. Brunfelt and E. Steinnes (Eds.), Activation Analysis in Geochemistry and Cosmochemistry, Universitetsforlaget, Oslo, 1971, pp. 113—128.
6 R. Sher, Handbook on Nuclear Activation Cross-Sections, IAEA Technical Report No. 156 (1974) pp. 1—14.
7 H. Albinsson, Handbook in Nuclear Activation Cross-Sections, IAEA Technical Report No. 156 (1974) pp. 15—86.
8 R. van der Linden, F. de Corte and J. Hoste, J. Radioanal. Chem., 20 (1974) 695.

Analytica Chimica Acta, 85 (1976) 203—208

Short Communication

A RAPID METHOD FOR THE DETERMINATION OF METHYLMERCURY CHLORIDE IN WATER SAMPLES BY GAS CHROMATOGRAPHY WITH A MICROWAVE EMISSION SPECTROMETRIC DETECTOR

YAIR TALMI** and V.E. NORVELL*

Analytical Chemistry Division, Oak Ridge National Laboratory, Oak Ridge, Tennessee 37830 (U.S.A.)

(Received 1st December 1975)

In the past three years, the gas chromatography—microwave emission spectrometric detector system (g.c.—m.e.s.) has been routinely applied to the determination of methylmercury(II) chloride in various environmental samples [1]. This m.e.s. detector is almost equally sensitive, 0.0005—0.002 ng, and selective (selectivity greater than 10,000) for all volatile mercury compounds, regardless of their molecular structure. These exceptional features of the detector greatly simplify the analytical procedures required for the determination of traces of methylmercury(II) chloride in complex matrices such as biological tissues and sediment samples. The relative sensitivities obtained for methylmercury(II) chloride (on a routine basis) have been better than 10 ng g^{-1} for solid samples (50—500 mg) and 100 ng l^{-1} for water samples.

Recent studies by Moore [2, 3] have demonstrated the excellent extractability of inorganic anionic complexes of mercury, from alkaline as well as acidic solutions, with quaternary amines (approximate m.w. 400) dissolved in various organic solvents. Another study [4] has shown that methylmercury(II) chloride and phenylmercury(II) acetate can also be efficiently extracted with quaternary amines dissolved in simple solvents. In the work described here, it was found that tertiary amines are preferable as extractants of methylmercury(II) chloride. With 0.5 % solutions of tertiary amine in benzene, a quantitative (95 ± 3 %) extraction of methylmercury(II) chloride (as a CH_3HgCl—amine complex) can be achieved for aqueous solvent volume ratios as high as 400. After the extraction, aliquots (1—10 μl) of the benzene layer are injected into the g.c. column. In the injection port, which is held at 200 °C, the CH_3HgCl—amine complex is instantly cleaved to release the volatile methylmercury(II) chloride which is then separated by the g.c. column in exactly the same manner as the pure methylmercury(II) chloride. When this technique is used, traces of methylmercury chloride as low as 1 ng l^{-1} can be determined in various water samples with an accuracy and

*Current Address: Department of Chemistry, University of Tennessee, Knoxville, Tennessee 37916.

**Current Address: Princeton Applied Research Corp., P.O. Box 2565, Princeton, N.J.08540

precision of 10—15 %. The excellent sensitivity and relative simplicity of this technique should be of interest to environmentalists concerned with the mechanisms of alkylmercury accumulation in various biological systems.

The general principle of the method, which is based on the interaction of a volatile analyte to form a non-volatile extractable complex, followed by the release of the analyte in the injection port, may be applicable to other analytical problems.

Experimental

Apparatus. The g.c.—m.e.s. system used has been described previously [1, 5]. Methylmercury(II) chloride, eluted into a low-power microwave argon plasma, is fragmented and its concentration is determined by measuring the atomic emission intensity produced by the excited mercury atoms at 253.7 nm. The instrumental conditions are listed in Table 1.

Reagents and solutions. Alamine 336-S (a mixture of tri-n-octyl- and decyl-amines; General Mills, Inc., Kankakee, Ill.) and Adogen 464 (methyltri [C_8—C_{10}] ammonium chloride; Archer Daniels Midland Co., Minneapolis, Minn.) were used. Benzene solutions (0.5 % v/v) of each amine were prepared in A.R.-grade benzene. Methylmercury(II) chloride (Alfa Inorganics) was dissolved in doubly distilled water or A.R.-grade benzene to prepare stock and standard solutions.

Synthetic sea water was made by dissolving A.R.-grade NaCl(42 g), K_2SO_4(1.6 g), $MgCl_2 \cdot 6\,H_2O$(14.4 g) and $CaSO_4 \cdot 2\,H_2O$(2 g) in 4 l of distilled water. Spring water, obtained from a nearby natural spring, was filtered through a Millipore filter (0.45-μm pore diameter) before analysis.

Extraction procedure. Water samples spiked with CH_3HgCl in the range 2.5 pg ml^{-1} to 1.25 ng ml^{-1} were prepared. The pH was adjusted to 9 for sea water and 6.5—7.5 for spring water. The CH_3HgCl was extracted with 5 ml of 0.5 % amine solution in benzene. The extractions (after pH adjustment) were done at aqueous/solvent volume ratios of 10:1, 50:1, 100:1, 200:1 and 400:1 in 100, 250, 500, 1000 and 2000-ml separatory funnels, respectively. Each funnel was shaken vigorously for 5—10 min, either by hand or by a Burrell wrist-action shaker. After phase separation (10—20 min) each organic layer was collected and transferred to a 3-ml bottle capped with a Teflon-coated rubber diaphragm. Aliquots (1—10 μl) of these extracts were injected into the g.c. column. The peak heights obtained from the injected samples were compared to those obtained from standard solutions of CH_3HgCl in benzene.

TABLE 1

G.c.—m.e.s. operating conditions

Pyrex column	3 ft. long, 5 mm i.d., 6.5 mm o.d.
Column packing	6 % FFAP on 80/100 mesh Gas Chrom Q
Quartz capillary	12 in. long, 0.5 mm i.d., 6.5 mm o.d.
Carrier gas	Argon; plasma operated at 5—10 torr.
Flow rate	130—150 ml min^{-1}
Column temperature	180—190 °C
Injector temperature	200°C
Capillary heater	220°C
Microwave generator output	18 W
Monochromator	Jarrell-Ash 0.5-m Ebert mounting scanning monochromator with 1180 grooves mm^{-1}; grating blazed at 190 nm. slit 8—10 mm high, 50 μm wide
Wavelength	253.65 nm
Photomultiplier tube	1P28
Optics	Lens focal length, 100 mm; diameter, 50 mm. Plasma image focussed on entrance slit

Results and discussion

The effect of pH and salt on the extraction efficiency. Various studies [6] concerning the extraction of methylmercury(II) salts (Cl^-, Br^-, I^-, OH^-, etc.) have demonstrated the suitability of benzene, toluene, chloroform, carbon tetrachloride and a few other solvents as extractants. The bromide and iodide forms of CH_3HgX are more efficiently extracted than the chloride form [7, 8]. Nevertheless, extraction with these pure solvents is not very satisfactory because efficiencies are usually 80—85 % at best, and aqueous/solvent volume ratios are practically limited to 10—20. Moore has recently shown [4] that 0.1 M Aliquat 336-S (a quaternary amine hydrochloride) in diethylbenzene is a better extractant than the pure solvent, for CH_3HgCl. When 0.5 % Adogen 464 in benzene was examined for extraction of 10—50 ng ml^{-1} of methylmercury chloride at aqueous/solvent volume ratios of 1—5, 88 % was extracted, compared to 65 % for the pure solvent; but with 0.5 ng ml^{-1} at aqueous/solvent ratios of 100, percentage extraction was only 25 %, whether or not the amine was present. When a 5 % Adogen 464 solution was used, 99.5 % extraction of 5 ng ml^{-1} CH_3HgCl at volume ratio 10 was achieved. Unfortunately, the requirement for a relatively high concentration of amine (0.1 M or 5 %) was prohibitive in the g.c.—m.e.s. work because of the introduction of excessive amounts of organic matter into the microwave plasma (see below). The extraction efficiency of CH_3HgCl with quaternary amines was virtually unaffected by pH in the range 1—7. Above pH 9, however, it was drastically reduced.

In clear contrast to the quaternary amines, the tertiary amine Alamine 336-S in benzene solutions is a very effective extractant, even at relatively low concentration levels. Thus, with 0.5 % Alamine 336-S in benzene,

quantitative extractions were achieved (at neutral pH) even at aqueous/solvent volume ratio of 200:1 (Fig. 1). In fact, the highest usable volume ratio was not limited by the extraction efficiency but rather by incomplete phase separation. Recovery was significantly reduced at low pH values, and above pH 9 recovery dropped gradually with increase in phase ratio; sodium chloride (1 %) in the water caused a very similar effect (Fig. 1). Because of this salt effect, the extraction of CH_3HgCl from sea water was not as complete and was less reproducible than from fresh water. At neutral pH, low and erratic percentage extraction (10—60 %) was obtained (with 0.5 % Alamine 336-S in benzene), and at lower pH levels recoveries were even worse. Above pH 9, recovery was essentially quantitative even at a volume ratio of 200:1 although the reproducibility was inferior (r.s.d. ±15 %) compared to fresh water. At pH 11, magnesium hydroxide precipitated, which rendered phase separation difficult, although it did not affect the extraction recovery. These experiments indicate that CH_3HgCl reacts with R_3N to form adduct products such as $R_3N \cdot CH_3HgCl$ rather than the $R_4N^+(CH_3HgCl_2)^-$ type of product formed with quaternary amines [4].

G.c. considerations. Once injected into the g.c. column, the CH_3HgCl is instantly released from its tertiary or quaternary adduct. The retention times obtained for pure CH_3HgCl and CH_3HgCl—amine samples were identical, indicating that the release time was negligible compared to the retention time.

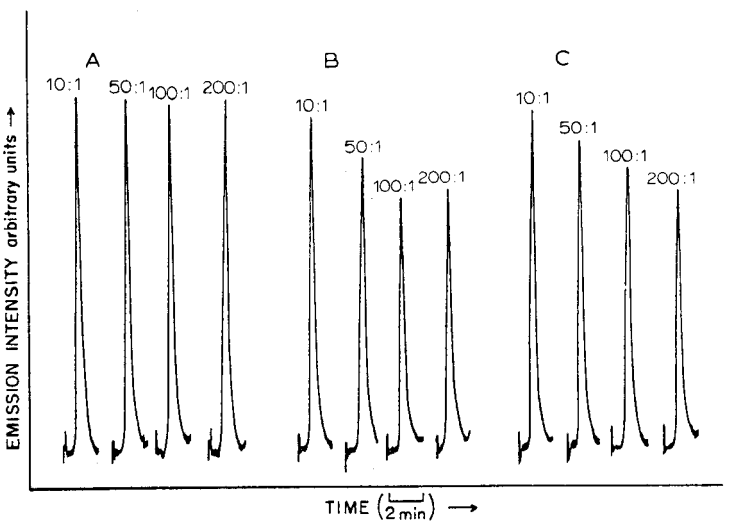

Fig. 1. The effect of volume ratios, pH, and chloride on the extraction of CH_3HgCl. (A) pH 6.6. (B) pH 6.6, 1 % NaCl. (C) pH 9 (NaOH). The numbers on the peaks indicate the volume ratios.

Quaternary amine hydrochlorides were not eluted from the column and slowly accumulated near the injection port. Alamine injections produced four chromatographic peaks corresponding to the four amines which make up Alamine 336-S (Fig. 2). In both cases, the separation performance of the column slowly deteriorated. Nevertheless, the column could be totally rejuvenated by simply repacking its upper portion (inlet) every 200—500 injections.

Spectroscopic consideration. The amount of amines eluted into the plasma, with each injection, is 10^4—10^5 times larger than that of the CH_3HgCl. Since the selectivity of the m.e.s. to mercury is about 10^4 [1], it is not surprising that the emission signals (molecular and continuum) of these amines were observed (Fig. 2). However, because the amine peaks were well separated from the CH_3HgCl peak, their spectral interference was negligible. Even so, complete elution of the amines (15—25 min) was necessary before a second sample could be injected, to avoid deposition of carbonaceous material on the quartz capillary. To shorten the delay between consecutive injections, the plasma was operated under reduced pressure (5—10 torr) instead of atmospheric pressure. At reduced pressures, the low power plasma tolerated larger amounts of organic matter, because of its increased capability for fragmentation and atomization; the coating of the inner capillary walls with solid deposits was thus eliminated and the selectivity

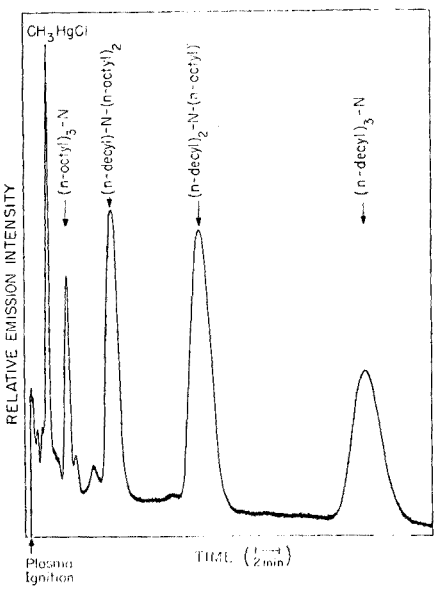

Fig. 2. A chromatogram of CH_3HgCl (5 μl) in 1 % Alamine—benzene solution.(Plasma operating at atmospheric pressure.)

of the detector to mercury further increased. In fact, the emission intensity from the amines became low enough to allow sample injections every 200 s with minimal spectral interferences.

Sensitivity. When properly optimized and handled, the g.c.—m.e.s. method is capable of detecting less than $5 \cdot 10^{-13}$ g CH_3HgCl. When the system is (routinely) applied to "real" analytical problems, a more realistic detection limit is $4—10 \cdot 10^{-12}$ g. Since 10-μl injections are easily tolerated and since a preconcentration factor of 400 can be achieved, the relative sensitivity for CH_3HgCl in water samples is 1—2.5 ng l^{-1}. The relative standard deviation (at 10 ng l^{-1}) is approximately ±10 % for fresh water and ±15 % for "sea water" samples.

REFERENCES

1 Y. Talmi, Anal. Chim. Acta, 74 (1975) 107.
2 F. L. Moore, Environ. Sci. Technol., 6 (1972) 525.
3 F. L. Moore, Sep. Sci., 7 (1972) 505.
4 F. L. Moore, Environ. Lett., in press.
5 Y. Talmi and A. W. Andren, Anal. Chem., 46 (1974) 2122.
6 P. A. Krenkel, Crit. Rev. Environ. Control, CRC, 3 (1973) 303.
7 R. B. Simpson, J. Amer. Chem. Soc., 83 (1961) 4711.
8 J. A. Ealy, M.Sc. Dissertation, University of Tennessee, Knoxville, 1971.

Analytica Chimica Acta, 85 (1976) 209—211

Short Communication

COMPLEXIMETRIC DETERMINATION OF ANTIMONY(III)

KIYOAKI KUWADA and AKIRA OUCHI
College of General Education, University of Tokyo, Meguro, Tokyo 153 (Japan)
TOSHIO TAKEUCHI
Faculty of Science, and Engineering, Sophia University, Chiyoda, Tokyo 102 (Japan)
(Received 16th January 1976)

Titrations with potassium bromate or iodimetry are commonly used for the determination of antimony(III) [1]. Bromate titrations do not give correct values when reducing agents such as ethanol, acetone, etc., or arsenite are present in the sample. For iodimetry, it is not easy to oxidize Sb(III) to Sb(V) quantitatively. Titrations of antimony with ethylenedinitrilotetraacetic acid (EDTA) have been reported [2, 3], but these methods are not easy to apply, as the conditions seem to be rather critical and the end-points are not always clear. Although the formation constant of the Sb—EDTA complex is about 24.8 [4], which is apparently much higher than the values for the zinc(II) or copper(II) complexes [5], this value pertains only to acidic media. The chelate is stable between pH 2 and 3; below pH 2, it decomposes, and above pH 3, antimony(III) is hydrolyzed. Moreover, the chelate formation is slow at low temperature. In the present communication the use of trans-cyclohexanedinitrilotetraacetic acid (CyDTA) is proposed in place of EDTA. A more stable chelate is formed, and the excess of CyDTA can be back-titrated with lead acetate or nitrate solution at about pH 4.3, and 0 °C.

Experimental

Standard CyDTA solution. Dissolve 0.05 mol of the free acid (Dotite GR-grade) and 0.11 mol of sodium hydroxide in water, and dilute to 500 ml. Standardize against a standard solution of copper sulfate or zinc chloride (pure zinc in hydrochloric acid), using xylenol orange (Dotite XO; Dojindo Laboratories) or eriochrome black T indicator, respectively.

Antimony trichloride solution. Dissolve antimony trichloride (EP grade, Wako Pure Chemicals) in acetone. This solution was stable for over a month. Standardize with potassium bromate standard solution, after mixing with an equal volume of 1 M sodium hydroxide, evaporating on a water bath, and taking up the residue in 6 M hydrochloric acid. Solutions in 6 M hydrochloric acid were unstable.

Standard lead solution (0.05 M). Dissolve lead acetate (GR grade, Wako Pure Chemicals) in 1 l of 0.01 M acetic acid or water. Standardize with the standard CyDTA solution or a standard EDTA solution. The other reagents were of reagent grade (Wako Pure Chemicals).

Procedure. To 10 ml of 0.05 M antimony trichloride solution (HCl or acetone solution), add 30 ml of water and 10 ml of 0.06 M CyDTA standard solution; a 5 % molar excess of CyDTA is sufficient. Adjust the pH to 2—3 by adding sodium hydroxide solution, especially when a hydrochloric acid solution is used. Then add 5 ml of 1 M acetic acid and raise the pH of the solution to 2.5—3.0 by dropwise addition of 1 M sodium acetate solution. Warm the solution to 30—40 °C for about 5 min, while stirring, to complete the chelate formation. Do not boil the solution. Then cool to 0—5 °C, add sodium acetate to give pH 4.0—4.5, and back-titrate the excess of CyDTA with the lead standard solution using xylenol orange (aqueous 0.1 % w/v) as indicator. At the end-point, the color of the solution changes from yellow to violet for at least 1—2 min. The addition of pure ethanol may make the end-point clearer.

Results

A comparison of the analysis of antimony trichloride solution by this complexometric titration and by the bromate titration after complete expulsion of the organic solvent, is shown in Table 1. The results coincide well within the normal range of error.

The results of titrations of samples containing various quantities of antimony trichloride in acetone solution are shown in Table 2. When the CyDTA titration was applied to samples containing 0.1 mM (12.2 mg) Sb^{3+}, the results were not affected by the presence of sodium chloride up to 42.7 mM, acetone up to 40 ml, ethanol up to 60 ml, or arsenic trioxide up to 1.76 mM. However, copper iron, and sulfate interfered.

This titration can be used for the determination of $2 \cdot 10^{-2}$—2 mM Sb^{3+}, and is especially convenient for applications to solutions in organic solvents.

TABLE 1

Titration of antimony(III) with CyDTA and with bromate

Samples	Sb^{3+} found (mM)	
dissolved in	$KBrO_3$	CyDTA
6M HCl	0.501_2	0.498_0
6M HCl	0.198_8	0.197_4
Acetone	0.474_1	0.474_6
Acetone	0.237_2	0.236_9

TABLE 2

Titration of antimony in acetone solutions (mM)

Sb^{3+} present[a]	CyDTA added	Pb^{2+} added	Sb^{3+} found
0.098_8	0.2442	0.1456	0.098_6
0.173_0	0.2442	0.0713	0.172_9
0.197_7	0.2442	0.0452	0.199_0
0.222_4	0.2442	0.0201	0.224_1
0.234_7	0.2442	0.0095	0.234_7
0.098_8	0.1465	0.0477	0.098_8
0.135_9	0.1465	0.0105	0.136_0

[a]Standardized by $KBrO_3$ titration.

REFERENCES

1 N. H. Furman (Ed.), Scott's Standard Methods of Chemical Analysis, Vol. 1, 6th edn., Van Nostrand, New York, 1962, p. 92.
2 S. Takamoto, Nippon Kagaku Zasshi, 76 (1955) 1339.
3 I. M. Yurist, Zavod. Lab., 32 (1966) 1050; Chem. Abstr., 66 (1967) 25750.
4 V. A. Ermahov, V. V. Vorob'eva, A. A. Zartsev and G. N. Yakovlev, Radiokhimiya, 13 (1971) 840.
5 L. G. Sillen and A. E. Martell, Stability Constants of Metal—Ion Complexes, 2nd edn., Chemical Society, London, (1964).

Analytica Chimica Acta, 85 (1976) 213—218

Book Reviews

Eugene D. Olsen, *Modern Optical Methods of Analysis*, McGraw-Hill, New York, 1975, ix + 629 pp., price £11.75.

"The proper use of any instrumental technique for chemical analysis requires a clear understanding of what is being measured as well as how it is being measured. Only with a balanced knowledge of both the physicochemical theory behind the measurement and the instrumental principles involved can the scientist extract the maximum information from the instrument." These words form the introduction to the Preface of this book, and they summarize concisely the philosophy, aims, and approach of its author.

After a chapter on unifying principles, thirteen chapters deal with all the established spectroscopic methods — ultraviolet, visible, infrared, emission, flame photometry, atomic absorption and fluorescence, Raman, microwave, fluorimetry and phosphorimetry, refractometry and interferometry, spectropolarimetry and circular dichroism, turbidimetry and nephelometry, x-ray methods, n.m.r. and e.s.r., γ-ray and Mössbauer spectroscopy. There are two appendices and a good subject index.

This is a sound, well-written text, suitable for first or second-year undergraduates in British universities. Each chapter ends with a number of interesting exercises and calculations, to which answers are given, and with selected references that offer a good choice for further reading. The book is illustrated adequately throughout with good Tables and Figures, and with circuit and block diagrams showing the design principles of the instruments. Although these certainly include many of the models in use at the present time, there is a trend for particular designs to become outdated surprisingly quickly, and it is this aspect that will lead to this text becoming obsolete, unnecessarily prematurely, unless revised editions are issued.

This book can be recommended; students who are encouraged to use it at the appropriate stage of their chemical education will acquire a solid, sensible background on which to base their practical experience.

D. M. W. Anderson

R. Rosset, M. Caude and A. Jardy, *Manuel Pratique de Chromatographie en Phase Liquide*, Varian S.A., Orsay, 1975, xv + 280 pp., price 85.60 Fr. francs.

In the six years since its inception, high-pressure liquid chromatography (h.p.l.c.) has become accepted as a standard analytical method in many industrial companies and research centres. This book is one of several to appear recently which caters for the increasing number of newcomers to the field of h.p.l.c. and as its title suggests, it is written primarily for the practis-

ing chromatographer. There are chapters on the theory of chromatography, optimization of analytical conditions, equipment and column packing techniques, the various modes of chromatography (adsorption, liquid/liquid partition and ion exchange) and gel permeation chromatography, as well as short chapters on quantitative analysis and preparative h.p.l.c. For those with prior knowledge of thin-layer chromatography (t.l.c.) or gas chromatography (g.c.) there are notes on the conversion of a t.l.c. analysis into an h.p.l.c. one, and on the comparison of g.c. with h.p.l.c.

Throughout the book emphasis is laid on practical methods of improving a chromatographic analysis and the authors draw on their own research experience to demonstrate the factors which influence the separation of phenothiazines by adsorption chromatography (particle size, column dimensions and the nature of the mobile phase) as well as the separation of some carboxylic acids by ion-exchange chromatography (pH, ionic strength and the nature of the co-ion in the mobile phase). The chapter on ion exchange illustrates one of the difficulties in writing a book on a rapidly changing topic such as h.p.l.c., in that the accent is placed on ion exchange materials based on polystyrene beads whereas (as the authors predict) these have effectively been superseded by the mechanically more stable ion exchangers based on silica or silica-coated glass beads.

Each chapter concludes with a short list of literature references, and at the end of the book there is a useful collection of some 350 references covering various topics (detectors, preparative h.p.l.c. etc.) and applications of h.p.l.c. (antibiotics, steroids etc.). The references are up-to-date covering the literature to the beginning of 1975. In spite of the obvious language barrier, this paperbacked book should have considerable appeal and can be warmly recommended to all practising chromatographers.

Andrew Pryde

Donald T. Sawyer and Julian L. Roberts, Jr., *Experimental Electrochemistry for Chemists*, Wiley, New York, 1974. x + 435 pp., price £9.90.

The recent renaissance of electroanalytical methods has been accompanied by numerous applications of electrochemical techniques in various studies such as reaction mechanisms, kinetics and adsorption processes. The purpose of this book is to provide sufficient information on the basic principles and procedures of electrochemistry for the non-specialist to utilize the methods successfully.

The brief introduction is followed by chapters which cover 300 pp., on indicator and reference electrodes, electrochemical cells, solvents and electrolytes, and instrumentation; these provide the information necessary for voltammetry, polarography, potentiometry, conductimetry, and coulometry in all their varieties. Descriptions are clear; tables and diagrams are numerous. The chapter on instrumentation is particularly admirable.

The subsequent four chapters are much less successful. These deal with basic principles, methodology and applications with potentiometric measurements, controlled potential and controlled current methods and electrochemical titrations. The text reads almost as if the authors, awed by their own temerity in reducing the theory to an absolute minimum and appalled by the overwhelming bulk of the electrochemical and electroanalytical literature, had opted out. Of the 87 references in these four chapters, only 6 are to work published after 1970, and only 15 to material printed after 1965. The discussion of potentiometry is particularly confused, similar information appearing in different parts of the text; moreover, the ammonia electrode has been with us for some years and is not a mere possibility (p. 317).

Had the final chapters been as up-to-date and thorough in treatment as the first 300 pages, this book could have been recommended strongly to all practical chemists. It contains much useful practical information which is hard to find collated elsewhere, but its concluding chapters must be treated with reserve and considerable caution.

A. M. G. Macdonald

Extraction Chromatography, edited by T. Braun and G. Ghersini. Akademiai Kiado — Elsevier, Amsterdam, 1975, xvii + 565 pp., price Dfl 130.00 (U.S.$54.25).

This book, printed in the format of the Journal of Chromatography, is volume 2 of the new J. Chrom. Library Series. Extraction chromatography is defined here as "The separation of inorganic substances by means of chromatographic systems involving an organic compound as the supported stationary phase and an aqueous solution as the mobile phase". The emphasis is on column chromatography, and the 15 chapters, contributed by Russian and European authors, deal with theoretical aspects, correlation and liquid-liquid extraction, techniques, stationary phases, inert supports, separations of ions, actinides, lanthanides and fission products, uses in radiotoxicology, chelating agents, concentration of trace metals, use of cellular plastics, and correlation with laminar techniques.

In general, the treatment is comprehensive, and the book is useful in collecting together the available information on extraction chromatography, which is becoming increasingly important as greater column selectivity is achieved.

There are, however, various irritating features. The English is frequently stilted, and the type too often blurred. The indiscriminate use of the term "organophosphorous compounds" for alkylphosphates and similar substances is quite wrong. The final chapter (153 pp.) comprises a detailed bibliography (629 references), giving author(s), address, title of paper and reference; a tabular survey of experimental data on relevant investigations; a table of stationary phases; an author index (to the bibliography, not to the book);

and a "corporate index" listing the institutes and companies to which these authors are affiliated. Since the individual chapters are adequately referenced, this extensive and essentially bibliographic chapter seems to be superfluous. It has undoubtedly added considerably to the cost, which will doom this book to appear only on the library shelves of wealthy institutes.

Electroanalytical Chemistry, edited by H. W. Nürnberg, (Advances in Analytical Chemistry and Instrumentation, Vol. 10), Wiley, London, 1974, xi + 609 pp., price £18.50.

This volume contains seven articles on different aspects of electroanalysis. The first, by D. J. Fisher (158 pp.), covers instrumentation for d.c. polarography and coulometry; the approach is based on system concepts with emphasis on optimizing sensitivity and precision, and the review is concerned largely with the sophisticated instrumental developments at ORNL over the past 15 years. Applications of polarography and coulometry to actinide analysis are described by G. W. C. Milner and G. Phillips (37 pp.) in a well-balanced review, which, however, covers the literature only to 1968.

The uses of voltammetry and polarography in organic analysis are discussed authoritatively by P. J. Elving (90 pp.), who also presents the results of a survey made in 1972, as to why polarographic methods, which have been studied so extensively, have been used so little in routine organic structural and quantitative analysis in America. This tendency is less apparent in Europe, where polarography is often used in pharmaceutical analysis. Progress in this area, up to about 1970, is reviewed (47 pp.) by H. Hoffmann and J. Volke, but polarographic methods offer advantages over competitive techniques and much has been published on this subject since that time.

Voltammetry in non-aqueous solvents and melts is described (85 pp.) by J. Badoz-Lambling and G. Cauquis, who deal not only with the technique and precautions necessary with these media, but also with their practical advantages. This review contains an extensive table of electroactivity ranges for over 20 solvents and melts.

The benefits to be gained in mechanistic studies by combining electrochemical and electron spin resonance techniques are described by B. Kastening (74 pp.). The final review by K. Schwabe (90 pp.) serves as a reminder that even well-established processes such as pH measurement are in a state of continuous change in terms of depth of understanding and breadth of application.

In general, this book is a good addition to the useful Reilley-Murray series.

Galen W. Ewing, *Instrumental Methods of Chemical Analysis, 4th Edn.*, McGraw-Hill, New York, 1975, viii + 560 pp., price £11.25.

A text book which tries to cover the whole range of instrumental chemical analysis cannot succeed in pleasing everyone, but Professor Ewing has been considerably more successful than most other authors in presenting comprehensive, sensible, and well-balanced surveys of the available techniques. Chapters on all the spectroscopic techniques are followed by electrometric methods, chromatography, thermal activation techniques, and electronic circuitry. This new edition follows the same pattern as that published in 1969; the main changes involve the addition of chapters on electron spectroscopy and automated analysis and expansion of the discussions of n.m.r. and mass spectrometry, but considerable updating is evident in most chapters. For example, non-flame atomizers in a.a.s., atomic fluorescence spectrometry, ion-selective electrodes, high-pressure liquid chromatography and instrument—computer interfacing are dealt with adequately, and plentiful references to more specialized texts of recent date are given. Nomenclature has been converted to S.I. units where this seems sensible. The set problems and the reference lists at the end of each chapter are very useful, and the retention of an author index as well as a subject index is a welcome sight in a student text.

This new edition can be recommended warmly to the final-year undergraduates and immediate post-graduates for whom it is intended, and also to their teachers.

Analysis Instrumentation, Volume 13., edited by R. S. Saltzman, L. Zinn and R. Sims, Instrument Society of America, Pittsburgh, 1975, v + 154 pp., price £8.25.

This paperback contains the texts of 23 of the 32 papers read at the 21st Annual ISA Analysis Instrumentation Symposium held in May, 1975, in Philadelphia. The standard of the papers is rather variable; at the price asked, the book cannot be considered good value.

Absorption Spectra in the Ultraviolet and Visible Region Volume XIX, edited by L. Lang, Akademiai Kiado, Budapest, 1975, 400 pp., price £8.75.

Absorption Spectra in the Ultraviolet and Visible Region Volume XX, edited by L. Lang, Akademiai Kiado, Budapest, 1975, 400 pp., price £14.20.

These two volumes contain spectral data for another 350 compounds. The pattern is the same as in all earlier volumes of the series.

Recent N.B.S. Publications

L. W. Finger and E. Prince, *A System of Fortran IV computer programs for crystal structure computations*, SD Cat. No.: C13.46:854, 133 pp., price $2.00.

Marine pollution monitoring, Proceedings of a Symposium held at NBS, Gaithersburg, 1974, edited by R. C. Junghans, SD Cat. No.: C13.10:409, 293 pp., price $3.90.

J. P. Cali et al., *Standard reference materials — the role of SRM's in measurement systems*, SD Cat. No.: C13.44:148, 54 pp., price $1.15.

H. M. Roder, *Liquid densities of oxygen, nitrogen, argon and parahydrogen*, SD Cat. No.: C13.46:361., 114 pp., price $1.25.

R. L. Powell and G. W. Burns, *Thermocouple reference tables based on the IPTS-68 — Reference tables in degrees fahrenheit for thermoelements versus platinum (Pt-67)*, SD Cat. No.: C13.44:125 Suppl. 1., 46 pp., price $1.05.

Howard F. McMurdie et al., *Standard x-ray diffraction powder patterns, Section 12 — Data for 57 substances*, SD Cat. No.: C13.44:25/12., 90 pp., price $1.50.

R. E. Drullinger, M. M. Hessel and E. W. Smith, *Analysis of optically excited mercury molecules*, SD Cat. No. C13.44:143, 51 pp., price $1.10.

R. K. Anderson and J. O. Harrison, Jr., *Computer program package for metric conversion — Reference manual*, SD Cat. No. 13.46:872, 145 pp., price $2.10.

Report on the 59th National Conference on Weights and Measures (1974), edited by S. J. Edgerly, SD Cat. No.: C13.10:407, 284 pp., price $3.75.

P. S. Shoenfeld, *Real-time acquisition and processing of fluorimetry data*, SD Cat. No.: C13.46:857, 45 pp., price $1.05.

Catalog of NBS Standard Reference Materials, SD Cat. No.: C13.10:260 — 1975—76 cat. 40 pp., price $1.50.

Copies of these documents are available from the U.S. Government Printing Office, Washington, D.C. 20402. S.D. Catalog numbers must be quoted. Orders must be prepaid. Foreign remittances must be in U.S. exchange and must include an additional 25% of the publication price to cover mailing costs.

Theory and Practice of MO Calculations on Organic Molecules

by **I.G. CSIZMADIA,** Department of Chemistry, University of Toronto.

PROGRESS IN THEORETICAL ORGANIC CHEMISTRY, Vol. 1.

1976 x+378 pages US $38.50/Dfl. 100.00 ISBN 0-444-41468-1

Current chemical theory is based on approximate quantum mechanical treatments and especially molecular orbital methods. In recent years, the theory has been developed to the point where quantitative calculations can be made on many physical properties of molecules and interacting molecular systems.

This book provides an introduction to rigorous *ab initio* molecular orbital calculations for the experimental organic chemist. The necessary mathematics and quantum mechanics are reviewed as background for the experimentalist wishing to begin theoretical work. The Hartree-Fock method for both open and closed shell molecules is derived in detail. Results of many recent theoretical studies are included to illustrate the practical application of molecular orbital theory to problems in organic chemistry.

This book should be of particular value to the experimental organic chemist interested in beginning MO calculations related to his research interests. It would serve as a text for a course in Theoretical Organic Chemistry and as a useful supplementary text in courses on Physical Organic Chemistry and Molecular Quantum Mechanics. This text provides an excellent introduction to theoretical organic chemistry for the experimental organic chemist.

CONTENTS: **A. Introduction.** I. Introductory Remarks. II. Mathematical Introduction. III. Quantum Mechanical Background. **B. Theory of Closed Electronic Shells.** IV. Non-Empirical or Hartree-Fock MO Theory. V. Semi-Empirical MO Theories. VI. Excited and Ionized States in the Framework of Closed Shell MO Theories. VII. Hybrid Atomic Orbitals (HAO) and Localized Molecular Orbitals (LMO). VIII. Limitations of Molecular Orbital Theories. IX. Applications of MO Theory to Closed Shell Problems. **C. Theory of Open Electronic Shells.** X. Open Shell SCF Theories. XI. Limitations and Applications of Open Shell SCF Theories. **D. Practical Aspects of MO Computations.** XII. Basis Sets for Molecular Orbital Calculations. XIII. Information on Selected Computer Programs. XIV. Closing Remarks. **E. Appendix.** XV. Detailed Formalisms of Roothaan's SCF Theories.

ELSEVIER SCIENTIFIC PUBLISHING COMPANY

P.O. Box 211, Amsterdam, The Netherlands

Distributor in the U.S.A. and Canada:
ELSEVIER/NORTH-HOLLAND, INC.,
52 Vanderbilt Ave., New York, N.Y. 10017

The Dutch guilder price is definitive. US $ prices are subject to exchange rate fluctuations.

960 E

Handbook of Atomic Data

by S. FRAGA, J. KARWOWSKI and K.M.S. SAXENA

1976 x + 554 pages US $49.75/Dfl. 129.00 ISBN 0-444-41461-4

This book provides a comprehensive description, at the Hartree-Fock level, of all the elements of the Periodic System and many of their positive ions. Hartree-Fock data represent a permanent point of reference for theoretical calculations. In addition, theoretical predictions constitute a valuable help to experimental researchers. Most of the data tabulated here are not available in the literature. The quantities considered have been tabulated for: the neutral atoms and all the positive ions (except one) of the elements Helium through Krypton; the neutral atoms and the first eleven positive ions of the elements Yttrium through Ytterbium; and the neutral atoms and first four positive ions of the elements Lutecium through Nobelium.
Both experimental and theoretical researchers will find this book of unique value because it provides easy access to data which may be useful either for reference or as a basis for future work.

CONTENTS: **Introduction. Theory of Atomic Structure.** Formulation. Hartree-Fock Results. **Description of the Quantities.** Configurations, States, and Functions. Energies and Interaction Constants. Interactions with External Fields. Coherent X-Ray Scattering Factors. Atomic Radius. **Tables. Configurations.** Electronic Configurations and States. Functions. Orbital Parameters. Energies. Total Energies. Normal Mass Effects. Hartree-Fock Energies. Specific Mass Effects. Total Relativistic Corrections. Relativistic Mass Corrections. Breit Corrections. **Spectra.** Electron Affinities. Energy Levels. Ionization Potentials. **Coupling Constants.** Spin-Orbit Coupling Constants. Spin-Spin Dipole Interaction Constants. Fermi Contact Interaction Constants. Magnetic Dipole Hyperfine Structure Constants. Electric Quadrupole Interaction Constants. Magnetic Octupole Coupling Constants. **External Interactions.** Electric Dipole Polarizabilities. Oscillator Strength Sums. Dispersion Coefficients. Nuclear Magnetic Shielding Constants. Magnetic Susceptibilities. Lande Factors. Coherent X-Ray Scattering Factors. **Integrals and Parameters.** Slater-Condon Integrals. Spin-Orbit Parameters; Marvin Radial Integrals. Orbital Energies. Atomic Radii. **Expectation Values.** Expectation Values $\langle r^2 \rangle$. Expectation Values $\langle r^4 \rangle$. Expectation Values $\langle r^6 \rangle$. Expectation Values $\langle r^{-3} \rangle$. Expectation Values $\langle r^{-5} \rangle$. **Data for Additional Configurations.** Hartree-Fock Energies. Energies, Coupling Constants and External Interactions. Ionization Potentials. Integrals and Parameters. **Appendix.** Nuclear Data. **References. Subject Index.**

ELSEVIER SCIENTIFIC PUBLISHING COMPANY

P.O. Box 211, Amsterdam, The Netherlands

Distributor in the U.S.A. and Canada:
ELSEVIER/NORTH-HOLLAND, INC.,
52 Vanderbilt Ave., New York, N.Y. 10017

The Dutch guilder price is definitive. US $ prices are subject to exchange rate fluctuations.

(Continued from page 4 of cover)

Short Communications

Printed in The Netherlands

VOL. 85 No. 1 ANALYTICA CHIMICA ACTA AUGUST 1976

CONTENTS

(continued on inside page of the cover)